

Load-Response and the Effect of
De-bonding on Structural Insulated Panels
Performance

By

Farhoud Delijani

A thesis submitted to the Faculty of Graduate Studies
in partial fulfilment of the requirements for the degree of

Doctor of Philosophy

Department of Biosystems Engineering
Faculty of Engineering
University of Manitoba
Winnipeg

Copyright © 2016 by Farhoud Delijani

Abstract

Series of full-scale tests were conducted on polyurethane foam-core Structural Insulated Panels (PUR SIPs) to study the load response and creep behaviour of such panels. The load response of PUR SIPs was compared with conventional stud wall panels. The effects of de-bonding between the foam-core and the OSB face-sheets were also studied to understand the effects of such change on the overall performance of PUR SIPs. At last, computer modelling was employed to simulate and predict the behaviour of PUR SIPs in different loading orientations and dis-bond ratios. It was found that PUR SIPs can outperform conventional stud-wall panels in every aspect. In the case of 165 mm (6.5 in.) thick PUR SIPs, 33% dis-bond between the PUR foam-core and the OSB face-sheets caused an average of 64% reduction in 'axial load' capacity, an average of 75.8% reduction in 'transverse load' capacity, and an average of 7.9% reduction in 'racking load' capacity of the panels compared to brand new fully-bonded SIPs. It was also found that 33% dis-bond in 165 mm (6.5 in.) thick PUR SIPs has minimal effect on the racking load capacity of the panels. In the case of 114 mm (4.5 in.) thick PUR SIPs, 33% dis-bond between the PUR foam-core and the OSB face-sheets caused an average of 63.3% reduction in 'axial load' capacity, an average of 79% reduction in 'transverse load' capacity, and an average of 29% increase in 'racking load' capacity of the panels compared to brand new fully-bonded SIPs. All tested panels satisfied the code requirements for the creep deflec-

tions (span/180) and they fully rebounded to their initial estate, 90 days after removal of the simulated snow loads. It was also found that weathering has minimal effect on the bond between the face-sheets and the PUR foam. After computer simulations of fully-bonded and dis-bonded PUR SIPs in two different thicknesses, it was found that SOLIDWORKS simulation software is a useful tool to predict the load response of PUR SIPs only when fully-bonded panels are exposed to transverse load orientation regardless of the thickness of the panel.

In general, available Canadian and American standards were followed in this study. Where applicable, standards were adopted from other material testing methods for testing PUR SIPs. It is believed that this independent research has addressed most frequently expressed concerns regarding the use and application of structural insulated panels such as de-bonding issues and creep behavior and their relationship to durability. The hope is that this research help increase the use and application of SIPs in green, high-performance, light-frame building construction in Canada.

Acknowledgments

For his skills, patience and cooperative assistance throughout the experimental work I ‘especially’ would like to express my special thanks to Peter Hildebrand at the Alternative Village. I also owe a great debt to my fellow graduate and undergraduate students: Jeremy Pinkos, Moe Yusim, Hossein Safavian, Garry Enns, and Natasha Jacobson.

My best regards go to my supervisor Dr. Kris Dick, who is an exceptional teacher and mentor. Without his guidance, mentorship and unlimited kindness, I would not have been able to complete this research.

Lastly, I would like to thank my beloved wife, Solmaz Nafez, and my son Ilya, who have always been there for me and dealt with the hardships we went through along this long journey.

This research study was not possible without the financial contribution of Emercor Ltd. And Industrial Research Assistance Program (IRAP) of National Research Council Canada.

Dedication

To my beloved son, ILYA.

Contents

Contents	iii
List of Tables	x
List of Figures	xvii
List of Symbols	xxxii
1 Introduction	1
1.1 Thesis Structure	3
1.2 Programme	5
1.3 What is a SIP?	5
1.3.1 Thermal Resistance, Temperature and Moisture	10
1.3.2 SIPs Installation	13
1.3.3 Challenges with SIPs in the Marketplace	15
1.4 Research Objectives	17
1.5 Research Approach	17
1.5.1 Structural Capacity Evaluation Baseline	17

1.5.2	Dis-bonded Panels	18
1.5.3	Bond Integrity Evaluation.....	18
1.5.4	Durability and Long-term Creep Study	19
1.6	Deliverables	20
1.7	Implications of the Research for the Construction Industry	21
2	Literature Review	25
2.1	Introduction.....	26
2.2	History of SIPs.....	26
2.3	Different Types of Sandwich Panels.....	29
2.4	Previous Studies on Creep Behaviour in Insulated Sandwich Panels.....	30
2.4.1	Creep in Material	30
2.4.2	Creep in Insulated Sandwich Panels	31
2.5	Previous Studies on Foam and De-bonding Issues in Insulated Sandwich Panels	
	35	
2.5.1	EPS Foam.....	35
2.5.2	XPS Foam	36
2.5.3	Polyurethane (Urethane or PUR) and Polyisocyanurate (PIR, polyiso, or ISO) Foams	37
2.5.4	Compressed Wheat or Rice Straw Core.....	38
2.5.5	Characteristics of OSB Facings	41

2.5.6	Failure Mode and De-bonding in Sandwich Panels.....	42
-------	---	----

3 Experimental Measurement of the Structural Capacity of PUR SIPs - Baseline

Tests		46
--------------	--	-----------

3.1	Test Samples	48
3.2	Baseline Tests	49
3.2.1	Tests on Structural Capacity of Stud Wall Panels	49
3.2.2	Tests on Structural Capacity of PUR SIPs.....	49
3.2.2.1.	Axial tests.....	51
3.2.2.2.	Transverse tests	57
3.2.2.3.	Racking tests	58
3.3	Baseline Test Results	62
3.3.1	Modes of failure.....	62
3.3.2	Relative Behavior of PUR SIP Types	63
3.3.3	Comparison to theoretical critical buckling load.....	68
3.4	Conclusions.....	69

4 Experimental Measurement of the Structural Capacity of Dis-bonded PUR SIPs71

4.1	Introduction.....	72
4.2	Sample Preparation	72
4.3	Test Procedure and Assembly.....	77

4.3.1	Axial Load Tests	77
4.3.2	Transverse Load Tests	79
4.3.3	Racking Load Tests.....	81
4.4	Experimental Results	82
4.4.1	Axial Load Test Results.....	83
4.4.2	Transverse Load Test Results	90
4.4.3	Racking Load Test Results	94
4.5	Conclusions.....	98
5	Experimental Measurement of the Flexural Creep Behaviour of PUR SIPs	101
5.1	Introduction.....	102
5.2	Material Description	102
5.3	Creep Pre-Tests	106
5.4	Creep Test Method.....	110
5.4.1	Duration of Applied Loads	113
5.4.2	Test Procedure and Assembly.....	117
5.5	Data Analysis	122
5.6	Test Results	130
5.7	Conclusions.....	140

6 Bond Strength as a Measure of Serviceability and Quality of Polyurethane Foam

Structural Insulated Panels (Pull-off Tests) 142

6.1	Introduction.....	143
6.2	Materials and Method	144
6.3	Results and Analysis	151
6.4	Conclusions.....	155

7 FEM Modelling of OSB- PUR SIPs 157

7.1	Introduction.....	158
7.2	Modelling of PUR SIPs under different loading orientations.....	159
7.2.1	Microscopic evaluations	160
7.2.2	Compression tests for determining mechanical properties of PUR SIPs	162
7.2.3	Experimental determination of modulus of elasticity of tested PUR SIP OSB face-sheets	165
7.3	Modelling.....	169
7.3.1	Number of nodes and element sizes for each simulated test	169
7.3.2	Loading	169
7.3.3	Mechanical and physical properties of the modeled PUR SIP components	172
7.4	Results.....	172

7.4.1	Axial tests results	174
7.4.2	Transverse tests results	179
7.4.3	Racking tests results.....	183
7.5	Conclusions.....	187
8	Summary and Conclusions	189
8.1	General.....	190
8.2	Overall Conclusions.....	190
8.2.1	PUR SIPs vs. stud wall panels	190
8.2.2	Thicker PUR SIPs vs. thinner PUR SIPs.....	191
8.2.3	Partially dis-bonded PUR SIPs vs. fully-bonded PUR SIPs.....	191
8.2.4	Creep load behaviour of PUR SIPs.....	192
8.2.5	Pull-off test conducted on brand new and weathered PUR SIPs	193
8.2.6	Load response computer simulation of PUR SIPs.....	193
8.3	Limitations and Further Recommended Tests	194
8.3.1	Limitations	194
8.3.2	Further Recommended Tests	194
	References.....	198
	Appendices.....	212
	Appendix A: Material Properties	213
	Appendix B: Test Setup Drawings	215

Appendix C: Baseline Test Results.....	219
Axial Test Results (Baseline tests)	220
Transverse Test Results (Baseline tests).....	221
Racking Test Results (Baseline tests).....	222
Appendix D: Dis-bonded Panels Test Results	223
Axial Test Results (Dis-bonded tests).....	224
Transverse Test Results (Dis-bonded tests).....	228
Racking Test Results (Dis-bonded tests)	230
Design Load on a Residential Wall (Location: Winnipeg, Manitoba)	232
Appendix E: Compression Coupon Test Results.....	234
Appendix F: Pull-off Test Results	236
Appendix G: Modelling Documents.....	245
Load vs. Deflection Curves of OSB Specimen Tested for the Evaluation of the ‘E’ Values	246
Axial Load Simulations of Fully-Bonded PUR SIPs (114mm, 4.5 in. thick).....	248
Axial Load Simulations of Dis-Bonded PUR SIPs (114mm, 4.5 in. thick).....	251
Transverse Load Simulations of Fully-Bonded PUR SIPs (114mm, 4.5 in. thick) ..	254
Transverse Load Simulations of Dis-Bonded PUR SIPs (114mm, 4.5 in. thick).....	257
Racking Load Simulations of Fully-Bonded PUR SIPs (114mm, 4.5 in. thick)	260
Racking Load Simulations of Dis-Bonded PUR SIPs (114mm, 4.5 in. thick)	263

List of Tables

Chapter 1

Table 1-1: RSI and R-values of EPS core SIPs at different temperatures (Premiersips, 2011).....	11
Table 1-2: Specimen quantity for PUR SIP baseline tests in accordance with ASTM E1803 (ASTM, 2006), ASTM E72 (ASTM, 2015) and APA (APA, 2013).....	18

Chapter 2

Table 2-1: Advantages and disadvantages of commonly used facing sheet materials for manufacturing SIPs (Panjehpour et al., 2013)	29
Table 2-2: Comparison of R and RSI values for the cellular foam insulation materials (Morley, 2000)	37
Table 2-3: Basic properties of CSA 0437.0 OSB and Waferboard ¹ (SBA, 2004).....	43
Table 2-4: Physical properties of OSB (SBA, 2004).....	44
Table 2-5: Minimum properties for facing materials used for SIP (APA, 2011)	45

Chapter 3

Table 3-1: Specification of PUR SIPs test specimens in accordance with ASTM E1803 (ASTM, 2006), ASTM E72 (ASTM, 2015) and APA (APA, 2013)	48
---	----

Table 3-2: Baseline test results for 114 mm (4.5 in.) thick PUR SIP	64
Table 3-3: Baseline test results for 165 mm (6.5 in.) thick PUR SIP	65
Table 3-4: Baseline test results for 38 × 140 mm (nominal 2 x 6 in.) and 38 × 89 mm (nominal 2 x 4 in.) stud walls.....	65
Table 3-5: Comparison between panel assemblies load capacity	66

Chapter 4

Table 4-1: Dimensions of intentionally dis-bonded PUR SIPs test specimens in accordance with ASTM E1803 (ASTM, 2006), ASTM E72 (ASTM, 2015) and APA (APA, 2013).....	72
Table 4-2: Test result of the dis-bonded 114 mm (4.5 in.) thick panels exposed to axial, transverse and racking loads	84
Table 4-3: Comparison between results in axial, racking and transverse test conducted on fully bonded 114 mm (4.5 in.) thick panels and dis-bonded panels	84
Table 4-4: Test result of the dis-bonded 165 mm (6.5 in.) thick panels exposed to axial, transverse and racking loads	85
Table 4-5: Comparison between results in axial, racking and transverse test conducted on fully bonded 165mm (6.5 in.) thick panels and dis-bonded panels	85
Table 4-6: Summary of ultimate load ratios for bonded compared to dis-bonded for 114 mm (4.5 in.) and 165 mm (6.5 in.) thick panels.....	86
Table 4-7: Vertical deformation of PUR SIPs under axial load	89

Table 4-8: Average maximum deflection (mid-height linear potentiometer reading) of the fully bonded 114mm (4.5 in.) and 165mm (6.5 in.) thick PUR SIPs vs. dis-bonded panels in axial load tests compared to code limits ($L/180=13.6$ mm) 89

Table 4-9: Average maximum deflection of the fully bonded 114mm (4.5 in.) and 165mm (6.5 in.) thick PUR SIPs vs. dis-bonded panels in transverse load tests (at the time of failure)..... 93

Table 4-10: Average maximum load at the deflection limit of $L/180$ for panels tested for transverse load capacity compared to the code requirement of 1.25 kN maximum load . 93

Chapter 5

Table 5-1: Specification of PUR SIPs tested for flexural creep behaviour in accordance with ASTM E1803 (ASTM, 2006), ASTM E72 (ASTM, 2015) and APA (APA, 2013) 103

Table 5-2: Technical requirements for closed-cell polyurethane and Polyisocyanurate foam thermal insulation tested to CAN/ULCS704-03 and CAN/ULC-S704-11 (Standards Council of Canada, 2011) 104

Table 5-3: Physical properties of the polyurethane foam-core provided by the foam manufacturer 104

Table 5-4: Physical properties of the OSB used in manufacturing of the tested PUR SIPs 105

Table 5-5: Mechanical properties of the OSB used to manufacture the tested PUR SIPs	105
Table 5-6: Compressive stress handled by PUR SIP coupons with different thicknesses	107
Table 5-7: Compression and rebounding values of PUR SIP coupons under axial compressive load.....	108
Table 5-8: Loading schedule for short-term creep test of SIPs (NRC, 2007).....	113
Table 5-9: Loading schedule for long-term creep test of SIPs	114
Table 5-10: Flexural creep test loads recommended by NRC's guideline (NRC, 2007)	114
Table 5-11: Actual weight of the tested panels.....	116
Table 5-12: Results of the physical measurements of the moisture content of the OSB face-sheets (dry basis) of the PUR SIPs tested for flexural creep behaviour	121
Table 5-13: Change in temperature and relative humidity of the test chamber during the 8 weeks of creep test	121
Table 5-14: Experimentally measured mechanical properties of PUR SIPs conducted by Taylor (1996)	129
Table 5-15: Results of the analysis of the negligibility check of the first and third terms in Equation 5.1	130
Table 5-16: Maximum deflection of each specimen under dead load only	135

Table 5-17: Maximum deflection of each specimen under combination of dead load plus live load.....	135
Table 5-18: Manual readings of deflection up to 90 days after removal of the design creep loads	136
Table 5-19: Average maximum deflection of tested panels under different creep load combinations	137
Table 5-20: Shear stress level created in foam core due to creep loads in tested panels	139
Table 5-21: Experimental maximum creep deflection of panels vs. the theoretical predicted creep deflection values (using Eq. 5.15)	140

Chapter 6

Table 6-1: Summary of failure modes based on panel type.....	152
Table 6-2: Comparison of load, vertical movement and stress in all failure modes combined.....	153
Table 6-3: Comparison of pull-off energy	154
Table 6-4: Comparison of pull-off energy (Joules) based on each side of panel	155

Chapter 7

Table 7-1: Average modulus of elasticity of 114 mm (4.5 in.) PUR SIP samples subjected to axial compressive load.....	163
Table 7-2: Average modulus of elasticity of 165 mm (6.5 in.) thick PUR SIP samples subjected to axial compression load	163

Table 7-3: Physical and mechanical properties of polyurethane foam with 25.6 kg/m ³ (1.6 lb./ft ³) density (Shim et al., 2000)	164
Table 7-4: Load points taken from the elastic region of load vs. deflection curves of tested OSB coupons	168
Table 7-5: Experimental average values of E based the data points provided in Table 7-4	169
Table 7-6: Specimen ID, number of nodes, element size and, total number of elements of simulated PUR SIPs	170
Table 7-7: Maximum load applied to modeled fully-bonded and dis-bonded 114 mm (4.5 in.) thick panels	171
Table 7-8: Maximum load applied to modeled fully-bonded and dis-bonded 165 mm (6.5 in.) thick panels	172
Table 7-9: Physical and mechanical properties of modeled PUR SIPs from available published literature.....	173
Table 7-10: Model ID's for simulated PUR SIPs under different loading scenarios	173

Appendix A

Table A - 1: Result of the foam density tests conducted and provided by the PUR SIP manufacturer (Emercor). Each panel (sample) was tested on five spots over the area of the panel	214
Table A - 2	216

Appendix F

Table F - 1: Results of all conducted pull-off tests.....237

Table F – 2: Results of pull-off tests for foam failure only.....238

List of Figures

Chapter 1

Figure 1-1: Schematic details of an ordinary Structural Insulated Panel (CCMC, 1996) ..	6
Figure 1-2: Different facing materials used in SIPs manufacturing (Photo courtesy of Vantem Panels formerly Winter Panel, United States, 2012).....	7
Figure 1-3: Assembly line of EPS core SIPs (Photo courtesy of Premier SIPS by Insulfoam, United States, 2012).....	8
Figure 1-4: SIP compared to an ‘I-beam’ (Foamlaminates, 2008)	9
Figure 1-5: Whole wall R-value comparisons between 3.5 in. core SIP wall and conventional 2x4 and 2x6 wood frame walls (Kosny, Desjarlais, & Christian, 1999).....	11
Figure 1-6: Most common panel to panel spline connection configuration for SIPs (Morley, 2000)	14
Figure 1-7: Special screws used in SIP connections and installations (Trufast, 2012)	14
Figure 1-8: De-bonding test sampling scheme (Source: Dick, 2011).....	20

Chapter 2

Figure 2-1: Typical material creep behaviour (Taylor, 1996)	31
---	----

Figure 2-2: Creep behaviour of regular polystyrene at various stresses [Source: Sauer et al., J. Appl. Phys., 20, 510- 1949] (Teach & Kiessling, 1960).....	36
Figure 2-4: Typical curve of compressive strength versus temperature in rigid Polyurethane foam (Hilado, 1967).....	39
Figure 2-4: Effects of 100% humidity and temperature on dimensional stability of typical rigid Polyurethane foam (Hilado, 1967).....	39
Figure 2-5: SIPs made of compressed wheat straw, Timber Strand sub-frame, Exposure 1 OSB, (7/16 in. - no urea formaldehyde added) and, non-toxic adhesives (Agriboard Industries , 2010)	39
Figure 2-6: OSB grade stamp	44
 Chapter 3	
Figure 3-1: Axial compression test setup diagram (APA, 2013).....	51
Figure 3-2: Axial test set-up	52
Figure 3-3: Legend for Equation 3.2 (Mousa & Uddin, 2011).....	54
Figure 3-4: Transverse test on stud wall in progress	57
Figure 3-5: Racking behaviour of sandwich wall panels with or without vertical loads (Bregulla, 2003)	58
Figure 3-6: Racking resistance test on 2240 x 2240mm (8 x 8 ft.) PUR SIPs.....	59
Figure 3-7: A typical spline-glue connection used to connect two Styrofoam foam core panels together (Fine Homebuilding, 2006)	61

Figure 3-8: Typical test setup for racking load tests (APA, 2013)	61
Figure 3-9: Typical transverse tests results comparing the performance of a 165mm thick (6.5 in.) PUR SIPs to a conventional 165mm (6.5 in.) stud wall panels	67
Figure 3-10: Typical racking tests results comparing the performance of a 165mm thick (6.5 in.) PUR SIP to a conventional stud wall panel	67
Figure 3-11: Typical axial tests results comparing the performance of a 165mm (6.5 in.) thick PUR SIP to a conventional 140mm (2 by 6) stud wall panels.....	68

Chapter 4

Figure 4-1: Darker OSB area indicates the dis-bonded/debonded region on the surface of the PUR SIP	74
Figure 4-2: Partially bond-less PUR SIPs ready for test. Waxed paper used between the OSB face-sheets and the PUR foam to avoid bond between the two materials	75
Figure 4-3: Connection details of two 1220x2440 mm (4x8 ft.) panels joined together for racking test purposes. OSB splines, construction adhesive, expandable spray PUR foam and nails used to join the panels together	76
Figure 4-4: Location of linear potentiometers on dis-bonded panels tested under eccentric compression axial load.....	78
Figure 4-5: Dis-bonded panel under direct eccentric axial load. Bucking occurred only at the disbonded area of the panel at the time of failure	78
Figure 4-6: A failed disbonded panel subjected to transverse load	80

Figure 4-7: Location of linear potentiometers on dis-bonded panels tested under transverse load	80
Figure 4-8: Location of the linear potentiometers on dis-bonded panels tested under racking load.....	83
Figure 4-9: Typical axial load resistance of 114mm (4.5 in.) thick dis-bonded PUR SIPs compared to fully-bonded panels with the same thickness. This graph shows the overall shortening of the SIP under axial load (top linear potentiometer only).....	87
Figure 4-10: Typical axial load resistance of 165mm (6.5 in.) thick dis-bonded PUR SIPs compared to fully bonded panels with the same thickness. This graph shows the overall shortening of the SIP under axial load (top linear potentiometer only).....	87
Figure 4-11: Typical axial load resistance of 114mm (4.5 in.) thick dis-bonded PUR SIPs compared to fully bonded panels with the same thickness. This graph shows the overall shortening of the SIP under axial load (mid-left linear potentiometer only). The first few millimetres of negative deformation is due to slight rotation of the I beam (located at the 1/3 of the panel thickness) before it is fully stabilized on under applied load.....	88
Figure 4-12: Typical axial load resistance of 114mm (4.5 in.) thick dis-bonded PUR SIPs compared to fully bonded panels with the same thickness. This graph shows the overall shortening of the SIP under axial load (mid-left linear potentiometer only)	89
Figure 4-13: Typical transverse load resistance of 114mm (4.5 in.) thick dis-bonded PUR SIPs compared to fully bonded panels with the same thickness. Red dotted line represents	

fully bonded panels and solid line represents dis-bonded panels. The vertical blue line indicates the serviceability deflection limit of L/180 (13 mm)..... 92

Figure 4-14: Typical transverse load resistance of 165mm (6.5 in.) thick dis-bonded PUR SIPs compared to fully bonded panels with the same thickness. The vertical blue line indicates the serviceability deflection limit of L/180 (13 mm)..... 92

Figure 4-15: Typical racking load resistance of 114mm (4.5 in.) thick dis-bonded PUR SIPs compared to fully bonded panels with the same thickness..... 94

Figure 4-16: Typical racking load resistance of 165mm (6.5 in.) thick dis-bonded PUR SIPs compared to fully bonded panels with the same thickness..... 95

Figure 4-17: Racking test on dis-bonded in progress. Bucking of the dis-bonded area of the left panel can be seen 95

Figure 4-18: Racking load trend-line comparison between dis-bonded panels and fully bonded panels for 114mm (4.5 in.) thick PUR SIPs..... 97

Figure 4-19: Racking load trend-line comparison between Dis-bonded panels and fully bonded panels for 165mm (6.5 in.) thick PUR SIPs..... 97

Chapter 5

Figure 5-1: PUR SIP coupon under compression load test with a maximum deflection limited to 25mm (1 in.)..... 106

Figure 5-2: A typical compressive test conducted on 165mm (6.5 in.) and 114mm (4.5 in.) thick PUR SIP coupons with the area of 152 by 152 mm (6 x 6 in.) and 25mm (1 in.) deflection limit	107
Figure 5-3: Relaxation and rebound behaviour of 165mm (6.5 in.) thick PUR SIP coupons under compressive load	109
Figure 5-4: Relaxation and rebound behaviour of 114mm (4.5 in.) thick PUR SIP coupons under compressive load	109
Figure 5-5: Loading scheme for short-term creep test of SIPs (NRC, 2007)	111
Figure 5-6: Schematic drawing of the PUR SIP flexural creep test set up	118
Figure 5-7: PUR SIP subjected to design creep loads	120
Figure 5-8: Flexural creep test of PUR SIP in progress.....	120
Figure 5-9: Physical specification of the flexural creep test span	123
Figure 5-10: Deflection of a sandwich beam (Allen, 1969)	126
Figure 5-11: Schematic diagram showing the critical points of a typical Deflection vs. Time creep curve (Taylor, 1996)	131
Figure 5-12: Load vs. Deflection curve of the specimen CT45-1	132
Figure 5-13: Load vs. Deflection curve of the specimen CT45-2	132
Figure 5-14: Load vs. Deflection curve of the specimen CT45-3	133
Figure 5-15: Load vs. Deflection curve of the specimen CT65-1	133
Figure 5-16: Load vs. Deflection curve of the specimen CT65-2	134

Figure 5-17: Load vs. Deflection curve of the specimen CT65-3 134

Chapter 6

Figure 6-1: Schematic detail of the hand-made pull-off tester 145

Figure 6-2: Hand-made pull-off tester used conduct pull off tests on PUR SIPs 145

Figure 6-3: PUR SIPs stored in a storage yard with minimum weather protection for more than four years..... 146

Figure 6-4: Pull-off test assembly (Source: Dick, 2014) 147

Figure 6-5: Steps in pull off test preparation 148

Figure 6-6: Schematic failure modes of the specimen plug (Source: Dick, 2014) 149

Figure 6-7: Actual failure modes of the specimen plug observed in pull-off tests..... 150

Figure 6-8: Typical load vs. deflection curve of the pill-off tests conducted on PUR SIPs 151

Chapter 7

Figure 7-1: Magnification (40x) of PUR foam-OSB bond area in PUR SIPs. Top part of the photo is the OSB and the bottom shows foam 161

Figure 7-2: Separating OSB face-sheets from the PUR foam-core 166

Figure 7-3: Test set-up for evaluation of E of the OSB face-sheet coupons 166

Figure 7-4: Mesh detail and deformation behaviour of modeled fully-bonded 165mm (6.5 in.) thick PUR SIPs under eccentric axial load (M65A) (Red indicates zone of greatest deformation)..... 175

Figure 7-5: Comparison between the experimental results and simulated results concluded from axial load test on fully-bonded 114 mm (4.5 in.) thick PUR SIPs	175
Figure 7-6: Comparison between the experimental results and simulated results concluded from axial load test on fully-bonded 165 mm (6.5 in.) thick PUR SIPs	177
Figure 7-7: Comparison between the experimental results and simulated results concluded from axial load test on partially dis-bonded 114 mm (4.5 in.) thick PUR SIPs	177
Figure 7-8: Comparison between the experimental results and simulated results concluded from axial load test on partially dis-bonded 114 mm (4.5 in.) thick PUR SIPs	178
Figure 7-9: Mesh detail and deformation behaviour of modeled 165mm (6.5 in.) thick partially dis-bonded PUR SIPs under eccentric axial load (MD65A) (Red indicates zone of greatest deformation)	178
Figure 7-10: Comparison between the experimental results and simulated results concluded from transverse load test on fully-bonded 114 mm (4.5 in.) thick PUR SIPs	180
Figure 7-11: Comparison between the experimental results and simulated results concluded from transverse load test on fully-bonded 165 mm (6.5 in.) thick PUR SIPs	180
Figure 7-12: Mesh detail and deflection behaviour of modeled 165mm (6.5 in.) thick fully-bonded PUR SIPs exposed to transverse load (M65T) (Red indicates zone of greatest deformation)	181

Figure 7-13: Comparison between the experimental results and simulated results concluded from transverse load test on partially dis-bonded 114 mm (4.5 in.) thick PUR SIPs	181
Figure 7-14: Comparison between the experimental results and simulated results concluded from transverse load test on partially dis-bonded 165 mm (6.5 in.) thick PUR SIPs	182
Figure 7-15: Mesh detail and deflection behaviour of modeled 165mm (6.5 in.) thick partially dis-bonded PUR SIPs exposed to transverse load (MD65T) (Red indicates zone of greatest deformation).....	182
Figure 7-16: Comparison between the experimental results and simulated results concluded from racking load test on fully-bonded 114 mm (4.5 in.) thick PUR SIPs ...	184
Figure 7-17: Comparison between the experimental results and simulated results concluded from racking load test on fully-bonded 165 mm (6.5 in.) thick PUR SIPs ...	184
Figure 7-18: Comparison between the experimental results and simulated results concluded from racking load test on partially dis-bonded 114 mm (4.5 in.) thick PUR SIPs	185
Figure 7-19: Comparison between the experimental results and simulated results concluded from racking load test on partially dis-bonded 165 mm (6.5 in.) thick PUR SIPs	185

Figure 7-20: Mesh detail and deformation behaviour of modeled 165mm (6.5 in.) thick PUR SIPs exposed to racking load (M65R) (Red indicates zone of greatest deformation) 186

Figure 7-21: Mesh detail and deformation behaviour of modeled 165mm (6.5 in.) thick partially dis-bonded PUR SIPs exposed to racking load (MD65R) (Red indicates zone of greatest deformation) 186

Appendix B

Figure B - 1: Axial test set-up top plate details (Source: Dick, 2011)..... 216

Figure B - 2: Axial test set-up details showing lateral stability holders (Source: Dick, 2011) 217

Figure B - 3: Axial test frame basic framing details (Source: Dick, 2011) 218

Appendix C

Figure C - 1: Axial tests results of five tested panels comparing the performance of 165mm (6.5 in) thick PUR SIPs to conventional 140mm (2 by 6) stud wall panels 220

Figure C - 2: Transverse tests results of five tested panels comparing the performance of 165mm thick (6.5 in) PUR SIPs to three tested conventional 165mm (6.5 in) stud wall panels 221

Figure C - 3: Racking tests results of five tested panels comparing the performance of 165mm thick (6.5 in) PUR SIPs to conventional stud wall panels. Solid lines represent the maximum load vs. deflection in 165mm thick (6.5 in) SIPs..... 222

Appendix D

- Figure D - 1: Axial load resistance of 114mm (4.5 in.) thick dis-bonded PUR SIPs compared to fully bonded panels with the same thickness. This graph shows the overall shortening of the SIP under axial load (top linear potentiometer only)..... 224
- Figure D - 2: Axial load resistance of 165mm (6.5 in.) thick dis-bonded PUR SIPs compared to fully bonded panels with the same thickness. This graph shows the overall shortening of the SIP under axial load (top linear potentiometer only)..... 225
- Figure D - 3: Axial load resistance of 114mm (4.5 in.) thick dis-bonded PUR SIPs compared to fully bonded panels with the same thickness. This graph shows the overall shortening of the SIP under axial load (mid-left linear potentiometer only). The first few millimetres of negative deformation is due to slight rotation of the I beam (located at the 1/3 of the panel thickness) before it is fully stabilized on under applied load..... 226
- Figure D - 4: Axial load resistance of 114mm (4.5 in.) thick dis-bonded PUR SIPs compared to fully bonded panels with the same thickness. This graph shows the overall shortening of the SIP under axial load (mid-left linear potentiometer only). The first few millimetres of negative deformation is due to slight rotation of the I beam (located at the 1/3 of the panel thickness) before it is fully stabilized on under applied load..... 227
- Figure D - 5: Transverse load resistance of 114mm (4.5 in.) thick dis-bonded PUR SIPs compared to fully bonded panels with the same thickness. The vertical blue line indicates the serviceability deflection limit of L/180 (13 mm)..... 228

Figure D - 6: Transverse load resistance of 165mm (6.5 in.) thick dis-bonded PUR SIPs compared to fully bonded panels with the same thickness. The vertical blue line indicates the serviceability deflection limit of L/180 (13 mm)..... 229

Figure D - 7: Racking load resistance of 114mm (4.5 in.) thick dis-bonded PUR SIPs compared to fully bonded panels with the same thickness 230

Figure D - 8: Racking load resistance of 165mm (6.5 in.) thick dis-bonded PUR SIPs compared to fully bonded panels with the same thickness 231

Appendix E

Figure E - 1: All in one compressive tests conducted on 165mm (6.5 in.) and 114mm (4.5 in.) thick PUR SIP coupons with the area of 152 by 152 mm (6 x 6 in.) and 25mm (1 in.) deflection limit..... 235

Appendix F

Figure F - 1: Pull-off test results of the New Panel 1 – Samples 1 to 10 Side A of the panel..... 239

Figure F - 2: Pull-off test results of the New Panel 1 – Samples 1 to 10 Side B of the panel..... 239

Figure F - 3: Pull-off test results of the New Panel 2 – Samples 1 to 10 Side A of the panel..... 240

Figure F - 4: Pull-off test results of the New Panel 2 – Samples 1 to 10 Side B of the panel..... 240

Figure F - 5: Pull-off test results of the New Panel 3 – Samples 1 to 10 Side B of the panel.....	241
Figure F - 6: Pull-off test results of the New Panel 3 – Samples 1 to 10 Side A of the panel.....	241
Figure F - 7: Pull-off test results of the Weathered Panel 1 – Samples 1 to 10 Side A of the panel	242
Figure F - 8: Pull-off test results of the Weathered Panel 1 – Samples 1 to 10 Side B of the panel	242
Figure F - 9: Pull-off test results of the Weathered Panel 2 – Samples 1 to 10 Side A of the panel	243
Figure F - 10: Pull-off test results of the Weathered Panel 2 – Samples 1 to 10 Side B of the panel	243
Figure F - 11: Pull-off test results of the Weathered Panel 3 – Samples 1 to 10 Side A of the panel	244
Figure F - 12: Pull-off test results of the Weathered Panel 3 – Samples 1 to 10 Side B of the panel	244

Appendix G

Figure G - 1: Load vs. deflection behaviour of the OSB face-sheet coupons under pure bending test.....	247
--	-----

Figure G - 2: Mesh detail of modeled 114mm (4.5 in.) thick fully-bonded PUR SIPs under eccentric axial load (M45A)	249
Figure G - 3: Deformation behaviour of modeled 114mm (4.5 in.) thick fully-bonded PUR SIPs under eccentric axial load (M45A) (Red indicates zone of greatest deformation).....	250
Figure G - 4: Mesh detail of modeled 114mm (4.5 in.) thick partially dis-bonded PUR SIPs under eccentric axial load (MD45A)	252
Figure G - 5: Deformation behaviour of modeled 114mm (4.5 in.) thick partially dis-bonded PUR SIPs under eccentric axial load (MD45A) (Red indicates zone of greatest deformation).....	253
Figure G - 6: Mesh detail of modeled 114mm (4.5 in.) thick fully-bonded PUR SIPs exposed to transverse load (M45T).....	255
Figure G - 7: Deflection behaviour of modeled 114mm (4.5 in.) thick fully-bonded PUR SIPs exposed to transverse load (M45T) (Red indicates zone of greatest deformation)	256
Figure G - 8: Mesh detail of modeled 114mm (4.5 in.) thick partially dis-bonded PUR SIPs exposed to transverse load (MD45T)	258
Figure G - 9: Deflection behaviour of modeled 114mm (4.5 in.) thick partially dis-bonded PUR SIPs exposed to transverse load (MD45T) (Red indicates zone of greatest deformation).....	259

Figure G - 10: Mesh detail of modeled 114mm (4.5 in.) thick fully-bonded PUR SIPs exposed to racking load (M45R)..... 261

Figure G - 11: Deformation behaviour of modeled 114mm (4.5 in.) thick-fully bonded PUR SIPs exposed to racking load (M45R) (Red indicates zone of greatest deformation) 262

Figure G - 12: Mesh detail of modeled 114mm (4.5 in.) thick partially dis-bonded PUR SIPs exposed to racking load (MD45R) 264

Figure G - 13: Deformation behaviour of modeled 114mm (4.5 in.) thick partially dis-bonded PUR SIPs exposed to racking load (MD45R) (Red indicates zone of greatest deformation)..... 265

List of Symbols

A	<i>Cross-sectional area</i>
A_v	<i>Shear area of the panel</i>
b	<i>Width of the face-sheet (in y direction)</i>
B	<i>Sandwich width</i>
c	<i>Core thickness</i>
C_a	<i>Shape factor</i>
C_b	<i>Basic roof snow load factor</i>
C_s	<i>Slope factor</i>
C_w	<i>Wind exposure factor</i>
d	<i>Total thickness of sandwich panel</i>
D	<i>Flexural rigidity of the SIP</i>
D_f	<i>Flexural stiffness of the beam/strut (face-sheet)</i>
d	<i>Sandwich thickness</i>
EA	<i>Axial Stiffness</i>

E_b	<i>SIP modulus of elasticity under transverse bending</i>
E_c	<i>Modulus of elasticity of the foam-core</i>
E_f	<i>Longitudinal modulus of elasticity of OSB face-sheets</i>
EI	<i>Bending Stiffness</i>
$FD_{Foam}(t)$	<i>Fractional deflection of foam-core material</i>
$FD_{OSB}(t)$	<i>Fractional deflection of OSB face material</i>
$FD_P(t)$	<i>Predicted fractional deflection</i>
F_s	<i>Core shear stress</i>
G	<i>Core shear modulus</i>
I	<i>Moment of inertia of facing sheet about the centroid of the panel</i>
I_s	<i>Importance factor for snow load</i>
K	<i>Constant to calibrate the long-term effects of dead load and live load</i>
K_B	<i>Bending behaviour of the face-sheet</i>
K_S	<i>The spring constant for the shear behaviour of the core</i>
l	<i>length of the de-bonded area</i>
L	<i>Beam or test span, panel length</i>
M_r	<i>Bending moment resistance</i>
P	<i>Applied at the third of the beam's span</i>

P	<i>Global buckling load of concentric loading sandwich panel</i>
P	<i>Axial load in the face-sheet due to eccentric loading</i>
P_E	<i>Critical buckling load</i>
P_r	<i>Axial Compressive Resistance</i>
Q	<i>Shear force</i>
S_r	<i>1-in-50 associated rain load</i>
S_s	<i>1-in-50 year ground snow load</i>
T	<i>Nominal facing thickness</i>
T_r	<i>Axial Tensile Resistance</i>
V_r	<i>Shear through thickness resistance</i>
V_{rb}	<i>Planar shear resistance due to bending</i>
w	<i>Displacement of the de-bonded part (in z-direction)</i>
w_2	<i>Deflection at x</i>
w_m	<i>the maximum displacement of the de-bonded part of the face-sheet</i>
$\Delta_{Short\ term}$	<i>Deflections under short term portions of design load</i>
Δ_B	<i>Predicted deflection due to bending</i>
$\Delta_{Long-term}$	<i>Immediate deflection under dead load + long-term portion of live load</i>
Δ_S	<i>Predicted deflection due to shear</i>

$\Delta_T(t)$	<i>Time dependent total deflection</i>
$\Delta_T(t)$	<i>Time dependent total deflection</i>
Π	<i>Mathematical constant (Pi)</i>
σ_z	<i>Tensile stress in face-sheet/core interface/bond</i>
ν_c	<i>Poisson's ratio of the foam core</i>
ν_{xy}	<i>Poisson's ratio of face-sheet in the xy-plane</i>

Chapter 1

Introduction

Structural Insulated Panels (SIPs) are an alternative wall system to conventional stud wall, joist and rafter systems in commercial and residential construction. SIPs can be used for wall, roof, floor, and foundation assemblies. SIPs are a composite material typically made of two Oriented Strand Boards (OSBs), metal, cement or plywood as facings and a foam-core. The foam-core acts as both an insulation material and provides rigidity to the system while the facings provide durability and strength (Butt, 2008). The foam-core is usually made of expanded polystyrene (EPS), extruded polystyrene (XPS) or polyurethane (PUR or PE). Some new alternative materials, such as compressed rice, wheat straws and bamboo particulate (Cortez-Barbosa et al., 2015) waste, are also being used to build SIPs.

SIPs are made in variety of sizes, but commonly, panel dimensions are 1220 by 2440 mm (4 x 8 ft.) up to 2743 by 8534 mm (9 by 28 ft.) with the thickness varying from 114 to 318 mm (4.5 to 12.5 inches). Construction with SIP is faster (one to four weeks faster than conventional stick frame technique). The finished walls are also straighter than conventional stud wall and their insulation properties better. Further, the SIP walls are stronger than the stick-frame construction (Morley, 2000).

The information related to the short-term mechanical behaviour, the effects of thermal and moisture conditions on serviceability, and the load duration on SIPs can provide a general objective on the matter. Although SIPs have been used in the construction industry since the 1950's, they didn't fully attract the construction industry's attention until the

1980s. The questions which this thesis investigates are the two major concerns about SIPs: their long-term durability, and the effect of de-bonding on their load-response.

1.1 Thesis Structure

This has been authored in a style where the manuscript is a collection of articles that together, contribute toward the overall theme of the thesis. Although each chapter includes its own conclusion, effort has been made to create a flow between the chapters and help draw an overall conclusion related to the original goal of the thesis. This thesis consists of a total of 8 chapters as follows:

1. Introduction
2. Literature Review
3. Experimental Measurement of the Structural Capacity of PUR SIPs - Baseline Tests
4. Experimental Measurement of the Structural Capacity of Dis-bonded PUR SIPs
5. Experimental Measurement of the Flexural Creep Behaviour of PUR SIPs
6. Bond Strength as a Measure of Serviceability and Quality of Polyurethane Foam Structural Insulated Panels (Pull-off Tests)
7. FEM Modelling of OSB- PUR SIPs
8. Summary and Conclusions

Chapter 1 introduces SIPs in general and explains the significance of the proposed research. This chapter also explains the research objectives and the overall deliverables of the programme. Chapter 2 presents a review of other research and examines the available literature on SIPs and SIP components including the history of SIPs, SIP types and their applications, and, creep in sandwich panels. Chapter 3 contains an evaluation of the structural capacity of conventional stud-wall and PUR SIPs in order to establish a baseline for comparison purposes. This comparison presents the results of the load response of PUR SIPs and conventional stud-wall panels in three different loading configurations: axial, transverse, and, racking. The findings of this chapter provide comparison baselines for the tests conducted in Chapter 4. Chapter 4 presents results of the load response of the purposely dis-bonded PUR SIPs and compares them to the baseline findings in Chapter 3 in order to find the relationship between dis-bond ratio and its effect on overall load carrying capacity of SIPs.

The creep behaviour of PUR SIPs is not well documented. The results of testing the behaviour of such panels exposed to creep loads for a period of eight weeks is discussed in Chapter 5. Chapter 6 presents the results of research focused on the evaluation of the bond strength between the OSB skins and the PUR foam core as one measure of service life and fabrication quality. Chapter 7 discusses the use of a commercially available FEM software program to model the load-response behaviour of the panels. Lastly, Chapter 8 summarizes the findings of this research program and provides recommendations for future work on PUR SIPs.

1.2 Programme

Industry and code officials in Canada are reluctant to certify SIPs due to a lack of information on long-term durability. Such resistance is understandable and so must be addressed. Where the Canadian Construction Materials Centre (CCMC) believes most assessments done on SIPs are circumstantial or subjective, rather than being scientific and standardized, it also suggests a need for universal evaluations to assess both existing and new assemblies. While there are scattered studies on Canadian polyurethane SIP products conducted by individual manufacturers, the absence of a regulatory organization in the Canadian SIP industry means that such information remains private, rarely getting shared. The research presented in this thesis was made possible with financial support from Emercor Ltd., an Alberta based polyurethane SIP manufacturer, and in consultation with CCMC. It aims to inform the “long-term durability of SIPs question”.

1.3 What is a SIP?

A SIP is an engineered composite construction material made of two layers of rigid facing and a rigid foam-core that performs as an insulating material (Figure 1-1). The core material sandwiched between two panels is foam made of expanded polystyrene (EPS), extruded polystyrene (XPS), isocyanurate, polyurethane or, compressed, insulating straw. Some manufacturers are investigating ways of using cementitious and rigid fibrous insulating materials as well (U.S. Department of Energy, 2011).

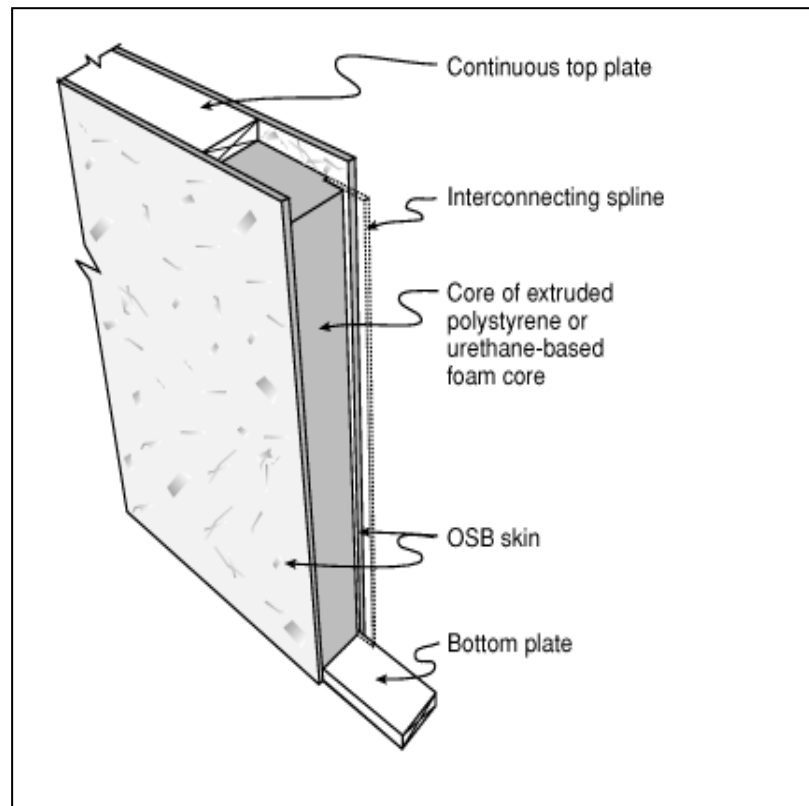


Figure 1-1: Schematic details of an ordinary Structural Insulated Panel (CCMC, 1996)

The facing sheets or boards can be sheet metal or aluminium, plywood, cement, or oriented strand board (OSB). Other materials, used as necessary, include pressure treated plywood, drywall, fiber reinforced plastic (FRP), and finish lumber can be used as necessary (Morley, 2000) (Figure 1-2). Individually, SIP components are not made of significant load bearing structural material. When joined together, however, they create a strong composite material which is much stronger than the individual components (Morley, 2000). To make a SIP panel with EPS foam, a block of foam is cut to size and then laminated or glued to the facing sheets using hydraulic press machines and liquid urethane moisture-cure adhesive. The bonding agent is a fast curing adhesive. Each panel needs only a few minutes in a press machine in order to set (Figure 1-3). In the case of isocya-

nates or polyurethane foam-cores, the facing sheets are kept apart from each other and then the liquid foam is injected between the boards to expand and cure. This is done in a horizontal orientation. The expanded foam fills the cavities and properly bonds with the top and bottom facing sheets when it is set. Structurally, when loaded perpendicular to facesheets, SIPs behave as 'I-beams'. Rigid foam-core acts as the web and the facings work as the flange of an 'I-beam' (Figure 1-4). When subjected to force, facing skins undergo tension or compression, while the core resists against shear and buckling (Mousa & Uddin, 2010). By keeping the face-sheets apart, the foam-core increases the stiffness of the panel (Mousa & Uddin, 2012). Thickening the foam-core adds to the moment of inertia while only slightly increasing the weight of the overall panel (Huang & Gibson, 1990). In a wall assembly, the OSB facings work as two slender columns, laterally and continuously supported by the foam-core. This helps the facings withstand compression force and avoid buckling (Morley, 2000) (Forest Products Laboratory, 2012).



Figure 1-2: Different facing materials used in SIPs manufacturing (Photo courtesy of Van-tem Panels formerly Winter Panel, United States, 2012)



Figure 1-3: Assembly line of EPS core SIPs (Photo courtesy of Premier SIPs by Insulfoam, United States, 2012)

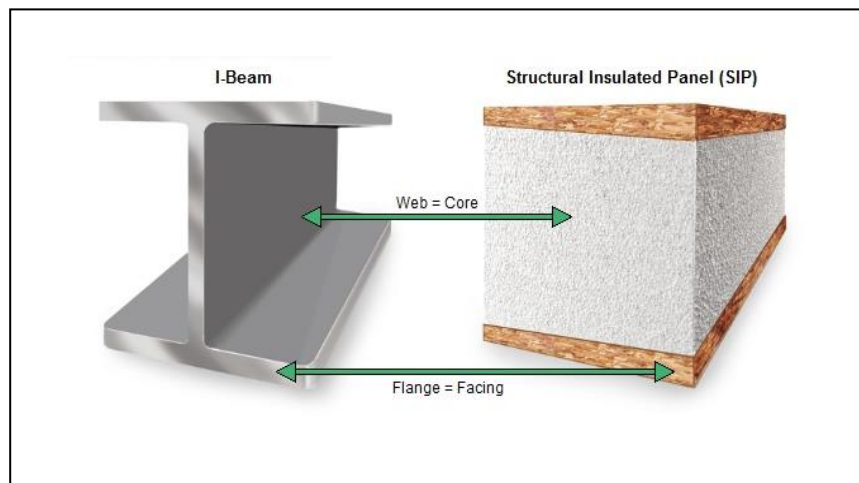


Figure 1-4: SIP compared to an 'I-beam' (Foamlaminates, 2008)

Some SIP producers claim that construction with SIP can reduce the time of construction by more than fifty percent and improve the energy efficiency of the building by up to fifty percent (PorterSIPS, 2012). Research conducted at the University of Oregon has shown that a house made with SIPs needed 161 fewer hours to complete compared with the control industry standard stick-framed house. Further, the SIP house required 34% less on-site construction time (Morley, 2000). The overall cost of construction with SIP is about one US dollar more per square foot in comparison with conventional construction methods (Mc Leister, 1998). SIPs resist wind and lateral loads and can be designed to withstand large seismic loads. Morley (2000) reports a SIP house withstood a tornado in Clement, Georgia, USA, in March 1998, with no structural damage, while 7 houses and 25 mature trees nearby the house were completely destroyed. Although authorities have reviewed several evaluation reports, SIPs have not been yet recognized by Canadian or American building codes (PATH, 2001) and no universal standards or codes of practice

are available for design and installation of SIPs (Rungthonkit & Yang, 2009). While the construction industry generally shows resistance to new products, the lack of acceptance in building codes has further slowed SIPs from entering the Canadian construction market.

1.3.1 Thermal Resistance, Temperature and Moisture

SIPs provide relatively uniform insulation compared to traditional construction methods like stud or stick frame, and also, if properly installed, a more airtight construction (Morley, 2000). In a specific research study (Shaw Environmental System Analysis Inc, 2009), a one-year monitoring of moisture and temperature showed no evidence of condensation or excessive moisture buildup during the cooling or heating season in a regular SIP assembly. Examination of the moisture content of the SIP members also showed constant values below 10 percent. Based on research conducted at the Oak Ridge National Laboratory in the United States (Kosny et al., 1999), a SIP wall with 89 mm (3.5 inch) thickness had an thermal resistance of $2.47\text{m}^2\text{K/W}$ ($14\text{ h ft}^2\text{°F/Btu}$) compared to a 38x89 mm (2x4 inch) stick-framed wall with regular fiberglass batt insulation, with an expected thermal resistance of $1.73\text{m}^2\text{K/W}$ ($9.8\text{ hft}^2\text{°F/Btu}$) (Figure 1-5). This means that an 89 mm (3.5 inch) thick SIP wall with EPS core has about 30% higher thermal resistance compared with a 38x89 mm (2x4 at 16 inch spacing) and 610 mm (24 in.) stick frame wall insulated with fiberglass batt.

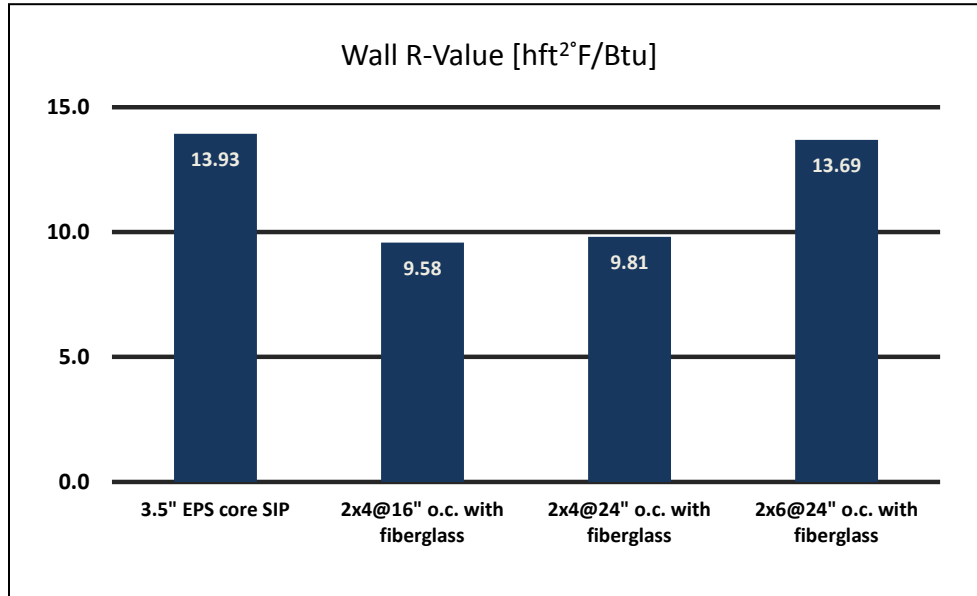


Figure 1-5: Whole wall R-value comparisons between 3.5 in. core SIP wall and conventional 2x4 and 2x6 wood frame walls (Kosny, Desjarlais, & Christian, 1999).

Some manufacturers publish their expected thermal resistance values for their products. This might be backed up by approved third party testing or just based on their private independent test results. Table 1-1 is an example of expected RSI and R-values published by a SIP manufacturer in the United States.

Table 1-1: RSI and R-values of EPS core SIPs at different temperatures (Premiersips, 2011)

Core Thickness	RSI [R-Value] @ 24° C [75° F]	RSI [R-Value] @ 4.4° C [40° F]	RSI [R-Value] @ 4° C [25° F]
89 mm (3.5 in.)	2.64 [15]	2.82 [16]	3.00 [17]
140 mm (5.5 in.)	4.05 [23]	4.40 [25]	4.58 [26]
191 mm (7 ¼ in.)	5.28 [30]	5.64 [32]	5.81 [33]
235 mm (9 ¼ in.)	6.52 [37]	7.04 [40]	7.40 [42]
286 mm (11 ¼ in.)	7.92 [45]	8.63 [49]	8.98 [51]

As seen in Table 1-1, as the temperature of the closed cell foams such as EPS decreases, the insulation value of the foam linearly increases. This is caused by the change in blowing agent's (Fluorocarbons gas such as CFC-11 or HCFC-141B etc.) characteristics due to temperature variation (DuPont, 2011).

There are also claims that a SIP wall assembly in a house can reduce the energy consumption by 60 to 70 percent (Butt, 2008). Tests have revealed that SIP construction may allow around 20% less air infiltration than wood stick framed construction method. This, in turn, will give occupants more control over their indoor environment (Medina et al., 2008). In the meantime, a well-designed, installed, and correctly operated mechanical ventilation system is needed to help prevent indoor moisture issues, which is important for achieving the energy-saving benefits of an SIP structure (U.S. Department of Energy, 2011).

The lack of proper mechanical ventilation system in an airtight building might cause mold issues and affect the indoor air quality of the inhabitant. Besides the effects on energy savings, the other advantage of the air-tightness can be better resistance against fire. Lack of oxygen within the wall system can cause fire to extinguish itself (U.S. Department of Energy, 2011).

1.3.2 SIPs Installation

Construction companies base their SIP orders on building plans. SIP manufacturers then pre-fabricate SIPs in a plant and ship them to the job site. The builder assembles the wall panels, following the instructions provided by the SIP manufacturer. SIP producers then assist in custom-making panels for specific jobs. They number the panels in sequence and, further, guide the builders in the installation of each panel. Additional modifications such as ducts and openings can be applied at the job site. This custom-made/pre-fabrication method, in turn, decreases the construction duration and provides a better installation quality with the minimum material waste. There is a risk of creating a thermal bridge if the panels are not joined together properly. Also, a well-joined panel system will increase the overall integrity of the structure.

Depending on the core material and the thickness, different SIP manufactures offer different connection systems for corner and middle connections. Figure 1-6 depicts the wall-spline connections commonly used in construction with SIPs. Construction glue and special long self-tapping screws (Figure 1-7) fasten the connection pieces once in place.

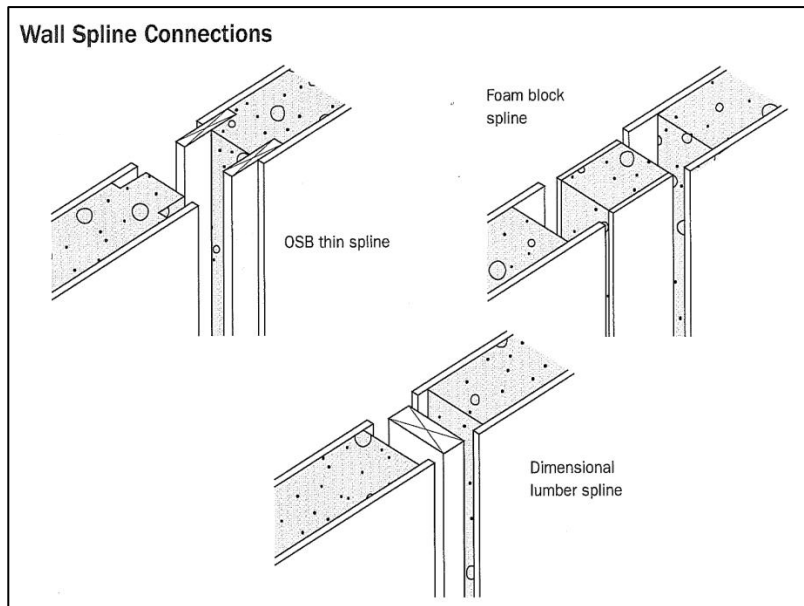


Figure 1-6: Most common panel to panel spline connection configuration for SIPs (Morley, 2000)



Figure 1-7: Special screws used in SIP connections and installations (Trufast, 2012)

1.3.3 Challenges with SIPs in the Marketplace

SIPs with wood-facing membranes need to be protected by fire retardant materials such as drywall (U.S. Department of Energy, 2011). This protects the foam and the OSB facing from fire for a length of time that may allow occupants to evacuate the house safely. Along with Blazeguard Fire-Rated sheathing, when applied by a licenced applicator, fire retardant paints are another option. Blazeguard panels have a layer of special cement called Pyrotite applied over an OSB substrate (International Barrier Technology, 2008). A good SIP installation provides improved air-tightness in a building. Also, some studies suggest that the level of toxicity of the burning material in SIPs is not worse than conventional building materials (Morley, 2000).

As with conventional construction methods, fire, poor resistance against wind borne debris, termite attack, insects, mold buildups, and rodents are areas of concern with SIPs (Mousa & Uddin, 2012). Foam insulation products can provide an ideal environment for insects and rodents to inhabit. Insects and rodents might tunnel throughout the SIPs and damage the integrity of the foam-core. Some producers suggest solutions of insecticides or boric acid, applied to the panels, locating yard vegetation 60 cm (2 feet) away from the building walls, and also keeping the indoor humidity below 50% percent, may help prevent these problems (U.S. Department of Energy, 2011).

Another concern is the thermal resistance reduction of polyurethane foam by aging. According to Morley (2000), an “aged” sample of polyurethane foam has an RSI value of

1.04 per 25.4 mm thickness of the material (R 5.88 per inch thickness of the material) in comparison with a 'fresh' polyurethane foam sample with an RSI value of 1.06 to 1.23 (R-value of around 6 to 7). Although even with this reduction, the thermal resistance of this foam is almost 50% better than the EPS foam with the same thickness. From the homeowner's perspective, chemicals in SIP components may introduce pollutants into the home. Small amount of chemicals in foam insulation, as well as formaldehyde in the OSB, might be released from SIPs and cause health problems. Although, the latter will not be an issue if the OSB used is formaldehyde-free.

Another possible issue with polyurethane SIPs is the foam density. It will be inconsistent throughout the panel if the foam components are not been mixed properly with the correct ratios. This inconsistency in foam density might cause local shrinkage, settlement, or even buckling of the panels in-service condition. This, in turn, might require expensive, time-consuming repairs. Susceptibility of the foam-core to temperature shocks may slightly alter the panel dimensions. When a SIP building is exposed to extreme temperature shocks, change in panels dimension might cause breakage in poor connection points within the wall, roof or floor assembly. This can cause air leakage from the building.

The long-term durability and longevity of panels are the major concerns of the industry and consumers. Although SIPs have been produced and used in the housing industry for more than 60 years, research and material testing on the long-term performance of the panels remain relatively limited. More scientific investigation is needed to understand the effects of de-bonding and delamination between the foam and the sheet facings.

1.4 Research Objectives

This research focused on two structural performance aspects of Emercor SIPs:

1. The effect of long-term bond degradation at the interface between the oriented strand board (OSB) skin and the polyurethane foam-core and its impact on structural performance corresponding to the degree and location of de-bonding was studied in this research.
2. As a function of the environment in which they are used, wood-based structural components are subject to creep effects. Moisture, temperature and magnitude of load all play a role in long-term creep behaviour. This research component evaluated the creep behaviour of panel specimens in different thicknesses.

1.5 Research Approach

The research approach used to investigate the two principal objectives is summarized below:

1.5.1 Structural Capacity Evaluation Baseline

Panels were tested to establish baseline values. These tests were conducted in accordance with ASTM E72 and E1803 standards. Table 1-2 outlines the tests and number of specimens for the baseline study.

1.5.2 Dis-bonded Panels

Axial compression, transverse, and racking tests will be conducted to investigate the impact of lack of zonal bonding on panel performance. The testing protocol is contained in Table 1-2.

1.5.3 Bond Integrity Evaluation

This component of the research evaluated the effect of bond strength between the OSB and the polyurethane foam on panel structural capacity. The intent behind this phase of the research was to investigate the load-deformation behaviour of panels with reduced bond. The following approach was used. Pull-off tests were conducted on a panel to evaluate the bond between the face-sheets and the PUR foam-core. Pull-off test locations were randomly selected (Figure 1-8).

Table 1-2: Specimen quantity for PUR SIP baseline tests in accordance with ASTM E1803 (ASTM, 2006), ASTM E72 (ASTM, 2015) and APA (APA, 2013)

Test Type	No. of Specimens ^{1,2}	Size mm [ft.]	Comments
Axial	5	1220x2440 [4x8]	Vertical axial load vs. lateral deflection at mid-height of panel
Transverse	5	1220x2440 [4x8]	Load applied at right angle to panel height to simulate wind loading
Racking	5 pairs	1220x2440 [4x8] x2	In-plane racking load applied to evaluate the lateral force resisting capacity of the panel, shear.

Note: 1. The number of specimens may be increased if an appropriate coefficient of variation (COV) is not met.
2. The number of specimens is indicated for each of 114mm (4.5 in.) and 165 mm (6.5 in) thick panels.

The research objective here is to investigate the relationship between percentage and location of facing de-lamination on overall structural performance. The data collected from this testing shall be compared with the fully-bonded panels or baseline values to develop a computer model to characterize this behaviour. This model could be used in further research and development to predict panel behaviour.

1.5.4 Durability and Long-term Creep Study

Facial and core material of the SIPs can undergo high creep behaviour. The main cause of creep in SIP is the foam material (Rungthonkit & Yang, 2009). The focus of this portion of the research was to investigate the effect of long-term loads and measure the mid-span creep deflections of SIPs. Based on ASTM E1803-06 Section 11, a minimum of three panels were tested. While the standard indicated a total test time of 30 days, these tests were conducted for a minimum of 8 weeks (56 days) to develop a more complete creep curve. Laufenberg et al. (1999) suggest such duration in order to simulate a typical snow load in service. Expected mode of failure in this test series was shear in core (foam), crushing, and de-bonding of the facial OSB. Further, it is proposed to use ASTM C393-06 to determine the core shear properties of the panel assembly. A total of 5 specimens were evaluated. The polyurethane SIPS in this research were fabricated horizontally. When injected inside the mould, polyurethane foam rises from the bottom OSB and

reaches the top OSB sheet. Hypothetically, the texture of the foam can be slightly different in top portion. There was an expectation the foam at the top area may have slightly lower density. Furthermore, pull-off tests (Chapter 6) were conducted on different sides of weathered and brand new panels to test the validity of this hypothesis.

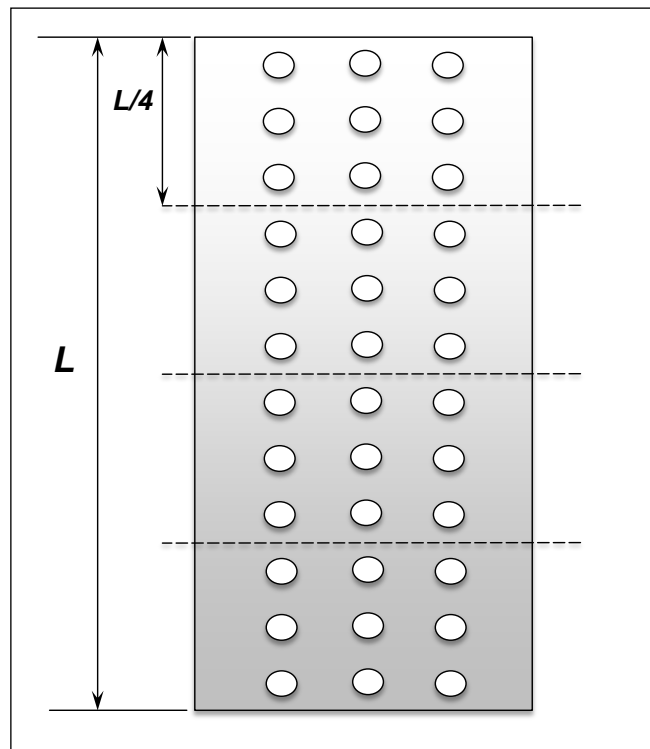


Figure 1-8: De-bonding test sampling scheme (Source: Dick, 2011)

1.6 Deliverables

The following are the principal outcomes of this research program:

1. A review of the literature written on previous research work
2. Re-establishing the baseline load values for Emercor polyurethane SIPS

3. Developing a relationship between percentage of de-bonding and change in structural capacity of the polyurethane SIPs
4. Characterizing the creep behaviour of PUR SIPs with two different thicknesses
5. Employing a computer model to characterize panel behaviour related to reduced bond strength. When used in conjunction with experimental data, this model could be used to predict aspects of load-response behaviour

1.7 Implications of the Research for the Construction

Industry

SIPs have been present in the construction for decades. The SIP industry holds a small share of wood products and building material industry. Due to advantages of SIP, there is potential for growth and a bigger market share (Gagnon & Adams, 1999). Although demand for SIPs has relatively increased in recent years (Mullens & Arif, 2006), their acceptance by building code officials, building authorities, builders, and general public is still overshadowed by uncertainty and doubt. Some of this doubt is based on lack of confidence in long-term durability.

This research aims to address some aspects of the above-mentioned issues which will assist the public to better understand SIPs and use them with much more confidence. SIPs reduce the overall energy consumption of a household. Therefore, their application will impact the overall national energy consumption.

Recently some of the local building code and city officials have demanded producers present their CCMC (The Canadian Construction Materials Centre) (CCMC, National Research Council Canada, 2013) licencing number in order to have their products used on construction sites within major cities. By conducting this research, the founder of the project will receive dependable research data that can be presented to CCMC to apply for a licence number and obtain a product stamp. This, in turn, enables the consumer to obtain the product from the local building material suppliers and use it for residential and possibly commercial building applications confidently.

There is a considerable body of knowledge generated by the individual manufacturer, both in the United States and in Canada. Most of the data has been generated and, therefore, owned by individual SIP manufacturers. Due to the proprietary nature of this data, the information remains scattered and unshared with other manufacturers and the public. Consequently, published experimental research data on SIPs is rare and very infrequently compared to the other residential and commercial construction wall, floor, and roof systems (Mullens & Arif, 2006).

Usually, every industry shows resistance to new products. Lack of information is the major reason for this reluctance by code officials, contractors, engineers, building material suppliers, and homeowners. Mullens and Arif (2006), in a case study, investigated the effect of SIP on the residential construction process. They observed the construction process of two Habitat for Humanity homes. One house was built using SIPs and the other

one was constructed with conventional stick-frame walls. The speed of construction, the amount of waste material, necessary skill levels, and equipment requirements were compared between the two buildings. Mullens and Arif (2006) found that using SIPs reduced the necessary effort-level of volunteer workers by 50% in comparison to using conventional wood-frame walls. They also found that using SIPs saved more than 60% of the needed site framing labor for the walls and roof systems.

Manufacturers' variable methods for framing, spline and connection design, fastener type, and spacing issues causes design differences which directly affect the wall panel assembly's strength. A unity among the SIP manufacturers is needed to harmonize the design values and installation guidelines in order to eventually promote the entrance of SIPs guidelines into the national building codes.

Connecting these scattered techniques and database of knowledge as well as the formation of Structural Insulated Panels Association of Canada (SIPA Canada) will hopefully unify the industry with building and code officials. Future co-operation and the creation of a common language for building code officials and manufacturers can cause the establishment of a Canadian SIP association similar to Structural Insulated Panel Association in the United States (SIPA). The mission of SIPA Canada subsequently similar to the goals set by SIPA in the United States (SIPA, About SIPA, 2011): *"To increase the use and acceptance of SIPs in green, high performance building by providing an industry*

forum for promotion, communication, education, quality assurance, and technical and marketing research”.

Chapter 2

Literature Review

2.1 Introduction

The term ‘building panels’ in construction industry, refers to modular construction methods. These methods can include the fabrication of stud walls or any composite pre-fabricated sandwich panel. The core of sandwich panels may contain insulation material or not. They may also work as load-bearing members or be used as cladding or partition walls only (Butt, 2008). There are research studies on the performance of the sandwich panels in general, but not many research studies on the long-term structural behaviour of SIPs.

The following matters will be reviewed in this chapter to better understand sandwich panels and their overall behaviour:

1. History of SIPs
2. Different types of insulated sandwich panels
3. Former studies on long-term creep in insulated sandwich panels
4. Previous studies on foam and de-bonding issues in insulated sandwich panels

2.2 History of SIPs

Although SIPs have been around since 1950s, they gained attention in the 1970s and 1980s. The first attempts of construction with SIPs started in 1930’s when Frank Lloyd Wright merged beauty with applicability in a low-cost housing project in Usonian in the

United States. His panels consisted of three layers of plywood and two layers of tar paper. These panels however were not commercially successful due to a lack of insulation (Morley, 2000). Around the same time, engineers at the Forest Production Laboratory (FLP), located in Madison, Wisconsin, produced panels consisting of insulation sandwiched between two skins with added framing members placed inside the panel for additional support. Panels were used to build test homes which went under continuous monitoring for about thirty years. Over time, they experimented with new methods and material as well. Used panels were eventually dismantled and re-examined by FLP for further studies (Butt, 2008). They sold those products for the next thirty years (Foamlaminates, 2008).

Lack of suitable insulation and concerns about energy efficiency encouraged Alden B. Dow, Frank Lloyd Wright's student, to continue experimenting with the SIP concept. In 1950, he created the first SIP with an insulation core. He has, therefore, been credited as the creator of the first SIPs. Dow's early SIPs were made of 41 mm (1 $\frac{5}{8}$ in) Styrofoam sandwiched in between two 8 mm (5/16 in) thick plywood facings. Those panels were used in homes located in Midland Michigan and can still be found in those homes today (Morley, 2000).

Dow's early success sparked the first major manufacturing of SIPs by Koppers Company who built the first automatic production plant in 1959 in Detroit. Koppers SIPs were

composed of blown pre-expanded Styrofoam beads between two sheets of plywood and glued together using steam and glue to create a rigid framework. Eventually, price, slow speed of production, and the resistance to their use by the carpenters' union, made Koppers SIPs not commercially successful (Foamlaminates, 2008).

Later in 1960s, Alside Hope Program started a new line of SIP production. But after making less than 100 SIP houses, lack of demand forced this company out of business too (Morley, 2000). There are also records that Woods Constructors of Santa Paula, California used SIP panel systems in their apartments and homes from 1965 to 1984 (All Canadian Construction, 2011).

In 1990, U.S. SIP manufacturers established SIPA in order to promote and introduce SIP to the construction industry. As of 2000, there are more than 100 SIP manufacturers in the United States. SIPA has reported 24% yearly growth rate in SIP industry from 1991 to 1994. Since then, the growth rate increased to more than 35% annually. In 2000, one hundred SIP manufacturers produced SIPs for 5% of the buildings built in the United States annually (Morley, 2000). Recently, the construction industry has been paying more attention to the SIP technology. This in turn, can encourage builders to use more environmentally friendly materials such as SIPs.

2.3 Different Types of Sandwich Panels

Foam-cores can be cast in or laminated with different types of facing materials, such as various cement boards, aluminum and steel sheet metal, fibre-reinforced polymers (plastics), plywood, and finish cladding products (Morley, 2000; Butt 2008). Table 2-1 provides some of the advantages and disadvantages of some facing materials that are being used by the SIP industry.

Table 2-1: Advantages and disadvantages of commonly used facing sheet materials for manufacturing SIPs (Panjehpour et al., 2013)

Type of skin	Advantages	Drawbacks
Oriented Strand Board (OSB)	Cost-effective	Flammable, Pervious to insects Vulnerable to moisture, Requirement of sheetrock to comply with fire codes
Aluminium and Steel	Non-flammable, Lightweight	Unable to insulate the core from heat, Requirement of sheetrock to comply with fire codes, Requirement of cosmetic finishes
Cement and Calcium silicate board	Fire resistant, Able to insulate the core from heat, Providing good axial compressive strength	Having brittle failure under compressive load, Unavailability with large size panels
Fibre Reinforced Polymer (FRP)	Lightweight, Impervious to insect, Waterproof	Potential flammability, Low compressive strength, Unable to insulate the core from heat, Requirement of sheetrock to comply with fire codes, Lacking of acoustic resistance

2.4 Previous Studies on Creep Behaviour in Insulated Sandwich Panels

There is limited literature on the structural performance of SIPs under long-term loads. A few studies have been conducted on SIPs with polystyrene foam but there is no study testing OSB-faced polyurethane foam-core full-sized SIPs. Although this research aims to study the polyurethane foam-core SIPs, studying the creep behaviour of general wood products and foam as a separate material core panels can be beneficial. Also, reviewing the existing reported work on EPS foam-core SIPs will help better understand and predict the behaviour of polyurethane SIPs.

2.4.1 Creep in Material

Creep, as an inelastic action (Pollack, 1988), is the tendency of solid materials to deform slightly or permanently due to the applied load or sustained mechanical stress over a time period. There is a direct relationship between creep, stress level, and the temperature which the solid material is subjected to. The higher the stress level and the temperature, the more the creep deflection will be. Creep happens when the strain continues to increase even though the stress level is constant. In this case, removing the stress will result in strain decrease (Pollack, 1988). Creep-rupture can also be defined as the ultimate failure due to loss of strength and increased deformation under a long-term load (Laufenberg et al., 1999).

Figure 2-1 depicts the typical creep behaviour of a viscoelastic material. The instantaneous region shows where the material reaches its immediate deflection. In the primary creep region, deflection increases at a decreasing rate. The secondary creep region depicts the region in which the deflection has a near-constant rate and in the tertiary region, the material ends in rupture. Deflection immediately decreases if the material or the structure is unloaded before the start of the tertiary stage (Taylor, 1996).

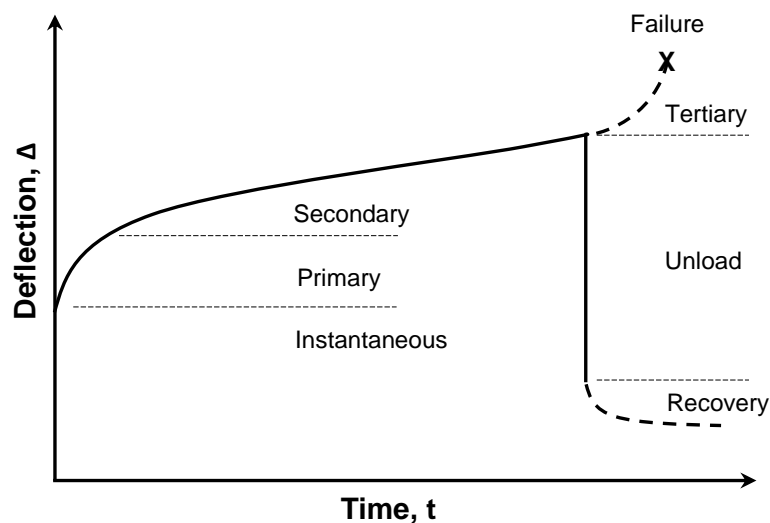


Figure 2-1: Typical material creep behaviour (Taylor, 1996)

2.4.2 Creep in Insulated Sandwich Panels

Time-dependent creep deformation in sandwich panels is related to load duration. Strength of wood based products has been known to be dependent of time under stress or duration of load (Laufenberg et al., 1999). Creep due to long-term loads has no influence

on SIPs when used in a wall assembly (Davies, 1987). The effect of creep on SIPs must be considered when the panels are used as roof or floor panels. The National Design Specification for Wood products (NDS) in the United States provides a formula for calculating the total deflection (Δ_{Total}) of wood products exposed to long-term loading (NFPA, 1991):

$$\Delta_{Total} = K (\Delta_{Long\ term}) + \Delta_{Short\ term} \quad (\text{Eq. 2.1})$$

Where:

K = Constant to calibrate the long-term effects of dead load and live load

$\Delta_{Long-term}$ = Immediate deflection under dead load + long-term portion of live load

$\Delta_{Short-term}$ = Deflections under short term portions of design load

The “ K ” factor, or “the long-term deflection constant”, ranges between 1.5 for seasoned lumber and glulam timber products to 2.0 for green lumber. Since there was no such information for SIPs at the time, Taylor (1996) conducted series of tests on EPS and polyurethane core SIP and recommended “ K ” factor values of 1.53 for EPS core SIPs and 1.97 for polyurethane core SIPs.

Davies (1987) reported on research conducted by Just (1983) on a series of creep tests on sandwich beams with several different polyurethane foam-core and plain metal facings for ten years. Just (1983) found that the foam continued to creep even after 10 years. He also concluded that the creep function was nearly linear (on the double logarithmic scale) and the fact that 50% of the creep deflection is reversible but the recovery speed is slower than the initial creep deflection.

Wong et al. (1988) researched the creep behaviour of OSB, S-P-F lumber, and stressed skin panel (SSP) specimen for 90 days and concluded that the fluctuation in environmental conditions have a negative impact on creep behaviour of OSB and SSP. The effect of humidity on creep is greater than the effects of temperature in an indoor test environment. They also found that linear viscoelastic theories (under low stress levels and controlled environment) can be used to characterize the time-dependent flexural behaviour of OSB and SSP.

Based on Haung and Gibson's (1990) simple model conjoined with Just's findings (1983), a 10-year creep behaviour in metal faced sandwich panels with any density foam-core under any design load is predictable only when the foam-core is a linear viscoelastic material such as urethane foam.

Taylor (1996) conducted a 90 day creep test on strips of EPS and polyurethane core OSB faced SIPs. Taylor considered a static four-point-loading scheme and measured the mid-span deflections. Based on his findings, the behaviour of EPS and urethane SIPs are linearly viscoelastic to the $2/3$ and $1/3$ of stress level respectively. A research program between the United States Department of Agriculture (USDA) Forest Service, Forest Products Laboratory (FPL), in Madison, Wisconsin, and Forintek Canada, Corporation in Vancouver, British Columbia, Canada conducted on creep and creep-rupture behaviour of wood-based structural panels (Laufenberg et al., 1999), showed that plywood, OSB, and waferboard (in that order) are more sensitive to environmental conditions than lumber. This six month period creep test was conducted on large specimens under three environmental conditions at two low constant-load levels. Laufenberg et al. (1999) suggest that Creep and creep-rupture for panel products are extremely sensitive to both constant or changing environmental conditions and constant-load levels. Butt (2008) conducted flexural and creep tests on 53 full-sized OSB faced SIPs with EPS cores. Based on his experimental findings, regardless of connection between panels, his entire specimen met the serviceability limit state design with a minimum safety factor of 3 or more. He also concluded that deflection and the load carrying capacity due to live load in panels with lumber-spline is less than deflection in panels with foam-spline connections.

2.5 Previous Studies on Foam and De-bonding Issues in Insulated Sandwich Panels

Since the main focus of this study is to evaluate the possible de-bonding characteristics of Polyurethane foam from the OSB skins, the de-bonding mode in sandwich panels with foam-cores needs to be investigated. First and foremost, the foam itself needs to be better understood. Three major types of foam are currently being used to make SIPs: XPS, EPS and polyurethane foam (PUR) which are individually discussed below.

2.5.1 EPS Foam

The BASF chemical company invented expandable polystyrene (EPS) in 1950 (BASF, 2007). Based on Morley's findings, as of 2000, 85% of SIPs manufactured in the United States uses EPS foam in their SIPs. EPS foam has a closed cell structure that makes it moisture resistant. High thermal resistance in EPS is due to air pockets within the foam's body. A 16.02 kg/m^3 (1.0 lb./ft^3) foam density provides an RSI value of 0.63 per inch thickness (R-value of 3.85 per 254 mm thickness) (Morley, 2000). EPS, which fungi and microorganisms do not attack and damage, is non-toxic. EPS starts deflecting at $80 \text{ }^\circ\text{C}$ (175°F) and its melting point is about $100 \text{ }^\circ\text{C}$ (212°F). EPS is a slow-burning material according to ASTM classification (Teach & Kiessling, 1960). Like other plastics, maximum stress capacity of EPS depends on the load duration. EPS cannot handle long-term tensile

stresses larger than 17 MPa (2500 psi). As seen in Figure 2-2, when loads are larger than 17.8 MPa (2580 psi) fracture occurs in less than 1000 hours.

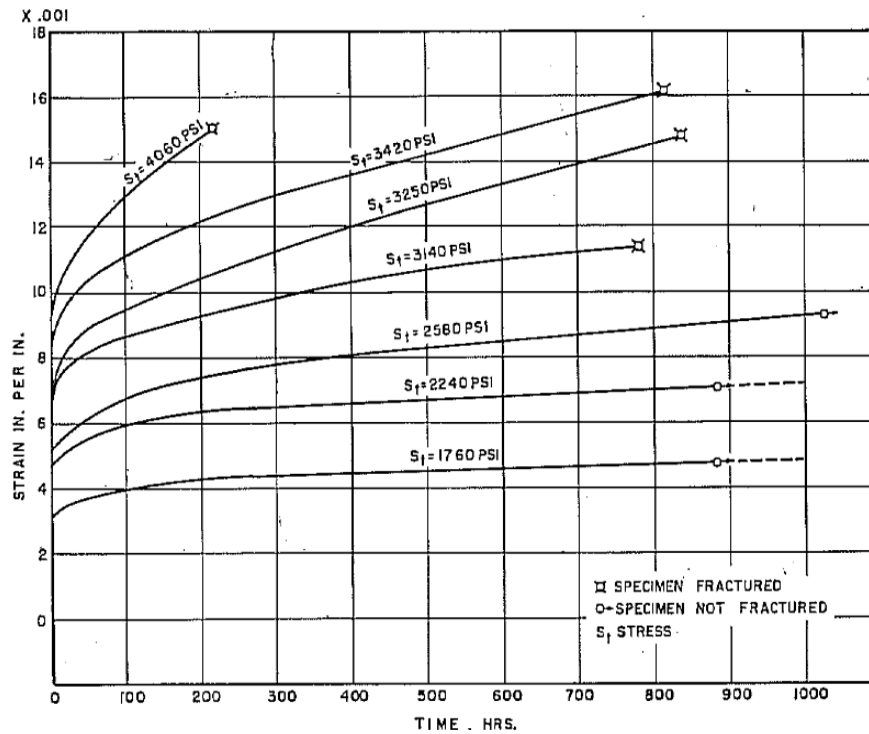


Figure 2-2: Creep behaviour of regular polystyrene at various stresses
 [Source: Sauer et al., J. Appl. Phys., 20, 510- 1949] (Teach & Kiessling, 1960)

2.5.2 XPS Foam

Although extruded polystyrene, or XPS, has better compressive and flexural strength, better shear resistance and thermal resistance for unit of thickness, it is not used by the major SIP manufacturers. Higher price, foam slab thickness limitations (up to maximum 4" or 100mm), and dimension instability are the major reasons for the lack of acceptance by the SIP industry (Morley, 2000).

2.5.3 Polyurethane (Urethane or PUR) and Polyisocyanurate (PIR, poly-iso, or ISO) Foams

Bayer developed polyurethane foams 1941 to 1945. In 1952, Hochtlen introduced the flexible format of the Polyurethane foams (Frisch & Saunders, 1973). Polyurethanes are formed by combining polyol with a diisocyanate (an isocyanate that has two isocyanate groups) or a polymeric isocyanate (American Chemistry Council, 2012). Although polyisocyanurate foam is chemically comparable to polyurethane foam, the production methods as well as the physical properties of the foams are different. Foams made of 100% isocyanate have better thermal resistance than polyurethane foams but they are expensive and break down over time. Urethanes or polyurethanes are made with equal parts of polyol and isocyanurate molecules (Morley, 2000). Table 2-2 provides RSI and R-values for three major foam types used in SIP industry. Polyisocyanurate foams tend to show better fire resistance properties in comparison with Polyurethane foam. In general, an increase in the isocyanate excess, expressed as the isocyanat index, will enhance the isocyanate index, which in turn, will enhance the fire performance of the foam (Vairo et al., 2010).

Table 2-2: Comparison of R and RSI values for the cellular foam insulation materials (Morley, 2000)

Cellular Foam Insulation RSI [R-Values]				
Temperature		EPS	XPS	Urethane
75°F	24 °C	0.63 [3.57]	0.68 [3.85]	1.21 [6.88]
30°F	-1°C	0.68 [3.85]	0.73 [4.17]	1.21 [6.88]
0°F	-18°C	0.73 [4.17]	0.80 [4.55]	1.21 [6.88]

Service condition affects the dimensional stability and performance of the rigid Polyurethane foam. For example, low temperature in combination with low humidity may significantly affect foam integrity. Changes in Polyurethane foams, due to environmental effects, are grouped as reversible and irreversible changes. Thermal expansion and compressive strength are all categorized as reversible changes. Although the thermal expansion in rigid polyurethane foam is reversible, but since the facing material has a different expansion coefficient, there might be added stress produced in the structure causing breaks in joints and thermal bridge (Hilado, 1967). Briody et al. (2012) conducted creep compression tests over a variety of temperatures on viscoelastic polyurethane foam samples. Based on their findings, higher temperatures accelerate the creep deflection. As seen in Figure 2-3, compressive strength of rigid Polyurethane foam decreases remarkably with increasing temperature. Long exposure to high dry temperature above 150 °C (302 °F) results in permanent changes (Figure 2-4) (Hilado, 1967). Polyurethane foam (PUR, HFC-245fa) provides superb adhesion to the OSB skins and offers the best insulation protection for moisture transferring (Panjehpour, Abang Ali, & Voo, 2013).

2.5.4 Compressed Wheat or Rice Straw Core

Compressed wheat or rice straw is a new kind of core material (Figure 2-5). In 1935 in Sweden Theodor Dieden, successfully compressed straw and used it as construction material. Stramit was the commercial brand for the developed and patented version of the product made in in England in the late 1940s (Morley, 2000).

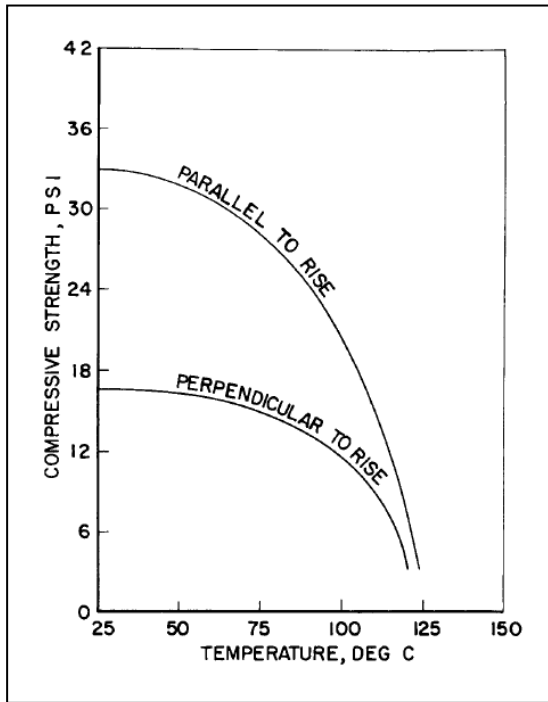


Figure 2-4: Typical curve of compressive strength versus temperature in rigid Polyurethane foam (Hilado, 1967)

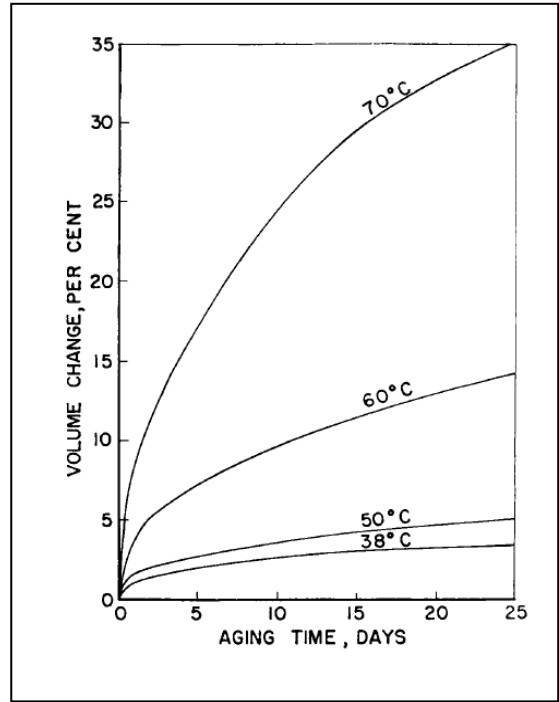


Figure 2-4: Effects of 100% humidity and temperature on dimensional stability of typical rigid Polyurethane foam (Hilado, 1967)



Figure 2-5: SIPs made of compressed wheat straw, Timber Strand sub-frame, Exposure 1 OSB, (7/16 in. - no urea formaldehyde added) and, non-toxic adhesives (Agriboard Industries , 2010)

Rectangular 1000 lb. wheat or rice straw bales are brought to mill then prepared and groomed. The material is then pressed together using a 15000 lb. ram while the natural binder inside the material is activated due to added heat (around 400°F/200°C). The final product is a slab of compressed straw which is 1220 mm (4 ft.) wide and 89 mm (3.5 in.) thick. The slab is then heated again and cut to size. Compressed board is then glued and molded into panels consisting of OSB facings and engineered lumber frame. Panels are made up to 7.3 m (24 ft.) long, 102 to 203 mm (4 to 8 in.) thick depending in the application. Compressed wheat-core SIPs are blast resistant, have up to 2.5 hour fire rating, insect and mold resistant, high and are believed to be 7 times more air-tight than conventional construction.

This environmentally friendly material has a negative carbon footprint because the farmers do not have to spend energy disposing their agricultural waste product and instead, can use their unwanted waste as income. The relative heft of panels (for the RSI and R-Value they offer) has delayed their acceptance (133kg/m³, 8.4 pcf, versus 16kg/m³, 1 pcf in the case of EPS foam-core SIPs) for the thermal resistance they offer. The thermal resistance, on the other hand, is not as good as has been claimed. The realistic value ranges from RSI 0.25 to 0.35 for 25.4 mm (R 1.4 to R 2.0 per inch) of compressed product, while the manufacturers claim twice those values (Morley, 2000).

2.5.5 Characteristics of OSB Facings

The Structural Board Association defines OSB as: “a structural panel suitable for a wide range of construction and industrial applications. It is a mat-formed panel made of strands sliced in the long direction from small diameter, fast growing round wood logs and bonded with an exterior type binder under heat and pressure” (SBA, 2004).

OSB has been used as the facing material for SIPs for two major reasons. First, it is an engineered wood material which can properly handle load and, second, it is available in the large sizes demanded by the SIP industry (Morley, 2000). OSB is widely available in most parts of North America and is inexpensive. OSB is available in common thicknesses of 8, 9.5, 11, 12.5, 15.5 and 18.5 mm ($\frac{5}{16}$, $\frac{3}{8}$, $\frac{7}{16}$, $\frac{1}{2}$, $\frac{5}{8}$ and, $\frac{3}{4}$ of an inch). OSB Panels are available in 1220 x 2440 mm (4 x 8 in.) sheets or cut to size dimensions. Larger sizes, up to 2440 x 7320 mm (8 x 24 ft.), are available by special order. Some new mills manufacture jumbo panels are as large as 3660 x 7320 mm (12 x 24 in.) (SBA, 2004). Table 2-3 and Table 2-4 provide the basic and physical properties of the OSB. OSB panels used in the SIP industry are usually rated as Exposure 1 (Figure 2-6) in order to protect them from weathering and possible moisture exposure during construction (APA, 2011). APA’s recommendation for minimum panel properties for the OSB used in SIP manufacturing is listed in Table 2-5.

2.5.6 Failure Mode and De-bonding in Sandwich Panels

Failure mode and face de-bonding of sandwich beams under dynamic load have been studied by several researchers. Daniel et al. (2002) summarizes them as face-sheet compressive failure, face-sheet de-bonding, indentation failure, core failure and face-sheet wrinkling, all of which are dependent on the loading type, geometrical dimensions and basic material properties. On the other hand, failure mode and face de-bonding of sandwich wall panels include global buckling, wrinkling or local buckling and, foam-core failure (Mousa & Uddin, 2010). Major failure mode in Butt's (2008) creep tests on full-sized OSB faced SIPs with EPS cores and foam-spline connections proves to be due to horizontal shear between the facings and the EPS foam-core between the quarter points and the supports region. In general, de-bonding occurs when the tensile stress of the facing is more than the tensile stress of the core material.

Wrinkling of the facing in compression is the major cause of de-bonding of the facing sheets. Another cause for de-bonding is the manufacturing defect called 'dis-bond'. There are few formulas to calculate the global buckling but several studies have suggested simple formulas to calculate wrinkling (Mousa & Uddin, 2010).

Table 2-3: Basic properties of CSA 0437.0 OSB and Waferboard ¹ (SBA, 2004)

	Grade O-2		Grade O-1		Grade R-1 ³	
	Metric	Imperial	Metric	Imperial	Metric	Imperial
Dimensional tolerances, dry, as shipped ²						
Length and width, from stated dimensions	+0, -4 mm	+0, -5/32"	+0, -4 mm	+0, -5/32"	+0, -4 mm	+0, -5/32"
Squareness, maximum difference in diagonals	4 mm	5/32"	4 mm	5/32"	4 mm	5/32"
Straightness, maximum deviation from straight	1.5 mm/edge	1/16"/edge	1.5 mm/edge	1/16"/edge	1.5 mm/edge	1/16"/edge
Thickness ²						
- panel average from nominal	±0.75 mm	±0.030"	±0.75 mm	±0.030"	±0.75 mm	±0.030"
- within panel from panel average	±0.75 mm	±0.030"	±0.75 mm	±0.030"	±0.75 mm	±0.030"
Mechanical properties, dry, as shipped ⁴						
Modulus of rupture - parallel	29.0 MPa	4200 psi	23.4 MPa	3400 psi	17.2 MPa	2500 psi
Modulus of rupture - perpendicular	12.4 MPa	1800 psi	9.6 MPa	1400 psi	17.2 MPa	2500 psi
Modulus of elasticity - parallel	5500 MPa	800,000 psi	4500 MPa	650,000 psi	3100 MPa	450,000 psi
Modulus of elasticity - perpendicular	1500 MPa	225,000 psi	1300 MPa	190,000 psi	3100 MPa	450,000 psi
Internal bond	0.345 MPa	50 psi	0.345 MPa	50 psi	0.345 MPa	50 psi
Lateral nail resistance (t = thickness of panel, mm or inches as appropriate)	70t (N)	400t (lb)	70t (N)	400t (lb)	70t (N)	400t (lb)
Properties Following Moisture Exposure ⁴						
Modulus of rupture - parallel - after 2 hr boil	14.5 MPa	2100 psi	11.7 MPa	1700 psi	8.6 MPa	1250 psi
Thickness swell, after 24 hr soak, maximum	6.2 MPa	900 psi	4.8 MPa	700 psi	8.6 MPa	1250 psi
- 12.7 mm and thinner	15%	15%	15%	15%	15%	15%
- thicker than 12.7 mm	10%	10%	10%	10%	10%	10%
Linear expansion, oven dry to saturated, maximum						
- parallel	0.35%	0.35%	0.35%	0.35%	0.40%	0.40%
- perpendicular	0.50%	0.50%	0.50%	0.50%	0.40%	0.40%

Notes:

1. Minimum requirements (maximum where stated) are based on a 5-panel average, with no single panel more than 20% below (or above as appropriate) the stated requirement.
2. Tolerances are for rough/sized boards. Tolerances for sanded panels are ±0.40mm for variation from nominal, and ±0.25mm for within panel variation from panel average.
3. Grade R-1 is for waferboard, which is only produced by one Canadian mill.
4. These values are not for design purposes.

Table 2-4: Physical properties of OSB (SBA, 2004)

Nominal Panel Thickness [mm]	Weight [N/m ²]	Thermal Resistance [M ² C/w]	Vapour Permeance [ng/(Pa.s.m ²)]	Flame Spread Rating ¹	Smoke Developed Index ¹
9.5	60	0.08	145	148	137
11	69	0.09	120	148	137
12.5	79	0.11	85	148	137
15.5	97	0.13	65	148	137
18.5	116	0.16	65 ²	148	137

Notes:

1. These numbers are average test values obtained by APA, The Engineered Wood Association on several thicknesses of OSB.

2. Panel thicknesses greater than 15.5 mm were not tested, but can be assumed to provide a permeability resistance equal to or better than that of 15.5 mm panels. Vapour permeance values are given for 50% relative humidity (R.H.), and increase slightly with increasing R.H.

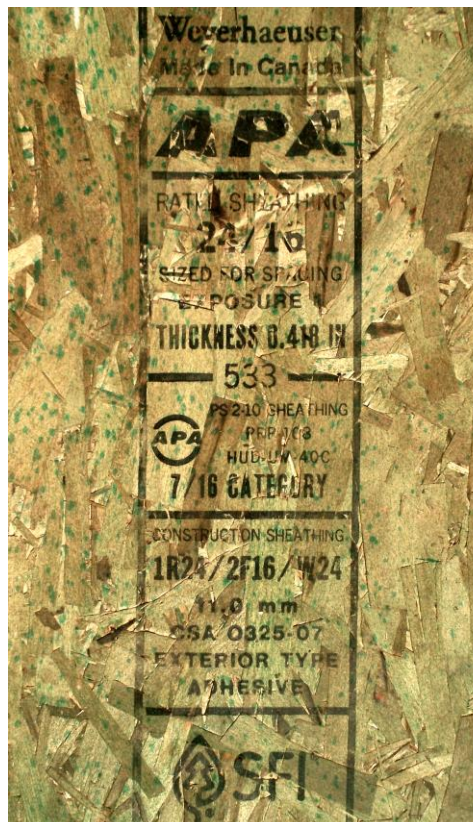
**Figure 2-6: OSB grade stamp**

Table 2-5: Minimum properties for facing materials used for SIP (APA, 2011)

Thickness	Flatwise Stiffness		Flatwise Strength		Tension		Density
	Along	Across	Along	Across	Along	Across	
7/16 in.	55600 (lbf- in. ² /ft.)	16500 (lbf- in. ² /ft.)	1040 (lbf-in./ft.)	460 (lbf-in./ft)	7450 (lbf/ft.)	5800 (lbf/ft.)	34 (pcf)
11 mm	0.523 (KN- m ² /m)	0.155 (KN- m ² /m)	0.386 (KN-m/m)	0.171 (KN-m/m)	108.8 (N/mm)	84.68 (N/mm)	544.6 (kg/m ³)

Chapter 3

Experimental Measurement of the Structural Capacity of PUR SIPs - Baseline Tests

Although building code authorities have reviewed several evaluation reports, SIPs have not yet been recognized by any major code in North America (PATH, 2001) and no universal standards or codes of practice are available for design and installation of SIPs (Rungthongkit & Yang, 2009). The only available set of standards for SIPs has been recently published by the American National Standard Institute (ANSI) and The Engineered Wood Association under the title Standard for Performance-Rated Structural Insulated Panels in Wall Applications (APA, 2013). The standard does not cover the horizontal application (floors and roofs) of SIPs. The Canadian wood design manual mentions SIPs only in its 2010 version and does not recommend any design procedure or test protocol for SIPs (CWC, 2010). The International Organization for Standardization recognizes SIPs in ISO 22452:2011 specifying test methods for determining the structural properties of double-sided, wood-based, load-bearing structural insulated panels (SIPs) for use in walls systems (International Organization for Standardization, 2011).

Baseline experimental tests in this research were conducted in accordance with available ASTM standards and guidelines and manuals provided by CCMC and APA, The Engineered Wood Association. Understanding the effects of de-bonding on overall structural capacity of PUR SIPs can provide a basis to answer some of the questions regulatory organizations have about the long-term behaviour and durability of PUR SIPs.

3.1 Test Samples

Table 3-1 provides the quantity and dimensions of panels tested in baseline test series. As seen in Table 3-1, for each thickness of PUR SIPs, five panels were be tested in axial loading mode, five in transverse loading mode, and five pairs (two single panels joined together) in racking load orientation. All panels were brand new and randomly selected by the manufacturer. All panels had 11mm (7/16 in.) thick OSB face-sheet on both sides. PUR SIPs were kept in the lab environment with the average temperature of 21°C and relative humidity of 35 to 40% for at least one week prior to testing in order to allow acclimatization of the material to occur.

Table 3-1: Specification of PUR SIPs test specimens in accordance with ASTM E1803 (ASTM, 2006), ASTM E72 (ASTM, 2015) and APA (APA, 2013)

Test Orientation	Test ID	Number of Specimens	Panel Dimensions: Width x Length x Overall Thickness		OSB Thickness mm [in.]
			mm	in.	
Axial	A45	5			
Transverse	T45	5	1220x2440x114	48x96x4.5	11 [7/16]
Racking	R45	5 (pairs)			
Axial	A65	5			
Transverse	T65	5	1220x2440x165	48x96x6.5	11 [7/16]
Racking	R65	5 (pairs)			

3.2 Baseline Tests

Baseline tests include testing structural capacity of conventional stud wall panels and PUR SIPs in axial, transverse and racking load condition.

3.2.1 Tests on Structural Capacity of Stud Wall Panels

A total of twelve wall panels were constructed using conventional stick frame method. Nine panels were made by 38×140 mm (2 x 6 in.) lumber with a stud spacing of 608 mm (24 in.) on centre and three were made by 38×89 mm (2 x 4 in.) lumber with a stud spacing of 608mm (24 in.) on centre. One side of the wall panels was faced with 11mm (7/16 in.) OSB sheathing. The opposing side was covered with 12.5 mm (0.5 in.) thick gypsum or drywall board. The nailing pattern was 150 mm (6 in.) on centre on both panel types. Fasteners used to connect the SIP facing panels to framing were 8d common nails (0.131 x 2.5 in.) conforming to ASTM F1667 (ASTM, 2013). This type of wall panel represents and simulates a typical wall assembly in the Winnipeg (Canada) area for residential construction applications.

3.2.2 Tests on Structural Capacity of PUR SIPs

PUR SIPs used in this study were manufactured and supplied by Emercor Ltd. (Calgary, AB, Canada). Two thicknesses of PUR SIPs were tested: 114 mm (4.5 in.) and 165 mm (6.5 in.). Each panel was comprised of two 11.9 mm (15/32 in.) OSB faces with a polyu-

urethane foam-core. Prior to testing, dimensional lumber was installed to simulate top and sill plates in accordance with standard construction practice. No lumber was added to the sides of the PUR SIPs.

According to the foam supplier's data sheet information, the density of the PUR foam-core is expected to be 32 kg/m^3 (2 lb/ft^3). Based on proprietary tests conducted by Emercor Ltd., the foam density was found to be about 40 kg/m^3 (2.48 lb/ft^3) (see Table A-1, Appendix A). The tests conducted on the stud wall assemblies were done in accordance with ASTM E72 (ASTM, 2015). Evaluation of the PUR SIPs structural capacity was conducted based on the following test standards and guidelines: ASTM E1803 (ASTM, 2006), ASTM E72 (ASTM, 2015) and APA (APA, 2013). All the tests were performed at an average room temperature of $21 \text{ }^\circ\text{C}$. The test frame in the Alternative Village at the University of Manitoba was used to test the wall panels. Load cells attached to the hydraulic ram systems on the test frame were used to measure the applied load. Linear potentiometers were used to measure deformation. The data were continuously recorded with a computer controlled Agilent data acquisition/data logger switch unit (34970A). Newly arrived PUR SIPs were kept in a lab environment for a few weeks for them to be acclimated.

3.2.2.1. Axial tests

Axial compression tests were conducted on panels set in the test frame (See Appendix B, Figure B-1 to B-3) with the load applied in accordance with APA standard (APA, 2013). Six linear potentiometers were attached to the panels to measure deflections due to applied loads (Figure 3-1). As guided by ASTM E1803 (ASTM, 2006), ASTM E72 (ASTM, 2015) and, APA (APA, 2013), the axial load must be vertically applied to one third of the thickness of the panel. This eccentric loading scheme will create off-centre loading, which in turn exposes the panel to compression and buckling deformations. NTA (2015) expresses such loading scheme ‘incidental’.

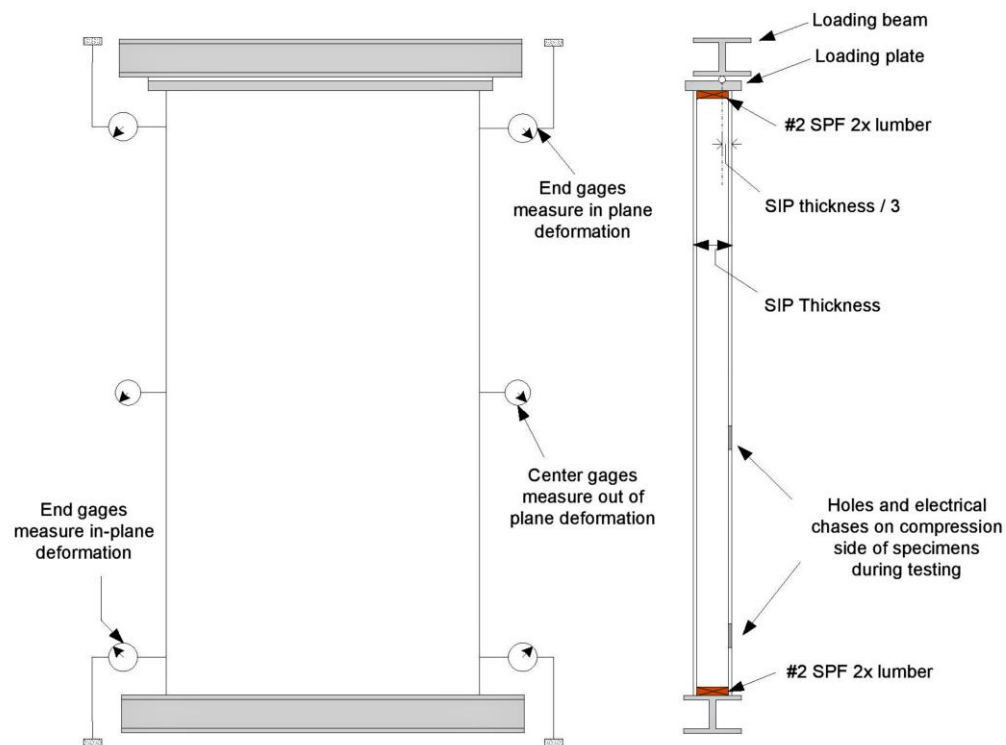


Figure 3-1: Axial compression test setup diagram (APA, 2013)

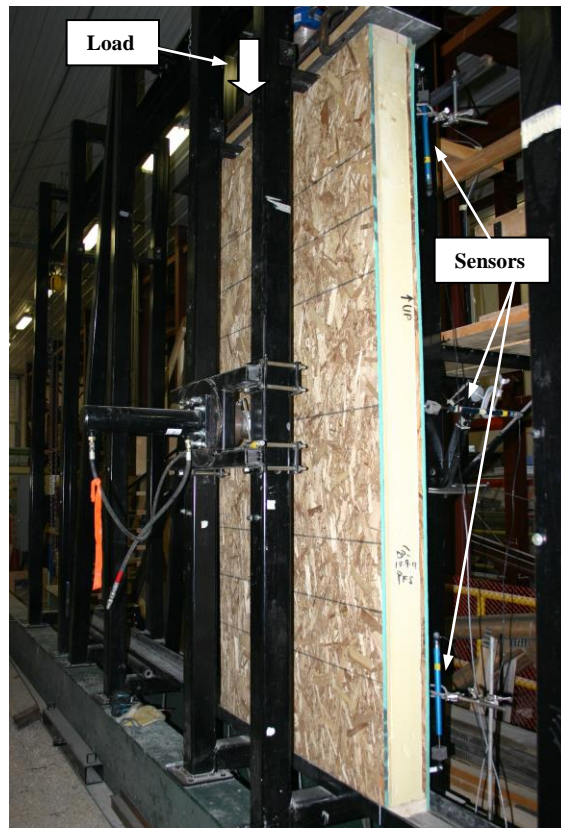


Figure 3-2: Axial test set-up

Following is a summary of the available studies on the prediction of the maximum axial load or critical buckling of the sandwich panels as follows:

According to Euler's formula, the critical buckling load (P_E) for a compression member with a height of L and pin-pin supports is given by (Mousa and Uddin, 2011):

$$P_E = \frac{\pi^2}{L^2} D \quad (\text{Eq. 3.1})$$

The flexural stiffness for a sandwich structure is given by ASTM C-393 as (Figure 3-3):

$$D = E_f I = \frac{E_f (d^3 - c^3) b}{12} \quad (\text{Eq. 3.2})$$

Eq. 3.2 assumes only isotropic face-sheets. To consider orthotropic face-sheets, such as OSB, E_f (longitudinal modulus of elasticity of face-sheets/skins) in Eq. 3.2 should be replaced by $E_f (1 - \nu_{xy}^2)$ where ν_{xy} is the in-plane Poisson's ratio of the orthotropic face-sheets in the xy -plane. This will consider the through-thickness anisotropy effect due to the orthotropic face-sheets. Therefore, Eq. 3.2 can be re-written as:

$$D = E_f I (1 - \nu_{xy}^2) = \frac{E_f (d^3 - c^3) b}{12} (1 - \nu_{xy}^2) \quad (\text{Eq. 3.3})$$

When the compression load P reaches the critical value for buckling P_{cr} , the sandwich member starts to buckle. Allen (1969) suggests the following formula for the calculation of general global buckling in sandwich panel with thin isotropic faces:

$$P = \frac{P_E}{1 + \left(\frac{P_E}{AG}\right)} \quad (\text{Eq. 3.4})$$

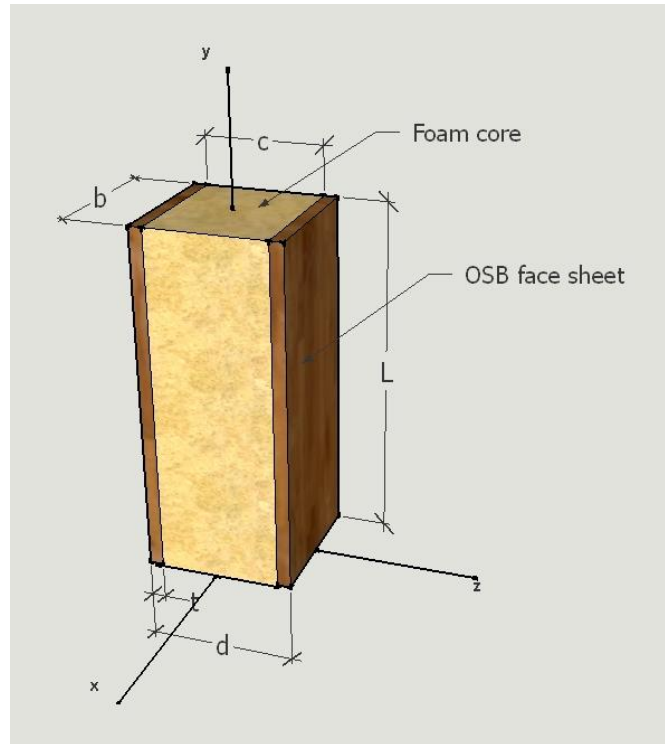


Figure 3-3: Legend for Equation 3.2 (Mousa & Uddin, 2011)

By substituting P_E from Eq. 3.1 into Eq. 3.4, then we can get:

$$P = \frac{\pi^2}{L^2} \frac{D}{\left(1 + \frac{\pi^2 D}{L^2 AG}\right)} \quad (\text{Eq. 3.5})$$

Flexural stiffness D can be determined from Eq. 3.3 for orthotropic face-sheets while the shear area A of a sandwich panel (Figure 3-1) is given as:

$$A = b \left(\frac{d + c}{2} \right) \quad (\text{Eq. 3.6})$$

Substituting Eq. 3.3 and Eq. 3.6 into Eq. 3.5, yields:

$$P = \frac{\pi^2}{L^2} \frac{E_{OSB} I}{\left(1 + \frac{\pi^2 E_{OSB} I (1 - \nu_{xy}^2)}{L^2 b \left(\frac{d + c}{2} \right) G} \right)} (1 - \nu_{xy}^2) \quad (\text{Eq. 3.7})$$

Where:

P = global buckling load of concentric loading sandwich panel (kN)

L = panel length (mm)

E_{OSB} = longitudinal modulus of elasticity of OSB face-sheets (MPa)

I = moment of inertia of facing sheet about the centroid of the panel (mm^4)

ν_{xy} = Poisson's ratio of face-sheet in the xy -plane

b = panel width (mm)

c = core thickness (mm)

d = total thickness of sandwich panel (mm)

G = core shear modulus (MPa)

Engineered design of SIP panels using listing report data of the NTA incorporated (NTA Inc., 2009) also recommends a similar formula for prediction of the critical buckling load for a pinned-pinned column under axial loading:

$$P_{cr} = \frac{\pi^2 E_b I}{3 \times (12L)^2 \left[1 + \frac{\pi^2 E_b I}{(12L^2) A_v G} \right]} \quad (\text{Eq. 3.8})$$

Where:

E_b = SIP modulus of elasticity under transverse bending

I = SIP moment of inertia (mm^4)

L = panel length or span length (mm)

A_v = shear area of panel. For symmetric panels $A_v = 6(h + c)$ (mm^2)

h = overall SIP thickness (mm)

c = core thickness (mm)

G = SIP shear modulus (MPa)

3.2.2.2. Transverse tests

Transverse tests simulate the lateral wind load that causes bending deflection in wall frames. As guided by ASTM E1803 (ASTM, 2006), ASTM E72 (ASTM, 2015), two linear potentiometers were attached to the compression side of the panel (loading face) in order to measure the overall deflection due to applied transverse loads. The test panels were loaded laterally up to failure. As seen in Figure 3-4, transverse tests in this study were conducted on five single 1220 x 2440 mm (4 x 8 ft.) panels in a vertical manner.

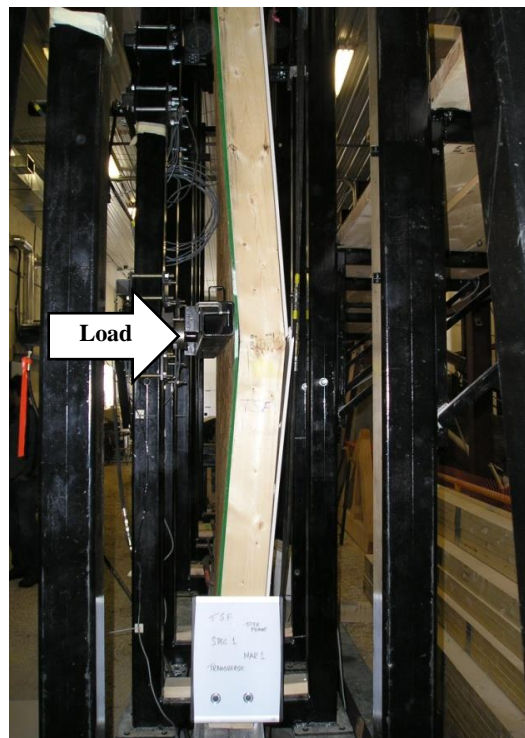


Figure 3-4: Transverse test on stud wall in progress

3.2.2.3. Racking tests

Free rotation of face-sheets can happen when wall panels are exposed to racking loads only (Figure 3-5). Racking load is a load applied in the plane of the panel assembly in such manner as to elongate one diagonal and shorten the other diagonal simulating deformation caused by wind or a seismic event (Figure 3-6).

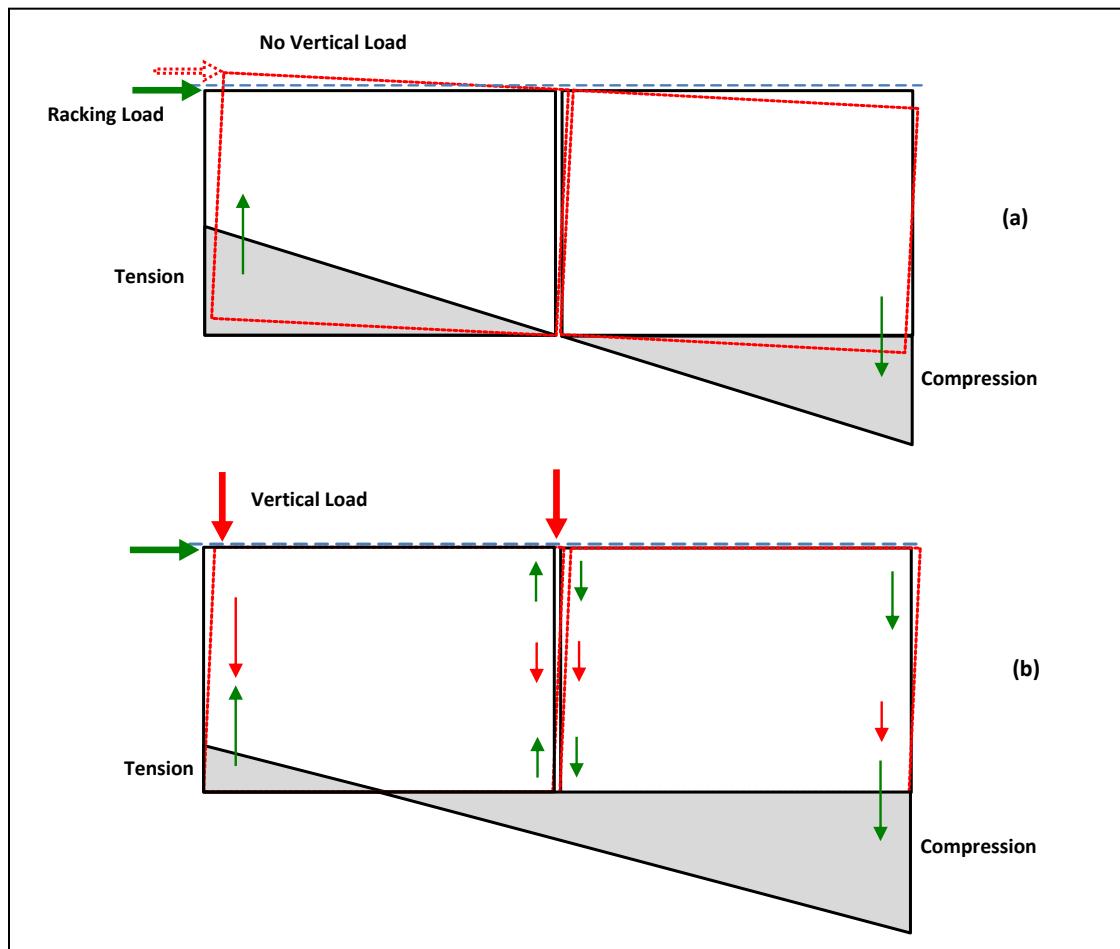


Figure 3-5: Racking behaviour of sandwich wall panels with or without vertical loads (Bregulla, 2003)

In a system of two panels, the whole system will freely rotate, causing compressive stress in the opposite side of the loading point and tensile-uptift force where the racking load is applied. On the other hand, when a vertical load is applied to the system, the compressive stress in the rear side is increased and the tensile stress is decreased. However, this increases the internal shear stress between the sandwich panel components (Bregulla, 2003).

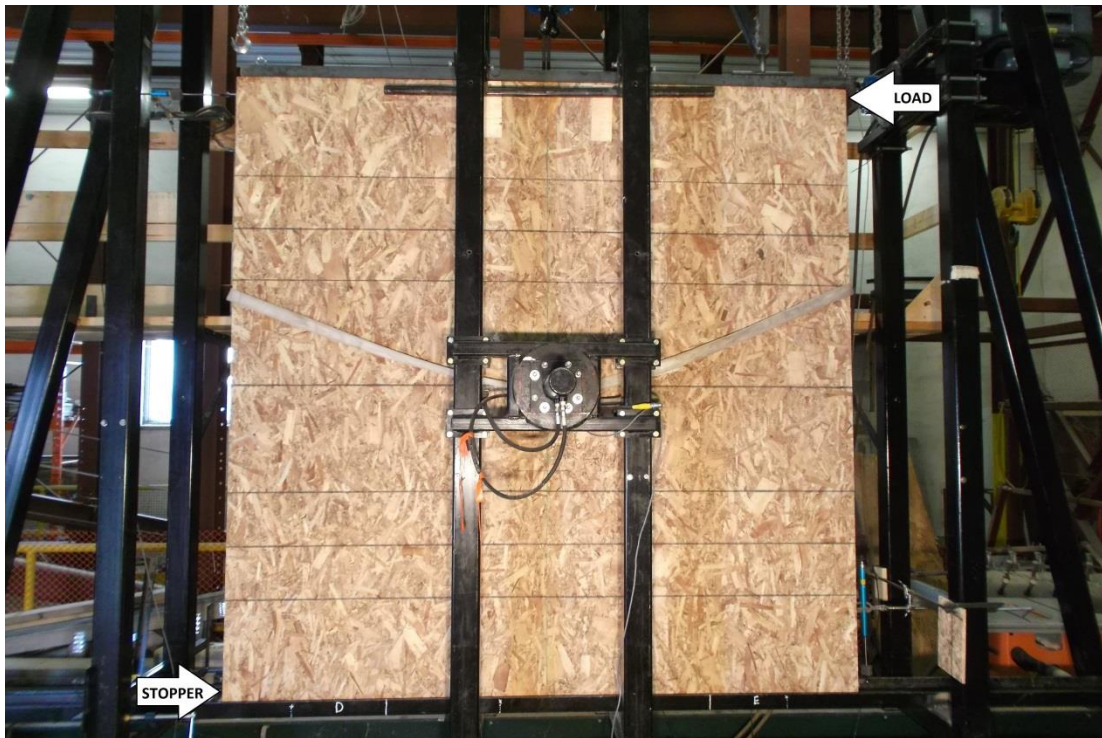


Figure 3-6: Racking resistance test on 2240 x 2240mm (8 x 8 ft.) PUR SIPs

ASTM E1803 (2006) and ASTM E72 (2015) recommend installation of a stopper system at the rear end of the walls in order to avoid horizontal movement of the system due to applied racking loads. Also a stopper had to be installed on top of the wall assembly in

order to eliminate any uplift or vertical movement when racking loads are being applied. Each racking load capacity tests were conducted on a pair of panels connected together using OSB splines forming a 2440 x 2440 mm (8 x 8 ft.) panel (Figure 3-7). The nailing pattern was 150 mm (6 in.) on centre and the nails used to connect the two SIPs together were 8d common nails (0.131 x 2.5 in.) conforming to ASTM F1667 (ASTM, 2013).

As guided by ASTM E1803 (2006) and ASTM E72 (2015), racking load was applied at a constant rate throughout the tests. Specimens were loaded in three stages of up to 3.5, 7.0, and 10.5 kN (790, 1570, and 2360 lbf). At the end of each stage, load was brought back to zero, paused for 5 seconds, and then increased to the next load level. After the third stage, the specimens were loaded to failure. As suggested by the above mentioned standards, the speed of the tests was such that the first cycle of loading 3.5 kN (790 lbf) was not completed in less than 2 minutes. In all racking tests, According to ASTM E72 (2015), if the failure did not occur before 102 mm (4 in.) of deflection, tests were stopped and considered complete. The same procedure was repeated for stud wall panels. As depicted in Figure 3-8, load was applied to the top corner of the wall assembly using a hydraulic jack. Stoppers were installed on the opposite bottom side of the panels in order to stop them from moving towards the force direction. As recommended by APA (2013), four linear potentiometers were installed on the panel to measure movements and deflections of the specimen. Five sets of panels were loaded to failure at a constant load rate recommended by ASTM E1803 (2006).



Figure 3-7: A typical spline-glue connection used to connect two Styrofoam foam core panels together (Fine Homebuilding, 2006)

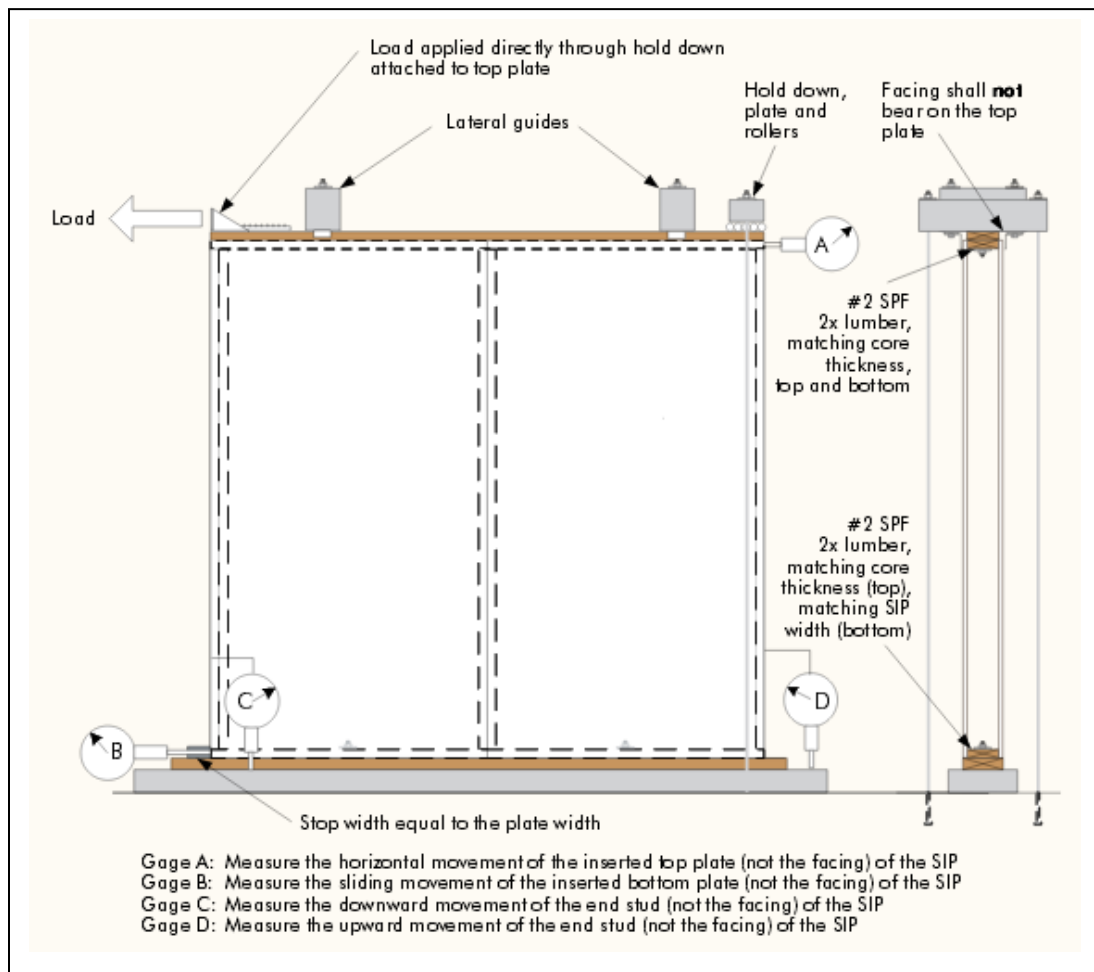


Figure 3-8: Typical test setup for racking load tests (APA, 2013)

3.3 Baseline Test Results

3.3.1 Modes of failure

Crushing of the top plate, the OSB, and, consequently, a slight rotation of the top plate, governed the failure mode of the PUR SIP under axial loads. The rotation angle normally widened on the compression due to intentional eccentricity adopted when the axial loads were applied. Buckling was not observed in any of the axial tests conducted in this part of the study. All panels, regardless of their thickness, crushed on the top right before the final failure and sudden drop in the handled load.

In terms of transverse loading, panels exhibited significant deflection before failure defined as a sudden drop in load or material failure. The failure mode was governed by crushing of the OSB on the compression side, visible stretching of OSB fibers on the tension side and then appearance of signs of shear fracture in the middle-height-zone of the foam-core. As for the foam-core, normally, a small crack would start from the tension side of the panel and the panel would suddenly fail with the crack propagating to the compression side and shearing the foam-core along the length of the panel.

Failure mode of the PUR SIPs in racking load capacity tests was much harder to detect and study. PUR SIPS tested for racking load capacity had upright dimensional lumbers

attached to their sides therefore the foam-core was not exposed for observation. Generally, rotation of the face-sheet OSBs was the only visible sign when the racking load was applied. In most cases, the panel would fail and the load would drop without an obvious sign of a physical failure. In a few cases, the panel would not fail and the loading had to be stopped at the deflection limit specified by the ASTM standard ASTM E1803 (2006) and ASTM E72 (2015) as 102mm (4 in.). The foam would deflect and rotate along with the face-sheets and the ultimate failure would occur when shear forces fully or partially separate the foam-core and the OSB face-sheets.

3.3.2 Relative Behavior of PUR SIP Types

Tables 3-2 to 3-5 represent the results for all the tests conducted on 165mm (6.5 in.) and 114mm (4.5 in.) thick PE SIPs and stud wall (stick-frame) panels. Table 3-5 represents the average values obtained for all the tests conducted. The overall structural performance of the tested PUR SIPs can be concluded from Table 3-5. In the case of axial compressive loads, thicker PUR SIPs had an ultimate load capacity 23% more than the thinner SIPs. In the case of transverse loading, 165mm (6.5 in.) thick SIPs handled 26% percent more ultimate load than the 114mm (4.5 in.) thick SIPs. However, at failure, when the panels were exposed to racking load, thicker panels handled 9% less ultimate load than the thinner panels.

As seen in Table 3-5, 165mm (6.5 in.) thick PUR SIPs can handle 25% more axial load compared to the same thickness of stud wall panels. PUR SIPs with 165mm (6.5 in.) can resist an average of 162 kN per linear meter. PUR SIPs with 114mm (4.5 in.) are able to carry an average of 131 kN per meter. In the case of transverse loading (which simulates wind load), 165mm (6.5 in.) thick PUR SIPs handled 37% more load than the stud wall panel. When the panels were exposed to racking loads, PUR SIPs performed more than 4 times better than the same thickness of stud wall assembly. This value was more than 3 times better when 114mm (4.5 in.) thick PUR SIPs were compared to the racking resistance of 114mm (4.5 in.) thick stud wall panels. The findings of this part of the test are in agreement with former studies conducted by Kermani and Hairstans (2006) claiming that a polystyrene SIP wall can outperform a conventional stud wall diaphragm.

Table 3-2: Baseline test results for 114 mm (4.5 in.) thick PUR SIP

Test number	114mm (4.5 in.) thick PUR SIP		
	Maximum Axial Load [kN]	Maximum Transverse Load [kN]	Maximum Racking Load [kN]
1	145.74	28.36	43.50
2	201.33	30.51	41.34
3	126.38	30.83	56.11
4	160.70	32.38	71.51
5	165.70	29.92	53.26
Avg.	159.97	30.40	53.14
STD	27.72	1.46	12.03

Table 3-3: Baseline test results for 165 mm (6.5 in.) thick PUR SIP

Test number	165 mm (6.5 in.) thick PUR SIP		
	Maximum Axial Load [kN]	Maximum Transverse Load [kN]	Maximum Racking Load [kN]
1	188.66	35.87	44.78
2	183.00	39.62	39.66
3	211.72	37.40	57.04
4	199.33	39.07	50.42
5	204.80	40.19	50.90
Avg.	197.50	38.43	48.56
STD	11.69	1.77	6.60

Table 3-4: Baseline test results for 38 × 140 mm (nominal 2 x 6 in.) and 38 × 89 mm (nominal 2 x 4 in.) stud walls

Test number	165 mm (6.5 in.) Stud wall panel			114mm (4.5 in.) Stud wall panel
	Maximum Axial Load [kN]	Maximum Transverse Load [kN]	Maximum Racking Load [kN]	Maximum Racking Load [kN]
1	149.76	30.26	11.75	14.92
2	129.80	27.11	12.34	15.22
3	192.66	27.06	10.75	16.42
Avg.	157.40	28.14	11.61	15.52
STD	32.12	1.84	0.80	0.79

Table 3-5: Comparison between panel assemblies load capacity

Test Orientation	114mm (4.5 in.) thick PUR SIP	165mm (6.5 in.) thick PUR SIP	Ratio of 165 mm (6.5 in.) to 114 mm (4.5 in.) PUR SIPs	165mm (6.5 in.) thick stud wall panel ¹	114mm (4.5 in.) thick stud wall panel ²	Ratio of 165 mm (6.5 in.) PUR SIP to 165 mm Stud Wall	Ratio of 114 mm (4.5 in.) PUR SIP to 114 mm Stud Wall
	Average max. load [kN]	Average max. load [kN]		Average max. load [kN]	Average max. load [kN]		
Axial	159.97	197.50	1.23	157.40	N/A	1.25	N/A
Transverse	30.40	38.43	1.26	28.14	N/A	1.37	N/A
Racking*	53.14	48.56	0.91	11.61	15.52	4.18	3.42

1. In the case of stud wall tests, single 1220 x 2440 mm (4 x 8 ft.) panels were tested while in the case of PUR SIP tests, two 1220 x 2440 mm (4 x 8 ft.) panels were joined together and tested to failure.

2. 1220 x 2440 mm (4 x 8 ft.) thick stud wall with OSB facings attached horizontally to simulate the actual end use condition.

Figures 3-9 to 3-11 represent the typical load-deflection curves of all panels tested. As seen in all three sets of curves, compared to stud walls, PUR SIPs exhibit a higher energy absorption capacity by having larger area under their load-deflection curves. As seen in Figure 3-9, although tested 165 mm (6.5 in.) thick PUR SIPs in transverse load orientation did not have any stud in them; they showed a similar behaviour except higher load capacity compared to stud wall panels. In the case of racking load capacity (Figure 3-10), 165 mm (6.5 in.) thick PUR SIPs not only exhibit ultimate load capacity of 4.18 times higher than stud wall panels with the same thickness, they had a steeper load vs. deflection curve suggesting higher stiffness in the specimen. As seen in Figure 3-11, when panels were exposed to axial load, even without any stud, 165 mm (6.5 in.) thick PUR SIPs exhibited 1.25 times higher ultimate load capacity than the stud wall panels with the same thickness.

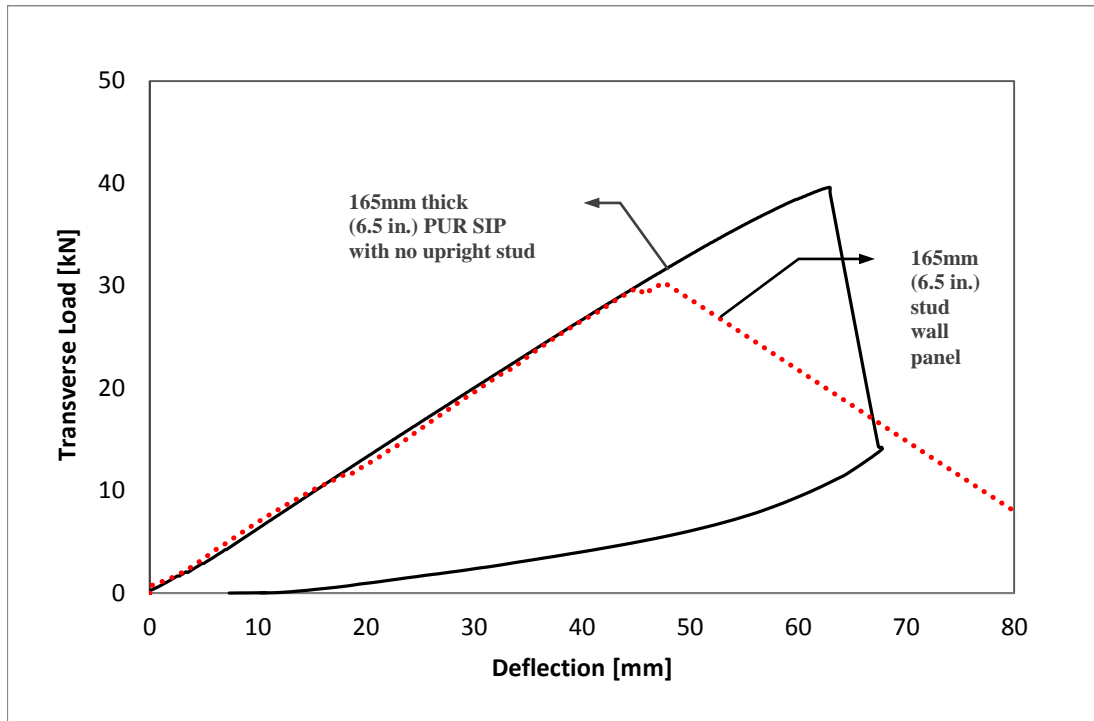


Figure 3-9: Typical transverse tests results comparing the performance of a 165mm thick (6.5 in.) PUR SIPs to a conventional 165mm (6.5 in.) stud wall panels

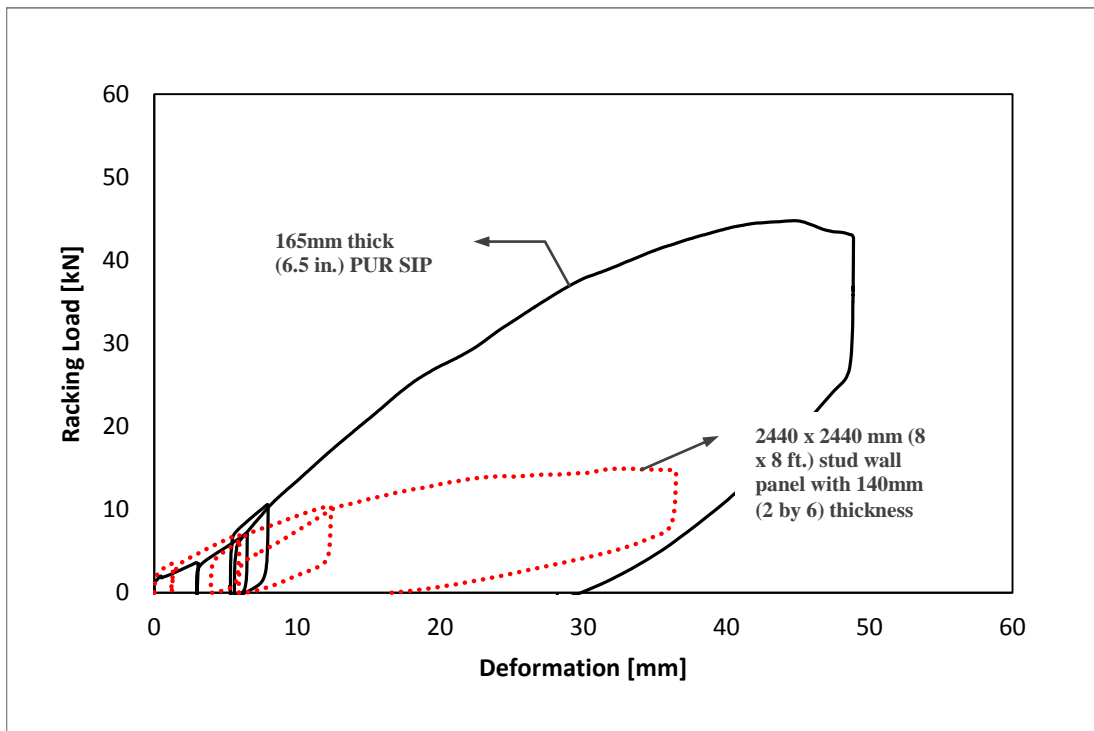


Figure 3-10: Typical racking tests results comparing the performance of a 165mm thick (6.5 in.) PUR SIP to a conventional stud wall panel

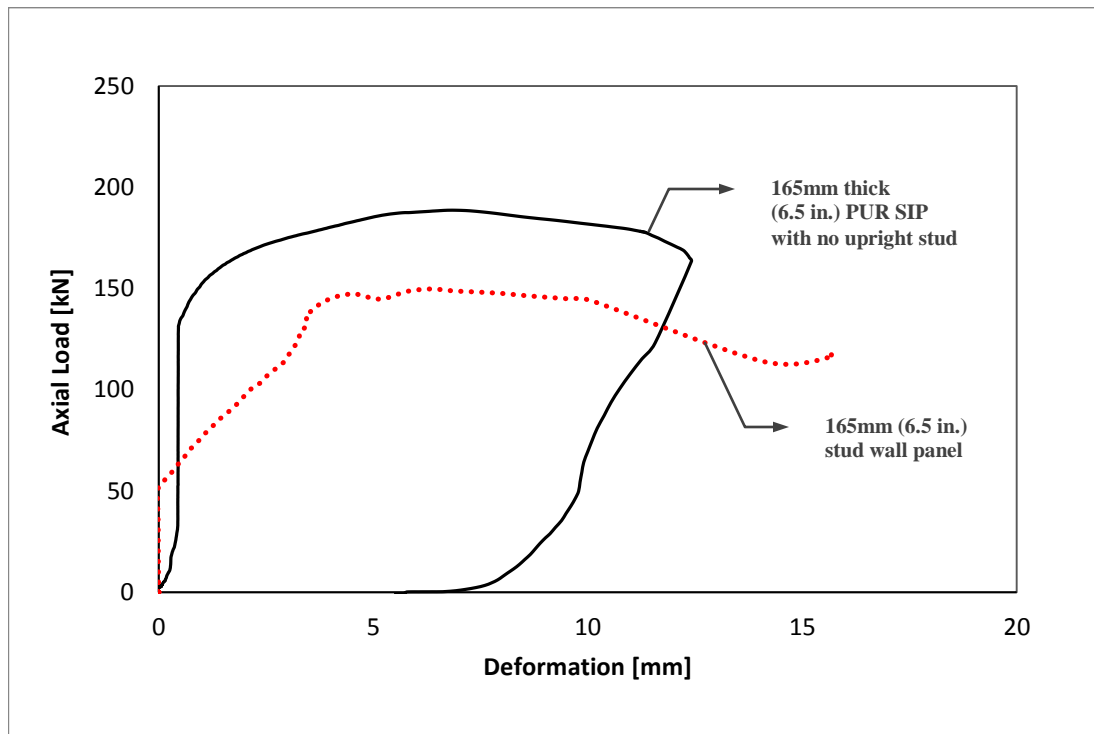


Figure 3-11: Typical axial tests results comparing the performance of a 165mm (6.5 in.) thick PUR SIP to a conventional 140mm (2 by 6) stud wall panels

3.3.3 Comparison to theoretical critical buckling load

Actual specifications and property values of the tested panels can be input in Eq. 3.7, in order to calculate the critical buckling load of the tested panels. Yielded theoretical values can be compared with the actual results obtained in experimental tests:

$$L = 2440 \text{ mm}$$

$$E_{OSB} = 5500 \text{ MPa}$$

$$I = 3'359'318'800 \text{ mm}^4$$

$$\nu_{xy} = 0.195 \text{ (Thomas, 2003)}$$

$$b = 1220 \text{ mm}$$

$$c = 142.8 \text{ mm}$$

$$d = 165 \text{ mm (6.5 in.)}$$

$$G = 0.84 \text{ MPa (PUR foam)}$$

P_{cr} (expected global buckling load of a concentric loaded 165 mm, 6.5 in. thick sandwich panel) = 157,578.94 N (157.58 kN)

This theoretical value is about 25% less than the average ultimate axial load found by experimental tests of 197.5 kN (Table 3-3).

3.4 Conclusions

1. Polyurethane core Structural Insulated Panels (PUR SIPs) tested in this study exhibited more rigidity, and overall load capacity than the conventional stud wall panels in all loading orientations of axial, racking, and transverse.
2. Under axial compression loads, 165mm (6.5 in.) PUR SIPs handled 23% more load than the thinner SIPs (114mm, 4.5 in. thick).

3. When subjected to transverse loading, 165mm (6.5 in.) PUR SIPs handled 26% more load than the 114mm (4.5 in.) thick PUR SIPs.
4. 165mm (6.5 in.) PUR SIPs exhibited 9% less load than 114mm (4.5 in.) thick PUR SIPs when they were exposed to racking load.
5. 165mm (6.5 in.) thick PUR SIPs can withstand 25% more axial load compared to the same thickness of stud wall panels.
6. In the case of transverse loading (which simulates wind load), 165mm (6.5 in.) thick PUR SIPs handled 37% more transverse load than the stud wall panel.
7. When the panels were exposed to racking load, PUR SIPs handled 4.18 times more load than the same thickness of stud wall assembly. This value was 3.42 times more when 114mm (4.5 in.) thick PUR SIPs were compared to the racking resistance of 114mm (4.5 in.) thick stud wall panels.
8. Compared to stud wall panels, PUR SIPs deflect less for the same racking load.

Chapter 4

Experimental Measurement of the Structural Capacity of
Dis-bonded PUR SIPs

4.1 Introduction

The effects of de-bonding and separation of SIP components on the overall behaviour of SIPs are currently unknown. Service conditions, weathering effects, and manufacturing malfunctions can cause partial separation. The main objective was to study the effects of a certain percentage of OSB-foam de-bonding on the overall structural capacity of the PUR SIPs. Intentionally de-bonded or dis-bonded panels were tested in order to investigate the effects of de-bonding of foam-core and OSB face-sheets of PUR SIPs on the overall structural capacity of the panels.

4.2 Sample Preparation

Table 4-1 represents the number of panels tested in this part of the study. As seen in this table, similar to fully-bonded panels tested in baseline test series (Chapter 3); five panels were tested in axial, five in transverse and five pairs in racking load orientations.

Table 4-1: Dimensions of intentionally dis-bonded PUR SIPs test specimens in accordance with ASTM E1803 (ASTM, 2006), ASTM E72 (ASTM, 2015) and APA (APA, 2013)

Test Orientation	Test ID	Number of Specimens	Panel Dimensions: Width x Length x Total Thickness		OSB Thickness mm [In.]
			mm	In.	
Axial	DA45	5			
Transverse	DT45	5	1220x2440x114	48x96x4.5	11 [7/16]
Racking	DR45	5 (pairs)			
Axial	DA65	5			
Transverse	DT65	5	1220x2440x165	48x96x6.5	11 [7/16]
Racking	DR65	5 (pairs)			

While there is no specific standard for testing disbonded panels, a decision was made to investigate the effect of disbonding on 1/3 of the panel length. It was decided to place the disbonded portion at the top in the test apparatus. The Emercor SIP manufacturing facility produced the partially bond-less or dis-bonded PUR SIPs. As seen in Figure 4-1, the panels were made with a total dis-bonded area of 33% (1220 x 814 mm, 0.993 m² or 4 x 2.67 ft, 10.7 sqft.). A comprehensive fire test study on SIPs conducted by Bregulla (2003) found that the top part of SIPs is the first zone to fail when SIPs are exposed to fire. In the case of transverse and racking loading situations, locating the dis-bond zone on the top or bottom area of the panel would cause asymmetry and simulate the worst possible loading condition. Similar asymmetric behaviour would be expected if the dis-bonded portion were oriented to the bottom of the test frame.

In order to make such panels, the designated area (darkened area seen in Figure 4-1), was covered by thick waxed paper (Figure 4-2) to prevent any contact between the injected liquid polyurethane foam and the OSB's internal surface. As a result, there was absolutely no bond between the OSB and the PUR foam on the desired dis-bond area of the panels. OSB face-sheets and PUR foam used to fabricate the dis-bonded panels was identical to those used to make the fully-bonded panels (tested and described in Chapter 3 of this thesis). Similar to regular panels, the soft side of the OSB faced the PUR foam-core and the rough side facing outside.

Panels arrived at the lab without any framing lumber. As for 114 mm (4.5 in.) thick panels, 38 x 89 mm (2 x 4) dimensional lumber was added to the top and bottom panels before being tested under axial and transverse load tests. In the case of 165 mm (6.5 in.) thick panels, 38 x 140 mm (2 x 6) dimensional lumber was added to the top and bottom of the panels.

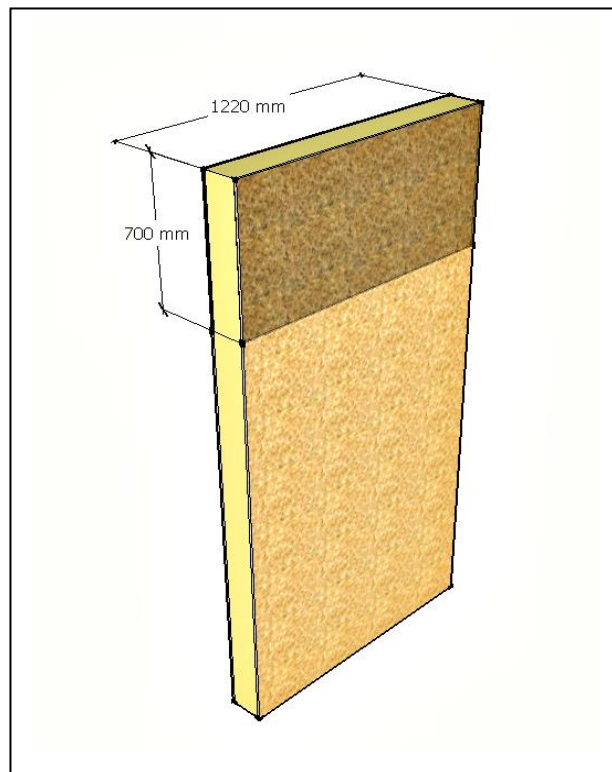


Figure 4-1: Darker OSB area indicates the debonded/debonded region on the surface of the PUR SIP



Figure 4-2: Partially bond-less PUR SIPs ready for test. Waxed paper used between the OSB face-sheets and the PUR foam to avoid bond between the two materials

Similar to racking tests conducted in baseline test series, OSB splines, construction adhesive, expandable spray PUR foam (Great Stuff Pro™), nails, along with two continuous 2438 mm (8 ft.) long dimensional lumber on top and bottom were employed to join two panels together (Figure 4-3). The framing lumber was attached to the panels using foam, construction adhesive (Lepage, PL Premium™). Similar to panels tested in baseline tests, the nailing pattern used was 150 mm (6 in.) on centre with 8d common nails (0.131 x 2.5 in.) conforming to ASTM F1667 (2011).

All panels were allowed to condition in the lab environment for at least 24 hours in order to allow the construction adhesive cure. All the tests were performed at an average room temperature of 21°C. The test frame at the Alternative Village at the University of Manitoba was used to test the wall panels. Load cells attached to a hydraulic ram system on the test frame were used to measure the applied loads. Linear potentiometers were used to measure deformation and deformation. The data were continuously recorded using a computer controlled Agilent data acquisition/data logger switch unit (34970A).



Figure 4-3: Connection details of two 1220x2440 mm (4x8 ft.) panels joined together for racking test purposes. OSB splines, construction adhesive, expandable spray PUR foam and nails used to join the panels together

4.3 Test Procedure and Assembly

4.3.1 Axial Load Tests

In order to be consistent with the control (baseline) tests, axial load tests on dis-bonded panels were conducted conforming to ASTM E1803 (ASTM, 2006), ASTM E72 (ASTM, 2015) and APA (APA, 2013). A load cell with a capacity of 45 ton (100,000 lbs) was used to conduct the tests. Linear potentiometers were used to measure deformations of the panels under the applied eccentric axial load. As seen in Figure 4-4, four linear potentiometers were attached to the wall panel to measure any in or out-of-plane movement or buckling. Two linear potentiometers were attached to the mid-height of the panel on the compression side and two linear potentiometers were attached to the mid-height of the dis-bonded region of the panel to detect and record possible buckling in those regions on both compression and tension side. Two other linear potentiometers also were attached to top of the panel to measure the shortening of the panel, one on the cross head of the loading machine and one on the highest possible part of the panel. The data was continuously recorded with a computer controlled Agilent data acquisition/data logger switch unit (34970A). All five specimens were loaded to failure. As seen in Figure 4-5, buckling only occurred on the dis-bonded region when the panels were exposed to axial load. This was an expected mode of failure since OSB sheet over the Dis-bonded area acted as slender columns with no lateral support to control or limit the buckling.

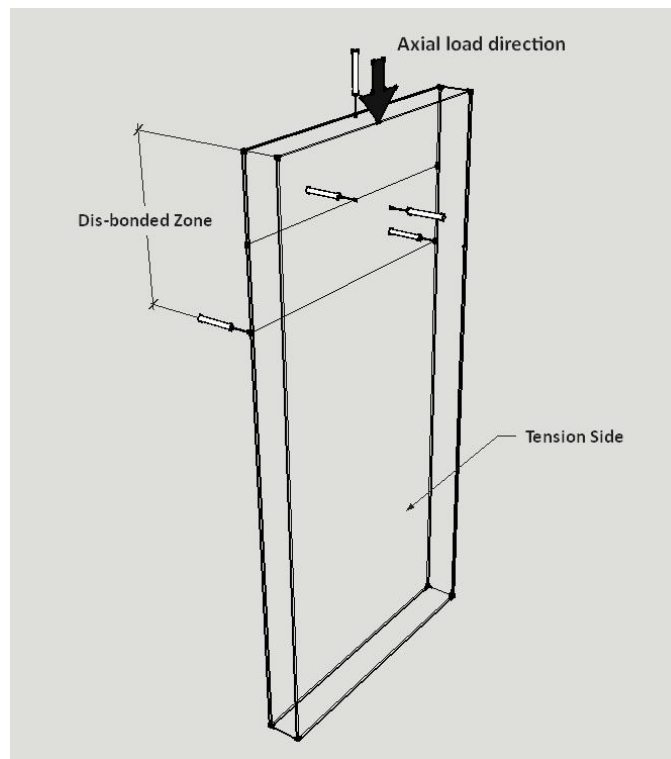


Figure 4-4: Location of linear potentiometers on dis-bonded panels tested under eccentric compression axial load



Figure 4-5: Dis-bonded panel under direct eccentric axial load. Buckling occurred only at the disbonded area of the panel at the time of failure

4.3.2 Transverse Load Tests

Similar to axial tests, ASTM E1803 (ASTM, 2006), ASTM E72 (ASTM, 2015) and APA (APA, 2013) standards were adopted to conduct transverse load tests. A 9,000 kg (20,000 lbs) capacity load cell was used to conduct the tests. Before testing, dimensional lumber was glued and nailed to top and bottom of the panels. Nail pattern and glue type were identical to those used in baseline tests described in Chapter 3 of this thesis.

Continuous, constant transverse load was applied to the mid-height of the dis-bonded panels until failure happened (Figure 4-6). Two linear potentiometers were attached to both sides of the compression side of the panels on the mid-height mark (Figure 4-7). Unlike fully-bonded panels (which failed at almost mid-height line), all five tested specimens failed in tension at the border of dis-bonded, bonded region of the panel. Shear failure in the foam first and then the tensile failure in OSB face-sheet dominated the general failure mode. The OSB sheet of the compression side also crushed and failed in compression.



Figure 4-6: A failed disbonded panel subjected to transverse load

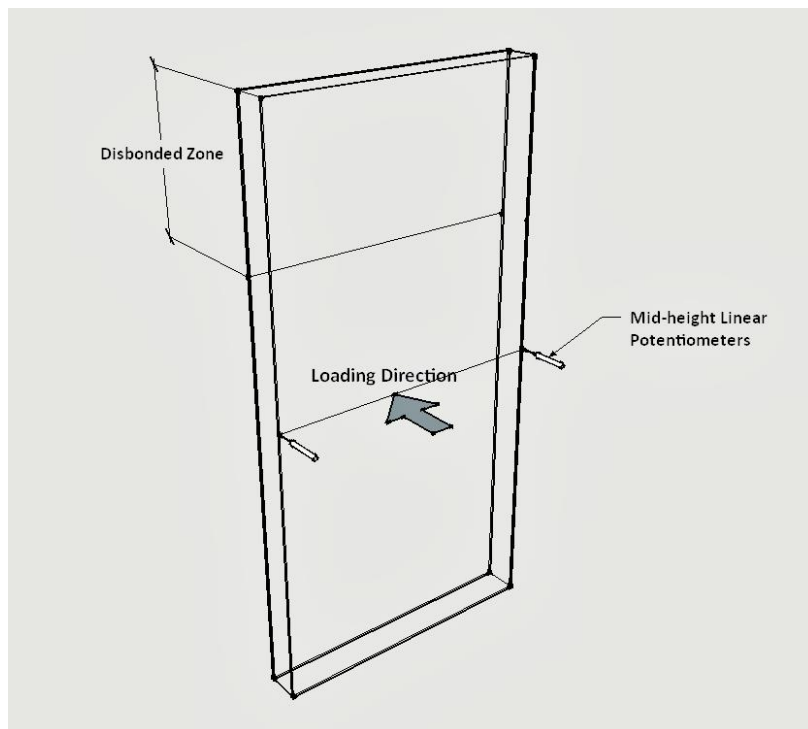


Figure 4-7: Location of linear potentiometers on dis-bonded panels tested under transverse load

4.3.3 Racking Load Tests

ASTM E1803 (ASTM, 2006), ASTM E72 (ASTM, 2015) and APA (APA, 2013) standards were adopted to conduct racking tests on dis-bonded panels as well. Before testing, two 1220 x 2440 mm (4 x 8 ft.) were joined together to form a 2440 x 2440 mm (8 x 8 ft.) panel. Similar to baseline tests, OSB splines, PUR foam, construction glue, and nail were used to join the panels together. Then, two 2440 mm (8 ft.) long dimensional lumbers were glued and nailed to the top and bottom of the assembly. The nail pattern and glue type were identical to those used in the baseline tests described in Chapter 3 of this thesis. As has been directed by ASTM E1803 (ASTM, 2006) and ASTM E72 (ASTM, 2015), the racking load was applied at a constant rate throughout the tests. A 50K lbs capacity load cell was used to conduct the tests. Specimens were loaded in three stages of 3.5, 7.0, and 10.5 kN (790, 1570, and 2360 lbf). At the end of each stage, the load was set back to zero, loading was paused for 5 seconds, and increased to the next load level. After the third stage, the specimens were loaded to failure.

According to ASTM E72 (ASTM, 2015), if the failure did not occur before 102 mm (4 in.) of deflection, the experiments were stopped and considered complete. As suggested by the above mentioned standards, the speed of tests were such that the first cycle of loading 3.5 kN (790 lbf) was not completed in less than 2 minutes from the start of the test. The racking loads were applied to the top (right) corner of the wall assembly (Figure

4-8) using a hydraulic jack connected to a load cell. A stopper was installed on the opposite bottom (left) side of the panels in order to block the specimen from moving towards the force direction. As seen in Figure 4-8, six linear potentiometers were attached on the panel(s) to measure in-plane and out-of-plane movement. One linear potentiometer was installed at the point of load application (top right) to measure horizontal in-plane displacement, one at the bottom side (bottom right) of the panel to detect any uplift movement and four linear potentiometers were installed at mid-height of the dis-bonded region on each side of the single panel to detect out-of-plane and bucking deformations. In total, five sets of panels were loaded to failure at a constant load rate and cycles as recommended by ASTM E1803 (ASTM, 2006).

4.4 Experimental Results

Tables 4-2 and 4-3 contain the results of axial, racking and transverse load tests conducted on dis-bonded panels. Table 4-4 and 4-5 compare the obtained results to those obtained from fully-bonded panels or the baseline tests described in Chapter 3 of this thesis.

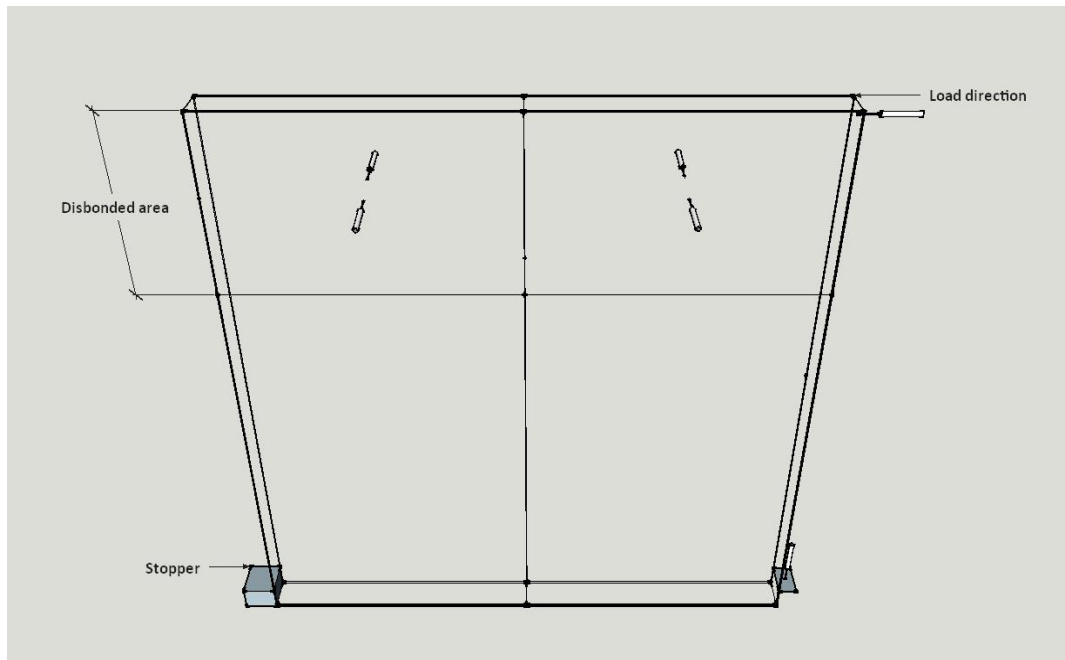


Figure 4-8: Location of the linear potentiometers on dis-bonded panels tested under racking load

4.4.1 Axial Load Test Results

As seen in Table 4-4 and Table 4-5, dis-bonded 114 mm (4.5 in.) and 165 (6.5 in.) thick PUR SIPs resisted maximum averages of 58.70 and 71.26 kN of eccentric axial loads respectively. As seen in Table 4.6, compared to fully-bonded panels, 33% dis-bond resulted in 2.73 times less axial load capacity in 114mm (4.5 in.) thick PUR SIPs. The 33% dis-bond caused 2.77 times less axial load capacity in thicker 165mm (6.5 in.) thick PUR SIPs.

Table 4-2: Test result of the dis-bonded 114 mm (4.5 in.) thick panels exposed to axial, transverse and racking loads

Test number	Dis-bonded 114mm (4.5 in.) thick PUR SIP		
	Maximum Axial Load [kN]	Maximum Transverse Load [kN]	Maximum Racking Load [kN]
1	53.82	6.90	74.99
2	64.01	6.35	56.73
3	53.44	6.35	61.57
4	64.50	6.07	84.72
5	57.73	6.21	64.67
Avg.	58.70	6.37	68.54
STD	5.35	0.32	11.25
COV (%)	9.11	4.97	16.42

Table 4-3: Comparison between results in axial, racking and transverse test conducted on fully bonded 114 mm (4.5 in.) thick panels and dis-bonded panels

Type of Panel	114mm (4.5 in.) thick PUR SIPs		
	Average Maximum Axial Load [kN]	Average Maximum Transverse Load [kN]	Average Maximum Racking Load [kN]
Dis-bonded	58.70	6.37	68.54
Fully Bonded	159.97	30.40	53.14
Difference [%]	-63.30	-79.03	28.98
Ratio [Bonded/Dis-bonded]	2.73	4.77	0.78

Table 4-4: Test result of the dis-bonded 165 mm (6.5 in.) thick panels exposed to axial, transverse and racking loads

Test number	Dis-bonded 165 mm (6.5 in.) thick PUR SIP		
	Maximum Axial Load [kN]	Maximum Transverse Load [kN]	Maximum Racking Load [kN]
1	67.91	9.68	42.68
2	72.42	8.99	44.13
3	68.47	9.34	52.14
4	66.86	8.73	40.96
5	80.65	9.74	43.74
Avg.	71.26	9.29	44.73
STD	5.66	0.43	4.32
COV (%)	7.94	4.68	9.65

Table 4-5: Comparison between results in axial, racking and transverse test conducted on fully bonded 165mm (6.5 in.) thick panels and dis-bonded panels

Type of Panel	165mm (6.5 in.) thick PUR SIPs		
	Average Maximum Axial Load [kN]	Average Maximum Transverse Load [kN]	Average Maximum Racking Load [kN]
Dis-bonded	71.26	9.29	44.73
Fully Bonded	197.50	38.43	48.56
Difference [%]	-63.92	-75.83	-7.89
Ratio [Bonded/Dis-bonded]	2.77	4.14	1.09

Table 4-6: Summary of ultimate load ratios for bonded compared to dis-bonded for 114 mm (4.5 in.) and 165 mm (6.5 in.) thick panels

Type of Panel	Axial Load	Transverse Load	Racking Load
114mm (4.5 in.) thick	2.73	4.77	0.78
165mm (6.5 in.) thick	2.77	4.14	1.09

Figures 4-9 to 4-12 present typical axial load versus vertical deformation behaviour for 114mm (4.5 in.) and 165mm (6.5 in.) thick PUR SIPs. Two graphs have been plotted for each panel thickness test. One curve shows the axial load versus deflection behaviour of the panel read from the top plate linear potentiometer, while the other one shows the mid-height deflection. Inclusive curves showing all of the five panels tested are shown in Figures D-1 to D-4 in Appendix D. As seen in the curves, regardless of the panel thickness, dis-bonded panels exhibited load versus deflection behaviour with lesser slope indicating reduced stiffness for the partially dis-bonded panels. While a basic implication is less load capacity, this has to be considered within the context of what an actual design load would be which will be dependant of the building size and environmental loads.

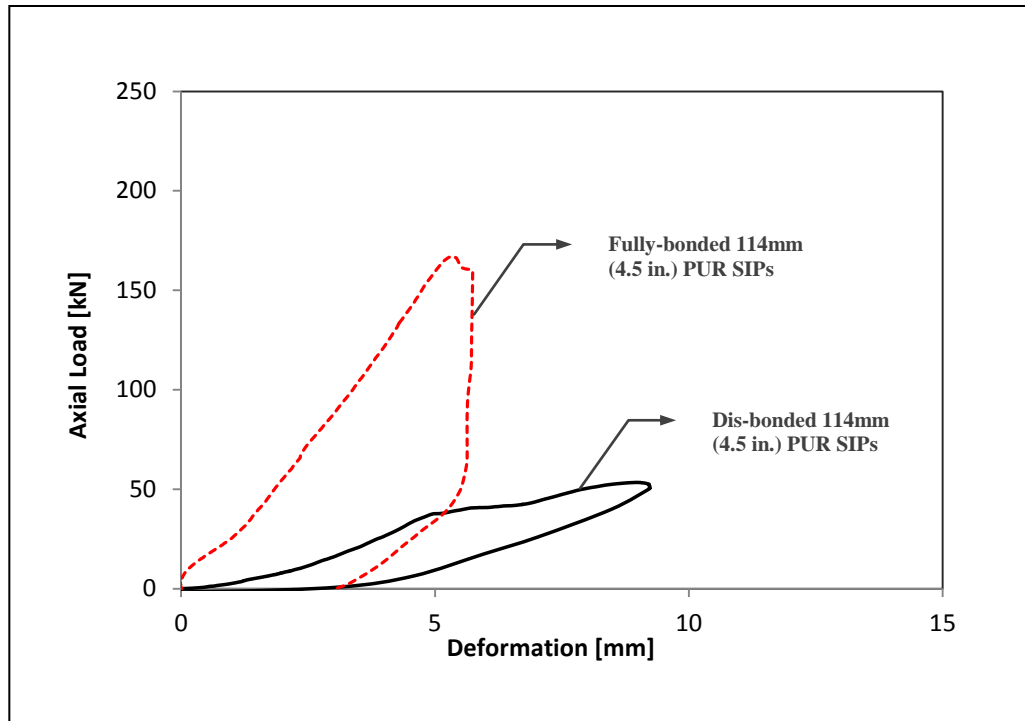


Figure 4-9: Typical axial load resistance of 114mm (4.5 in.) thick dis-bonded PUR SIPs compared to fully-bonded panels with the same thickness. This graph shows the overall shortening of the SIP under axial load (top linear potentiometer only)

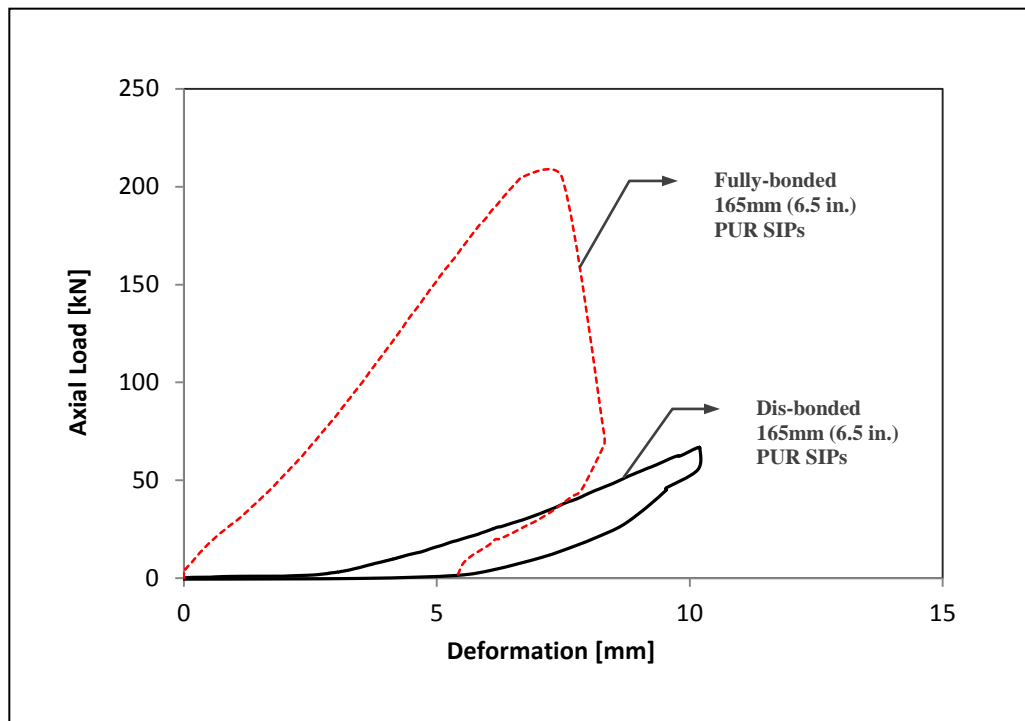


Figure 4-10: Typical axial load resistance of 165mm (6.5 in.) thick dis-bonded PUR SIPs compared to fully bonded panels with the same thickness. This graph shows the overall shortening of the SIP under axial load (top linear potentiometer only)

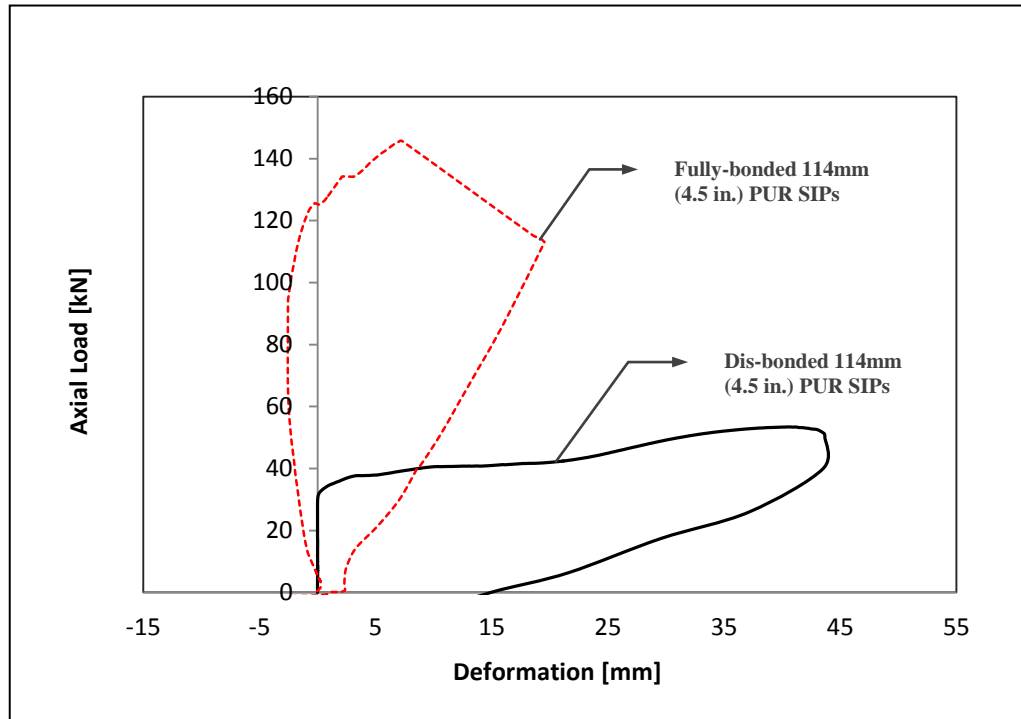


Figure 4-11: Typical axial load resistance of 114mm (4.5 in.) thick dis-bonded PUR SIPs compared to fully bonded panels with the same thickness. This graph shows the overall shortening of the SIP under axial load mid-left linear potentiometer only). The first few millimetres of negative deformation is due to slight rotation of the I beam (located at the 1/3 of the panel thickness) before it is fully stabilized on under applied load

As seen in Table 4-7, under the axial loads, 114 mm (4.5 in.) thick dis-bonded PUR SIPs shortened about 80% more than the fully-bonded panels. As for the 165 mm (6.5 in.) thick PUR SIPs, the overall shortening before failure was about 100%, suggesting the thicker panels experienced about 26% more shortening due to application of axial loads.

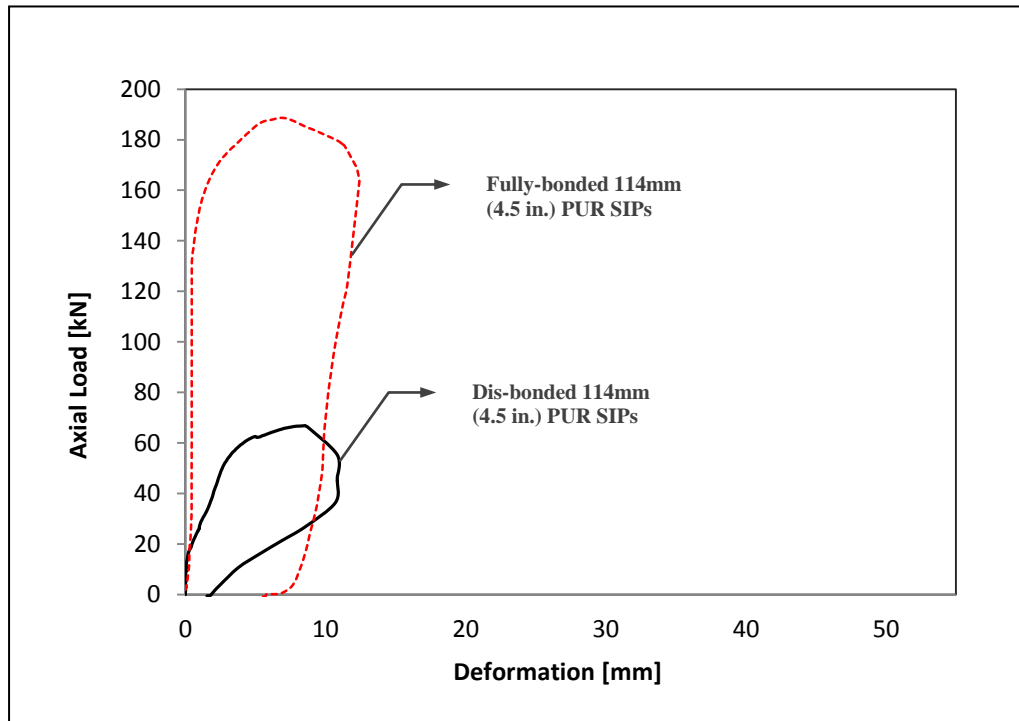


Figure 4-12: Typical axial load resistance of 114mm (4.5 in.) thick dis-bonded PUR SIPs compared to fully bonded panels with the same thickness. This graph shows the overall shortening of the SIP under axial load (mid-left linear potentiometer only)

Table 4-7: Vertical deformation of PUR SIPs under axial load

Thickness of the Panel	Average max axial deformation of dis-bonded PUR SIPs [mm]	Average max axial deformation of fully bonded PUR SIPs [mm]	Ratio of fully bonded to disbonded
114mm (4.5 in.)	8.19	4.57	1.79
165mm (6.5 in.)	9.66	4.82	2.00

Part 9 of the NBCC (NRC, 2010), Canadian Standard Association (CSA 086, clause 4.5.2) and Wood Design Manual (2010) suggest a maximum acceptable mid-span elastic deflection of $L/180$ for structural members under the load combinations of serviceability

limit states. In the case of 2438 mm (8 ft.) tall SIPs tested in this experiment, the acceptable deflection must be limited to 13.6 mm (2438/180). As seen in Table 4-8, fully-bonded and dis-bonded panels with different thicknesses satisfy the deflection limits under axial load except for the dis-bonded 114 mm (4.5 in.) thick PUR SIPs. This means thinner panels (114mm, 4.5 in. thick) experienced two times acceptable deflection (13.6 mm) prior to failure.

When the axial load capacity of the panels is considered, even dis-bonded thinner (114mm, 4.5 in. thick) panels will have enough load carrying capacity for a small single storey residential building (See Appendix D). Nevertheless, dis-bonded panels (114mm, 4.5 in. thick) do not satisfy the deflection limit criterion. On the other hand, with regards to axial load conditions, 33% dis-bond in thicker (165mm, 6.5 in. thick) panels seems to meet both strength and deflection limits of the panel required by the codes.

4.4.2 Transverse Load Test Results

Figures 4-13 and 4-14 represent typical load versus lateral deflection behaviour of 114 mm (4.5 in.) and 165mm (6.5 in.) thick panels when subjected to transverse loads to failure. Inclusive curves showing the behaviour of all tested panels can be seen in Figures D-5 and D-6 in Appendix D. As seen in Figures 4-13 and 4-14, dis-bonded PUR SIPs experienced more deflection before final failure demonstrating a more ductile behaviour while fully-bonded panels exhibited less deflection and a sudden failure.

Based on observations during testing, it appeared shear in the foam occurred first as evidenced by cracking within the foam-core. This was followed by failure in OSB face-sheets. Similar to the axial test results, a maximum acceptable mid-span elastic deflection was checked in accordance with NBCC (NRC, 2010), Canadian Standard Association (CSA 086, clause 4.5.2), and Wood Design Manual (2010). In the case of 2438 mm (8 ft.) tall wall panels, 50mm (2 in.) on each side of the panel was considered as the support edge resulting in a clear span of 2338 mm ($2438 \text{ mm} - 100 \text{ mm} = 2338 \text{ mm}$). Therefore, the acceptable deflection is limited to 13 mm ($2338/180$). Table 4-9 provides average deflections of all tested fully-bonded and dis-bonded panels. As seen in Table 4-9, dis-bonded 114 mm (4.5 in.) and 165 mm (6.5 in.) panels experienced 39 and 34% more deflections than the fully-bonded panels respectively.

Appendix C of the NBCC (NRC, 2010) suggests a wind load of 0.42 kPa for the city of Winnipeg area in Canada. Multiplying the pressure by the area of each panel ($0.42 \times 1.22 \text{ m} \times 2.44 \text{ m}$) yields a service load of 1.25 kN which is smaller than all the values presented in Table 4-10. This means even with 33% dis-bond, all the panels satisfy the load capacity requirements at the maximum deflection of $L/180$ allowed by the building code.

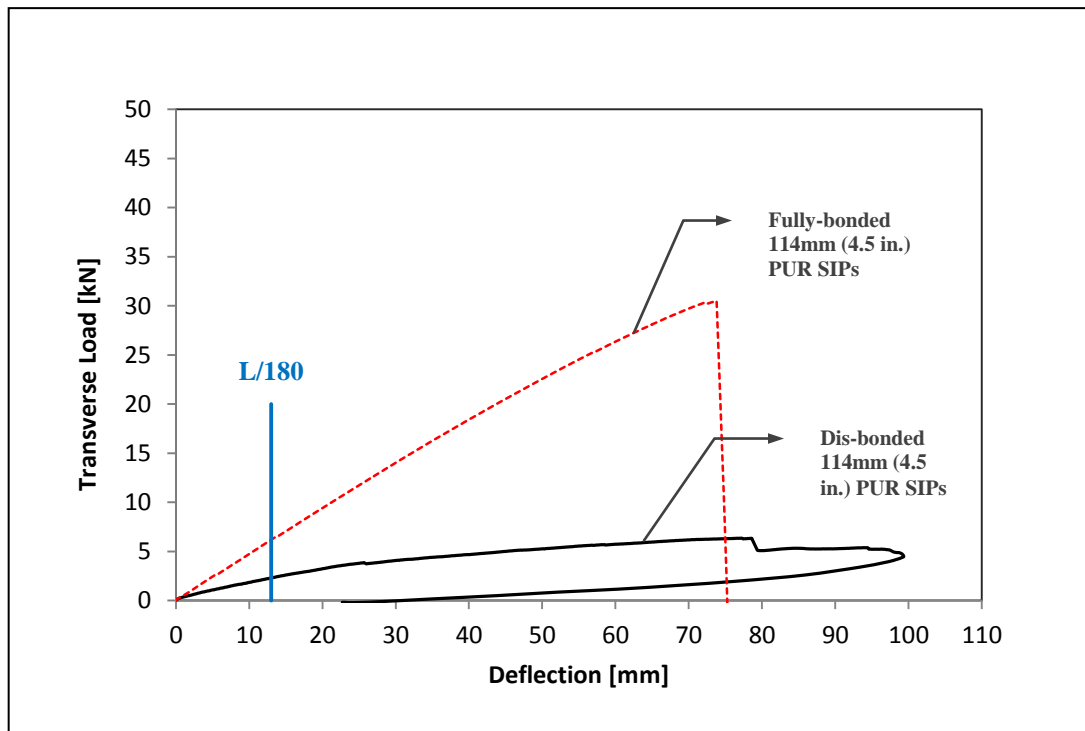


Figure 4-13: Typical transverse load resistance of 114mm (4.5 in.) thick dis-bonded PUR SIPs compared to fully bonded panels with the same thickness. Red dotted line represents fully bonded panels and solid line represents dis-bonded panels. The vertical blue line indicates the serviceability deflection limit of L/180 (13 mm)

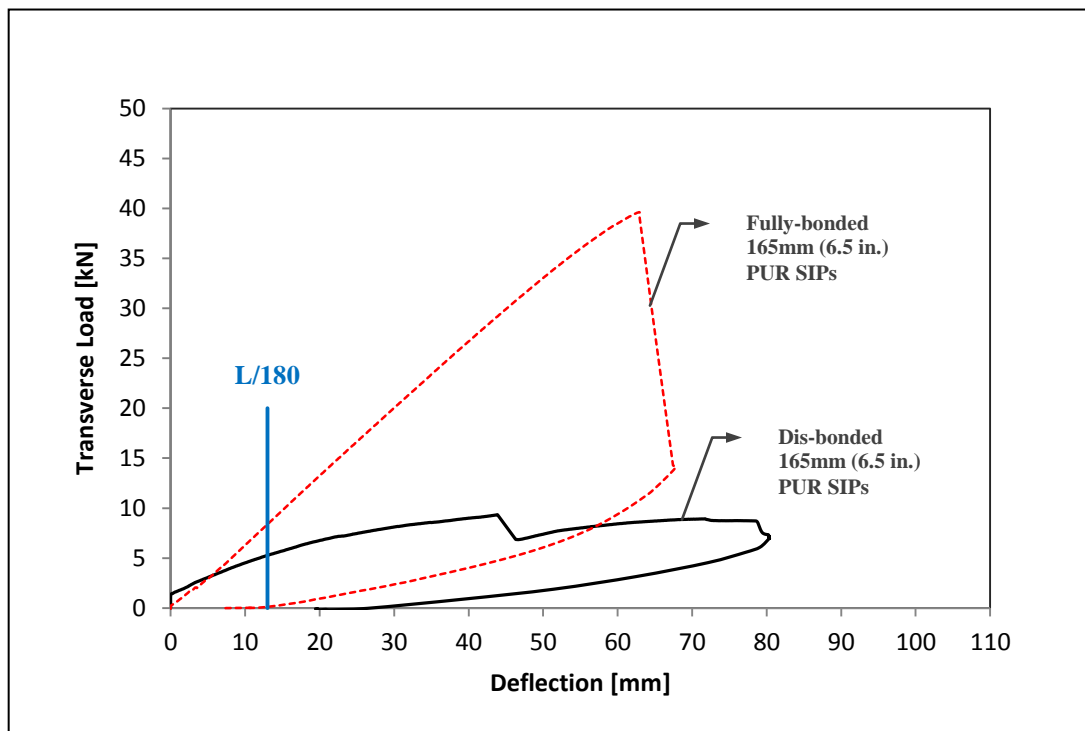


Figure 4-14: Typical transverse load resistance of 165mm (6.5 in.) thick dis-bonded PUR SIPs compared to fully bonded panels with the same thickness. The vertical blue line indicates the serviceability deflection limit of L/180 (13 mm)

Table 4-9: Average maximum deflection of the fully bonded 114mm (4.5 in.) and 165mm (6.5 in.) thick PUR SIPs vs. dis-bonded panels in transverse load tests (at the time of failure)

Thickness of the PUR SIP	Average max. deflection of dis-bonded PUR SIPs [mm]	Average max. deflection of fully-bonded PUR SIPs [mm]	Difference [%]
114mm (4.5 in.)	101.00	72.60	39.11
165mm (6.5 in.)	80.60	59.99	34.36

Table 4-10: Average maximum load at the deflection limit of L/180 for panels tested for transverse load capacity compared to the code requirement of 1.25 kN maximum load

Thickness of the PUR SIP	Average max load at the deflection limit of L/180 [kN]	
	Dis-Bonded	Fully Bonded
114mm (4.5 in.)	2.25	6.15
165mm (6.5 in.)	4.57	9.05

Based on the data presented in Table 4-4 and 4-5, 33% dis-bonding between the PUR foam-core and the OSB face-sheets of SIPs caused 4.77 times less transverse load capacity in 114mm (4.5 in.) thick PUR SIPs (6.37 vs. 30.40 kN) and resulted in 4.14 times less transverse load capacity in 165mm (6.5 in.) thick PUR SIPs (9.29 vs. 38.43 kN).

4.4.3 Racking Load Test Results

Figures 4-15 and 4-16 represent typical load versus lateral deformation behaviour of 114 mm (4.5 in.) and 165mm (6.5 in.) thick panels when subjected to racking loads to failure. Unlike fully-bonded panels, the deflection of the dis-bonded panels tested for racking load capacity was not limited only to in-plane deformation. An image of dis-bonded panel subjected to a racking load is shown in Figure 4-17. It can be seen that out-of-plane buckling occurred at the panel connection. Buckling behaviour of the OSB facing sheets at the connection was not observed in fully bonded panels. It is postulated that the reason for this is the bond between the foam and the OSB face sheets is resisting out-of-plane behaviour.

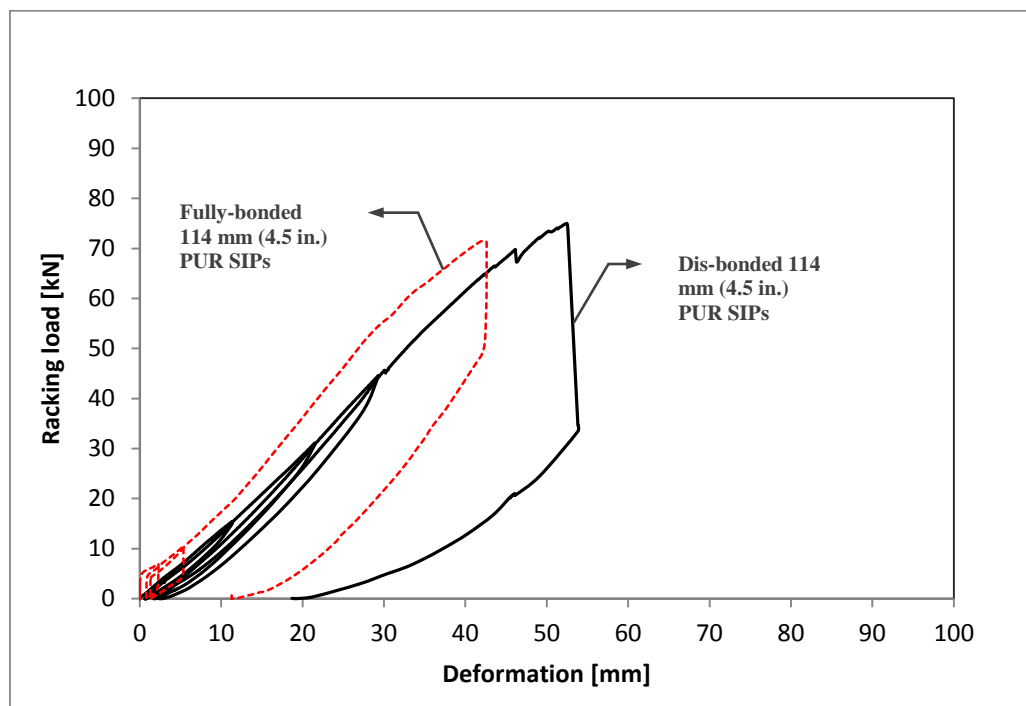


Figure 4-15: Typical racking load resistance of 114mm (4.5 in.) thick dis-bonded PUR SIPs compared to fully bonded panels with the same thickness

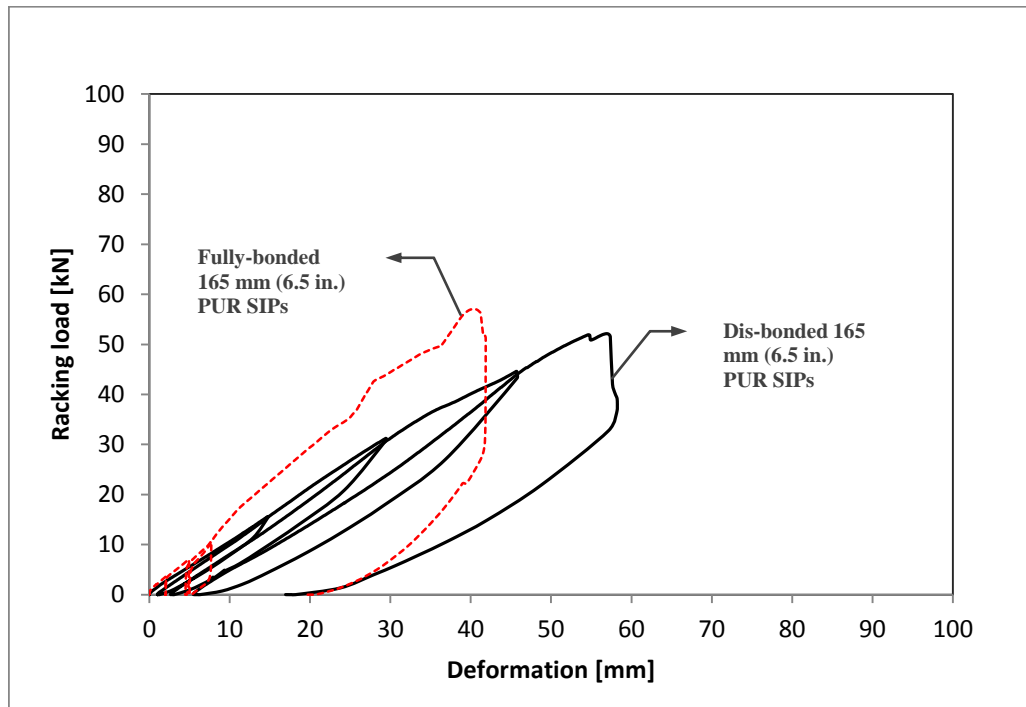


Figure 4-16: Typical racking load resistance of 165mm (6.5 in.) thick dis-bonded PUR SIPs compared to fully bonded panels with the same thickness



Figure 4-17: Racking test on dis-bonded in progress. Buckling of the dis-bonded area of the left panel can be seen

Based on data contained in Table 4-4, dis-bonded 114mm (4.5 in.) thick panels handled about 29% more maximum racking load than the fully-bonded panels with the same thickness (68.45 vs. 53.14 kN) when the deflection is disregarded. Figure 4-18 compares the trend lines of the zero to failure curves of the dis-bonded panels (114mm, 4.5 in. thick) and fully-bonded panels. As seen in the figure, despite the overall higher maximum racking load capacity, dis-bonded thinner panels clearly have less stiffness and rigidity and exhibit more deflection before failure due to no out-of-plane resistance in the dis-bonded region.

On the other hand, as seen in Table 4-5, dis-bonded 165mm (6.5 in.) thick panels handled about 8% less racking load than the fully-bonded panels with the same thickness. This can also be seen in Figure 4-19 where the trend lines of the zero to failure curves of the dis-bonded panels are compared to the fully-bonded panels (165mm, 6.5 in. thick) where minor difference in slopes is obvious.

Out-of-plane buckling of dis-bonded panels under racking loads was measured on both sides of the panels in the middle zone on both singles panels (Figure 4-8). Based on the data obtained from linear potentiometers, unlike 165mm (6.5 in.) thick panels, all the buckling values of 114mm (4.5 in.) thick PUR SIPs were in excess of an $h/360$ deflection criterion when exposed to racking loads.

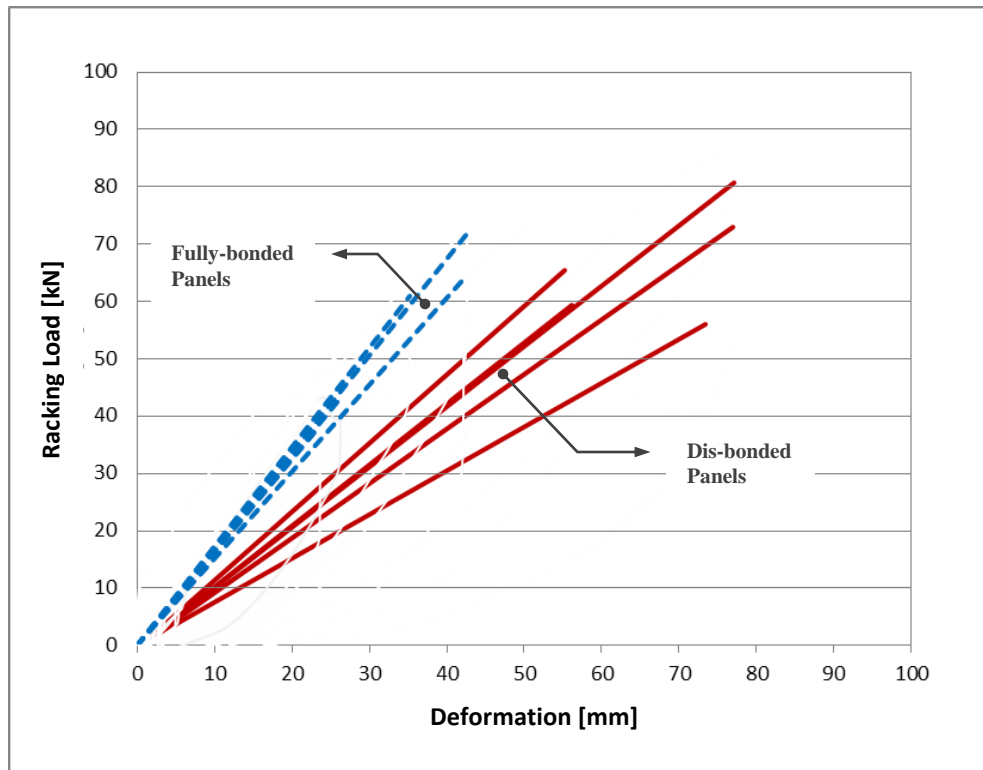


Figure 4-18: Racking load trend-line comparison between dis-bonded panels and fully bonded panels for 114mm (4.5 in.) thick PUR SIPs

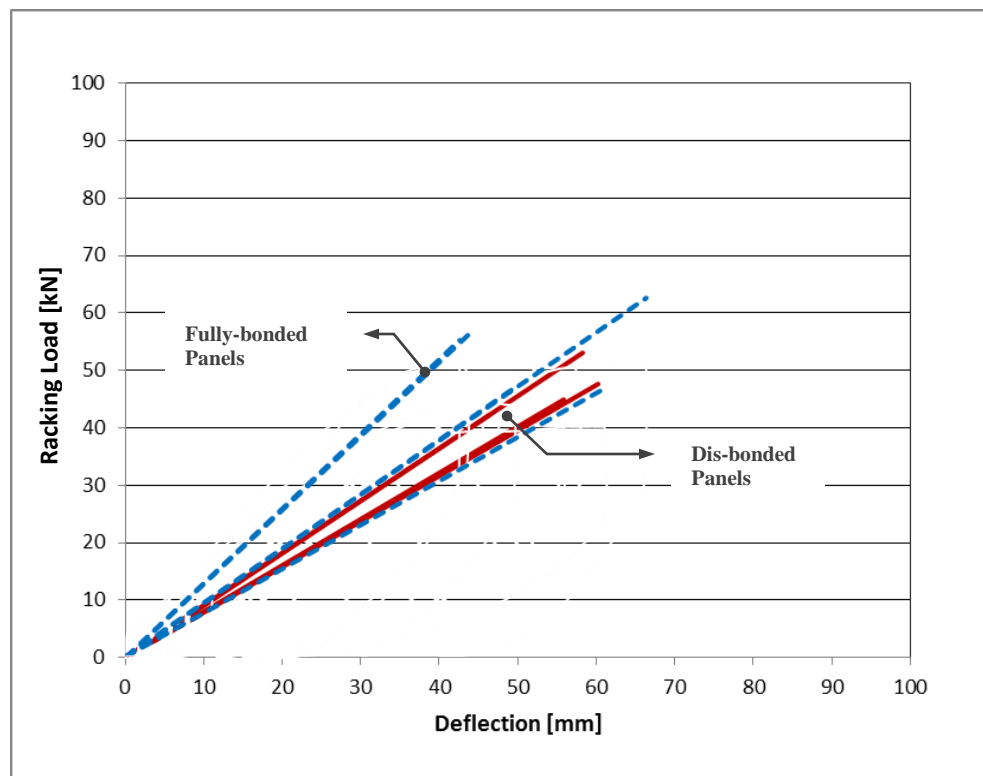


Figure 4-19: Racking load trend-line comparison between Dis-bonded panels and fully bonded panels for 165mm (6.5 in.) thick PUR SIPs

4.5 Conclusions

The following conclusions can be drawn from the experiments conducted in this part of the research study. In the case of 165 mm (6.5 in.) thick PUR SIPs, 33% dis-bond between the PUR foam-core and the OSB face-sheets caused the following result:

- a) Dis-bonded panels exhibited an average of 2.77 times less ‘axial load’ capacity when compared to disbonded panels (71.26 vs. 197.5 kN). Vertical displacement of dis-bonded panels was an average of 2 times (9.66 vs. 4.82 mm) more than fully-bonded panels. Based on observation during the test, most of the deformation occurred in the form of skin (OSB) out-of-plane buckling in the dis-bond region of the panel
- b) An average 4.14 times reduction in ‘transverse load’ capacity of the panel (38.43 vs. 9.29 kN) compared to brand new fully-bonded SIP. Dis-bonded panels deflected an average 1.3 times more than fully-bonded panels (34.3%) in mid-height of the panels. Even with 33% dis-bond, panels still satisfy load-carrying capacity requirements at a maximum deflection criterion of $L/180$.
- c) Thirty percent dis-bond between the foam-core and the OSB face-sheets over area of both sides of each SIP caused an average 1.1 times reduction in ‘rack-

ing load' capacity of the panel (48.56 vs. 44.73 kN) compared to a brand new fully-bonded SIP. Dis-bonded 165 mm (6.5 in.) thick PUR SIPs handled only a slightly higher ultimate racking load before failure compared to fully-bonded panels. This means that 33% dis-bond in 114 mm (4.5 in.) thick PUR SIPs has minimal effect on the racking load capacity of the panels.

In the case of 114 mm (4.5 in.) thick PUR SIPs, 33% dis-bond between the PUR foam-core and the OSB face-sheets caused the following results:

- a) An average 2.73 times reduction in 'axial load' capacity of the panel compared to a brand new fully-bonded PUR SIPs (159.97 vs. 58.7 kN). Dis-bonded panels shortened an average 1.79 times (8.19 vs. 4.57 mm) more than fully-bonded panels and experienced 4.4 times more deflection in mid-height compared to fully-bonded panels (27.89 vs. 6.34 mm).
- b) An average 4.77 times reduction in 'transverse load' capacity of the panel (30.40 vs. 6.37 kN) compared to a brand new fully-bonded SIP. Dis-bonded panels deflected an average 1.4 times (39.1%) more than fully-bonded panels at the mid-height of the panels. Even with 33% dis-bond, tested panels still

satisfy load carrying capacity requirements at the maximum deflection of $L/180$ allowed by the building codes.

- c) Dis-bond between the foam-core and the OSB face-sheets over both sides of each SIP caused an average 1.29 times increase in ‘racking load’ capacity of the panel (68.54 vs. 53.14 kN) compared to a brand new fully-bonded SIP. Although dis-bonded 114 mm (4.5 in.) thick PUR SIPs handled more ultimate racking load before failure, they experienced more deflection before failure and showed less stiffness than the fully-bonded PUR SIPs with a similar thickness.

Chapter 5

Experimental Measurement of the Flexural Creep Behaviour of PUR SIPs

5.1 Introduction

This part of the study investigated creep behaviour of two different thicknesses of PUR SIPs under sustained load. For the ‘time’ or creep test duration, Huang and Gibson (Huang & Gibson, 1990) proposed a thousand-hour period for the creep test of sandwich beams with polymer foam-cores. They based their findings on Just (1983) and Davies (1987) who suggested creep parameters estimated from a thousand-hour test can give a good prediction of creep of specimen after 10 years. Laufenberg et al. (1999) also conducted series of creep tests on some composite panel products. They monitored deflection of their specimens for 8 weeks (56 days) in order to correspond to a typical snow load in service condition.

This author was not able to find a specific time-length or definition for long-term creep test of wood-based sandwich materials in any research paper or standard. Some studies (Laufenberg, et al., 1999) refer to a six months creep test as a long-term test, while others (Taylor, 1996) suggest a three or nine months (Zarghooni, 2009) as a long-term test.

5.2 Material Description

As seen in Table 5-1, two sets of three PUR SIPs with different thickness were tested under sustained dead-load for a period of 8 weeks. The panels were oriented in creep test apparatus the same way they are manufactured in the manufacturing facility.

The panels tested for creep were manufactured by Emercor Ltd. Alberta, Canada, randomly sampled and shipped to the University of Manitoba. Based on technical requirements for closed-cell polyurethane and polyisocyanurate foam thermal insulation tested to CAN/ULCS704-03 and CAN/ULC-S704-11 (Standards Council of Canada, 2011) the foam-core must meet and demonstrate the minimum strength characteristics and specifications suggested in Table 5-2. Actual mechanical properties of the foam-core provided by the polyurethane foam manufacturer are contained in Table 5-3. The OSB face-sheets used by the SIP manufacturer to fabricate the PUR SIPs were stamped as 1R24/2F16/W24 with a nominal thickness of 11 mm (7/16 or 0.418 in.). The mechanical properties for OBS sheets, as supplied by the manufacturer are specified in Table 5-4. Table 5-5 also provides the physical properties of type 1R24/2F16/W24 OSB specified by OSB Design Manual (SBA, 2004).

Table 5-1: Specification of PUR SIPs tested for flexural creep behaviour in accordance with ASTM E1803 (ASTM, 2006), ASTM E72 (ASTM, 2015) and APA (APA, 2013)

Test Number	Test ID	Panel dimensions: width x height x overall thickness		OSB Thickness mm [in.]
		mm	In.	
1	CT45-1	1220x2440x114	48x96x4.5	11 [7/16]
2	CT45-2	1220x2440x114	48x96x4.5	11 [7/16]
3	CT45-3	1220x2440x114	48x96x4.5	11 [7/16]
4	CT65-1	1220x2440x165	48x96x6.5	11 [7/16]
5	CT65-2	1220x2440x165	48x96x6.5	11 [7/16]
6	CT65-3	1220x2440x165	48x96x6.5	11 [7/16]

Table 5-2: Technical requirements for closed-cell polyurethane and Polyisocyanurate foam thermal insulation tested to CAN/ULCS704-03 and CAN/ULC-S704-11 (Standards Council of Canada, 2011)

Properties	Physical Property Requirements		
	Type 1	Type 2	Type 3
Compressive strength, min, kPa	110	140	170
Tensile strength, min, kPa, perpendicular to the plane of the face-sheet	24	35	35
Flexural strength, min, kPa	170	275	275
Thermal resistance (m ² C/W):	after conditioning, min per 25 mm (1 in.) thick	0.97	
	long-term thermal resistance (LTTR), min. for 50 mm thick product ¹	1.90 (CAN/ULCS 704-03)	
		1.80 (CAN/ULC S704-11)	

1. The LTTR of the material shall be reported for the purpose of energy calculations. The LTTR value shall also be reported for the 25 mm and 75 mm thick products

Table 5-3: Physical properties of the polyurethane foam-core provided by the foam manufacturer

Property	Value	Unit
Core Density	31 (1.94)	kg/m ³ (pcf)
Density of molded panel	36 (2.25)	kg/m ³ (pcf)
Actual foam density based on SIP manufacturer's in-situ tests	40 (2.48)	kg/m ³ (pcf)
Perpendicular Compressive Strength at 10% deflection	110 (16)	kPa (psi)
Perpendicular Compressive Modulus	2985 (433)	kPa (psi)
Parallel Compressive Strength at 10% deflection	214 (31)	kPa (psi)
Parallel Compressive Modulus	4971 (721)	kPa (psi)
Porosity (Closed Cells)	92	%

Table 5-4: Physical properties of the OSB used in manufacturing of the tested PUR SIPs

Mechanical properties (dry, as shipped)	MPa	psi
Modulus of rupture (parallel)	29	4200
Modulus of rupture (perpendicular)	12.4	1800
Modulus of elasticity (parallel)	5500	800,000
Modulus of elasticity (perpendicular)	1500	225,000
Internal bond	0.345	50

Table 5-5: Mechanical properties of the OSB used to manufacture the tested PUR SIPs

Property	Value	Unit
Bending Moment Resistance, M_r	228	N·mm/mm
Axial Tensile Resistance, T_r	57	N/mm
Axial Compressive Resistance, P_r	67	N/mm
Shear Through Thickness Resistance, V_r	44	N/mm
Planar Shear Resistance Due to bending, V_{rb}	4.6	N/mm
Bending Stiffness (EI)	730000	N·mm ² /mm
Axial Stiffness (EA)	38000	N/mm
Shear Through Thickness Rigidity, G	11000	N/mm

* Orientation of applied force relative to panel length = 0°

5.3 Creep Pre-Tests

Prior to creep tests, it was of interest to gain some insight into relative compressive behavior of the two panel thicknesses and an indication of modulus of elasticity. A series of tests were conducted on PUR SIP coupons. Six coupons of 165mm (6.5 in.) and six coupons of 114mm (4.5 in.) thick PUR SIPs with the area of 152 by 152 mm (6 x 6 in.) cut from different brand new panels were exposed to axial compressive load with a constant speed of 2 mm/min. Compression tests were limited to 25 mm (1 in.) and the specimens were unloaded after the deflection limit had reached (Figure 5-1). The rebound percentage was also monitored and measured at the time of failure. The amount of rebound was measured up to 56 days (8 weeks) after the completion of the compression tests. Figure 5-2 represents the load deformation behaviour of all tested coupons.

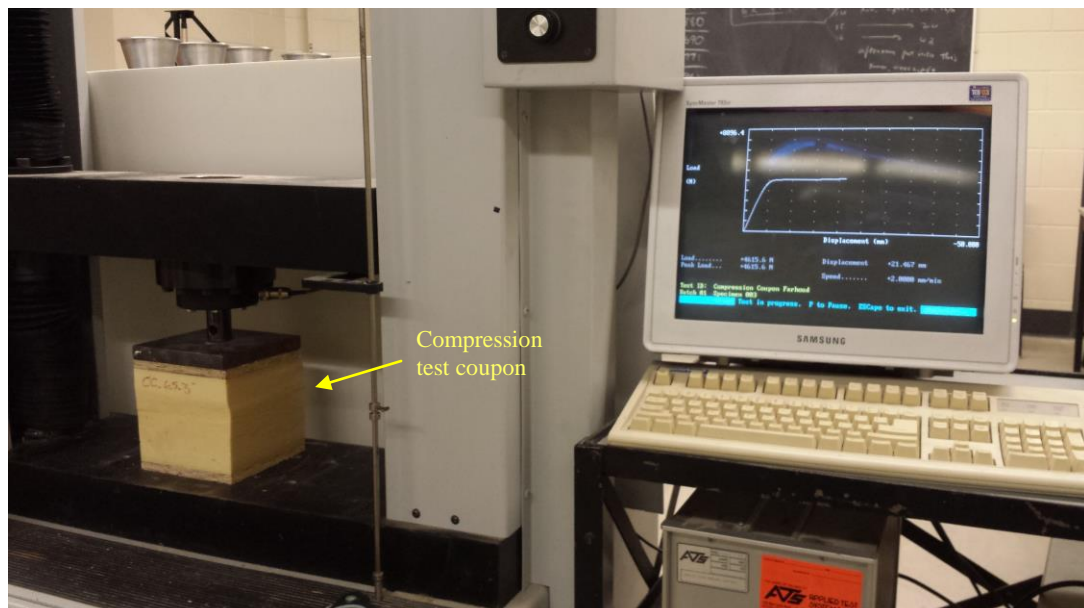


Figure 5-1: PUR SIP coupon under compression load test with a maximum deflection limited to 25mm (1 in.)

Although compared to thicker (165mm, 6.5 in.) PUR SIP coupons/cubes, thinner (114mm, 4.5 in.) samples seem to have higher initial stiffness as indicated by their steeper load vs. deflection curve (an average of 1520 vs. 929 N/mm) (Figure 5-2). The overall difference in compressive strength limits to only 9.7% (Table 5-6) between the two specimen thicknesses. With increasing core thickness, deformation is greater for the same given compressive force.

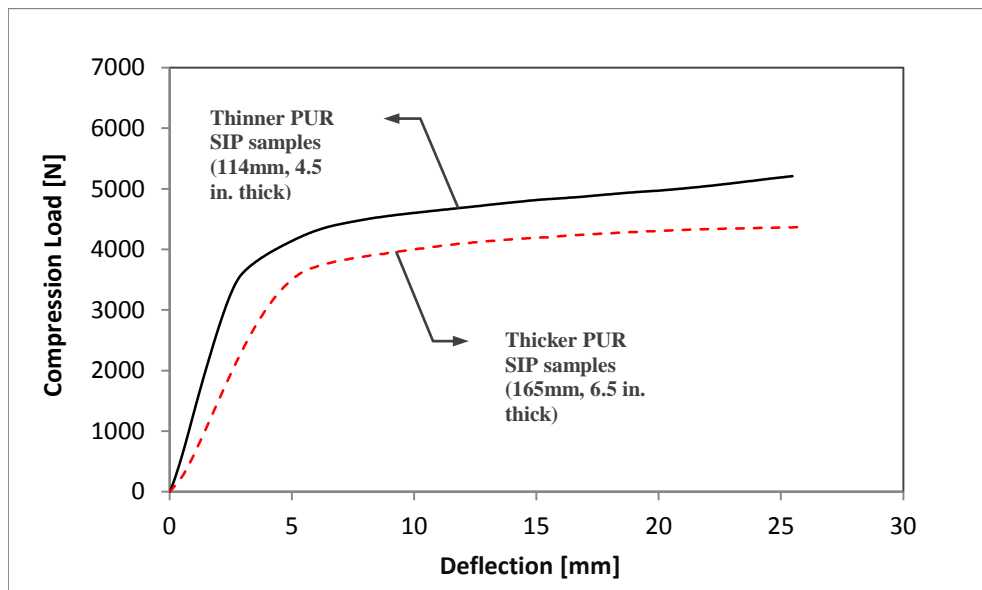


Figure 5-2: A typical compressive test conducted on 165mm (6.5 in.) and 114mm (4.5 in.) thick PUR SIP coupons with the area of 152 by 152 mm (6 x 6 in.) and 25mm (1 in.) deflection limit

Table 5-6: Compressive stress handled by PUR SIP coupons with different thicknesses

Thickness of the PUR SIP coupon	Average max compression load [N]	Average max compressive stress [MPa]	Difference [%]
114mm (4.5 in.)	5101.27	0.22	9.69
165mm (6.5 in.)	4650.73	0.20	

The rebound behaviour of the compressed coupons was observed to study the resiliency of the PUR SIPs tested in this thesis under compressive loads. Tested coupons were monitored for 56 days (8 weeks) in order to measure the rebound amount and compare the behaviour of the two different PUR SIP coupons tested. Table 5-7 represents the data compiled from rebound/deflection measurements of the compression coupons tested. As seen in Table 5-7, Figure 5-3 and Figure 5-4, right after the removal of the compression load, thinner panel coupons (114mm, 4.5 in. thick) exhibited about 15% shortening compared to their original thickness (114 vs. 99.5 mm) while thicker panels (165mm, 6.5 in. thick) shortened only 6% compared to their original thickness (165 vs. 155.5 mm). After 56 days (8 weeks) of relaxation, thicker panels rebounded about 97% (160.67 vs. 165 mm), while the thinner panels rebounded 92% compared to their original thickness (104.83 vs 114 mm).

Table 5-7: Compression and rebounding values of PUR SIP coupons under axial compressive load

Thickness of the PUR SIP coupon	Average Compression [mm]	Average Rebound [mm]			Total Rebound [%]
	Right after removal of the load	After 24 hours	After 30 days	After 56 days (8 weeks)	After 57 days (8 weeks)
114mm (4.5 in.)	99.5	104.17	104.67	104.83	88.55
165mm (6.5 in.)	155.5	160.33	160.33	160.67	95.02



Figure 5-3: Relaxation and rebound behaviour of 165mm (6.5 in.) thick PUR SIP coupons under compressive load



Figure 5-4: Relaxation and rebound behaviour of 114mm (4.5 in.) thick PUR SIP coupons under compressive load

5.4 Creep Test Method

Based on the definition provided in ASTM C480 (ASTM, 2008), a flexural creep test of sandwich construction involves subjecting a beam of the specimen to a sustained force normal to the plane of the beam, using either a 3-point or a 4-point loading fixture. The above mentioned ASTM test method standard, along with the available guideline provided by the National Research Council Canada (NRC) and The Canadian Construction Materials Centre (CCMC) that describe the technical requirements and performance criteria for the assessment of stressed skin panels for walls and roofs, were adopted as the test standards for the creep tests. Standard AC04 (ICCES, 2011) provided by ICC Evaluation Services (subsidiary of the International Code Council in the United States), was also reviewed in the development of this test. Figure 5-5 and Table 5-8 represent the loading schedule for the short-term creep test of SIPs recommended by the technical guide for stressed skin panels for walls and roofs published in 2007 by the National Research Council Canada (NRC).

NRC's technical guide (2007) also defines the following criteria for the determination of creep and recovery performance under load and ultimate load capacity of SIPs:

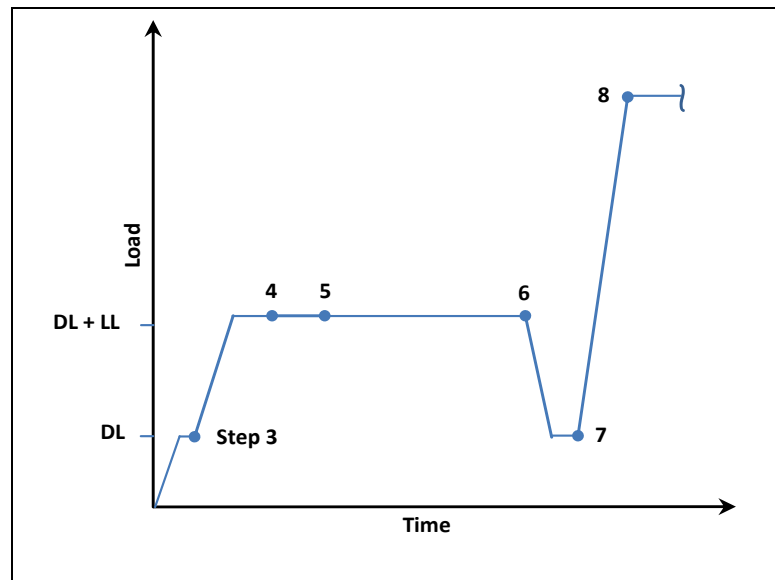


Figure 5-5: Loading scheme for short-term creep test of SIPs (NRC, 2007)

- Deflection under the action of live loads

The maximum difference in the deflections measured in Step 4 of Table 5-8 (dead load(s) plus live load) and Step 3 (dead load only) shall not exceed $L/360$ of the span.

- Creep deflection criterion

The difference in deflection at any one point, as measured between Step 6 and Step 4 of Table 5-8, shall not exceed 25% of that measured in Step 4 (attributable to the creep produced by the dead load(s) plus live load in place for approximately 24 hours).

- Recovery from creep criterion

The lack of recovery determined by the maximum difference in the deflections measured in Step 3 (dead load(s) only) Table 5-8 and that measured in Step 7 (on removal of live load) Table 6 shall not exceed $L/1440$ of the span.

- Sustained load capacity

The system shall survive the load exerted in Step 6 of Table 5-8 without collapse. The system shall then be taken to destruction, and the maximum load and mode of failure shall be recorded. Based on NRC's recommendation guideline (2007), a product is considered acceptable for flexural creep capacity only if the results of all tests on three panels successfully meet the above mentioned criteria. The guideline recommends one additional panel to be tested if the results of one of the tests do not meet the criteria.

The design is considered unacceptable and design values must be adjusted if the results of the retest or of two of the original tests do not meet the criteria. Since the creep tests conducted on PUR SIPs were subjected to long-term loads, instead of the short-term creep test procedure expressed in Table 5-8, steps stated in Table 5-9 were followed.

Table 5-8: Loading schedule for short-term creep test of SIPs (NRC, 2007)

Step	Task (refer to Figure 5-3)
1	Measure the moisture content of wood members at a sufficient number of points to give a representative picture of the overall moisture condition of the members at the time of the test. If members are not accessible, moisture contents may be obtained shortly after the test.
2	Take zero deflection readings before applying any load.
3	Apply test load (D), representing the superimposed dead load, at the uniform rate without shock to the system. At the conclusion, following a full five minutes (300 s) for the deflection to stabilize, take the deflection readings. Photograph the assembly.
4	Apply test load (L), representing the superimposed live load, at the uniform rate without shock to the system. At the conclusion, following a full five minutes (300 s) for the deflection to stabilize, take the deflection readings. For members continuous over two spans, the test load (L) shall be placed on one span only. Photograph the assembly.
5	Measure the deflections at one hour from the beginning of loading (Step 3).
6	Maintain these loads (D + L) for an additional full 23 hours and take deflection readings again
7	Remove test load (L) [Design Live Load] and take deflection readings five minutes (300 s) after its complete removal.
8	Reapply the test load (L) and increase the load to twice the total of all loads described in Table 1, i.e. 2 (D + L), and maintain for 24 hours. Photograph the assembly. If applicable, at the conclusion of this period and before removing the load, take close-up photographs of any portion of the assembly that may show visible distress.
9	<i>Note: For members continuous over two or more spans, this overload shall be applied to each span, one span at a time, while maintaining test loads (D) and (L) on the other span, and then to all spans at the same time. Maintain each complete loading cycle for 24 hours.</i> Take sufficient samples from the members for measuring relative density to give a representative measure of the overall density of the lumber and panel materials used in the construction of the panel.

5.4.1 Duration of Applied Loads

Table 5-10 adopted from NRC's guideline (NRC, 2007) was used in order to calculate the dead and live loads required to be applied to the specimens. Five panels of each

thickness of PUR SIPs were weighted in order to find the average self-weight of the specimens.

Table 5-9: Loading schedule for long-term creep test of SIPs

Step	Task
1	Measure the moisture content of wood members at a sufficient number of points to give a representative picture of the overall moisture condition of the members at the time of the test. If members are not accessible, moisture contents may be obtained shortly after the test.
2	Take zero deflection readings before applying any load.
3	Apply test load (D), representing the superimposed dead load, at the uniform rate without shock to the system. At the conclusion, following a full five minutes (300 s) for the deflection to stabilize, take the deflection readings.
4	Apply test load (L), representing the superimposed live load, at the uniform rate without shock to the system. At the conclusion, following a full five minutes (300 s) for the deflection to stabilize, take the deflection readings.
5	Measure the deflections at one hour from the beginning of loading (Step 3).
6	Maintain these loads (D + L) for an additional 8 weeks (1344 hrs) and take deflection readings again
7	Remove test load (L) [Design Live Load] and take deflection readings five minutes (300 s) after its complete removal.
8	Remove test load (D) and take deflection readings five minutes (300 s) after its complete removal.
9	Remove test load (D) and take deflection readings five minutes (300 s) after its complete removal.
10	Take sufficient samples from the members for measuring relative density to give a representative measure of the overall density of the lumber and panel materials used in the construction of the panel.

Table 5-10: Flexural creep test loads recommended by NRC's guideline (NRC, 2007)

Test Load	Weight (kN/m ²)	Parameter Simulated by the Test Load
Dead Load	0.5	Dead weight of superimposed finished roofing and ceiling materials. (For heavier roofing materials this value must be increased, e.g., to 1 kN/m ² for concrete tile.)
Live Load	The anticipated snow and rain loads for the anticipated geographical areas.	Design live load

The test panels were weighed:

- Average weight of a 165 mm (6.5 in.) thick PUR SIP = 65 kg (Table 5-11)
- Average weight of a 114 mm (4.5 in.) thick PUR SIP = 57 kg (Table 5-11)
- Surface area of a PUR SIP over the support span = $1.220 \times 2.360 = 2.879 \text{ m}^2$
- $0.5 \text{ kPa} = 500 \text{ N/m}^2 = 51 \text{ kg/m}^2$ (Dead weight of superimposed finished roofing and ceiling materials)
- $2.879 \times 51 = 146.84 \text{ kg}$
- $146.84 - 65 = 81.84 \text{ kg}$
- $146.84 - 57 = 89.84 \text{ kg}$

Therefore, the required dead load for 165 mm (6.5 in.) thick PUR SIPs was 81.84 kg (180 lbs.) and the dead load needed for 114 mm (4.5 in.) thick PUR SIPs was 89.84 kg (198 lbs.). A dead load of 500 N/m^2 (10 lbs/ft²), including self-weight of the PUR SIPs, was used to simulate roofing and ceiling material. In terms of the live load, the following equation taken from part IV of the National Building Code of Canada (NRC, 2010) was adopted as follows:

$$\text{Live load or specified Snow Load, } S = I_s[S_s(C_b C_w C_s C_a) + S_r] \quad (\text{Eq. 5.1})$$

Where:

$$I_s = 1.0 \text{ (Importance factor for snow load)}$$

$$S_s = 1.9 \text{ (1-in-50 year ground snow load in kPa)}$$

$$C_b = 0.8 \text{ (Basic roof snow load factor)}$$

$$C_w = 1.0 \text{ (Wind exposure factor)}$$

$$C_s = 1.0 \text{ (Slope factor)}$$

$$C_a = 1.0 \text{ (Shape factor)}$$

$$S_r = 0.2 \text{ (1-in-50 associated rain load in kPa)}$$

Table 5-11: Actual weight of the tested panels

Panel #	165 mm (6.5 in.) thick PUR SIP	114 mm (4.5 in.) thick PUR SIP
1	65.3	56.2
2	65.7	56.0
3	66.1	56.7
4	63.5	57.7
5	64.2	57.2
6	65.3	56.5
7	64.9	57.1
8	65.0	59.6
9	65.8	55.5
10	64.7	57.8
Average Weight	65.05 kg	57.03 kg

Inserting the above mentioned factors in Eq. 5.1, yields:

Live load or Specified Snow Load :

$$S = 1[1.9(0.8 \times 1 \times 1 \times 1) + 0.2] = 1.72 \text{ kPa} = 1720 \text{ N/m}^2$$

- Surface area of a PUR SIP over the support span = $1.220 \times 2.360 = 2.879 \text{ m}^2$
- $1720 / 2.879 = 597.43 \text{ kg}$

Therefore, the required live load for both the 165 mm (6.5 in.) and 114 mm (4.5 in.) thick PUR SIPs was 597.43 kg or 5860 N.

5.4.2 Test Procedure and Assembly

In order to accommodate the creep test frame assemblies, a chamber was built using donated PUR SIPs at the Alternative Village of the University of Manitoba. This relatively air-tight, heated, and air conditioned chamber allowed the researcher to control and maintain the ambient temperature and relative humidity as shown in Table 5-13. The specimens were tested in two sets from July to January 2014. Panels with 165 mm (6.5 in.) thickness were tested first and then 114 mm (4.5 in.) panels were tested. All panels were adequately covered with impermeable protection covers and arrived at the lab in intact/dry condition. Panels were allowed to acclimate in the lab environment for at least 3 weeks before being tested. As seen in Figure 5-6, a steel frame and pulley systems were designed, built, and employed in order to apply the calculated sustained dead and live loads to the panels. Two 10,000 lbs load cells (Omega Engineering Inc.) and two 100 mm (4 in.) linear potentiometers (Penny and Giles) were attached to each specimen to record load vs. displacement data. All three similar sized specimens were tested concurrently while an Agilent 34972A LXI DAQ was simultaneously recording all the data. The specimens were simply supported over a 2360 mm (93 in.) span. A non-standard 4-point (third-span) loading (as defined by ASTM C393/C393 (ASTM, 2011)) was adopted with the load acting on one-third of the support span to provide a 787 by 1220 mm (31 by 48

The pulley system was capable of multiplying the load to six times. Therefore, 100 kg of water created approximately 300 kg of load on each load point (total of 600 kg, very close to 597.43 kg calculated required live load) on the panel. The load magnitude was adjusted using control valves and the real time load level readings on the DAQ. Water was shut as soon as the load cells readings reached the required amount of load. Prior to each test session, moisture content of the OSB facings of all three panels was measured and recorded using a digital moisture content reader (Mastercraft SW582). Table 5-12 represents such moisture content data. Moreover, a standalone Onset U12-011 Hobo data logger (temp/RH) was installed in order to record the relative humidity and the ambient temperature of the chamber on an hourly basis (Table 5-13). Once the instrumentations and test setups were completed, the scanning started to record the zero deflection condition for at least 24 hours. This allowed the specimens to stabilize before any load was added to the system. Then, the dead load was added to the panels while the DAQ was scanning and recording the deflection every 60 seconds. The DAQ's scan rate was changed to one-hour interval after 24 hours. The live load was added 48 hours later. The scan rate was changed to 24 hour intervals 4 days after the live load was added. In addition to DAQ's recordings, the panel's deflections were also physically measured and recorded in a log-book. The live load was kept on each panel for about 8 weeks (56 days) and then removed. The dead load was removed 4 days after the removal of the live load. Scanning continued to record the re-bound amount for 5 days. Overall rebound was physically measured after 30, 60 and 90 days. Pictures were taken from all steps.

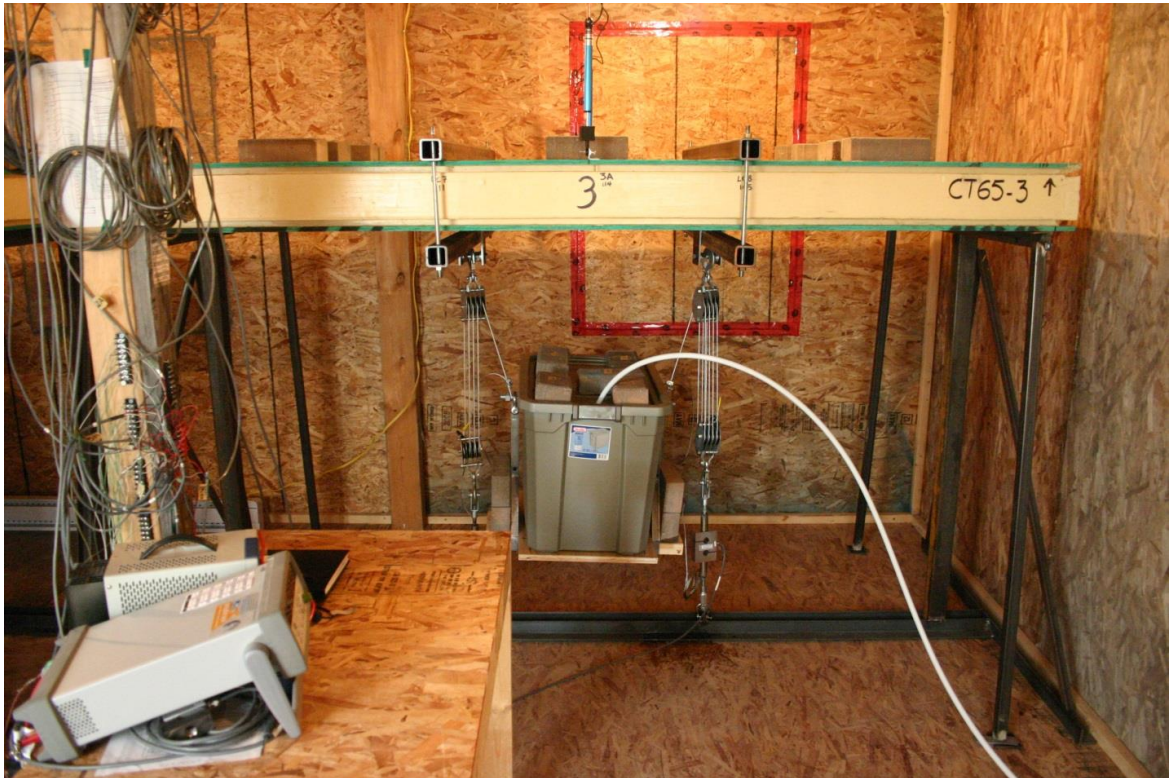


Figure 5-7: PUR SIP subjected to design creep loads



Figure 5-8: Flexural creep test of PUR SIP in progress

Table 5-12: Results of the physical measurements of the moisture content of the OSB face-sheets (dry basis) of the PUR SIPs tested for flexural creep behaviour

Reading #	Specimen ID					
	CT65-1	CT65-2	CT65-3	CT45-1	CT45-2	CT45-3
1	6	6	6	6	6	6
2	6	7	7	6	6	6
3	6	6	6	6	6	7
4	6	6	6	6	6	6
5	6	6	6	7	6	6
6	7	6	6	7	6	6
7	6	7	6	6	6	6
8	6	6	6	6	6	6
9	7	6	6	6	7	6
10	6	6	6	6	6	6
11	6	6	6	6	6	7
12	6	6	6	6	6	7
Average Moisture Content [%]	6.17	6.17	6.08	6.17	6.08	6.25

Table 5-13: Change in temperature and relative humidity of the test chamber during the 8 weeks of creep test

Test Series	Min Temperature [°C]	Max Temperature [°C]	Average Temperature [°C]	Min RH [%]	Max RH [%]	Average RH [%]
CT45	4.01	26.60	17.61	4.38	30.80	11.92
CT65	14.48	28.42	21.22	14.47	68.62	45.37

5.5 Data Analysis

The analysis procedure, presented by Allen (1969) and reported by Taylor (1996), can be used to predict the elastic mid-span deflection behaviour of PUR SIPs. The overall flexural rigidity “D” or “EI” of a sandwich beam or panel illustrated in Figure 5-9, with two thin face-sheets of thickness “t”, core material of thickness “c”, overall thickness of “h” and, the width of “b” can be expressed as:

$$D = E_f \frac{bt^3}{6} + E_f \frac{btd^2}{2} + E_c \frac{bc^3}{12} \quad (\text{Eq. 5.2})$$

Where:

E_f = Modulus of elasticity of the face-sheets

E_c = Modulus of elasticity of the foam-core

d = The distance between the neutral axis of the upper and lower face-sheets

And:

$$\frac{d}{t} > 5.77 \quad (\text{Eq. 5.4})$$

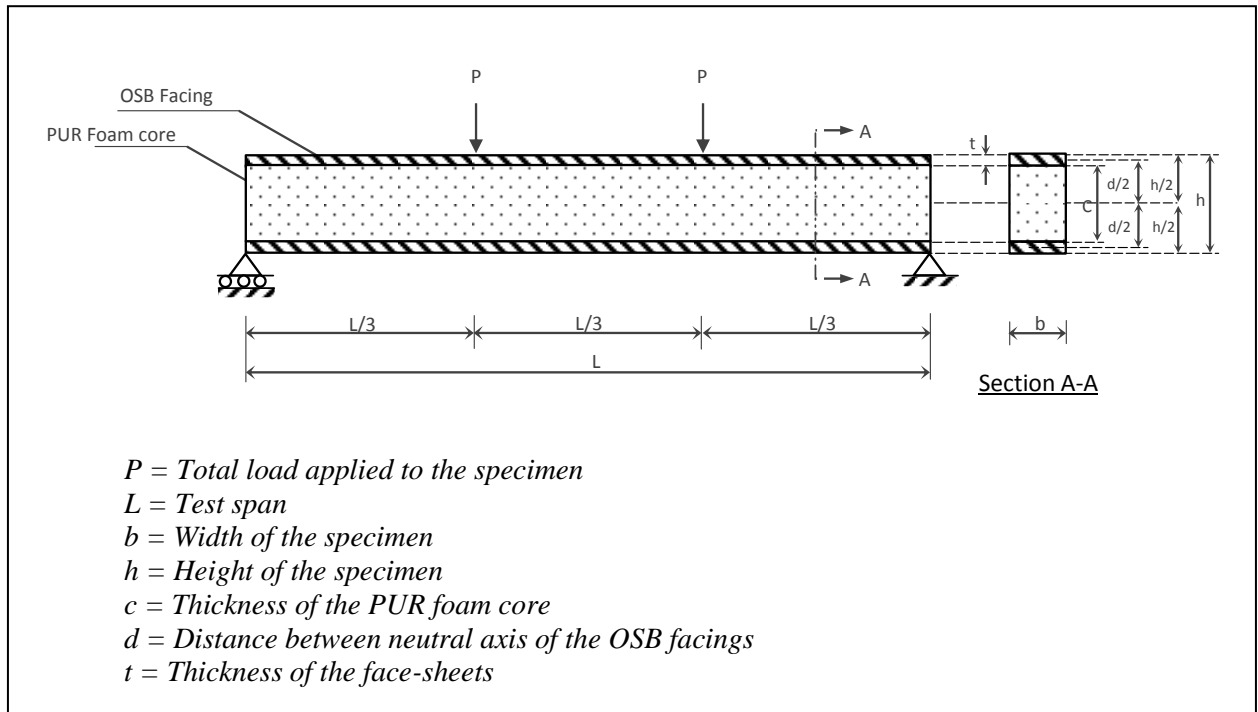


Figure 5-9: Physical specification of the flexural creep test span

The third term of the Equation 5.2 can be consequently considered negligible because it contributes to less than 1% of the second when:

$$6 \frac{E_f}{E_c} \frac{t}{c} \left(\frac{d}{c} \right)^2 > 100 \quad (\text{Eq. 5.5})$$

Based on Euler-Bernoulli's beam theory, the maximum bending deflection of a simply supported homogenous beam can be calculated using the following equation:

$$\Delta_{max} = \frac{Pa}{24EI} (3L^2 - 4a^2) \quad (\text{Eq. 5.6})$$

Where:

$L =$ Loading span

$a =$ The distance between the support and the action point of load “P”

In the case of a third point loading scheme where the load “P” is applied at the third of the beam’s span ($a = L/3$), the mid-span elastic bending deflection (Δ_B) can be expressed as:

$$\Delta_B = \frac{23PL^3}{648EI} \quad (\text{Eq. 5.7})$$

Or:

$$\Delta_B = \frac{23PL^3}{648D} \quad (\text{Eq. 5.8})$$

When conditions of Eq. 5.3, 5.4 and, 5.5 are satisfied, the maximum bending deflection (Δ_B) of the sandwich panel can be written as:

$$\Delta_B = \frac{23 PL^3}{648 E_f \frac{btd^2}{2}} \quad (\text{Eq. 5.9})$$

Allen (1969) and Supplement 4 of the Plywood Design Specification published by APA (1998), both cited and reported by Zarghooni (2009), defined the total mid-span deflection of a sandwich beam (Δ_T) as summation of deflections due to bending (Δ_B) and shear (Δ_S) as:

$$\Delta_T = \Delta_B + \Delta_S \quad (\text{Eq. 5.10})$$

Allen (1969) also suggested that in the case of sandwich beams with thin face-sheets (Figure 5-10), integration of equation dw_2/dx can be used to find the deflection of the beam due to shear as follows:

$$\Delta_S = \int \frac{dw_2}{dx} = \frac{Q}{AG} \quad (\text{Eq. 5.11})$$

Where:

$w_2 =$ Deflection at x

$Q =$ Shear force

$G =$ Foam-core shear modulus

$A =$ Cross sectional area

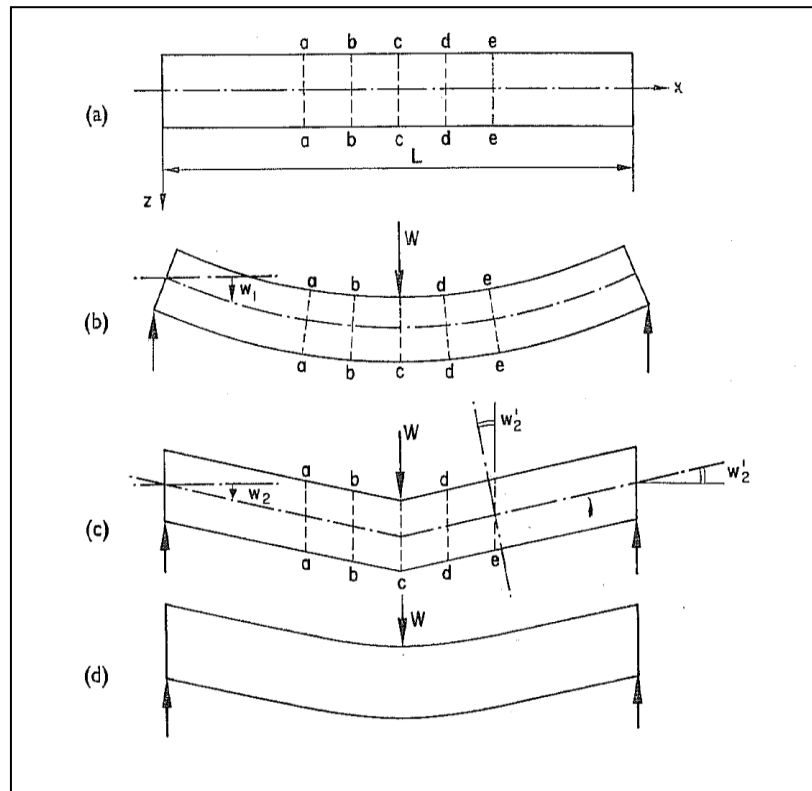


Figure 5-10: Deflection of a sandwich beam (Allen, 1969)

And:

$$A = \frac{bd^2}{c} \quad (\text{Eq. 5.12})$$

As for a non-standard 4-point (third-span) loading case where $x=L/3$, the deflection due to shear can be defined by Eq. 5.12 as follows:

$$\Delta_S = w_{2 \max} = \frac{PL}{6AG} \quad (\text{Eq. 5.13})$$

Therefore the total deflection of a sandwich beam exposed to load P at $L/3$ from each support can be predicted using the following equation:

$$\Delta_T = \Delta_B + \Delta_S = \frac{23 PL^3}{648 E_f \frac{btd^2}{2}} + \frac{PL}{6AG} \quad (\text{Eq. 5.14})$$

Referring to the work presented by Wong et. al (1988), Taylor (1996) recommends the following equation as an analysis technique to predict the creep behaviour of SIP from the individual creep behaviour of the face and the core material:

$$\Delta_T(t) = \left[\frac{23 PL^3}{648 D} (FD_{OSB}(t)) \right] + \left[\frac{PL}{6AG} (FD_{Foam}(t)) \right] \quad (\text{Eq. 5.15})$$

Where:

$\Delta_T(t)$ = Time dependent total deflection

P = Applied at the third of the beam's span

L = Beam or test span

D = Flexural rigidity of the SIP

$FD_{OSB}(t)$ = Fractional deflection of OSB face material

A = Cross sectional area

G = Foam-core shear modulus

$FD_{Foam}(t)$ = Fractional deflection of foam-core material

As per Taylor (1996), Equation 5.15 can be used to determine the creep behaviour of the SIPs by using only spring constants and the fractional deflection relationship of the component material. He found that the three month predicted fractional deflection can be calculated by dividing Equation 5.16 by the predicted initial deflection of the SIP as follows:

$$FD_P(t) = \frac{\Delta_T(t)}{(\Delta_S + \Delta_B)} = \frac{\Delta_T(t)}{\left(\frac{P}{K_S} + \frac{P}{K_B}\right)} \quad (\text{Eq. 5.16})$$

Where:

$FD_P(t)$ = Predicted fractional deflection

$\Delta_T(t)$ = Time dependent total deflection

Δ_S = Predicted deflection due to shear

Δ_B = Predicted deflection due to bending

K_S = The spring constant for the shear behaviour of the core

K_B = Bending behaviour of the face-sheet

Based on experimental results, Taylor (1996) concluded that Equation 5.16 had the potential to predict of the creep behaviour of SIPs. Table 5-14 shows the mechanical properties of the components of the PUR SIPs found experimentally by Taylor (1996) and used for the prediction of the three month deflection of the tested PUR SIPs in this experimental study.

Table 5-14: Experimentally measured mechanical properties of PUR SIPs conducted by Taylor (1996)

Component Material	Property	Value	
OSB	Modulus of Elasticity (MOE)	5.41	GPa
	Three month fractional deflection at 1/3 of the bending stress level (FD_{OSB})	1.799	mm/mm
Urethane Foam-Core	Shear Modulus (G)	1.97	MPa
	Three month fractional deflection at 1/3 of the shear stress level (FD_{Foam})	1.806	mm/mm

Table 5-15 provides the analysis of the negligibility check of the first and third terms in Equation 5.1 using equations 5.4 and 5.5 for each thickness of panels tested. The table also provides the predicted three month total deflection of each thickness of panel tested. As seen in Table 5-15, both calculated values of Eq. 5.5 exceed 100 (1100.25 and 668.37 respectively). Therefore, in the case of the tested panels in this study, both first and third terms in Equation 5.1 are negligible.

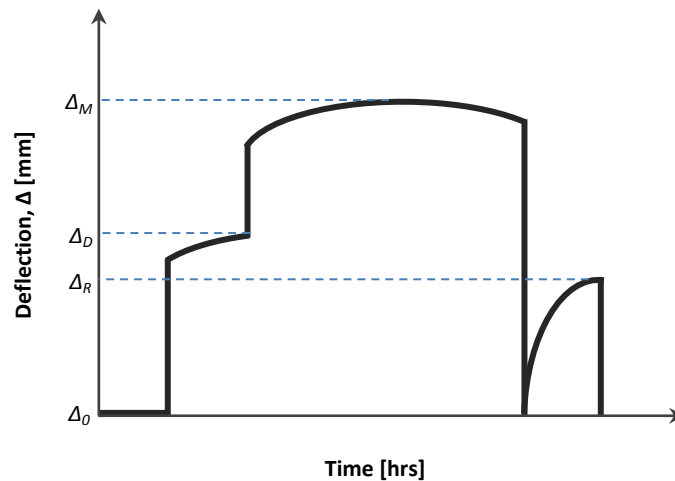
Table 5-15: Results of the analysis of the negligibility check of the first and third terms in Equation 5.1

Panel Thickness	d	t	c	b	L	E _f MOE of facing (OSB)	E _c MOE of core (PUR)	FD _{OSB}	FD _{Foam}	d/t	6(E _f /E _c)(t/c)(d/c) ²	P	Δ _T (t)
	[mm]					[MPa]	[mm/mm]					[N]	[mm]
114 mm (4.5 in.)	104	11	94	1220	2360	5410	4.21	1.799	1.806	9.482	1100.25	2929	19.67
165 mm (6.5 in.)	155	11	145	1220	2360	5410	4.21	1.799	1.806	14.09	668.37	2929	12.18

5.6 Test Results

Mid-span deflection readings from the two sides of each panel were used to plot time vs. deflection curves for all the tested panels. Figure 5-11 schematically represents major deflection points as a key to the actual time vs. deflection curves plotted using the experimental data. Figures 5-12 to 5-17, respectively, represent time (hours) vs. deflection (mm) curves for all the PUR SIPs tested under creep for a duration of 8 weeks (56 days). Table 5-16 represents the maximum deflection of each specimen under dead load only, while Table 5-17 provides the maximum deflection of each specimen under a combination of live load and dead load. As seen in Table 5-16, when subjected to dead loads only, the average deflection of thinner panels (114 mm, 4.5 in. thick) was 9.21 mm while the average deflection of thicker panels (165 mm, 6.5 in. thick) was 7.88 mm. This means that under the dead load, thinner panels deflected 16.9% more than thicker panels. In the

case of the dead load plus live load loading condition (Table 5-15), the average deflection of thinner panels (114 mm, 4.5 in. thick) was 18.36 mm while the average deflection of thicker panels (165 mm, 6.5 in. thick) was 15.53 mm. This means under the combination of dead load and live load, thinner panels deflected 18.2% more than thicker panels.



Legend:

Δ_0 = Zero Deflection Status

Δ_D = Deflection after application of dead load

Δ_M = Maximum deflection after application of dead load and live load

Figure 5-11: Schematic diagram showing the critical points of a typical Deflection vs. Time creep curve (Taylor, 1996)

As seen in Tables 5-14 and 5-15, the Coefficient of Variation (COV) of the deflections (in both dead load only and the combination of dead and live load stages) for thinner panels was consistently lower than the COV of the deflections of the thicker panels (3.44% vs. 5.41% and 3.31% vs. 4.52%), suggesting more uniformity in the average mid-span creep deflection behaviour of the thinner panels.

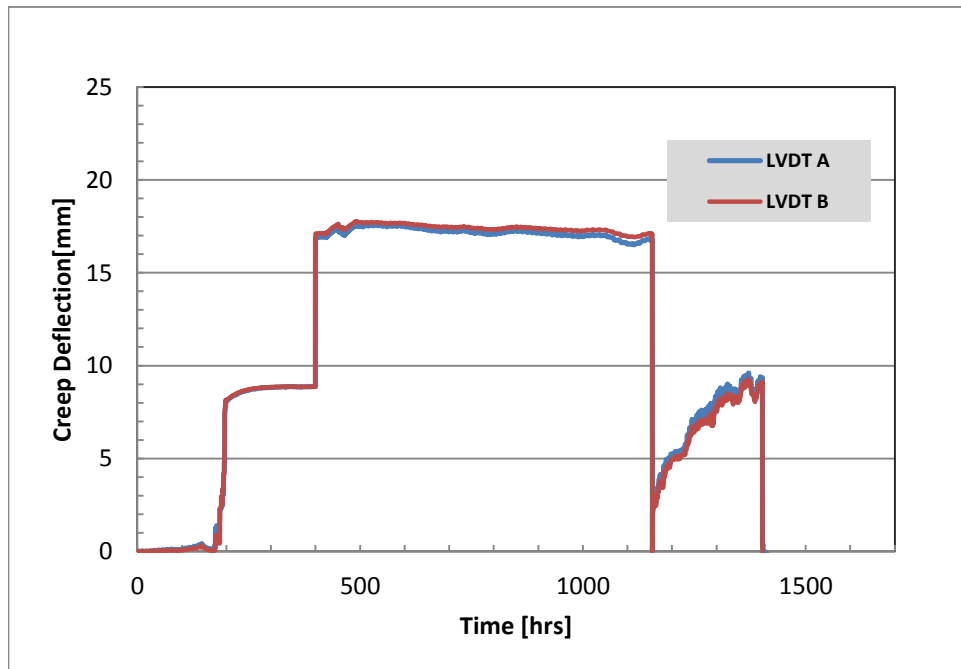


Figure 5-12: Load vs. Deflection curve of the specimen CT45-1

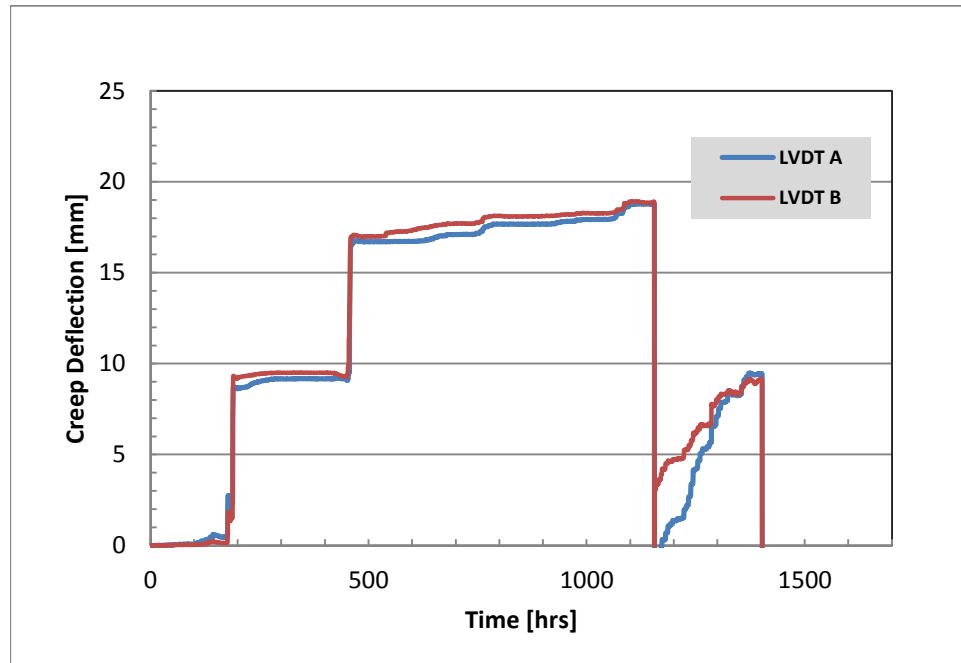


Figure 5-13: Load vs. Deflection curve of the specimen CT45-2

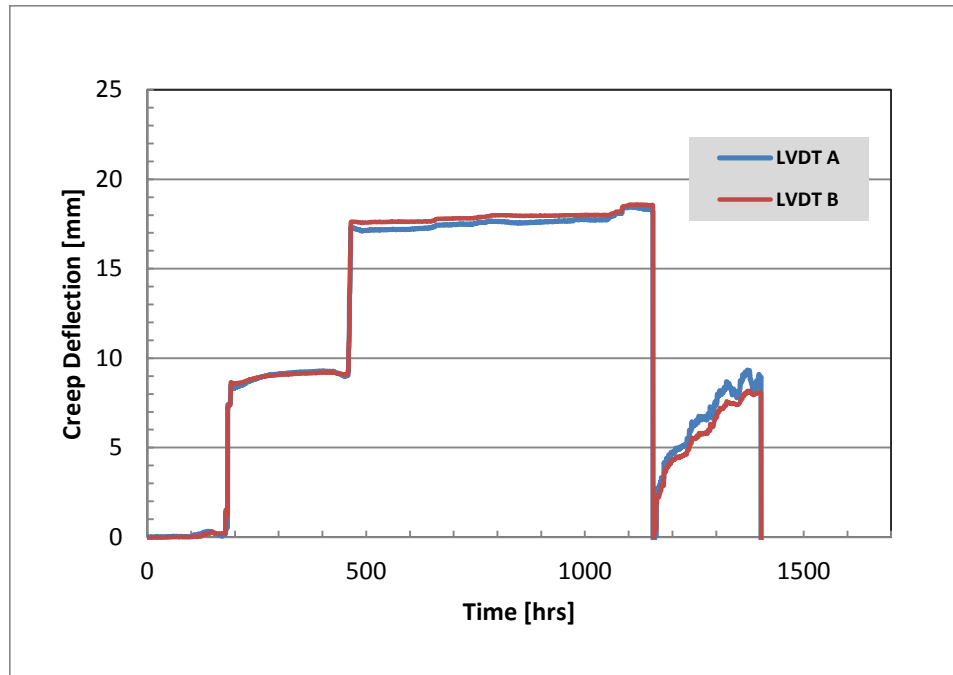


Figure 5-14: Load vs. Deflection curve of the specimen CT45-3

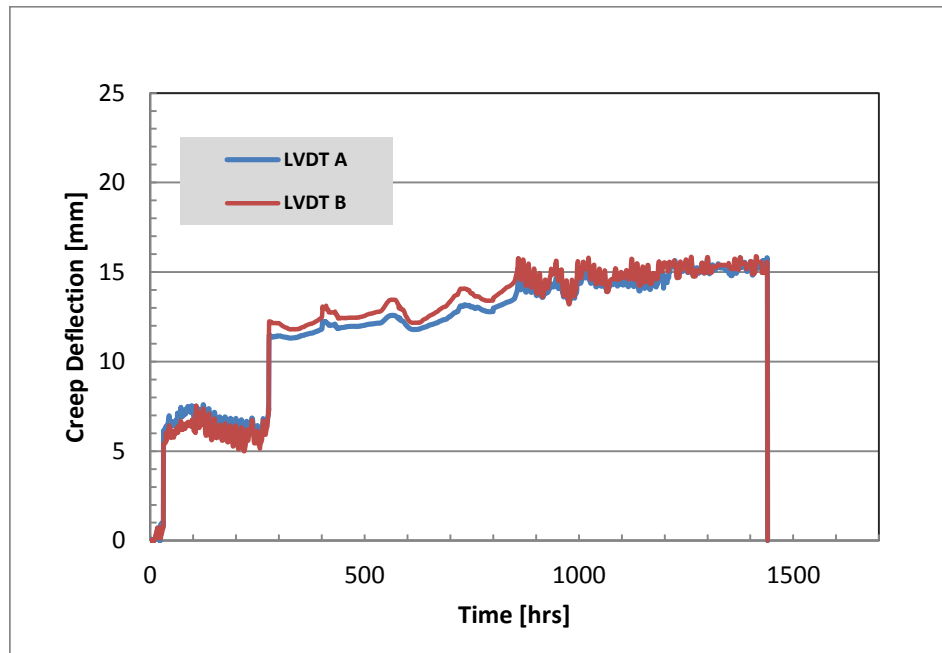


Figure 5-15: Load vs. Deflection curve of the specimen CT65-1

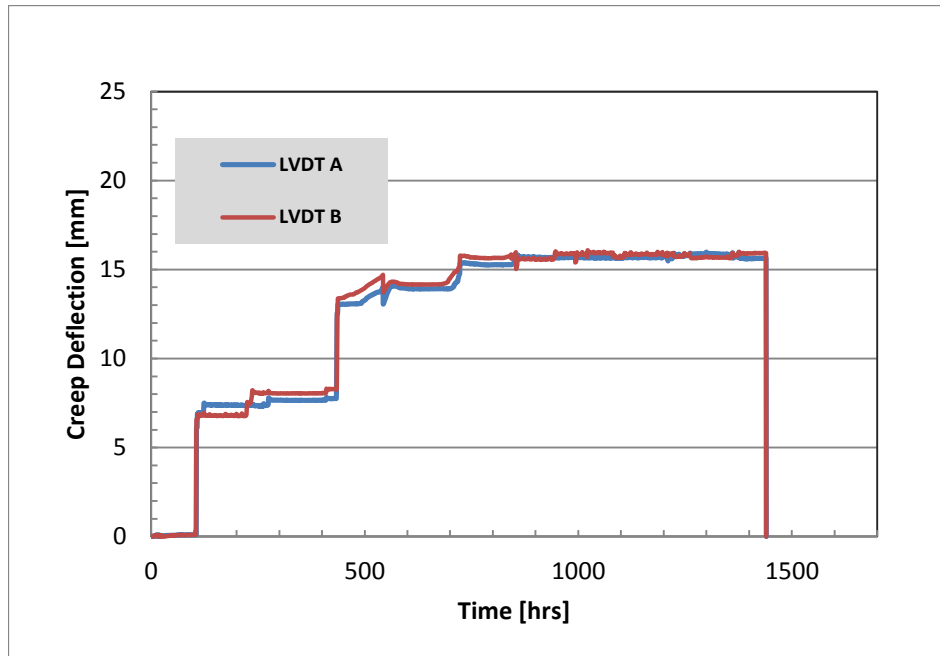


Figure 5-16: Load vs. Deflection curve of the specimen CT65-2

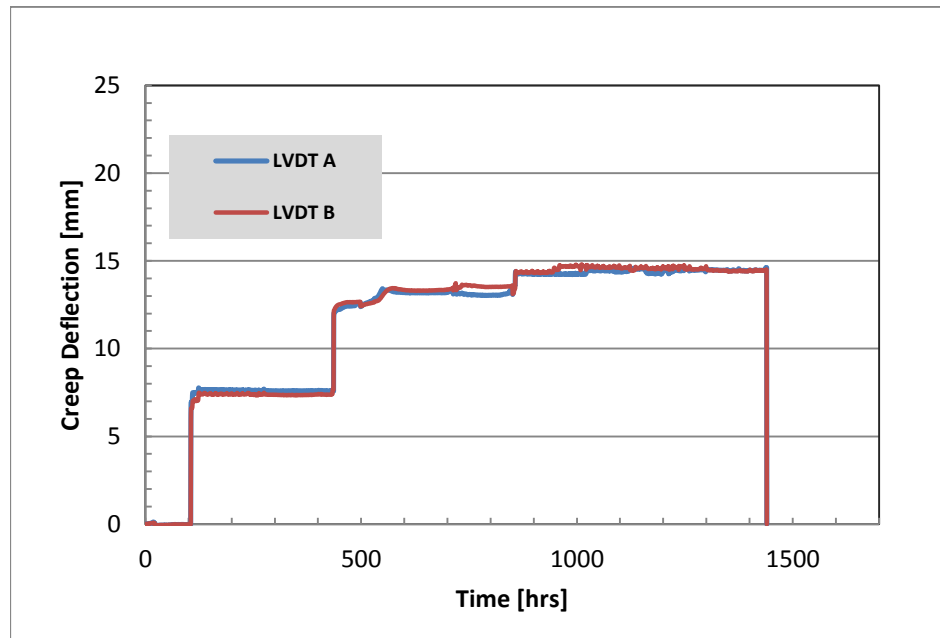


Figure 5-17: Load vs. Deflection curve of the specimen CT65-3

Table 5-16: Maximum deflection of each specimen under dead load only

Test Number	Test ID	Step 3, Maximum Deflection DL [mm]					
		LP A	LP B	Average	Total Average	STDEV	COV [%]
1	CT45-1	8.88	8.87	8.88			
2	CT45-2	9.52	9.49	9.51	9.21	0.32	3.44
3	CT45-3	9.28	9.21	9.25			
4	CT65-1	7.54	7.59	7.57			
5	CT65-2	8.42	8.31	8.37	7.88	0.43	5.41
6	CT65-3	7.76	7.66	7.71			

Table 5-17: Maximum deflection of each specimen under combination of dead load plus live load

Test Number	Test ID	Step 4, Maximum Deflection DL + LL [mm]					
		LP A	LP B	Average	Total Average	STDEV	COV [%]
1	CT45-1	17.60	17.78	17.69			
2	CT45-2	18.82	18.93	18.88	18.36	0.61	3.31
3	CT45-3	18.46	18.58	18.52			
4	CT65-1	15.80	15.88	15.84			
5	CT65-2	15.98	16.08	16.03	15.53	0.70	4.52
6	CT65-3	14.66	14.80	14.73			

The deflection of panels was monitored by manual measurement until 90 days after the removal of the dead and live loads. Table 5-18 provides the deflection of the tested panels after the removal of all loads. As seen in the table, all of the panels rebounded to their initial condition with no visible deflection.

Table 5-18: Manual readings of deflection up to 90 days after removal of the design creep loads

Test Number	Test ID	Permanent deflection after removal of all loads [mm]		
		After 30 Days	After 60 Days	After 90 Days
1	CT45-1	5	3	0
2	CT45-2	4	3	0
3	CT45-3	5	2	0
4	CT65-1	5	3	0
5	CT65-2	3	1	0
6	CT65-3	3	2	0

NRC's technical guide (2007) suggests that "The maximum difference in the deflections measured in Step 4 of Table 7 (dead loads plus live load) and Step 3 (dead load only) shall not exceed $L/360$ of the span". Table 5-19 provides the difference in deflections of the above mentioned steps for all tested panels. As seen in Table 5-19, thinner panels (114 mm, 4.5 in. thick) satisfy the ratios of mid-span deflection (Δ , mm) of, $L/268$, 252 and 254 respectively. Thicker panels (165 mm, 6.5 in. thick) also satisfy the ratios of mid-span deflection (Δ , mm) of $L/285$, 308 and 306 respectively. NRC's technical guide (2007) recommends the deflection limit of $L/360$ for roof panels under the action of the live load and the serviceability limits for wood construction under the total loads as $L/180$. CSA 086 (CSA, 2009) and Wood Design Manual (2010) suggest maximum acceptable mid-span deflection of $L/240$ for roofs under snow load. Part 9 of the NBCC (NRC, 2010) limits the deflections to $L/180$ when no ceiling is present, $L/240$ for ceilings

not covered with plaster or gypsum board and $L/360$ when plaster or gypsum board covers the ceiling.

Table 5-19: Average maximum deflection of tested panels under different creep load combinations

Test Number	Test ID	Average Deflection Due to 'LL+DL' [mm]	Average Deflection Due to 'DL' [mm]	Deflection due 'D+L' minus Deflection due 'D' [mm]	Satisfies the criteria of $\Delta = L/180$	Satisfies the criteria of $\Delta = L/240$	Satisfies the criteria of $\Delta = L/360$	Satisfying ratio of L/Δ
1	CT45-1	17.69	8.88	8.82	YES	YES	No	268
2	CT45-2	18.88	9.51	9.37	YES	YES	No	252
3	CT45-3	18.52	9.25	9.28	YES	YES	No	254
4	CT65-1	15.84	7.57	8.28	YES	YES	No	285
5	CT65-2	16.03	8.37	7.67	YES	YES	No	308
6	CT65-3	14.73	7.71	7.02	YES	YES	No	336

As seen in Table 5-19, over a span of 2360 mm (93 in.), both thicknesses of panels satisfied the ratios of $L/180$ and $L/240$, but none of the panels satisfied the $L/360$ ratio. This means that in service condition, the span width needs to be reduced so that the mid-span deflection meets the $L/360$ ratio. Based on PUR SIP's manufacturer suggestion, such panels are normally used over 1830 mm (72 in.) spans. Further tests are required in order to investigate if such panels will creep within the code limits over the above mentioned span.

In terms of creep deflection behaviour of sandwich panels, ASTM C480/C480M (2008) requires the total shear stress in core material to be reported. The standard suggests the following formula to calculate the average shear stress in foam-core of the SIPs:

$$F_s = \frac{P}{(d + c) b} \quad (\text{Eq. 5.17})$$

Where:

F_s = core shear stress, kPa

b = sandwich width, mm

c = core thickness, mm

d = sandwich thickness, mm

t = nominal facing thickness, mm

Equation 5.17 was used to calculate the average shear stress in tested PUR SIPs for the two different thicknesses of panels tested. As seen in Table 5-20, when exposed to designed dead and live loads, the PUR foam-core of the 165 mm (6.5 in.) thick panels experienced 16.05 kPa of shear stress while the foam-core of the 114 mm (4.5 in.) thick panels experienced 24.18 kPa of shear stress. This indicates the shear stress in the foam-core of the thinner panels was 51% more than the shear stress in the foam-core experienced by the thicker panels.

Table 5-20: Shear stress level created in foam core due to creep loads in tested panels

Panel Thickness	P	d	c	b	F _s
	[N]	[mm]	[mm]	[mm]	[kPa]
114 mm (4.5 in.)	5858.6	104.3	94.3	1220	24.18
165 mm (6.5 in.)	5858.6	155	145	1220	16.01

Table 5-21 provides a comparison between the experimental flexural creep of PUR SUIPs vs. the predicted values calculated using Equation 5.15 (developed by Taylor 1996). As seen in Table 5-21, the experimentally measured average maximum flexural creep deflection of 114 mm (4.5 in.) PUR SIPs was 18.36 mm (0.722 in.) while the value derived from Equation 5.15 is 19.67 mm (0.774 in.). This means the actual creep deflection was 7.14% larger than the predicted value. In the case of the 165 mm (6.5 in.) thick PUR SIPs, the experimentally measured average maximum flexural creep deflection was 15.53 mm (0.611 in.) vs. 12.18 mm (0.48 in.) resulted from Equation 5.15. This means the actual creep deflection was 27.5% larger than the predicted value. It can be concluded that the proposed formula for prediction of flexural creep deflection (Equation 5.15) was in agreement with the experimental findings in the case of the thinner 114 mm (45 in) panels, but it was not the case for the 165 mm (6.5 in.) thick panels.

Table 5-21: Experimental maximum creep deflection of panels vs. the theoretical predicted creep deflection values (using Eq. 5.15)

Panel Thickness	Average Maximum Deflection [mm]		Ratio of the Experimental over Theoretical Results	Difference [%]
	From the Experimental Results	Predicted using Eq. 5.15		
114 mm (4.5 in)	18.36	19.67	0.93	7.14
165 mm (6.5 in)	15.53	12.18	1.28	27.50

5.7 Conclusions

1. When exposed to the design live and dead loads, the panels with 114 mm (4.5 in.) thickness tested for flexural creep deflection over a span of 2360 mm (93 in.) satisfied the creep deflection limitations of $L/180$ and $L/240$ while they failed to satisfy the $L/360$ limitations. If panels are to meet the $L/360$ limit then the span would need to be shortened for the load conditions.

2. The test panels with 165 mm (6.5 in.) thickness satisfied the creep deflection limitations of $L/180$ and $L/240$ but failed to satisfy the $L/360$ limitations. Similar to thinner panels, in order to meet the criteria, loading span must be reduced accordingly for more restrictive deflection limits and greater loading.

3. No permanent deflection was detected 90 days after removal of the applied loads to both thicknesses of PUR SIPs tested for flexural creep deflection.
4. The flexural creep deflection prediction Equation (5.15) proposed by Taylor (1996) was in good agreement with the experimental findings of creep deflection of 114 mm (4.5 in.) thick PUR SIPs.
5. The flexural creep deflection prediction Equation (5.15) proposed by Taylor (1996) was not in good agreement with the experimental findings of creep deflection of 165 mm (6.5 in.) thick PUR SIPs.

Chapter 6

Bond Strength as a Measure of Serviceability and Quality of Polyurethane Foam Structural Insulated Panels (Pull-off Tests)

6.1 Introduction

Possibilities of de-bonding of the OSB face-sheets–foam-core interface under service conditions and its effect on the overall structural capacity of the SIPs is another unanswered question affecting the acceptance of SIPs as a construction material. This experiment investigated the effects of weathering and service conditions on the bond between oriented strand board (OSB) face-sheets and the polyurethane (PUR) foam-core of PUR SIPs. In order to do so, random pull-off tests were performed on new and highly weathered PUR SIPs. Based on ASTM D4541 (ASTM, 2009), a pull-off test is a procedure for measuring the bond or adhesion strength between two different materials using a destructive method. A steel disk is glued to the surface of the coating, or the upper material, and pulled by a mechanical device in order to measure the tensile strength of the bond between the coating and the substrate material. In the case of coating systems, this test method evaluates whether the surface remains intact due to applied perpendicular force (in tension) or if a plug of material is detached from the system and the bond. As defined in ASTM D4541 (ASTM, 2009), in a system consisting of test fixture, adhesive, coating system, and substrate, the failure will happen along the weakest plane within the system and exposed by the fracture surface. Three different failure scenarios are expected when this is conducted on SIPs: failure in the OSB material, failure in the foam-core, or failure in bond intersection between the OSB and the foam-core. Testing the bond strength between the OSB face-sheet and the foam-core in SIPs has not been directly addressed in

ASTM. The best available standard is C1583/C1583M (ASTM, 2009), which, based on its definition, is a suitable test standard for evaluating the bond strength between rigid substrates, such as plastic and wood.

Pull-off or pull-out testers are portable hand driven tools. Such machines are capable of applying a tensile force perpendicular to a disk attached to a surface. Pull-off testers are equipped with a manual or digital gauge to show and record the ultimate load at the time of failure. Not all available testing machines are equipped with displacement measuring devices.

6.2 Materials and Method

Available pull-off testers in the market can only record the final failure load with no capability of recording the displacement of the specimen. Therefore, it was decided to design and build a pull-off tester that was capable of being connected to a computer and a Data Acquisition System (DAQ). This allowed the researcher to record and plot the load versus displacement curve of each test. As seen in Figures 6-1 and 6-2, the pull-off tester consisted of a steel frame, a 2000 lb load cell (Omega Engineering Inc.), a 100 mm (4 in.) linear potentiometer, or, displacement sensor (Penny and Giles), 12.5 mm diameter threaded rod, and a cracking handle. The load cell and the linear potentiometer were connected to a DAQ in order to record load versus displacement data. Forty steel disks were

cut from a solid steel shaft with a thickness of 10 mm with a diameter of 57 mm (2 ¼ in.). A 10 mm diameter nut was welded at the centre of each disk to connect the disk to the pull-off tester.

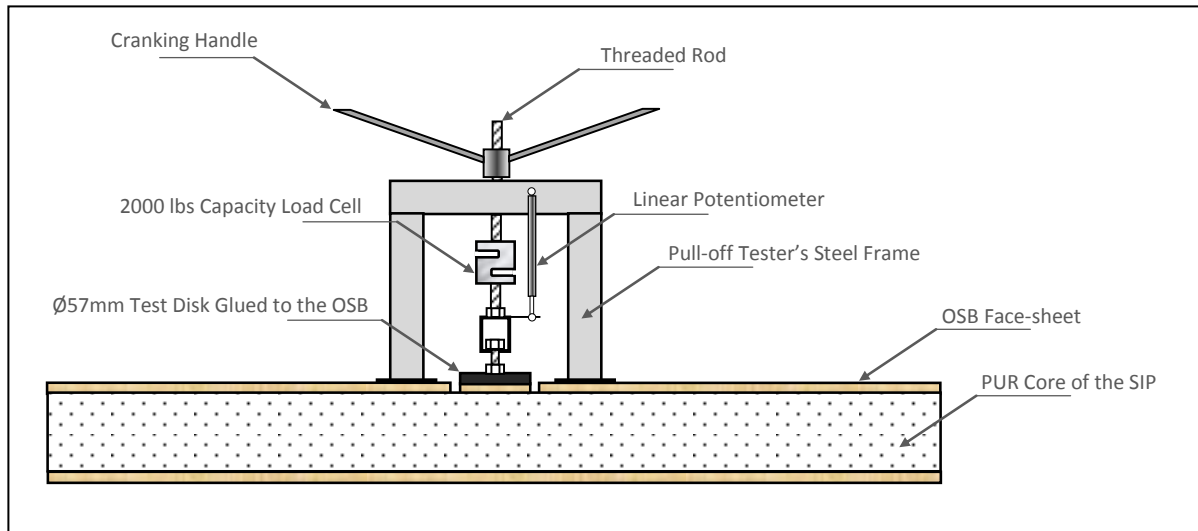


Figure 6-1: Schematic detail of the hand-made pull-off tester



Figure 6-2: Hand-made pull-off tester used conduct pull off tests on PUR SIPs

Pull-off tests were conducted on two sets of PUR SIPs. Three brand new 1220 x 2438 mm (4 x 8 ft.) panels were selected to represent the control samples, and three 1220 x 2438 mm (4 x 8 ft.) naturally weathered panels were selected to represent in-service, or used panels. Weathered panels were exposed to harsh environmental conditions, such as direct sunlight (UV), rain, and snow for at least two, and up to four years before being tested (Figure 6-3). As explained in Chapter 2 (page 56), for both sets, each side of the panel surface was divided into four sections. Each quarter consisted of nine possible sampling locations, for a total of 36 locations on each side of a panel. A computer program was used to generate random numbers between 1 and 36 to select ten sampling locations on each side of the surface of the panel. A total of 120 pull-off tests were performed.



Figure 6-3: PUR SIPs stored in a storage yard with minimum weather protection for more than four years

Once the sample locations were determined, a 63.5 mm outside diameter hole-saw was used to cut through the OSB face layer to the foam as shown in Figure 6-4. The surface of the steel disks and the OSB were cleaned using alcohol on the steel and vacuuming the OSB to remove possible debris or dirt. A five-minute fast curing epoxy gel was applied to both the steel disk and the OSB surface to secure the disk at the test location (Fig. 6-5). The epoxy was allowed to cure for 24 hours before conducting a pull-off test. To conduct a test, the sliding grip on the pull-off tester was engaged with the lifting bolt of the steel disk (Figure 6-5). The crank was turned to take up any slack between the grip and the bolt head. A pull-off test was conducted by cranking the handle of the pull-off tester in as smooth and continuous a manner as possible until the coupon failed.

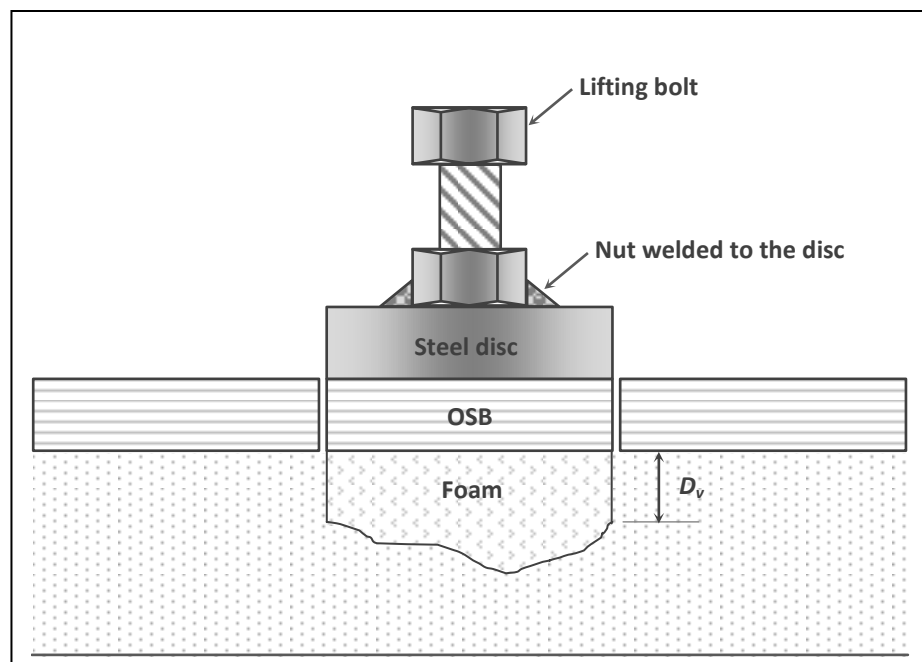


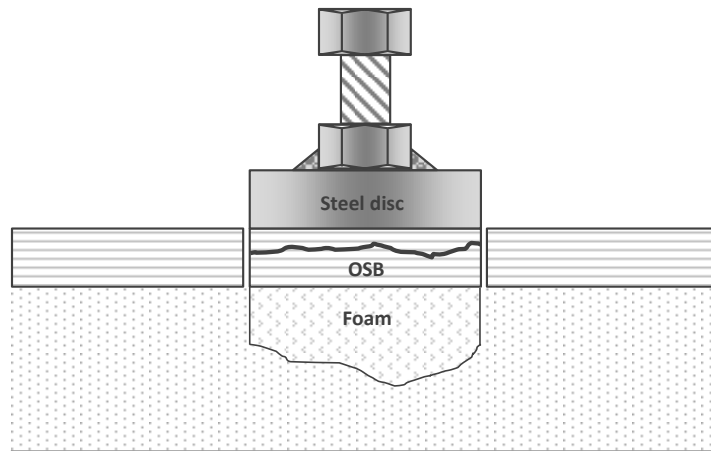
Figure 6-4: Pull-off test assembly (Source: Dick, 2014)



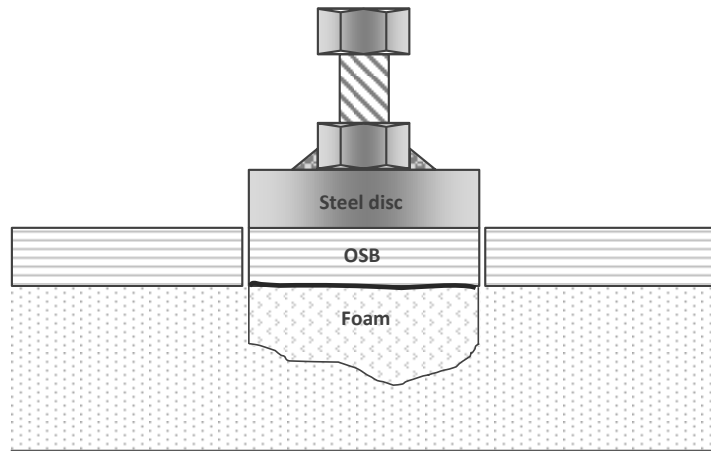
Figure 6-5: Steps in pull off test preparation

A load rate of 35 ± 15 kPa/s (5 ± 2 psi/s) was adopted, as recommended by the ASTM C1583/C1583M (ASTM, 2013) standard. Pre-tests were performed in order to find the number of cranks per unit time to meet the standard criteria. In general, each test continued until one of the following three failure modes was observed (Figure 6-6 and 6-7):

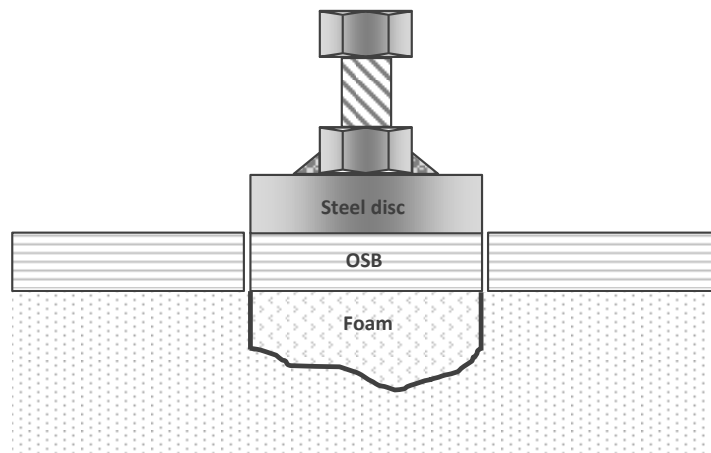
- i.) Bond failure at the OSB-foam interface
- ii.) Foam failure
- iii.) Delamination of the OSB face-sheet



(a) Failure within the OSB face-sheet



(b) Failure at the OSB-foam interface



(c) Failure within the foam

Figure 6-6: Schematic failure modes of the specimen plug
(Source: Dick, 2014)



(a) Partially de-bond failure



(b) Failure within the foam-core



(c) Failure within the OSB face-sheet

Figure 6-7: Actual failure modes of the specimen plug observed in pull-off tests

It should be noted that no failure of the epoxy bond between the pull-off disk and the OSB interface occurred in any of the 120 tests.

6.3 Results and Analysis

Table 6-1 summarizes the modes of failure of all 120 pull-off tests conducted on brand new and weathered PUR SIPs. Figure 6-8 illustrates a typical load (tensile/pulling force) versus vertical movement (deflection) of the test plugs. The area under the load-vertical movement plot was used to determine the energy or work done to pull the plug away from the panel. Table 6-3 summarizes the average pull-off energy for various specimen types and failure modes. The energy was calculated by measuring the area under the load-deformation curve. Based on the comparison presented in Table 6-3, there is minimal difference between the energy required to remove the pull-off plug from a panel.

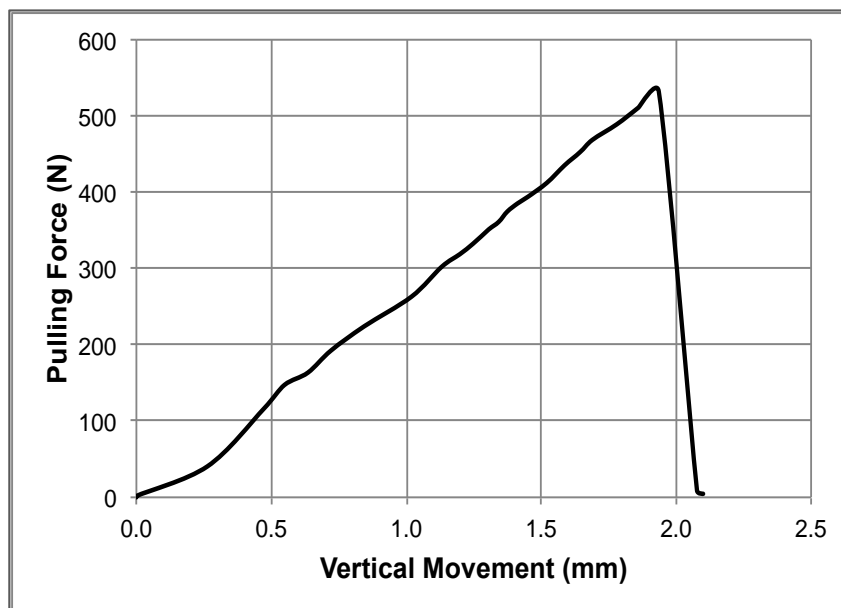


Figure 6-8: Typical load vs. deflection curve of the pull-off tests conducted on PUR SIPs

Table 6-1: Summary of failure modes based on panel type

Mode of Failure	Panel Type		Ratio of New to Weathered	Percentage of Total Tests ¹
	New	Weathered		
OSB Face-sheet	13	11	0.94	20
Foam	45	48	1.18	77.5
Bond Interface	2	1	2	2.5

Note. 1: Based on total of 120 specimens

A principal reason for conducting pull-off tests was to investigate the bond behaviour between new and weathered panels. A key result as illustrated in Table 6-1 is that only 2.5% of all failures occurred at the OSB-foam interface. Furthermore, the other failure modes occurred essentially equally between the new and weathered panels.

As shown in Figure 6-7, in all three cases of this type of failure mode, the de-bonding was incomplete separation. Only an average of 50% of the bond area failed, with the remainder of the OSB-foam interface staying intact (Figure 6-7 a).

A t-test statistical analysis of the pull-off energy data (Table 6-4) assuming equal variance indicated that there was no significant difference between the means, $p = 0.197 > 0.05$. Therefore, there is no significant difference between the new and weathered panels.

As seen in table 6-2 (and Table F-1 in Appendix F), the average tensile or normal stress of all pull-off tests in both weathered and new panels is 0.198 and 0.18 MPa respectively. The average tensile or normal stress in pull-off tests failed in foam region is 0.35 and 0.26 MPa for new and weathered panels respectively (see Table F-2 in Appendix F). The average direct shear stress in pull-off tests failed in foam region is 0.20 and 0.18 MPa for new and weathered panels respectively.

The area under the load vs. deflection curve of all tested samples was calculated in order to compare the magnitude of needed energy to pull-off the disks in both cases of new and weathered panels.

Table 6-2: Comparison of load, vertical movement and stress in all failure modes combined

	Average Maximum Load All Specimens	Average Vertical Movement at Max Load	Average Normal Stress All Specimens ¹	Average Normal Stress (Foam Failure)	Average Shear Stress (Foam Failure) ²
Panel Type	(N)	(mm)	(MPa)	(MPa)	(MPa)
New	552.63	2.04	0.20	0.35	0.20
St. Dev.	78.97	0.18	28.40	160.40	34.11
COV ³	0.14	0.09	0.14	0.19	0.17
Weathered	501.44	2.12	0.18	0.26	0.18
St. Dev.	73.40	0.28	26.40	246.44	22.51
COV ³	0.15	0.13	0.15	0.39	0.13
Ratio of Weathered to New ⁴	0.91	1.04	0.91	0.74	0.89

Note:

1. Based on maximum load acting over area of specimen.
2. Shear stress for specimens that failed in the foam. Based on the depth of foam sheared D_v (Fig. 5) times perimeter.
3. Coefficient of Variation (COV) is a ratio and does not have the units of the column.
4. Ratio does not have the units of the column.

Table 6-3: Comparison of pull-off energy

Parameter	Average Pull-Off Energy (Joules)
All specimens - new panels	0.82
All specimens - weathered panels	0.85
Foam failure all specimens	0.86
Foam failure new panels	0.82
Foam failure weathered panels	0.89
All specimens OSB failure	0.71
Bond failure (3 specimens)	0.79

The panels tested in this research were manufactured by injecting the polyurethane foam between two OSB faces with the sheets in a horizontal orientation. The bond between the foam and OSB is formed as the foam expands against the sheets and cures. A comparison of the pull-off energy for each side of the panel was done to see if there might be a difference as foam injection mode could influence bond strength. Table 6-4 presents the average energy values for the test panels for each side based on ten specimens per side. The results presented in Table 6-4 were statistically analyzed (T-test) and indicated there was no significant difference between the sides of the panels or between panel types. Based on the results of this testing it appears that there is little impact of weathering and aging on the foam quality and the bond integrity between OSB facing sheets and polyurethane for the panel tested in this study.

Table 6-4: Comparison of pull-off energy (Joules) based on each side of panel

Panel Type	Panel Number					
	1		2		3	
	Side A	Side B	Side A	Side B	Side A	Side B
	(J)		(J)		(J)	
New	1.02	0.98	0.62	0.71	0.74	0.82
Weathered	0.99	0.98	0.66	0.76	1.01	0.72
T-test result ($p > 0.05$ no significant difference):						
New	0.406	Comparison of Side A to Side B for the new panels				
Weathered	0.644	Comparison of Side A to Side B for the weathered panels				
New to Weathered	0.593					

6.4 Conclusions

A total of 120 pull-off tests were conducted on new and weathered structural insulated panels to evaluate the bond quality between polyurethane foam and OSB facing sheets.

The following conclusions were drawn from this study:

1. No significant difference was found in the bond strength between the opposing sides of the panels.

2. Based on shear stress for specimens that failed within the foam, there was no apparent degradation of the foam.
3. Only 2.5% of the specimens exhibited a partial failure at the interface between the OSB facing sheet and foam-core. Of the three that failed, two specimens were found in new panels. Thus, the failure was not related to aging or weathering.
4. Even with highly weathered panels, the bond strength still performed well. Therefore, structural performance of the SIP is a function of the integrity of the facing sheets. But this does not negate the need to provide a cladding system to protect the OSB from degradation.

Chapter 7

FEM Modelling of OSB- PUR SIPs

7.1 Introduction

The intent of modeling within the context of this research programme was to see if a computer-aided design (CAD)/computer-aided engineering (CAE) software could be used to create a simple model that would simulate what was determined experimentally. While it can be argued that the variability of wood and foam materials might make modeling problematic, it was of interest to investigate if a simple model created in SOLIDWORKS™ could be used to predict panel behaviour based on a comparison with experimental data.

Vast research has been conducted on creep, stress, and constant rate stressing of viscoelastic materials (Findley et al. 1976; Taylor 1996). Among the materials being researched, viscoelastic materials, such as wood and PUR foam, have been a point of interest and have generated a lot of data in this regard, but there is a little work done on some composite materials such as OSB-foam in SIPs (Taylor, 1996). It was of interest to develop analytical models that could be used to predict the overall behaviour of PUR SIPs for both thicknesses of PUR SIPs including bonded and partially dis-bonded panels were developed. The model was created using SOLIDWORKS™ software program (Dassault Systèmes, 2015).

7.2 Modelling of PUR SIPs under different loading orientations

A few available commercial finite element software programs such as RISA-3D (RISA Technologies, 2015), ATENA (Cervenka Consulting, 2015) and, SeismoStruct (Seismosoft Ltd., 2015) were studied in terms of their compatibility of modeling composite materials such as SIPs. Ultimately, the commercial finite element software of SOLIDWORKS (Dassault Systèmes, 2015) was selected and used to perform simulations of the load-response behaviour of PUR SIPs with two different thicknesses and bond conditions (fully-bonded and partially dis-bonded). The displacement formulation of the finite element method is the technique SOLIDWORKS employs to calculate displacement, stress and strain formed in a rigid body under internal and external loads. SOLIDWORKS uses non-linear stress analysis methods for the analysis of non-metallic components such as PUR foams or OSB sheets (Dassault Systèmes, 2015).

As for the component materials of PUR SIPs, OSB facings were presumed as orthotropic and the PUR foam core was presumed as isotropic material. Timber studs were added to the racking load models in order to simulate the experimental specimens. Full bond between the two panels was considered instead of spline, nail and, glue connection method used in experimental racking tests. The timber studs added to the racking load models were presumed orthotropic and the available published mechanical properties of Douglas-

fir were used. It was also assumed that the components of the SIP model including the OSB face-sheets and the PUR foam-core were fully-bonded with no possibility of slippage between the two materials. Failure criteria were defined as the average ultimate load, determined from experimental testing. Modulus of elasticity and Poisson's ratio used in the modelling, either from the publication or experimental tests, were taken from the linear portion of the stress-strain curves. Therefore, the expectation was not to accurately model the non-linear portion of the model's behaviour but to see if there was an approximation within the linear portion which is the design range zone of the load response curves.

Similar to partially dis-bonded panels tested in Chapter 4, dis-bonded panels were also modeled. In both cases, panels were exposed to different load orientations of racking, axial (eccentric) and transverse representing loading directions on x, y, and z axis. Two different thicknesses of 114 mm (4.5 in.) and 165 mm (6.5 in.) thick models were modeled and analyzed.

7.2.1 Microscopic evaluations

Coupons of PUR SIPs were cut and the bond region between the OSB and PUR foam-core was visually inspected using a microscope with 40x magnifying power. This inspection was conducted in order to see if there is any penetration of PUR foam within the

OSB body and texture and therefore formation of a third material zone with the characteristics of both PUR foam and OSB material.

The manufacturer of the tested PUR SIPs in this study uses the soft side (stamp side) of the OSB inside (facing the foam core) and leaves the rough side outside in order to allow better bond for the stucco and other exterior/cladding materials. Therefore, the smoother side of the OSB is facing the PUR foam and hence less penetration of the liquid PUR inside the OSB material is viable. As seen in the magnified OSB- PUR foam bond area in Figure 7-1, there is a distinct line between the two materials meaning a third composite material does not exist.

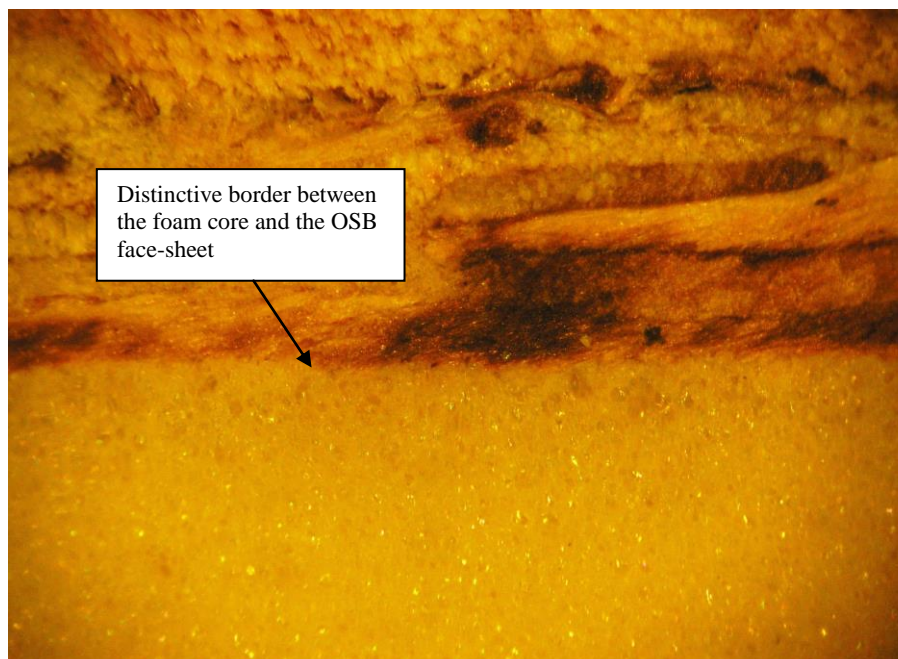


Figure 7-1: Magnification (40x) of PUR foam-OSB bond area in PUR SIPs. Top part of the photo is the OSB and the bottom shows foam

7.2.2 Compression tests for determining mechanical properties of PUR SIPs

As explained in Chapter 5, blocks of PUR SIP coupons were subjected to pure compressive force and compressed for at least 25 mm (1 in.). Results of those tests were used to find the modulus of elasticity (E) of the PUR foam core in compression. It was presumed that the soft foam-core would deflect earlier than the OSB face-sheets. Therefore the calculated 'E' represents the modulus of elasticity of the PUR foam only.

Table 7-1 and 7-2 provide the average compressive stress obtained from such tests. The linear portion of the strain versus stress curves of all tested specimens were used to calculate and average the modulus of elasticity of the PUR foam. As seen in the above mentioned tables, average E found from both thicknesses of PUR SIP coupons are within an acceptable STD of 0.44 and 0.75, suggesting data points to be close to the mean value. Averaging the two average values (6.55 and 6.12 MPa), it can be concluded that the compressive modulus of elasticity of the PUR foam used in the production of tested PUR SIPs in this research was 6.34 MPa.

Table 7-1: Average modulus of elasticity of 114 mm (4.5 in.) PUR SIP samples subjected to axial compressive load

Sample Number	Max load [N]	Experimental Modulus of Elasticity, E [mPa]
CC45-1	5325.88	6.57
CC45-2	4880.88	6.58
CC45-3	5209.04	6.79
CC45-4	5302.17	6.67
CC45-5	4786.46	6.98
CC45-6	5103.17	5.71
Average	5101.27	6.55
STD		0.44
COV [%]		6.70

Table 7-2: Average modulus of elasticity of 165 mm (6.5 in.) thick PUR SIP samples subjected to axial compression load

Sample Number	Max load [N]	Experimental Modulus of Elasticity, E [MPa]
CC65-1	4366.99	6.06
CC65-2	4734.30	6.95
CC65-3	4649.03	5.27
CC65-4	4741.17	6.15
CC65-5	4618.03	6.96
CC65-6	4794.88	5.31
Average	4650.73	6.12
STD		0.75
COV [%]		12.19

Table 5-3, 5-4 and, 5-5 (Chapter 5) of this thesis also provides the published physical and mechanical properties of the rigid PUR foam and the OSB face-sheets. As seen in Table 5-3, the actual core density of the PUR foam is 31 kg/m^3 (1.94 pcf) and the density of the molded panel is 36 kg/m^3 (2.25 pcf). This information is based on the data sheet provided by the SIP manufacturer. Some available published values have been provided in Table 7-3. It has to be noted that the following values resulted from the PUR foam with density of 25.6 kg/m^3 (1.6 lb./ft³) which is about 20% lighter than the foam used in tested PUR SIPs in this study. The author was not able to find published values for the PUR foams with density of 31 kg/m^3 (1.94 lb./ft³).

Table 7-3: Physical and mechanical properties of polyurethane foam with 25.6 kg/m^3 (1.6 lb./ft³) density (Shim et al., 2000)

Property	Value
Density [kg/m^3]	25.6
Shear modulus [MPa]	0.84
Plateau stress [MPa]	0.12
Compressive yield strain	5%
Strain at onset of densification	80%
Maximum tensile strain	5%
Maximum shear strain	10%

7.2.3 Experimental determination of modulus of elasticity of tested PUR SIP OSB face-sheets

Following ASTM D3043 (ASTM, 2011), coupons were prepared for a three point loading scheme to evaluate the modulus of elasticity of the OSB face-sheets used in the tested PUR SIPs. A brand new PUR SIP was cut in pieces and strips of OSB were separated from the PUR foam-core using a table saw (Figure 7-2). Three specimens were cut parallel (major axis) and three were cut perpendicular (minor axis) to the OSB strands. This would allow the E value of the OSB face-sheet material to be evaluated in the x and y directions. Each specimen was 500 mm long (19.7 in.), 11.1 mm (7/16 in.) thick (h), and 47.6 mm (1 7/8 in.) wide (b). All specimens were loaded to failure with a crosshead movement rate of 6.5 mm/min (1/4 in./min). The overall deflection (Δ) of the specimen was measured and recorded using the DAQ attached to the test-frame (Figure 7-3). The test-frame was an ATS machine (Series 1410, Computer controlled universal testing machine) equipped with an Interface 10000 lbs. load-cell capacity.

Based on Euler-Bernoulli's beam deflection theory, the mid-span elastic deflection of a simply supported beam, loaded exactly in the middle of its span, can be calculated using the following equation:

$$\Delta = \frac{FL^3}{48EI} \quad (\text{Eq. 7.9})$$



Figure 7-2: Separating OSB face-sheets from the PUR foam-core

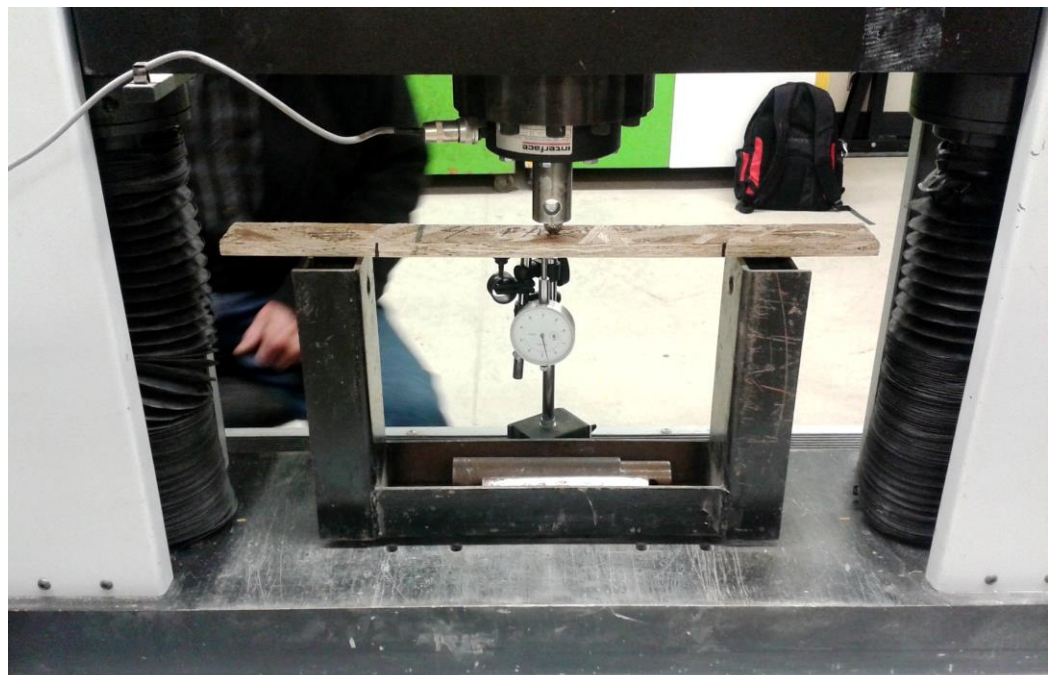


Figure 7-3: Test set-up for evaluation of E of the OSB face-sheet coupons

Where:

$F =$ Mid-span point-load

$L =$ Clear span

$E =$ Modulus of elasticity

$I =$ Moment of Inertia

Since the moment of inertia (I) of a rectangular section with a base width of 'b' and height of 'h', can be calculated using the following equation:

$$I = \frac{bh^3}{12} \quad (\text{Eq. 7.10})$$

Equation 7-9 can be re-written for E:

$$E = \frac{FL^3}{48 \Delta I} = \frac{FL^3}{4 \Delta b h^3} \quad (\text{Eq. 7.11})$$

The load vs. deflection curves of all tested OSB specimens can be seen in Figure G- 1 of the Appendix G. In order to find the E values, the load vs. deflection coordinates of three points within the elastic region of the load vs. deflection curves were used. Calculated E's were then averaged (Table 7-4). As for the parallel-to-strands specimens, 50, 100, and

150 N intervals were selected and as for the perpendicular-to-strands specimens, 30, 60, and 90 N intervals were selected.

As seen in Table 7-5, the average experimentally-found parallel-to-strands (major axis) modulus of elasticity of the OSB face-sheet is 4624.66 MPa, and 1845.76 MPa for perpendicular-to-strands (minor axis) coupons. The published values of E for OSB's (with different grades, densities, and different wood strand species sources), ranges from 3100 (SBA, 2004) to 7900 MPa (Forest Products Laboratory, 2010) for the parallel (major axis), and 1300 to 3100 MPa (SBA, 2004) for the perpendicular to strand directions (minor axis).

Table 7-4: Load points taken from the elastic region of load vs. deflection curves of tested OSB coupons

Specimen	Deflection [mm]	Load [N]	Deflection [mm]	Load [N]	Deflection [mm]	Load [N]
Parallel 1	0.97	49.68	2.03	99.76	3.15	150.47
Parallel 2	1.37	50.83	2.24	99.50	3.15	149.32
Parallel 3	1.22	50.83	2.39	99.23	3.66	150.61
Perpendicular 1	1.88	30.32	3.81	60.49	5.84	90.11
Perpendicular 2	1.53	30.18	3.25	60.94	5.03	90.52
Perpendicular 3	1.58	30.75	3.25	60.80	4.98	90.25

Table 7-5: Experimental average values of E based the data points provided in Table 7-4

Specimen	E [MPa]	Avg. E			
		[MPa]	[MPa]		
Parallel 1	5325.47	5085.65	4949.76	5120.29	
Parallel 2	3841.45	4610.84	4915.68	4455.99	4624.66
Parallel 3	4317.84	4305.69	4269.52	4297.68	
Perpendicular 1	1671.64	1645.03	1598.67	1638.45	
Perpendicular 2	2050.04	1942.01	1865.35	1952.47	1845.76
Perpendicular 3	2021.44	1938.99	1878.63	1946.35	

7.3 Modelling

7.3.1 Number of nodes and element sizes for each simulated test

Table 7-6 represents the number of nodes, element size and total number of elements defined in numerical models as generated automatically by the software. Each element had three degrees of freedom at each node consisting of translations in the nodal x, y, and z directions.

7.3.2 Loading

The average maximum loads that the panels resisted in different loading orientations in the experimental tests were used for loading the models. Therefore, FEM calculations

were executed until the maximum load in the modeling reached the maximum loads observed in the experimental tests. In terms of the axial load tests, similar to the experimental tests, the eccentric axial load was applied to the top of the panels. Supports and boundaries were set identical to the experimental tests, simulating the service conditions and based on the available ASTM standards of E72 (ASTM, 2015) and E1803 (ASTM, 2006). A similar approach was taken for transverse and racking load orientations in the modelling procedure. Experimentally found maximum loads were applied to the models in increments of 10kN and resulting deflections were recorded.

Table 7-6: Specimen ID, number of nodes, element size and, total number of elements of simulated PUR SIPs

Test Type	Model ID	Panel thickness mm [in.]	Total number of nodes	Element size mm	Total elements
Fully-bonded Axial	M45A	114 [4.5]	15599	89.43	9945
	M65A	165 [6.5]	16971	89.98	10891
Fully-bonded Transverse	M45T	114 [4.5]	14188	90.76	9001
	M65T	165 [6.5]	14850	90.76	9421
Fully- bonded Racking	M45R	114 [4.5]	15951	126.04	10096
	M65R	165 [6.5]	29891	90.75	19244
Dis-bonded Axial	MD45A	114 [4.5]	15513	90.85	9323
	MD65A	165 [6.5]	16520	90.86	10002
Dis-bonded Transverse	MD45T	114 [4.5]	15502	90.86	9295
	MD65T	165 [6.5]	16481	90.86	9954
Dis-bonded Racking	MD45R	114 [4.5]	15535	128.95	9292
	MD65R	165 [6.5]	16138	130.17	9731

The generated data points were used to plot the simulated load versus deflection curves for all the simulated panels. Calibration of the simulation process was verified by superimposing simulated curves over the experimental ones. In terms of axial load orientation, the axial load was distributed along the top line nodes located at $d/6$ from the panel center or $1/3$ of the overall thickness of the panel. All the nodes on the bottom of the panel were constrained in the ‘y’ direction. To simulate test setup, lateral constraint (‘z’ direction) was also applied to both sides of the panel, top and bottom, for a height of 60 mm (2.35 in.). As for the transverse and racking loading, the loading and boundary conditions were applied to the model identical to the experimental ones. Table 7-7 (also 4-4 in Chapter 4) and 7-8 (also 4-5 in Chapter 4), represent the maximum loads applied to fully-bonded and dis-bonded models in different loading orientations.

Table 7-7: Maximum load applied to modeled fully-bonded and dis-bonded 114 mm (4.5 in.) thick panels

Type of Panel	114mm [4.5 in.] thick PUR SIPs		
	Maximum Axial Load [kN]	Maximum Transverse Load [kN]	Maximum Racking Load [kN]
Dis-bonded	58.70	6.37	68.54
Fully-Bonded	159.97	30.40	53.14

Table 7-8: Maximum load applied to modeled fully-bonded and dis-bonded 165 mm (6.5 in.) thick panels

Type of Panel	165mm [6.5 in.] thick PUR SIPs		
	Maximum Axial Load [kN]	Maximum Transverse Load [kN]	Maximum Racking Load [kN]
Dis-bonded	71.26	9.29	44.73
Fully-Bonded	197.50	38.43	48.56

7.3.3 Mechanical and physical properties of the modeled PUR SIP components

Table 7-9 provides the published mechanical and physical properties of the PUR SIP materials that were used in the simulation process of the composite PUR SIPs. Table 7-10 represents the number of panels modeled along with their ID's.

7.4 Results

As seen in Table 7-10, a total of 12 models were created. Each loading orientation (axial, transverse and, racking) was modeled once. Both available thicknesses of PUR SIPs were modeled in this simulation experiment. Figure 7-4 to 7-16 represent the simulation results for 165 mm (6.5 in.) thick PUR SIPs.

Table 7-9: Physical and mechanical properties of modeled PUR SIPs from available published literature

Material	Properties	Value	Unit
Polyurethane Rigid Foam (Shim et al., 2000)	Elastic Modulus in X	4.61	MPa
	Poisson's Ration in XY	0.29	-
	Shear Modulus in XY	0.84	MPa
	Mass Density	48	kg/m ³
OSB (Dry condition) (SBA, 2004)	Elastic Modulus in X, Y	3100	MPa
	Elastic Modulus in Z	12.4	MPa
	Shear Modulus in XY	1000	MPa
	Poisson's Ration in X, Y	0.195	-
	Mass Density	650	kg/m ³
Douglas Fir 2x6 (38 x 140 mm) (Forest Products Laboratory, 2010)	Elastic Modulus in X	13440	MPa
	Poisson's Ration in X, Y	0.29	-
	Mass Density	500	kg/m ³

Table 7-10: Model ID's for simulated PUR SIPs under different loading scenarios

Model ID	114 mm [4.5 in.] thick PUR SIPs	Model ID	165 mm [6.5 in.] thick PUR SIPs
	Fully-Bonded		Fully-Bonded
M45A	Axial	M65A	Axial
M45T	Transverse	M65T	Transverse
M45R	Racking	M65R	Racking
	Dis-bonded		Dis-bonded
MD45A	Axial	MD65A	Axial
MD45T	Transverse	MD65T	Transverse
MD45R	Racking	MD65R	Racking

The simulation mesh detail and deformation behaviour or the deformation concentration results of the 114 mm (4.5 in.) panels can be found in Appendix G (Figures G - 2 to G - 13). All models were created using published values of the modulus of elasticity for the OSB face-sheets (Table 7-9) once, and once using the experimentally evaluated E values (Table 7-5). The entire loads vs. deflection curves contain three curves: experimental, simulated behaviour of the panel using the published values of E, and another one with the experimental value of E.

7.4.1 Axial tests results

In the case of axial loads, the load-deflection curves resulting from the computer simulation were compared with those obtained from the experimental tests in Figures 7-5 to 7-8. Experimental curves were plotted using the data readings of the top linear potentiometer. Figures 7-4, 7-5, and 7-6 represent the load vs. deflection behaviour of fully-bonded panels and 7-7, 7-8, and 7-9, represent partially dis-bonded panels. As seen in the load-deflection curves of fully-bonded PUR SIPS, when experimentally found values of E for OSB were used, the simulated model exhibited a load-deflection curve with smaller slope than the experimental curve. As seen in Figure 7-5, the simulated and experimental curves were almost identical when the published values of E for OSB were used. The deflection prediction in the simulated model with experimental E values is 3.15 mm higher than the simulated model with published E values at the peak of the load.

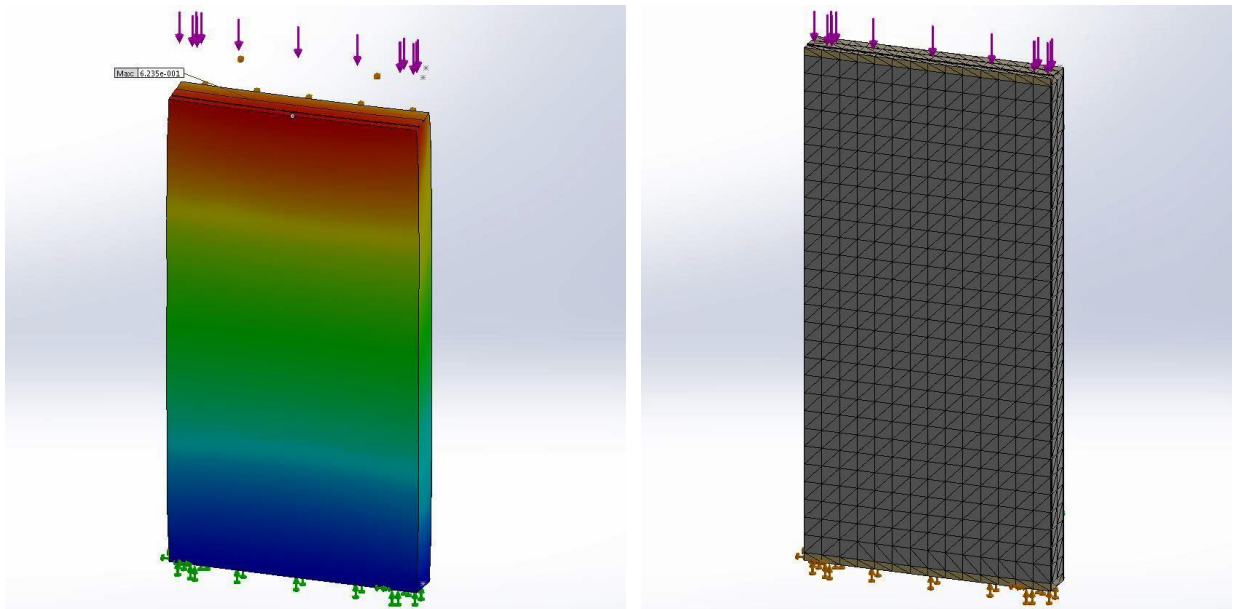


Figure 7-4: Mesh detail and deformation behaviour of modeled fully-bonded 165mm (6.5 in.) thick PUR SIPs under eccentric axial load (M65A) (Red indicates zone of greatest deformation)

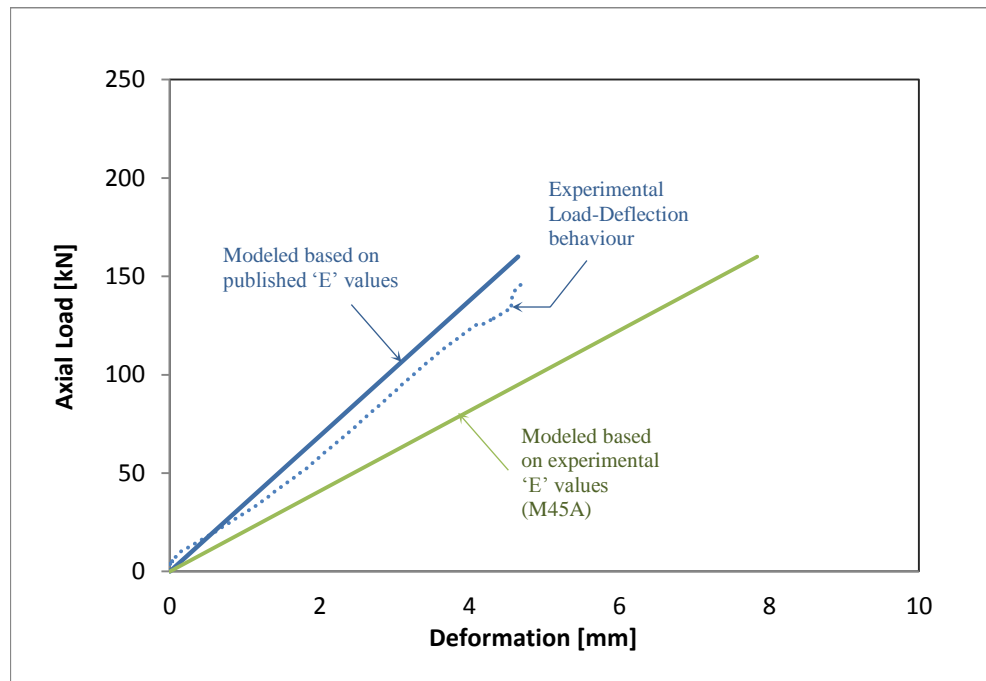


Figure 7-5: Comparison between the experimental results and simulated results concluded from axial load test on fully-bonded 114 mm (4.5 in.) thick PUR SIPs

As for the dis-bonded PUR SIPs, (Figure 7-7 and 7-8), both models stay linear. The experimental test did not behave in a linear manner because considerable amounts of deformation occurred in the dis-bonded area as soon as the axial load was applied to the panel. In experimental tests, buckling on both sides of the dis-bonded OSB happened almost immediately after the application of loads. Such phenomenon caused rapid change in the modulus of elasticity of the material, specifically OSB, initiating non-linear behaviour in the material(s).

As seen in Figure 7-7 and 7-8, unlike the behaviour of the test specimen, the deflection in both elastic models with constant modulus of elasticity, though different (experimental vs. published), remains proportional to the applied load. The overall effect of published values of E vs. experimental values is limited to a difference of 1.2 and 1.4 mm at the maximum load.

Based on these observations, the linear elastic modelling done with SOLIDWORKS cannot be accurate when significant localized deflection and deformation in material occurs during the application of loads. As seen in Figure 7-9, when exposed to eccentric axial loads, the concentration of stress is on top region of the specimen where the deflection is the highest.

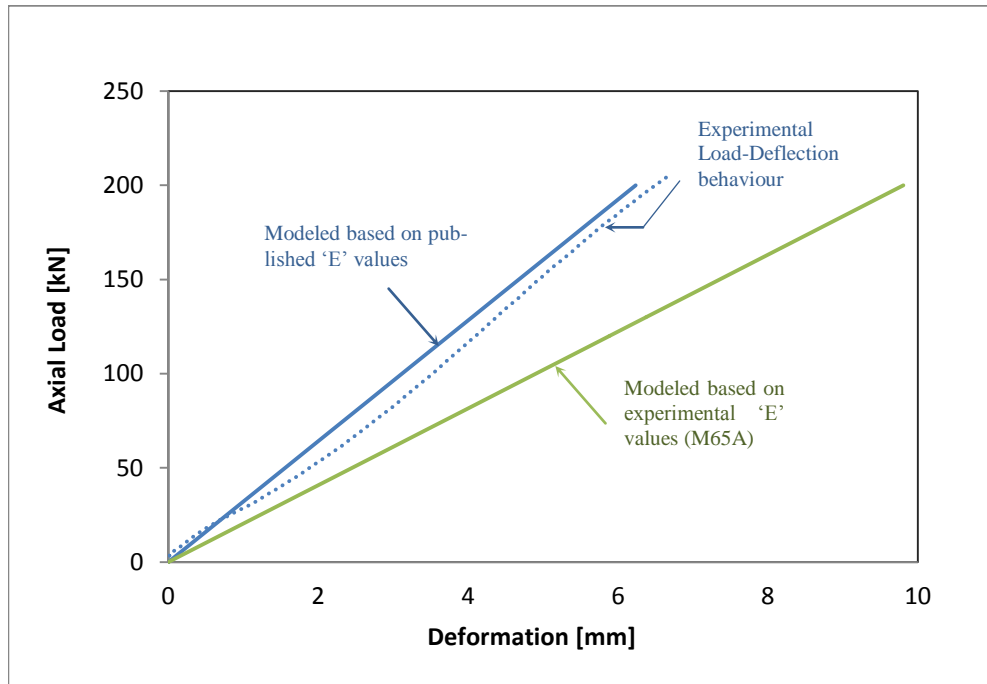


Figure 7-6: Comparison between the experimental results and simulated results concluded from axial load test on fully-bonded 165 mm (6.5 in.) thick PUR SIPs

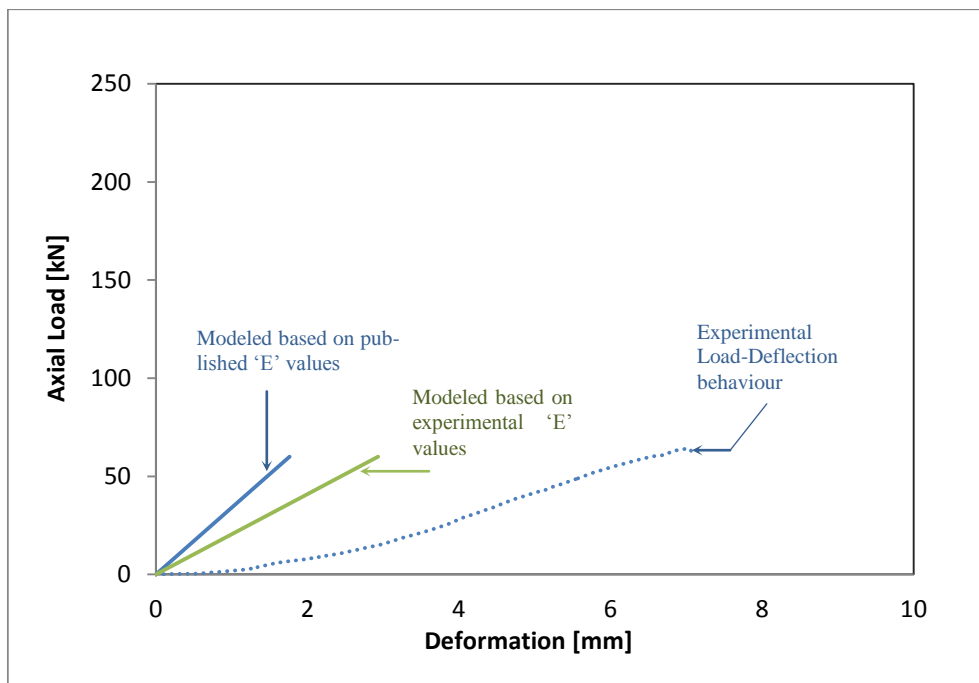


Figure 7-7: Comparison between the experimental results and simulated results concluded from axial load test on partially dis-bonded 114 mm (4.5 in.) thick PUR SIPs

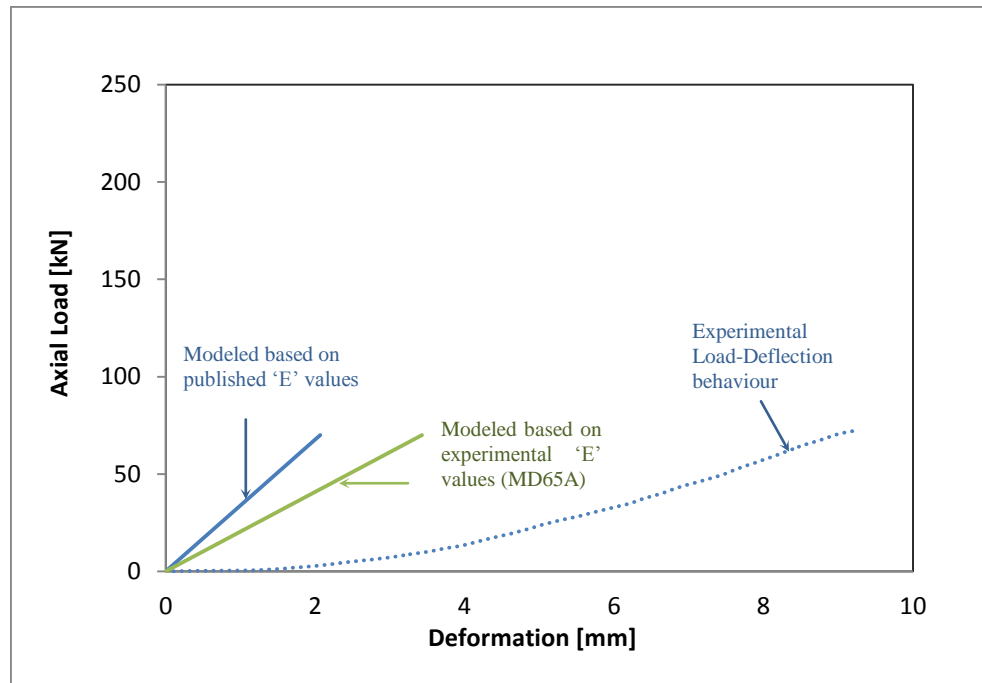


Figure 7-8: Comparison between the experimental results and simulated results concluded from axial load test on partially dis-bonded 114 mm (4.5 in.) thick PUR SIPs

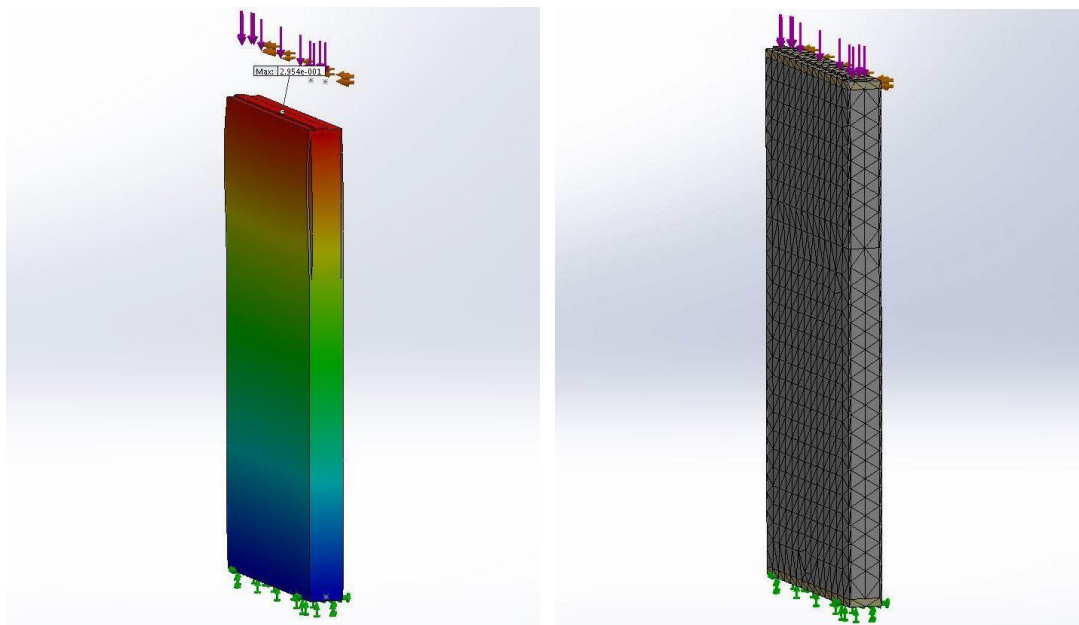


Figure 7-9: Mesh detail and deformation behaviour of modeled 165mm (6.5 in.) thick partially dis-bonded PUR SIPs under eccentric axial load (MD65A) (Red indicates zone of greatest deformation)

7.4.2 Transverse tests results

The load-deflection curves resulting from the computer modeling compared with those obtained from the experimental tests with a transverse load applied to the mid-height of the PUR SIPs are shown in Figure 7-10 and 7-11, for fully-bonded panels and Figure 7-13 and 7-14, for partially dis-bonded panels respectively. As seen in the load-deflection curves of fully-bonded panels, the behaviour of both modeled and experimental specimens are almost identical.

As for the partially dis-bonded PUR SIPs (Figures 7-13 and 7-14), some deformation was observed in the experimental tests when panels were subjected to transverse loads. As seen in Figures 7-13 and 7-14 (dotted curves), the pre-mature early deformation and deflection initiated some non-linear behaviour in the dis-bonded panel that does not match the linear behaviour predicted by the computer simulation. As seen in Figure 7-15, when exposed to transverse loads, partially dis-bonded PUR SIPs experienced an asymmetrical deflection with more deformation in the dis-bonded area dominating the final failure of the panel.

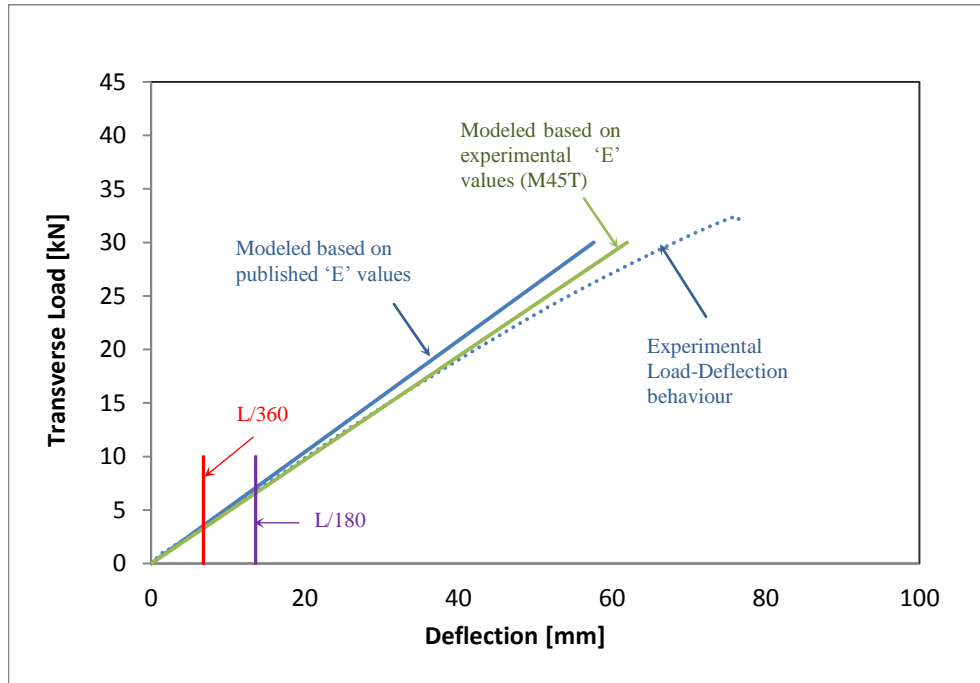


Figure 7-10: Comparison between the experimental results and simulated results concluded from transverse load test on fully-bonded 114 mm (4.5 in.) thick PUR SIPs

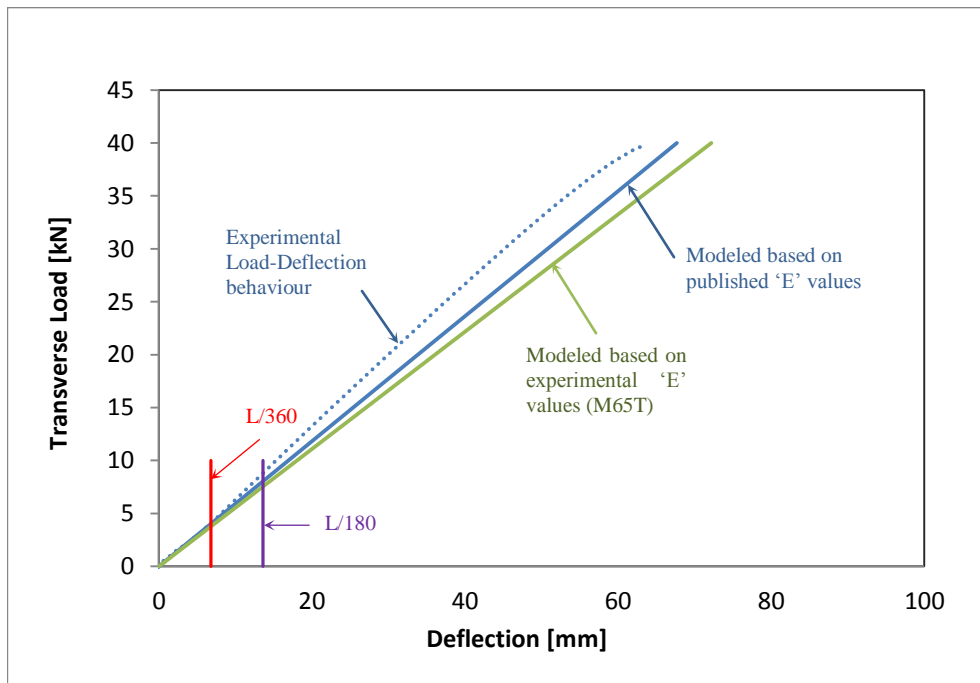


Figure 7-11: Comparison between the experimental results and simulated results concluded from transverse load test on fully-bonded 165 mm (6.5 in.) thick PUR SIPs

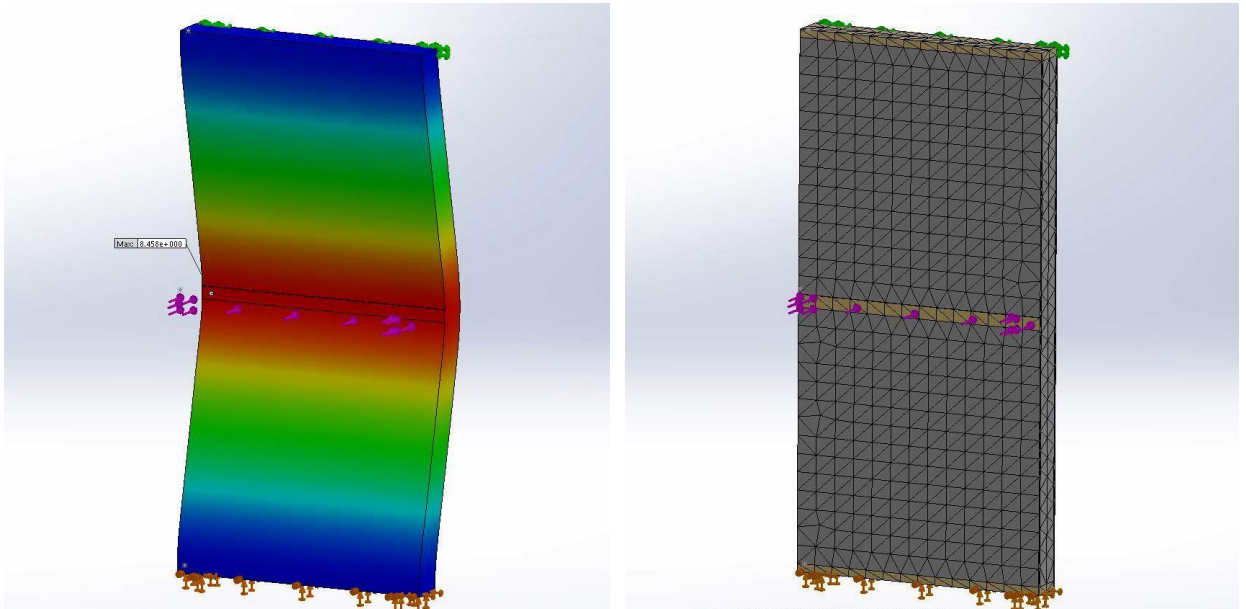


Figure 7-12: Mesh detail and deflection behaviour of modeled 165mm (6.5 in.) thick fully-bonded PUR SIPs exposed to transverse load (M65T) (Red indicates zone of greatest deformation)

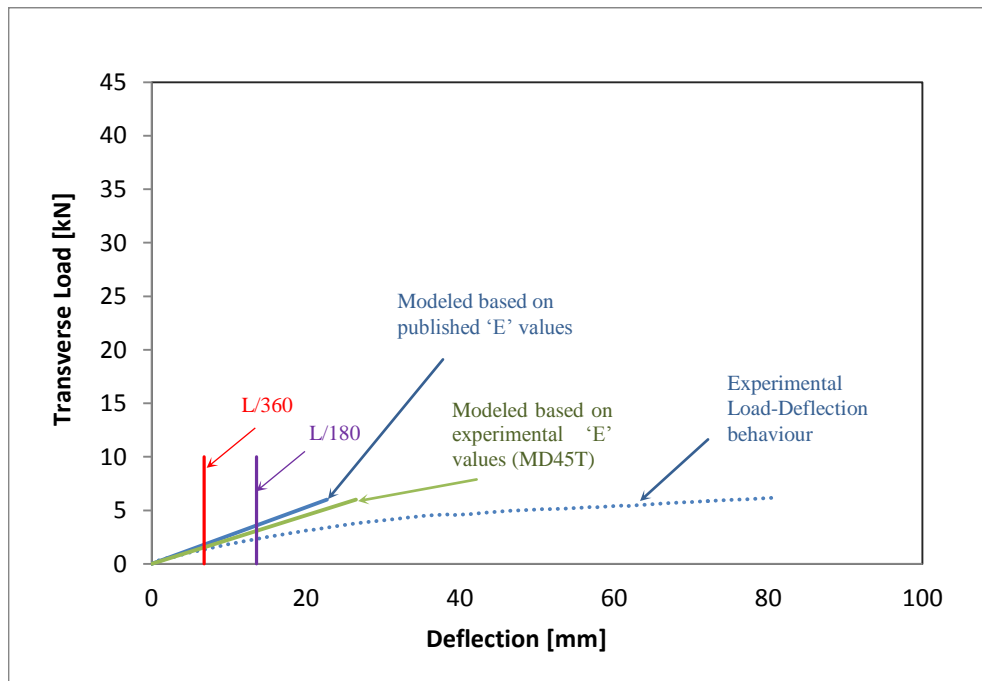


Figure 7-13: Comparison between the experimental results and simulated results concluded from transverse load test on partially dis-bonded 114 mm (4.5 in.) thick PUR SIPs

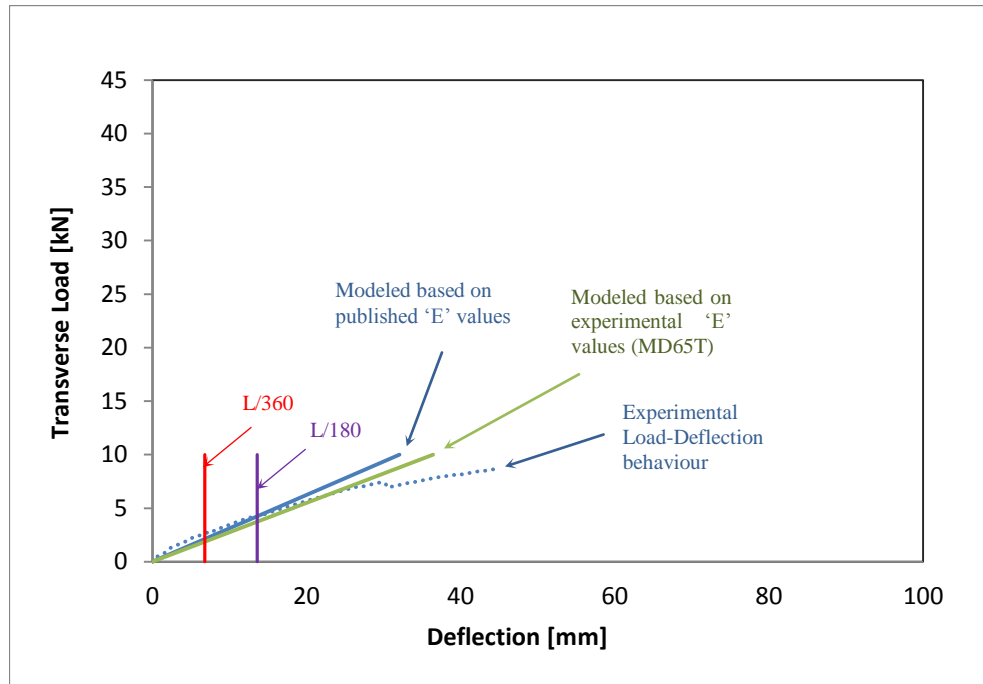


Figure 7-14: Comparison between the experimental results and simulated results concluded from transverse load test on partially dis-bonded 165 mm (6.5 in.) thick PUR SIPs

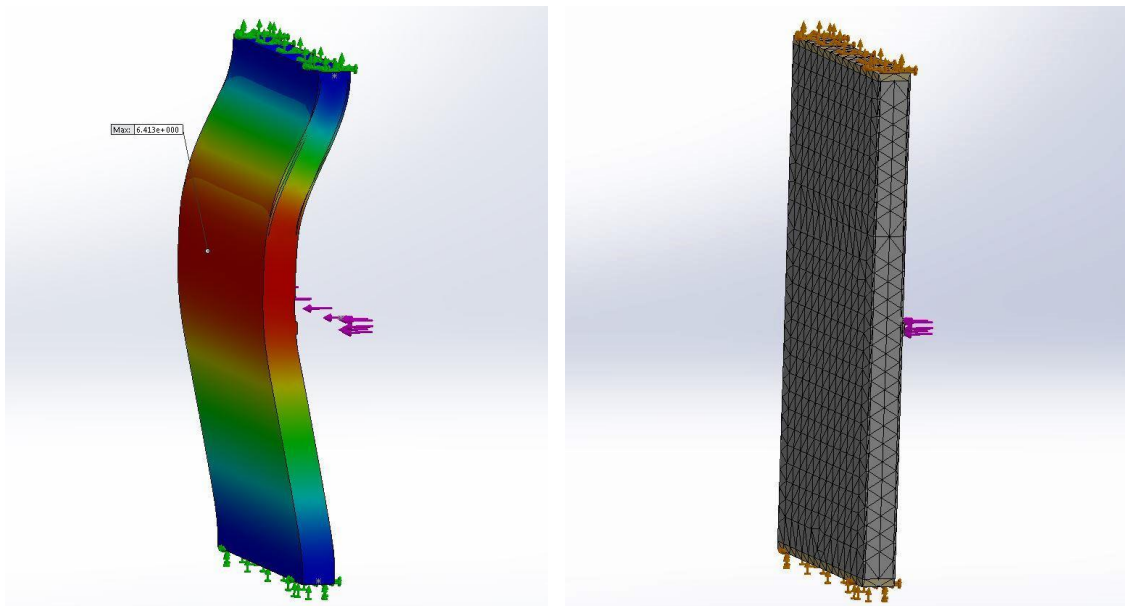


Figure 7-15: Mesh detail and deflection behaviour of modeled 165mm (6.5 in.) thick partially dis-bonded PUR SIPs exposed to transverse load (MD65T) (Red indicates zone of greatest deformation)

7.4.3 Racking tests results

As for the racking load response test simulations, the load-deflection curves resulting from the computer modeling compared with those obtained from the experimental tests of the panels are shown in Figure 7-16 and 7-17 for fully-bonded panels, and Figure 7-18 and 7-19, for partially dis-bonded panels. As seen in all load-deflection curves, the computer predicted behaviour of the composite model does not follow the experimentally found behaviour of the specimens.

Significant localized deformation at the load application area was observed (i.e. crushing of side and top lumber) when PUR SIPs were tested in racking load orientation. Similar to other tests with localized early deformation in material, the specimen tended to undergo a non-linear load-deflection experience. That in turn, caused the same gradual change in modulus of elasticity that is the source of inconsistency between the linear behaviour predicted by the simulation process and the experimental results. The assumption here is that in racking test simulations, localized deformation at the point of applied load is beyond the yield point and linear elastic behaviour, therefore, the model fails before it reaches the expected seen-in-experimental-tests deflection.

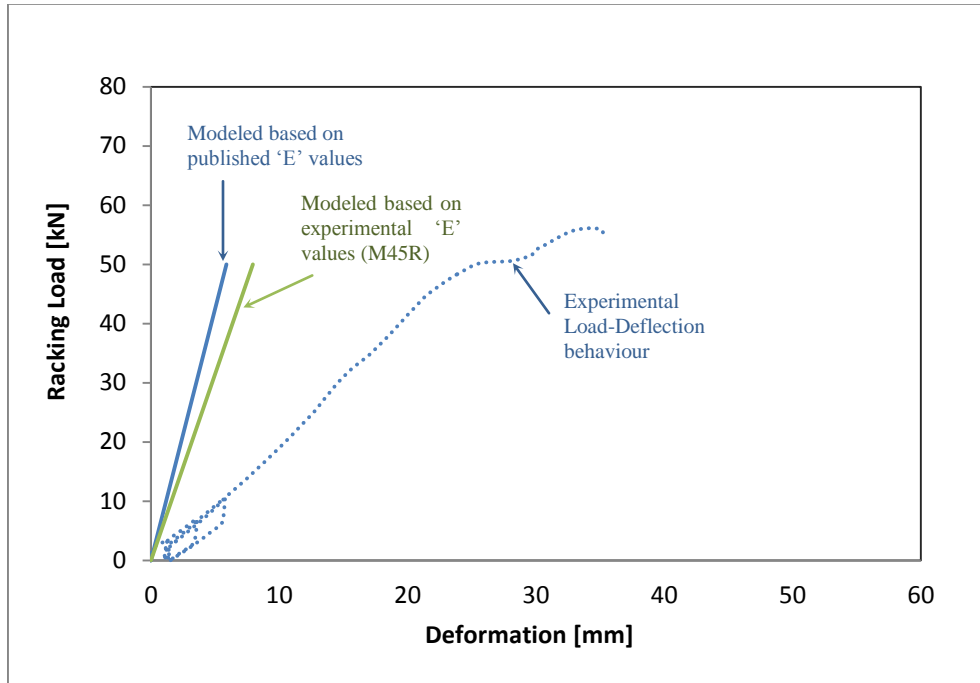


Figure 7-16: Comparison between the experimental results and simulated results concluded from racking load test on fully-bonded 114 mm (4.5 in.) thick PUR SIPs

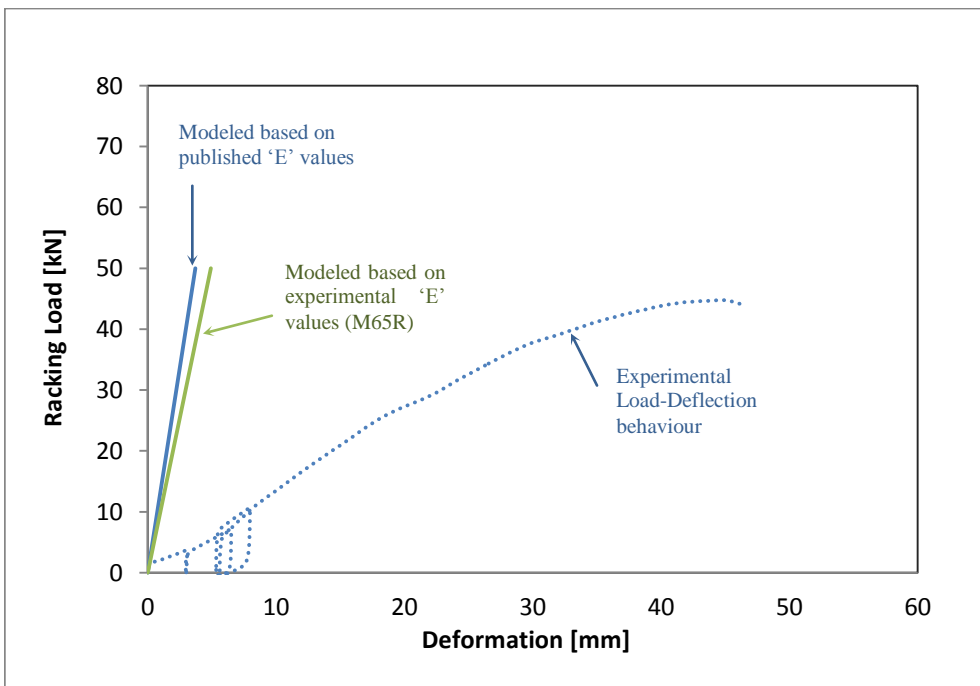


Figure 7-17: Comparison between the experimental results and simulated results concluded from racking load test on fully-bonded 165 mm (6.5 in.) thick PUR SIPs

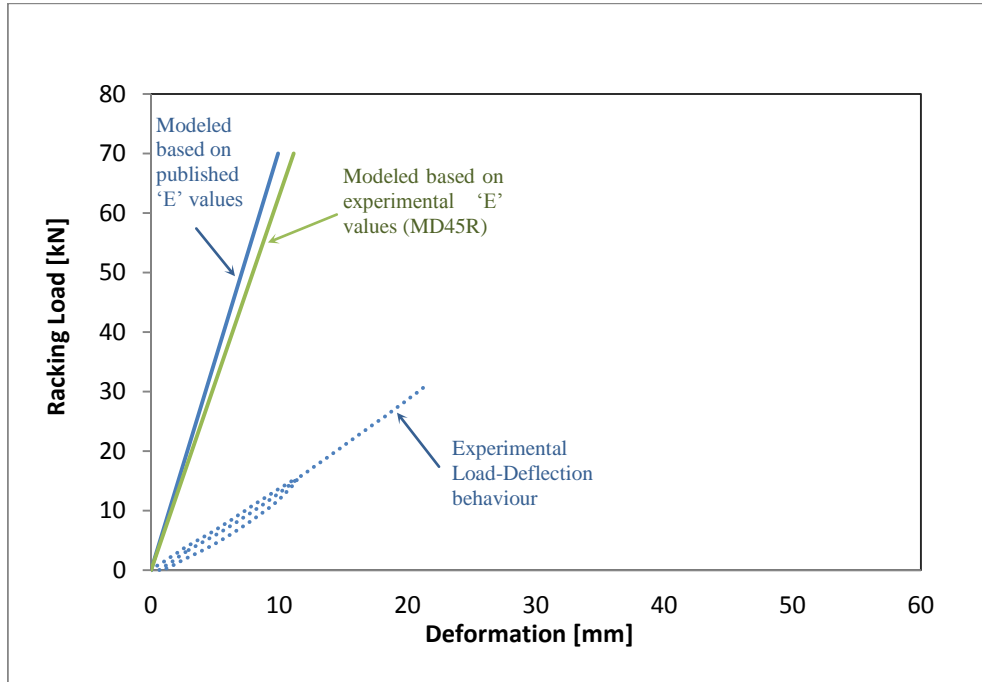


Figure 7-18: Comparison between the experimental results and simulated results concluded from racking load test on partially dis-bonded 114 mm (4.5 in.) thick PUR SIPs

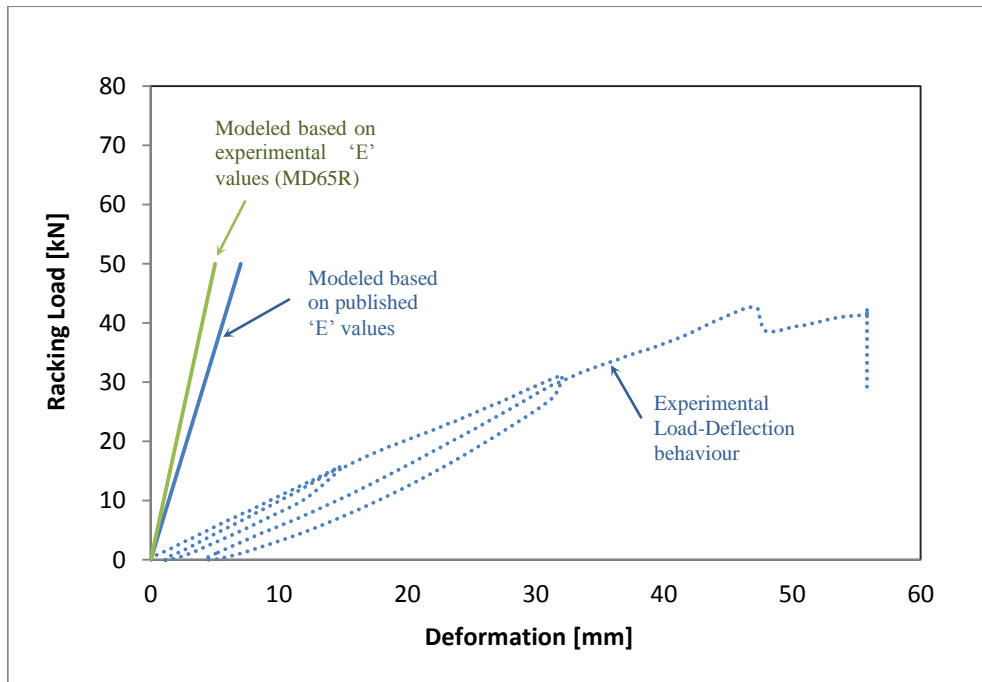


Figure 7-19: Comparison between the experimental results and simulated results concluded from racking load test on partially dis-bonded 165 mm (6.5 in.) thick PUR SIPs

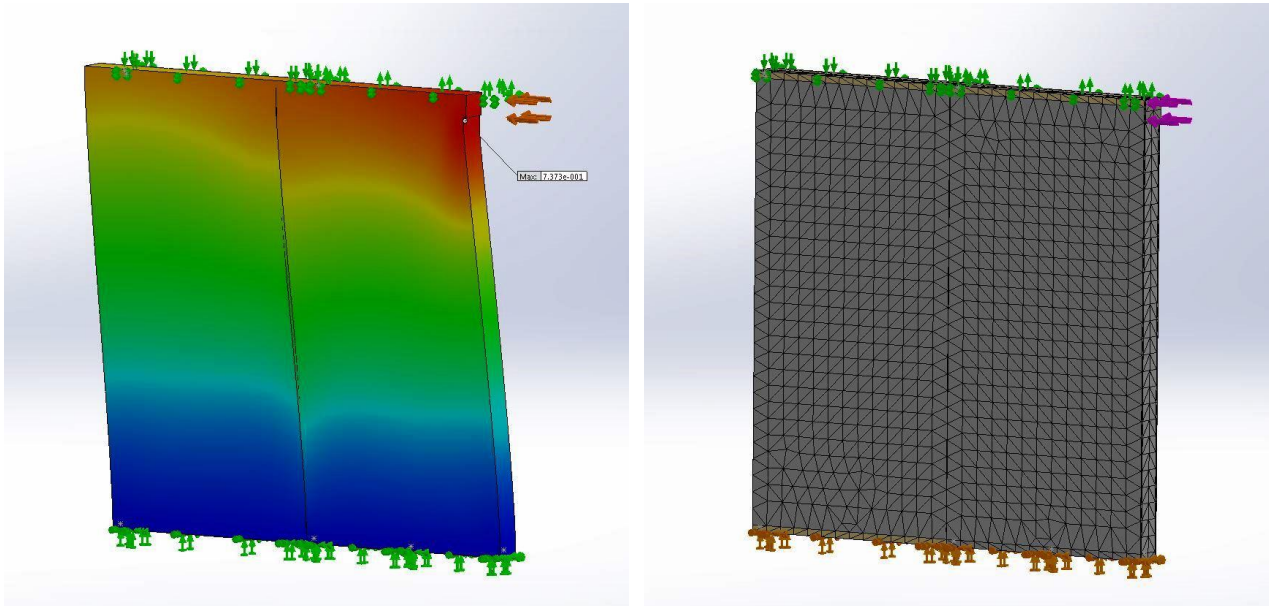


Figure 7-20: Mesh detail and deformation behaviour of modeled 165mm (6.5 in.) thick PUR SIPs exposed to racking load (M65R) (Red indicates zone of greatest deformation)

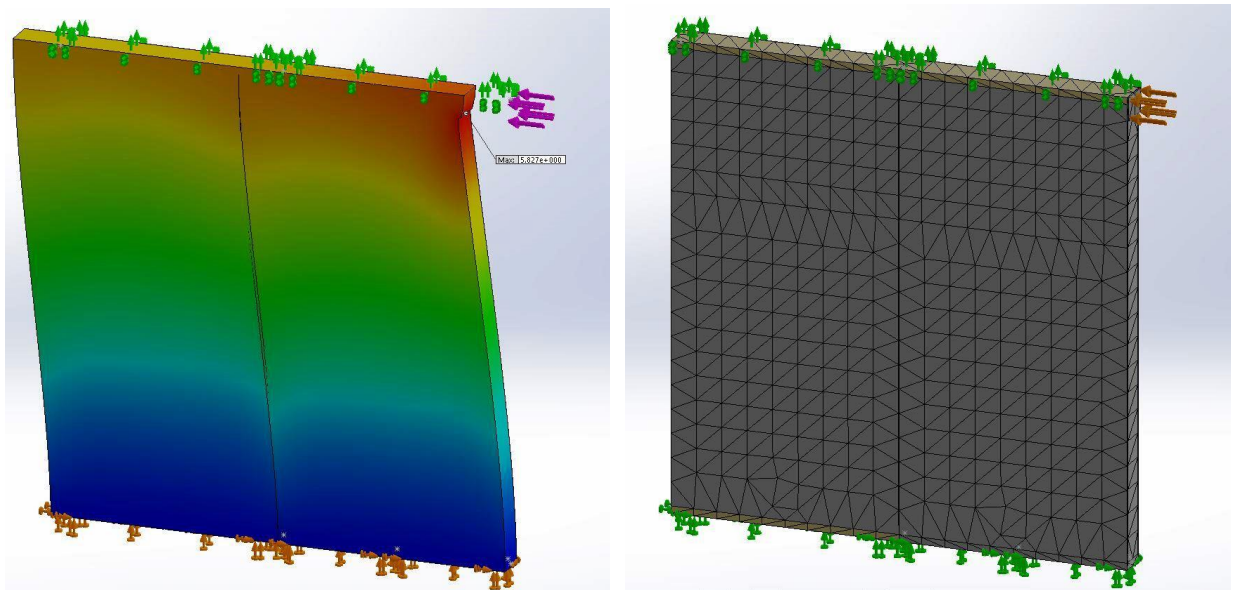


Figure 7-21: Mesh detail and deformation behaviour of modeled 165mm (6.5 in.) thick partially dis-bonded PUR SIPs exposed to racking load (MD65R) (Red indicates zone of greatest deformation)

7.5 Conclusions

After verifying the reliability of the FEM modeling using the experimental results data for full-scale fully-bonded and partially dis-bonded PUR SIPs, the FEM modeling conducted via SOLIDWORKS software was shown to be an effective tool in investigating the behaviour of the proposed panels only when the specimen did not experience any localized immediate deformation. Localized deflections, mostly happening in racking and axial tests and majorly in dis-bonded panels, caused non-linear load-deflection behaviour in material that requires different modeling approach considering such behaviour.

Therefore, FEM modeling conducted via SOLIDWORKS software can be useful to predict the structural behaviour of PUR SIPs with different overall thicknesses, different skin materials with different mechanical properties and, different thicknesses of foam core materials with different densities only in transverse loading orientation. This is limited only to fully-bonded panels.

FEM modeling of PUR SIPs via SOLIDWORKS does not seem to be an adequate tool to simulate the load response and load vs deflection behaviour of PUR SIPs in racking. The model is reasonable for fully-bonded axial but not for dis-bonded panels. The model predicted the transverse behaviour well for both fully-bonded and dis-bonded panels within the design range.

This simulation method seems to be an adequate prediction tool to predict the load response of composite material which do not undergo a significant deformation, or for those with minimal deflection and deformation before their final failure.

Chapter 8

Summary and Conclusions

8.1 General

An extensive experimental program was carried out to investigate the load-response, structural capacity, flexural creep behaviour, and the effects of weathering and service conditions on the bond between foam-core and the OSB face-sheets in PUR SIPs with two different thicknesses of 114 and 165 mm (4.5 and 6.5 in.). A literature review was conducted to investigate the current studies conducted on SIPs in general. The applicability of PUR SIPs for use in residential and commercial building construction was studied considering the Canadian building code requirements.

8.2 Overall Conclusions

8.2.1 PUR SIPs vs. stud wall panels

Polyurethane core Structural Insulated Panels tested in this study exhibited more rigidity, toughness, and overall load capacity than the conventional stud wall panels axial, racking, and transverse loading orientations. When the PUR SIPs were compared to conventional stud wall panels with the identical dimensions, 165mm (6.5 in.) thick PUR SIPs handled 25% more axial loads. In the case of transverse loading orientation, 165mm (6.5 in.) thick PUR SIPs handled 37% more transverse load than the stud wall panels. As for the racking loads, PUR SIPs exhibited 4.18 times more load capacity than the same

thickness of stud wall assemblies. This value was 3.42 times better with 114mm (4.5 in.) thick PUR SIPs were compared to the racking resistance of 114mm (4.5 in.) thick stud wall panels. In general, PUR SIPs go under less deformation and deflection before failure when exposed to racking load.

8.2.2 Thicker PUR SIPs vs. thinner PUR SIPs

When the two different thicknesses of available PUR SIPs were compared, under axial loads, 165mm (6.5 in.) thick PUR SIPs handled 23% more load than the thinner SIPs (114mm, 4.5 in.). When subjected to transverse loads, 165mm (6.5 in.) PUR SIPs handled 26% more load than the thinner SIPs (114mm, 4.5 in.). In terms of racking loads, 165mm (6.5 in.) thick PUR SIPs handled 9% less load than 114mm (4.5 in.) thick PUR SIPs.

8.2.3 Partially dis-bonded PUR SIPs vs. fully-bonded PUR SIPs

Partially dis-bonded (33% dis-bond between the PUR foam-core and the OSB face-sheets) PUR SIPs were compared to fully-bonded PUR SIPs in two different thicknesses. In the case of 165 mm (6.5 in.) thick PUR SIPs, dis-bonding resulted in an average of 64% reduction in axial load capacity of the panel compared to brand new fully-bonded PUR SIPs. The same dis-bond percentage caused an average 75.8% reduction in transverse load capacity and an average 7.9% reduction in racking load capacity of the panels.

In general, 33% dis-bond in 165 mm (6.5 in.) thick PUR SIPs had a minimal effect on the racking load capacity of the panels.

In the case of 114 mm (4.5 in.) thick PUR SIPs, 33% dis-bond between the PUR foam-core and the OSB face-sheets resulted in an average 63.3% reduction in axial load capacity of the panel compared to a brand new fully-bonded PUR SIPs. Same dis-bond ration caused an average 79% reduction in transverse load capacity of the panel compared to a brand new fully-bonded SIP. Thirty percent dis-bond between the foam-core and the OSB face-sheets over both sides of each SIP caused an average 29% increase in racking load capacity of the panel compared to a brand new fully-bonded SIP. Although dis-bonded 114 mm (4.5 in.) thick PUR SIPs handled more ultimate racking load before failure, they experienced more deflection before failure and showed less stiffness than the fully-bonded PUR SIPs with a similar thickness.

8.2.4 Creep load behaviour of PUR SIPs

When exposed to design live and dead loads, panels with 114 mm (4.5 in.) thickness tested for flexural creep deflection over a span of 2360 mm (93 in) satisfied the creep deflection limitations of $L/180$ and $L/240$ while they failed to satisfy the $L/360$ limitations. Panels with 165 mm (6.5 in.) thickness satisfied the creep deflection limitations of $L/180$ and $L/240$ but failed to satisfy the $L/360$ limitations. Similar to thinner panels, in order to

meet the criteria, loading span must be reduced accordingly. No permanent deflection was detected 90 days after removal of the applied loads to both thicknesses of PUR SIPs tested for flexural creep deflection.

8.2.5 Pull-off test conducted on brand new and weathered PUR SIPs

A total of 120 pull-off tests were conducted on new and weathered structural insulated panels to evaluate the bond quality between polyurethane foam and OSB facing sheets. No significant difference was found in the bond strength between the sides of the panels. Based on shear stress for specimens that failed within the foam, there was no apparent degradation of the foam. Only 2.5% of the specimen exhibited a partial failure at the interface between the OSB facing sheet and foam-core. Of the three that failed, two specimens were found in new panels. Thus, the failure was not related to aging or weathering. Even though there is no significant difference in bond performance between new and weathered panels, this does not negate the need to provide appropriate cladding for the wall system to minimize degradation of the exterior OSB face-sheets.

8.2.6 Load response computer simulation of PUR SIPs

A commercially available software program SOLIDWORKS™ (Dassault Systèmes, 2015) was used to model panel behaviour. It was shown to be an effective tool to predict load-deformation behaviour when the specimen did not experience any localized imme-

diate deformation. Therefore, such modeling method can be useful to predict the axial load response of fully-bonded PUR SIPs and transverse behaviour of both fully-bonded panels and dis-bonded panels.

8.3 Limitations and Further Recommended Tests

8.3.1 Limitations

The original intention was to test dis-bonded panels with several dis-bond percentages. That required more time and funding to manufacture the specimens. Due to such limitations, only 33% dis-bond ratio was selected.

As for creep tests, five specimens per PUR SIP thickness were intended to be tested in order to generate a stronger data pool. Due to lab space limitations, the number was reduced to three samples per thickness.

8.3.2 Further Recommended Tests

1. A set of weathered panels in both 114 and 165 mm (4.5 and 6.5 in.) thicknesses needs to be tested for structural capacity and flexural creep behaviour. The panels can be kept in environmental chamber with the exposure to freeze thaw cycles. Also, a set should be tested for creep in different sizes after being weathered.

Such a test would evaluate the effects of weathering and service conditions on the load-response and overall structural behaviour of PUR SIPs.

2. Since the majority of the SIPs manufactured in Canada have EPS foam-core, all the above mentioned tests can be repeated for EPS SIPs.
3. A set of panels in both 114 and 165 mm (4.5 and 6.5 in.) thicknesses should be tested for flexural creep with smaller spans than the tested 2338 mm (92 in.). This includes 1830 mm (72 in.) which based on the manufacture's suggestion is the norm in practice and application of PUR SIPs.
4. PUR and EPS SIPs of both 114 and 165 mm (4.5 and 6.5 in.) thicknesses made with 40% and 50% dis-bonding ratios should be tested for structural capacity and load-response as well as flexural creep behaviour. Results of such study, along with the results of the current research, would decide if there is a linear relationship between the de-bonding ration and the reduction in structural capacity of PUR or EPS SIPs.
5. Development of a non-destructive inspection test for Structural Insulated Panels.
The aim of such a study would be to determine a reliable and efficient non-

destructive test method for inspection of Structural Insulated Panels (SIPs). Ultrasonic inspection technology can be used to choose a suitable device. Simulated flawed samples can be tested in the laboratory in order to calibrate test images based on the type of defect and relate them to deterioration or imperfections. At the completion of this step, a database consisting of images gathered from testing several houses built with SIPs in the United States and Canada can be generated. The gathered data can be used to relate aging of SIPs with their long-term durability and integrity. The findings may answer some of the questions surrounding the long-term durability and the service life of SIPs.

6. More modelling and computer simulation can be conducted to find the effects of the different dis-bonding ratios on available EPS and PUR SIPs with different thicknesses.
7. The effects of the foam-core density on the overall structural capacity of the PUR SIPs can be studied via computer simulation and modelling as well. Deflections and stress distribution over the panel can be studied using this method.

8. Modelling and computer simulation can also be employed to study the effects of different face-sheets, such as drywall, plywood, or magnesium oxide board, on the overall behaviour of such panels. Panels with different thicknesses, foam-core density, and dis-bonding ratios can be studied.

References

1. *Agriboard Industries* . (2010). Retrieved 10 6, 2013, from www.agriboard.com:
http://www.agriboard.com/panels_from_agriboard.htm
2. *All Canadian Construction*. (2011). Retrieved 02 05, 2013, from
www.allcanadianconstruction.ca: <http://www.allcanadianconstruction.ca/SIP.html>
3. Allen, H. G. (1969). *Analysis and Design of Structural Sandwich Panels*. Oxford, England: Pergamon Press Ltd.
4. *American Chemistry Council*. (2012). Retrieved 04 05, 2012, from
<http://www.americanchemistry.com/>
5. APA. (1998). *Plywood Design Specification*. Tacoma, WA, USA: The Engineered Wood Association, APA.
6. APA. (2008). *Standardization Testing of Structural Insulated Panels (SIP) – BASF Polyurethane*. Washington, USA: The Engineered Wood Association (Keith, Edward L.).

7. APA. (2011). *Qualified OSB Facing Materials for SIPs - PR N610*. Tacoma, Washington: APA- The Engineered Wood Association.
8. APA. (2013). *ANSI/APA PRS 610.1 - 2013: Standard for Performance-Rated Structural Insulated Panels in Wall Applications*. Tacoma, WA, USA: The Engineered Wood Association (APA) and Approved American National Standard (ANSI).
9. ASTM. (2006). Standard Test Methods for Determining Strength Capacities of Structural Insulated Panels. *Designation: E1803 – 06*. West Conshohocken, USA, PA, United States: ASTM International.
10. ASTM. (2008). Standard Test Method for Flexure Creep of Sandwich Constructions. *Designation: C480/C480M – 08*. West Conshohocken, PA 19428-2959, United States: ASTM International.
11. ASTM. (2009). Standard Test Method for Pull-Off Strength of Coatings Using Portable Adhesion Testers. *D4541 – 09*. West Conshohocken, PA, USA: ASTM International.
12. ASTM. (2011). Standard Test Method for Core Shear Properties of Sandwich Constructions by Beam Flexure. *Designation: C393/C393M – 11*. West Conshohocken, PA, USA: ASTM International.

13. ASTM. (2011). Standard Test Methods for Structural Panels in Flexure.
Designation: ASTM D3043 - 00(2011). West Conshohocken, PA 19428-2959,
United States: ASTM International.
14. ASTM. (2013). Standard Practice for Contact Ultrasonic Testing of Weldments.
ASTM E164. West Conshohocken, PA, United States: ASTM International.
15. ASTM. (2013). Standard Specification for Driven Fasteners: Nails, Spikes, and
Staples. *Designation: F1667 - 13*. West Conshohocken, PA 19428-2959, United
State: ASTM Internationa.
16. ASTM. (2013). Standard Test Method for Tensile Strength of Concrete Surfaces
and the Bond Strength or Tensile Strength of Concrete Repair and Overlay
Materials by Direct Tension (Pull-off Method). *Designation: C1583/C1583M –
13*. West Conshohocken, PA 19428-2959, United States: ASTM International.
17. ASTM. (2013). Standard Test Method for Tensile Strength of Concrete Surfaces
and the Bond Strength or Tensile Strength of Concrete Repair and Overlay
Materials by Direct Tension (Pull-off Method). *C1583/C1583M – 13*. West
Conshohocken, PA, USA: ASTM International.
18. ASTM. (2015). Standard Test Methods of Conducting Strength Tests of Panels
for Building Construction. *Designation: E72-15*. West Conshohocken, PA, United
States: ASTM International.

19. AWC. (1992). *Wood Structural Design Data*. Washington DC: American Forest and Paper Association, American Wood Council.
20. BASF. (2007). Retrieved 06 12, 2012, from BASF:

http://www.basf.com/group/corporate/en/brand/STYROPOR_PERIPOR
21. BBA. (2009). *SIP Load Bearing Wall and Roof Panels*. British Board of Agreement.
22. Branz. (1999). *Asphalt Shingle Roofing*. Porirua City, New Zealand: Branz.
23. Bregulla, J. (2003). Investigation into the fire and racking behaviour of structural sandwich panel walls. *A methodology to assess loadbearing sandwich panels in fire*. Civil Engineering, School of Engineering, University of Surrey.
24. Briody, C., Duignan, B., Jerrams, S., & Ronan, S. (2012). Prediction of compressive creep behaviour in flexible polyurethane foam over long time scales and at elevated temperatures. *Polymer Testing*, DOI:

10.1016/j.polymertesting.2012.07.006.
25. Butt, A. S. (2008). Experimental study on the flexural behavior of structural insulated sandwich timber panels. *Thesis for Master of Applied Science (MAsc)*. Ontario, Canada: Ryerson University.
26. Cai, Z., & Ross, R. J. (2010). Chapter 12: Mechanical Properties of Wood-Based Composite Materials. In R. Bergman, *Wood Handbook, Wood as an Engineering*

- Material*. Madison, WI: U.S. Department of Agriculture: Forest Products Laboratory: 508 p.
27. Cas, B., Saje, M., & Planinc, I. (2007). Buckling of layered wood columns. *Advances in Engineering Software* , 38: 586–597.
28. Cathcart, C. M. (1998). SIPs, Not Studs. *Architecture*, 152: 148-153.
29. CCMC. (1996). Retrieved 01 25, 2012, from National Research Council Canada: <http://archive.nrc-cnrc.gc.ca/obj/irc/images/ci/v2no1/p4figB.gif>
30. CCMC. (2010). CCMC. Retrieved 08 25, 2012, from National Research Council Canada: <http://www.nrc-cnrc.gc.ca/eng/ibp/irc/ci/volume-2-n4-5.html>
31. CCMC. (2013). Retrieved 02 13, 2013, from National Research Council Canada: <http://www.nrc-cnrc.gc.ca/eng/index.html>
32. Cervenka Consulting. (2015). *ATENA 5*. Retrieved 10 05, 2015, from <http://www.cervenka.cz/products/atena/>
33. Cortez-Barbosa, J., Morales, E. A., Lahr, F. A., Nascimento, M. F., De Araujo, V. A., & Zaia, U. J. (2015). Bamboo Particulate Waste - Production of High Performance Structural Panels. In F. A. Lahr, H. Savastano Júnior, & J. Fiorelli, *Non-conventional Building Materials based on Agro-industrial Wastes* (pp. 9-48). Bauru, SP, Brazil: Tiliform.
34. CSA. (2009). *CSA 086-09 (Engineered Design in Wood)*. Mississauga, ON: Canadian Standard Association.

35. CSA. (2014). 086-14 Engineering design in wood. 5.4.2 *Elastic deflection*. Toronto, ON, Canada: CSA Group.
36. CWC. (2010). Wood Design Manual. Ottawa: Canadian Wood Council.
37. Dai, L. (2006). Fatigue Behaviour and Design of Wood Composites as Furniture Components. *SEM Annual Conference & Exposition on Experimental and Applied Mechanics*. Dept. of Forest Products, Mississippi State: Mississippi State University.
38. Daniel, I., Gdoutos, E. E., Wang, K. A., & Abot, J. L. (2002). Failure Modes of Composite Sandwich Beams. *International Journal of Damage Mechanics*, Vol. 11, 309 - 334, DOI: 10.1106/105678902027247.
39. Dassault Systèmes. (2015, 09 24). <https://www.solidworks.com/>. Retrieved 2015, from <https://www.solidworks.com/sw/products/simulation/finite-element-analysis.htm>
40. Davies, J. M. (1987). Design Criteria for Structural Sandwich Panels. *The Structural Engineer*, Vol. 65A, No.12, 435-441.
41. DuPont. (2011). *Technical Information ABA-14, H-54876-1 11/11*. DuPont.
42. Findley, W. N., Lai, J. S., & Onaran, K. (1976). *Creep and Relaxation of Nonlinear Viscoelastic Materials*. ISBN-10: 0486660168: North-Holland Publishing Company, Dover Publications.
43. Fine Homebuilding. (2006). Photograph by John Ross, The Taunton Press, Inc.

44. Foamlaminates. (2008). *www.foamlaminates.com*. Retrieved 1 19, 2011, from
Foam Laminates of Vermont:
http://www.foamlaminates.com/history_of_sips_part_1.html
45. Forest Products Laboratory. (2010). Mechanical Properties of Wood-Based
Composite Materials. In *Wood Handbook, Wood as an Engineering Material,
Centennial Edition, General Technical Report FPL– GTR–190* (pp. 12-2).
Madison, Wisconsin: Forest Products Laboratory, United States Department of
Agriculture Forest Service.
46. *Forest Products Laboratory*. (2012, 07 01). Retrieved from United States
Department of Agriculture: <http://www.fpl.fs.fed.us/>
47. Frisch, K. C., & Saunders, J. H. (1973). *Plastic Foams*. New York: Marcel
Dekker, Inc.
48. Gagnon, M., & Adams, R. (1999). A Marketing Profile of the U.S. Structural
Insulated Panel Industry. *Forest Products Journal*, Vol. 49 Issue 7/8, p31, 5p, 4
Charts, 1 Map.
49. Glick, J. (1973). The Buckling Load of an Elastically Supported Cantilevered
Column with Continuously Varying Cross Section and Distributed Axial Load.
Ingenieur-Archiv, 42: 355-359.

50. Hilado, C. J. (1967). Effect of Accelerated and Environmental Aging on Rigid Polyurethane Foam. *Journal of Cellular Plastics* , 1967 3: 161, DOI: 10.1177/0021955X6700300403.
51. HSU, D. K. (2008). Nondestructive Inspection of Composite Structures: Methods and Practice. *17th World Conference on Nondestructive Testing* (p. 3437 (4 Vols)). Shanghai, China: Curran Associates, Inc.
52. Huang, J.-S., & Gibson, L. J. (1990). Creep of Sandwich Beams with Polymer Foam Cores. *Journal of Materials in Civil Engineering*, 2(171-182), pp. Vol. 2, No. 3, pp. 171-182.
53. ICCES. (2011). ICC-ES Acceptance Criteria for Sandwich Panels. *Revisions to the ICC-ES Acceptance Criteria for Sandwich Panels*. Birmingham, AL, USA: ICC Evaluation Services.
54. International Barrier Technology. (2008). *Fire-Resistance Treatment of Structural Insulated Panels (SIPs) for Commercial Roofing Systems*. Watkins, MN, USA: International Barrier Technology.
55. International Organization for Standardization. (2011). ISO 22452:2011 Timber structures - Structural insulated panel walls - Test methods. *2011*. International Organization for Standardization.

56. Just, M. (1983). Results of Experimental Tests Regarding the Long Term Behaviour of Supporting Building Components Made of PURE-hardfoam and the Conclusions for Their Use. *Ifl-Mitt*, 22((3) 95-104).
57. Kermani, A., & Hairstans, R. (2006). Racking Performance of Structural Insulated Panels. *Journal of Structural Engineering (ASCE)*, 132:1806-1812.
58. Kosny, J., Desjarlais, A., & Christian, J. (1999). *Whole Wall Rating/Label for Structural Insulated Panel: Steady-State Thermal Analysis*. Oak Ridge, TN, United States: Oak Ridge National Laboratory, Buildings Technology Center.
59. Laufenberg, T. L., Palka, L. C., & McNatt, J. D. (1999). *Creep and creep-rupture behavior of wood-based structural panels*. Madison, WI, U.S.A.: United States Department of Agriculture, Forest Service, Forest Products Laboratory.
60. Mc Leister, D. (1998). Structural insulated panels. *Professional Builder*, Vol. 63(11) 50-56.
61. Medina, M. A., King, J. B., & Zhang, M. (2008). On the Heat Transfer Rate of Structural Insulated Panels (SIPs) Outfitted with Phase Change Materials (PCMs). *Energy*, 33 (667-678).
62. Morley, M. (2000). *Structural Insulated Panels (SIPS)*. Newtown, CT: The Taunton Press.

63. Mousa, M. A., & Uddin, N. (2010). Debonding of Composites Structural Insulated Sandwich Panels. *Journal of Reinforced Plastics and Composites*, 29: 3380.
64. Mousa, M. A., & Uddin, N. (2011). Global buckling of composite structural insulated wall panels. *Materials and Design* , 32: 766–772.
65. Mousa, M. A., & Uddin, N. (2012). Structural behavior and modeling of full-scale composite structural insulated wall panels. *Engineering Structures*, Volume 41, 320–334.
66. Mullens, M. A., & Arif, M. (2006). Structural Insulated Panels: Impact on the Residential Construction Process. *Journal of Construction Engineering and Management*, Vol. 132, No.7, pp. 786-794.
67. NBC. (2010). National Building Code of Canada. *Clause 4.1.8.13 , Sentence 3, Division B*. Ottawa, Canada: NRC Construction.
68. NRC. (2007). National Building Code of Canada. 2. Ottawa: National Research Council Canada.
69. NTA Inc. (2009, 0 27). Engineered design of SIP panels using listing report data. *NTA IM 14 TIP 01 SIP Design Guide* . Nappanee, Indiana, USA.
70. Olympus. (2013, 11 01). *Application Notes*. Retrieved from <http://www.olympus-ims.com>: <http://www.olympus-ims.com/en/applications/non-destructive-bond-testing-aircraft-composites/>

71. Panjehpour, M., Abang Ali, A. A., & Voo, Y. L. (2013). Structural Insulated Panels: Past, Present, and Future. *Journal of Engineering, Project, and Production Management*, 3(1), 2-8.
72. PATH. (2001). *The Partnership for Advancing Technology in Housing (PATH)*. Retrieved 10 5, 2013, from <http://www.toolbase.org>:
http://www.toolbase.org/pdf/techinv/sips_techspeg.pdf
73. Plaut, R. H., & Yang, J.-G. (1993). Lateral Bracing Forces in Columns with Two Unequal Spans. *J. Struct. Eng.* , 119:2896-2912.
74. Pollack, H. W. (1988). *Materials Science and Metallurgy (4th Edition)*. Prentice Hall.
75. PorterCorp. (2011). <http://www.portersips.com/history.html>. Retrieved 06 28, 2011, from <http://www.portersips.com/>: <http://www.portersips.com/history.html>
76. PorterSIPS. (2012). *The evolution of the structural insulated panel*. Retrieved 10 10, 2013, from <http://www.portersips.com/>:
<http://www.portersips.com/history.html>
77. RISA Technologies. (2015). Retrieved 10 05, 2015, from <https://risa.com/index.html>
78. Rungthonkit, P., & Yang, J. (2009). Behaviour of structural insulated panels (SIPs) under both short-term and long-term loadings. *Proceedings of the 11th*

- International Conference on Non-conventional Materials and Technologies (NOCMAT 2009)*. Bath, UK.
79. SBA. (2004). *Oriented Strand Board in Wood Frame Construction - Canadian Edition. OSB Performance by Design*. Structural Board Association.
80. SBA. (2004). *OSB Performance by Design. Oriented Strand Board in Wood Frame Construction*. Edmonton, AB: Structural Board Association.
81. SBA. (2004). *OSB Performance by Design, Canadian Edition*. Edmonton, AB: Structural Board Association.
82. Seismosoft Ltd. (2015). *SeismoStruct*. Retrieved 10 05, 2015, from <http://www.seismosoft.com/seismostruct>
83. Shaw Environmental System Analysis Inc. (2009). *An in-situ Evaluation of the Thermal and Moisture Performance of the Therman SIPs*. St. Catharines, ON, Canada.
84. Shim, V., Tu, Z. H., & Lim, C. T. (2000). Two-dimensional response of crushable polyurethane foam to low velocity impact. *International Journal of Impact Engineering* , 24: 703- 731.
85. SIPA. (2011). *About SIPA*. Retrieved 02 13, 2013, from Structural Insulated Panel Association, United States: <http://www.sips.org/about>
86. SIPA. (2013). *Structural Insulated Panel Association*. Retrieved 12 13, 2013, from <http://www.sips.org/press-releases>

87. Song, X., & Lam, F. (2010). Stability Capacity and Lateral Bracing Requirements of Wood Beam-Columns. *Journal of Structural Engineering*, 211 - 218.
88. Standards Council of Canada. (2011). Standard for Thermal Insulation, Polyurethane and Polyisocyanurate, Boards, Faced. Ottawa: Standards Council of Canada.
89. Stirna, U. (2011). Mechanical properties of rigid polyurethane foams at room and cryogenic temperatures. *Journal of Cellular Plastics*, 2011 47: 337, DOI: 10.1177/0021955X11398381.
90. Taylor, S. B. (1996). *The Flexural Creep Behavior of Structural Insulated Panels (SIP) Sandwich beams*. The Pennsylvania State University.
91. Teach, W. C., & Kiessling, G. C. (1960). *Polystyrene*. New York: Reinhold Publishing Corporation.
92. Thomas, W. (2003). Poisson's ratios of an oriented strand board. *Wood Sci Technol* , 37: 259–268, DOI 10.1007/s00226-003-0171-y.
93. Titman, D. J. (2001). Applications of thermography in non-destructive testing of structures. *NDT&E International* , 34:149–154.
94. Tompos, E. J. (2015). *Engineered Design of Structural Insulated Panels*. Retrieved 04 23, 2015, from Federation of American Scientists: http://fas.org/programs/energy/btech/new_technologies/NTA%20SIP%20Design%202008-09-23b.pdf

95. Trufast. (2012). Retrieved 05 30, 2012, from <http://trufast.com/>:
http://trufast.com/products/sip_nail/index.html
96. U.S. Composites Inc. (2012). Retrieved 05 08, 2015, from
www.uscomposites.com: <http://www.uscomposites.com/foam.html>
97. U.S. Department of Energy. (2011). Retrieved 09 02, 2011, from U.S. Department of Energy:
http://www.energysavers.gov/your_home/insulation_airsealing/index.cfm/mytopic=11740
98. Vario, G., Pellacani, L., Bertucelli, L., Golini, P., & Lotti, L. (2010). Enhanced Polyisocyanurate Foams for Metal Faced Panels. Correggio, Italy: Dow Italia Srl.
99. Wong, P. C., Bach, L., & Roger, C. J. (1988). The Flexural Creep Behaviour of OSB Stressed Skin Panels. *Structural engineering report SER 158*. Alberta: University of Alberta.
100. Zarghooni, M. H. (2009). Flexural Creep Behavior of Structural Insulated Timber Panels. *MSc. Thesis*. Ryerson University.
101. Zhang, L., & Tong, G.-S. (2011). Lateral buckling of eccentrically braced RHS columns. *Thin-Walled Structures*, 49: 1452–1459.

Appendices

Appendix A: Material Properties

Table A - 1: Result of the foam density tests conducted and provided by the PUR SIP manufacturer (Emercor). Each panel (sample) was tested on five spots over the area of the panel

Panel Thickness	114 mm (4.5 in.)				165 mm (6.5 in.)					
Sample Number	1	2	3	4	1	2	3	4	5	6
Density (lb/ft ³)	2.430	2.496	3.390	2.218	2.490	2.440	2.910	2.260	2.500	2.100
	2.540	2.635	2.220	2.400	2.490	2.430	2.700	2.490	2.570	2.000
	2.490	2.639	2.496	2.357	2.620	2.550	3.270	2.240	2.700	2.200
	2.430	2.496	2.303	2.380	2.810	2.380	2.490	2.570	2.430	2.200
	2.430	2.209	2.371	2.300	2.490	2.410	2.700	2.160	2.700	2.300
Average	2.464	2.495	2.556	2.331	2.580	2.442	2.814	2.344	2.580	2.160
Overall average:	2.477		lb/ft³							
	39.677		kg/m³							

Appendix B: Test Setup Drawings

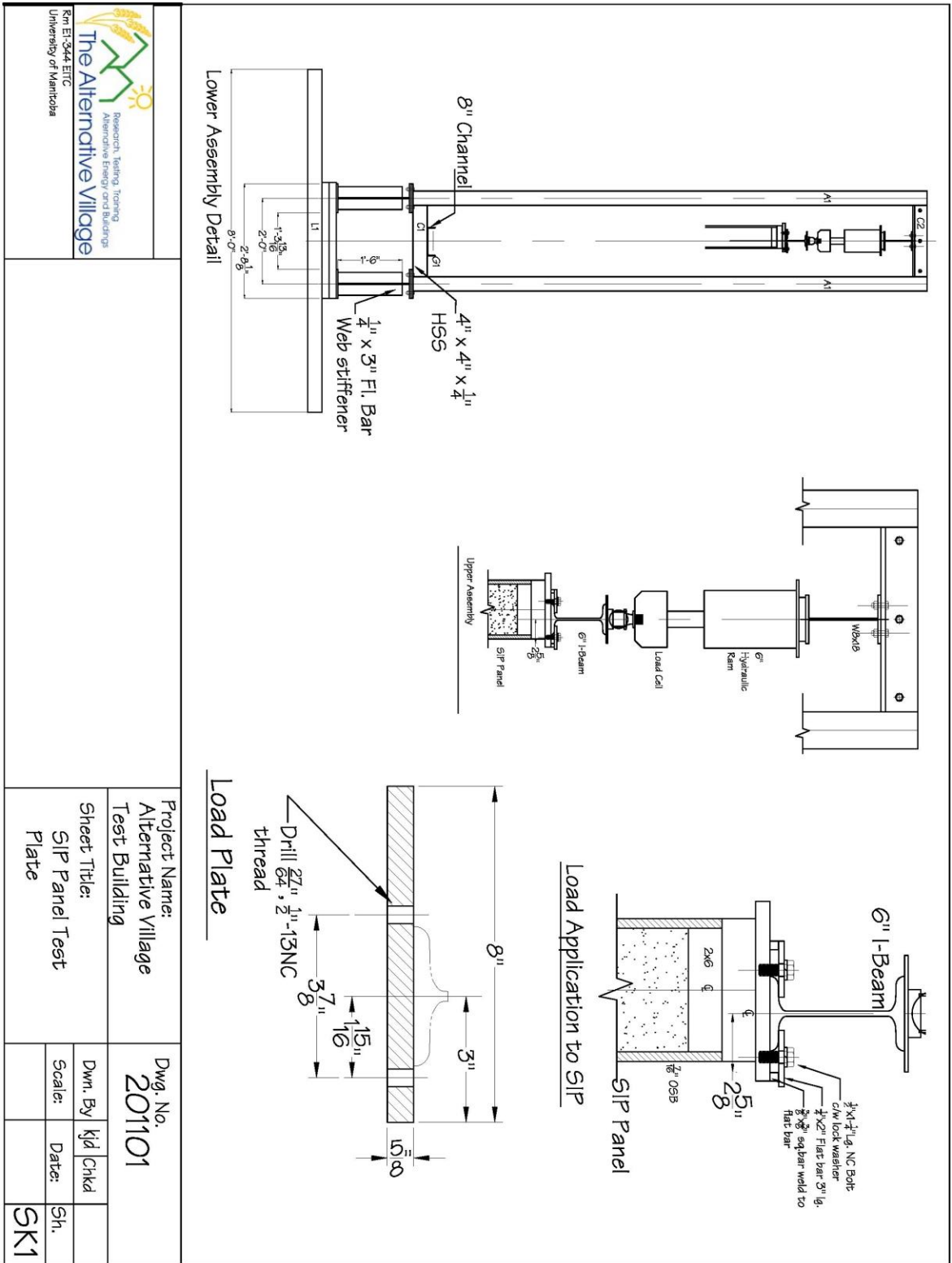


Figure B - 1: Axial test set-up top plate details (Source: Dick, 2011)

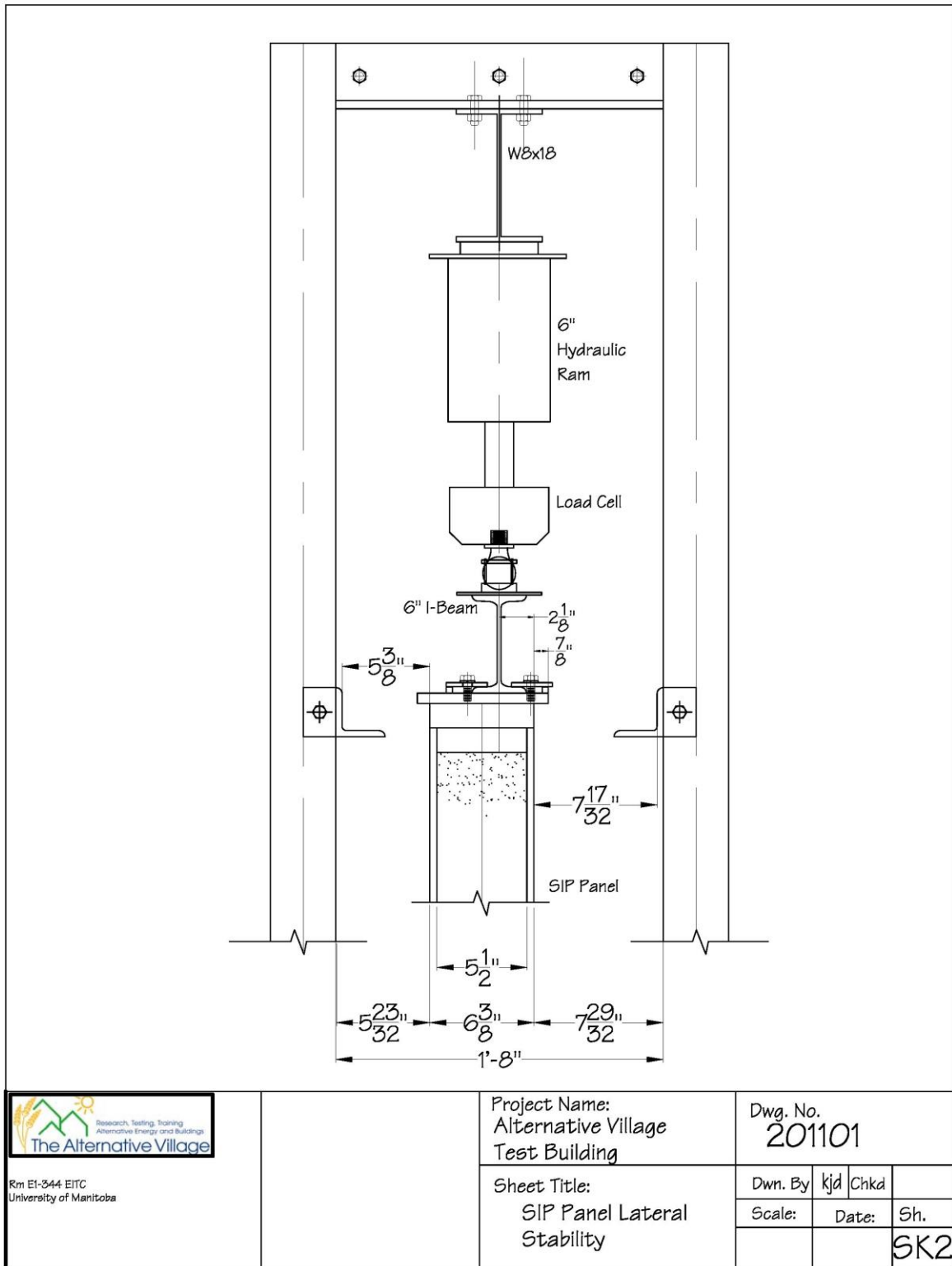


Figure B - 2: Axial test set-up details showing lateral stability holders (Source: Dick, 2011)

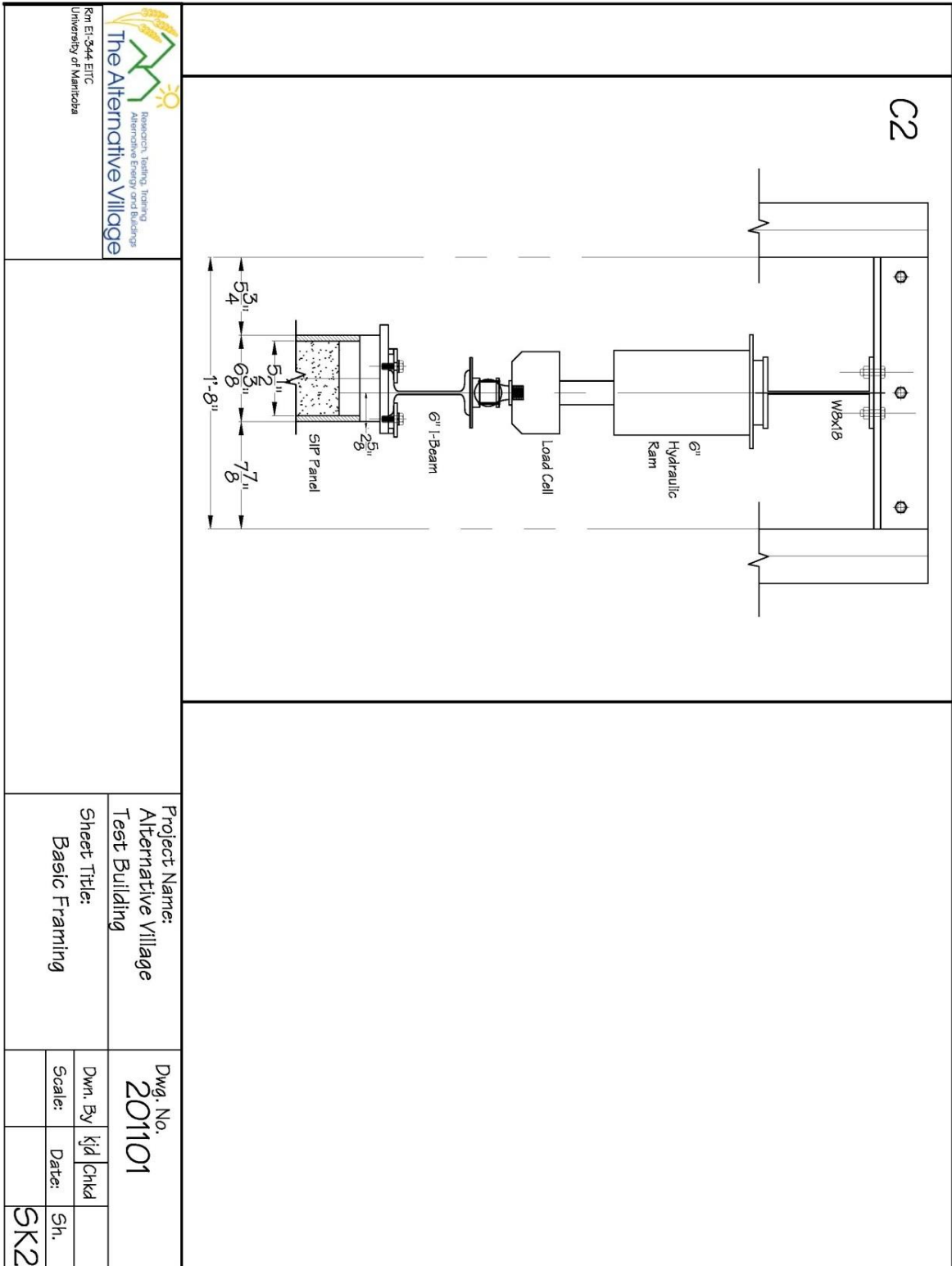


Figure B - 3: Axial test frame basic framing details (Source: Dick, 2011)

Appendix C: Baseline Test Results

Axial Test Results (Baseline tests)

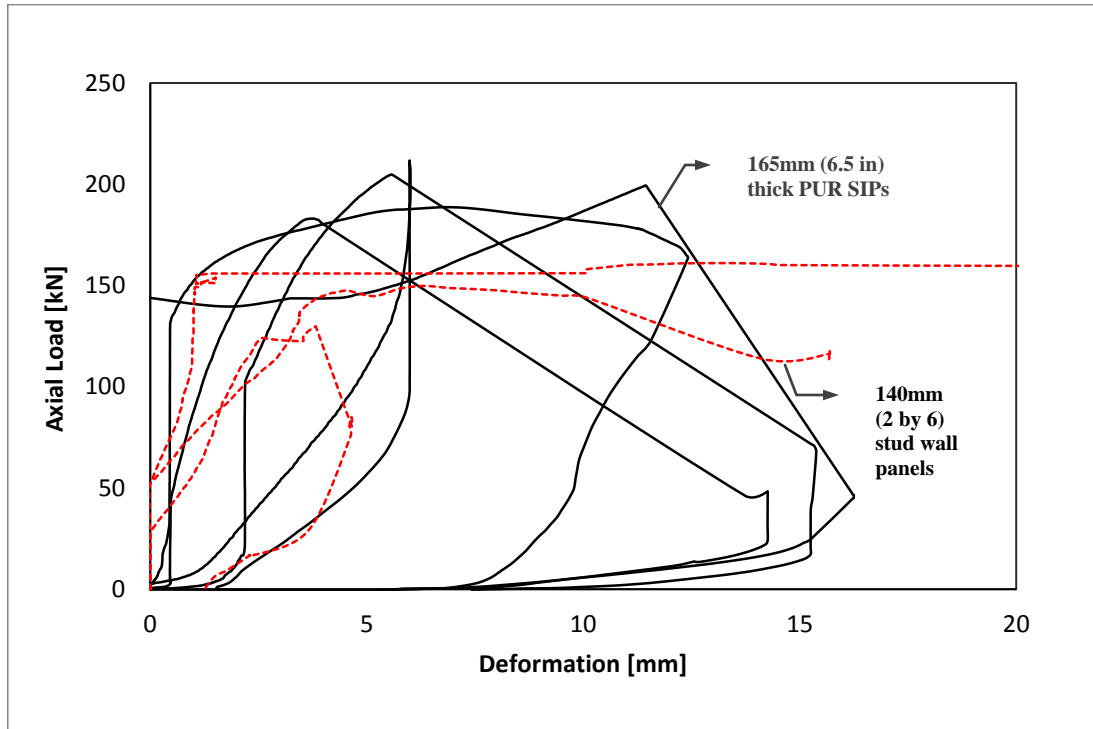


Figure C - 1: Axial tests results of five tested panels comparing the performance of 165mm (6.5 in) thick PUR SIPs to conventional 140mm (2 by 6) stud wall panels

Transverse Test Results (Baseline tests)

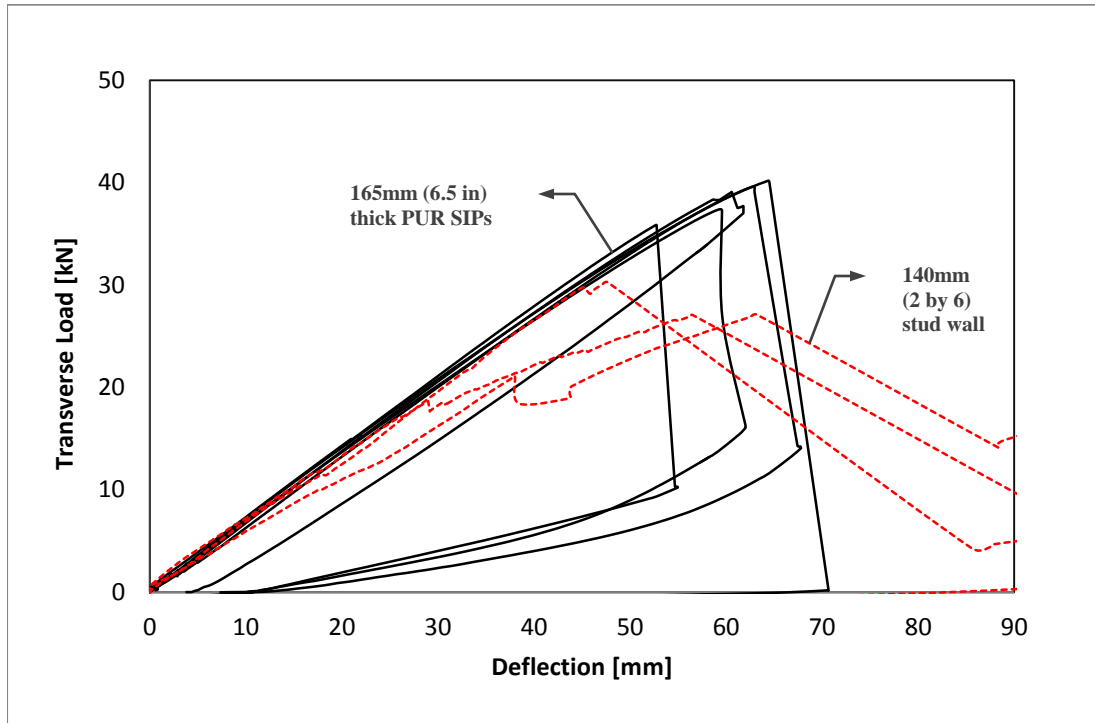


Figure C - 2: Transverse tests results of five tested panels comparing the performance of 165mm thick (6.5 in) PUR SIPs to three tested conventional 165mm (6.5 in) stud wall panels

Racking Test Results (Baseline tests)

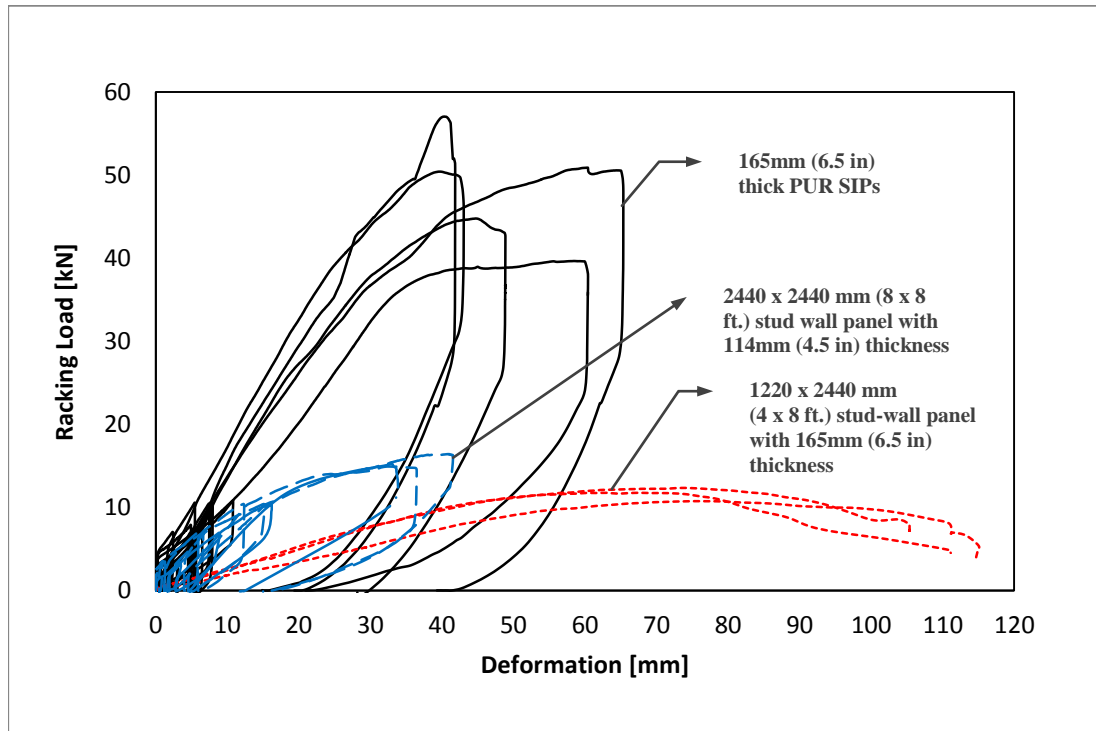


Figure C - 3: Racking tests results of five tested panels comparing the performance of 165mm thick (6.5 in) PUR SIPs to conventional stud wall panels. Solid lines represent the maximum load vs. deflection in 165mm thick (6.5 in) SIPs

Appendix D: Dis-bonded Panels Test Results

Axial Test Results (Dis-bonded tests)

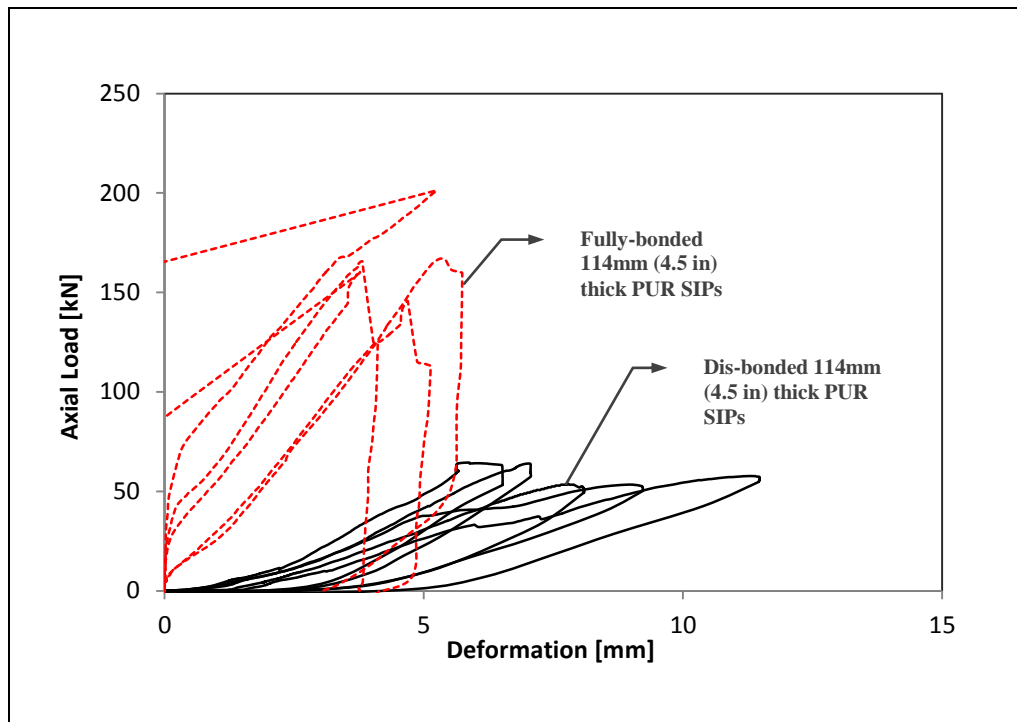


Figure D - 1: Axial load resistance of 114mm (4.5 in.) thick dis-bonded PUR SIPs compared to fully bonded panels with the same thickness. This graph shows the overall shortening of the SIP under axial load (top linear potentiometer only)

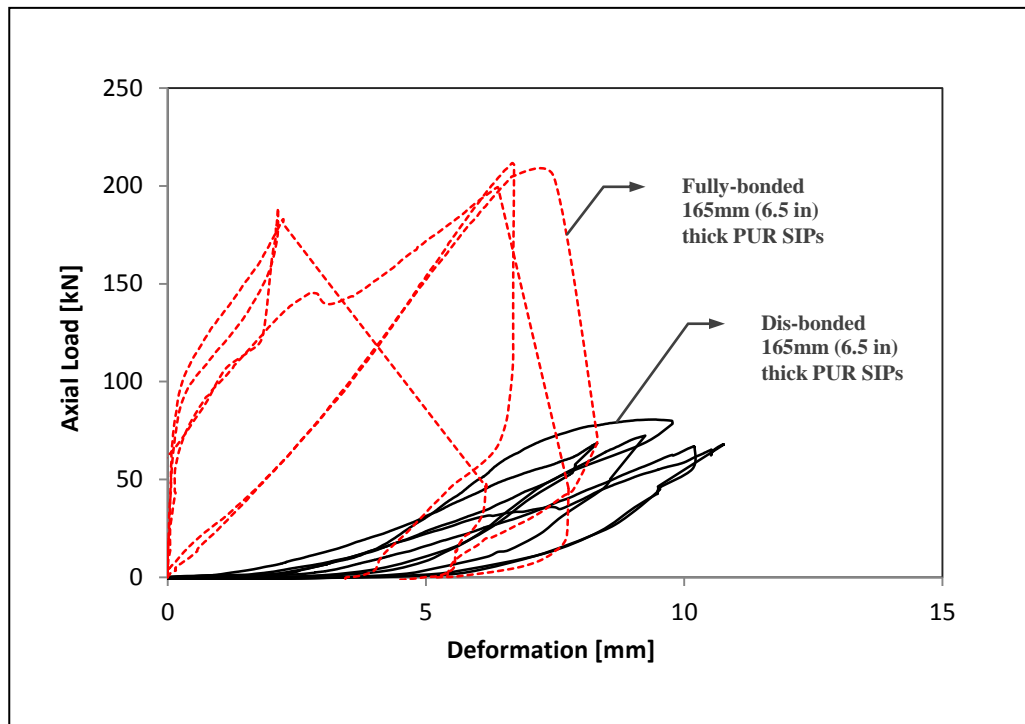


Figure D - 2: Axial load resistance of 165mm (6.5 in.) thick dis-bonded PUR SIPs compared to fully bonded panels with the same thickness. This graph shows the overall shortening of the SIP under axial load (top linear potentiometer only)

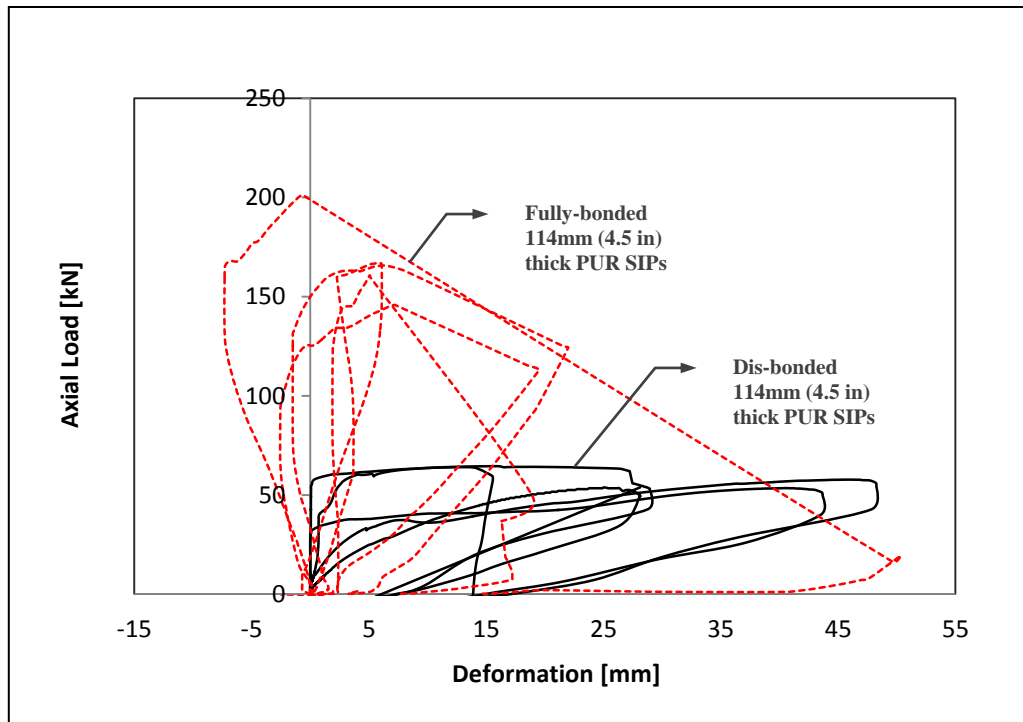


Figure D - 3: Axial load resistance of 114mm (4.5 in.) thick dis-bonded PUR SIPs compared to fully bonded panels with the same thickness. This graph shows the overall shortening of the SIP under axial load (mid-left linear potentiometer only). The first few millimetres of negative deformation is due to slight rotation of the I beam (located at the 1/3 of the panel thickness) before it is fully stabilized on under applied load

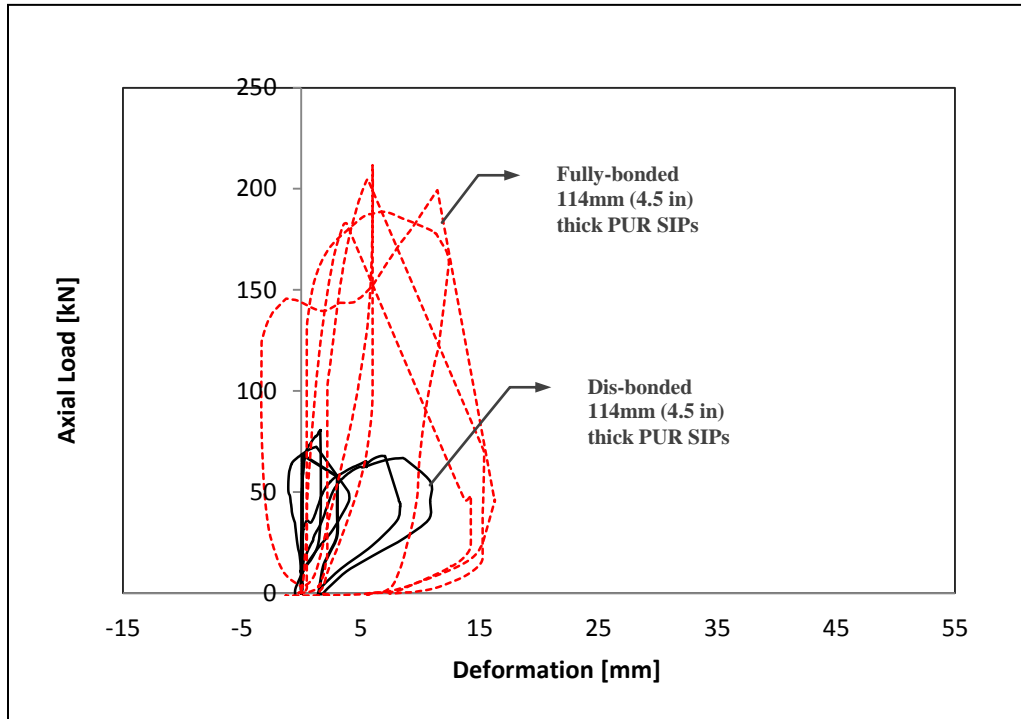


Figure D - 4: Axial load resistance of 114mm (4.5 in.) thick dis-bonded PUR SIPs compared to fully bonded panels with the same thickness. This graph shows the overall shortening of the SIP under axial load (mid-left linear potentiometer only). The first few millimetres of negative deformation is due to slight rotation of the I beam (located at the 1/3 of the panel thickness) before it is fully stabilized on under applied load

Transverse Test Results (Dis-bonded tests)

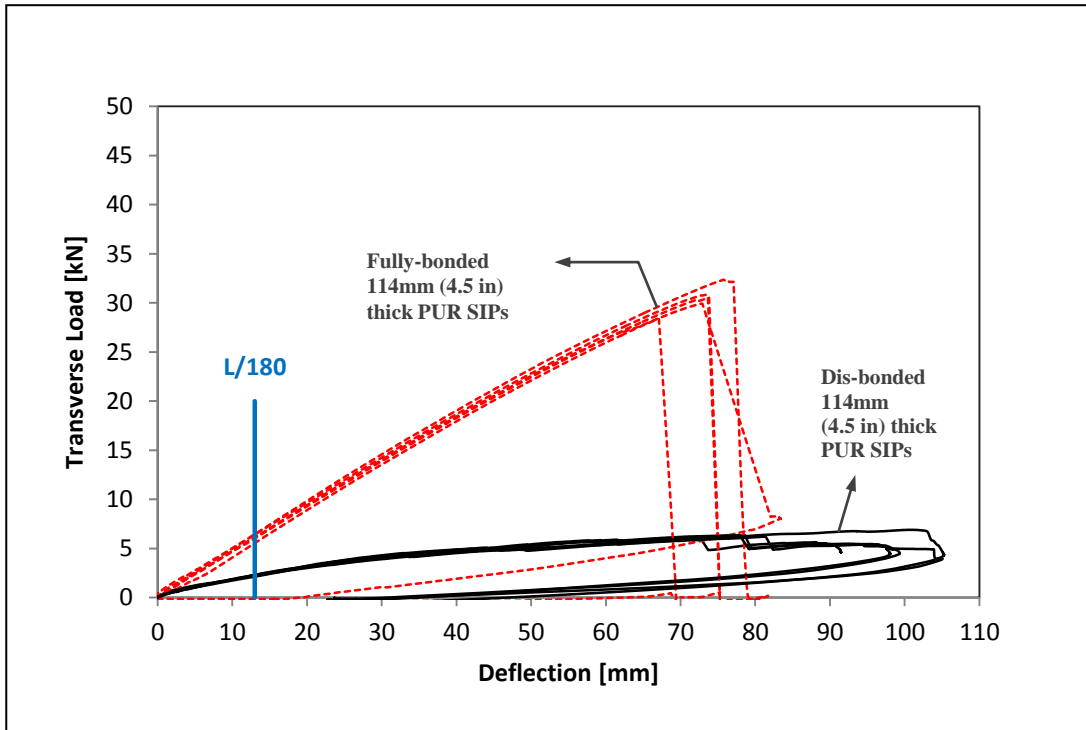


Figure D - 5: Transverse load resistance of 114mm (4.5 in.) thick dis-bonded PUR SIPs compared to fully bonded panels with the same thickness. The vertical blue line indicates the serviceability deflection limit of L/180 (13 mm)

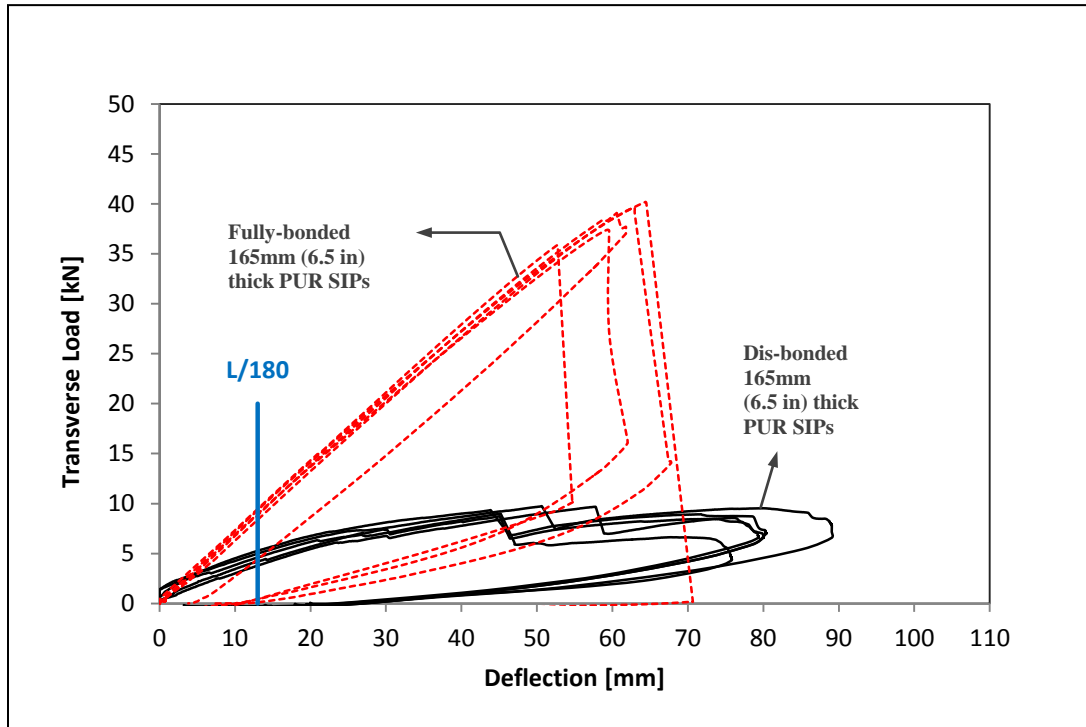


Figure D - 6: Transverse load resistance of 165mm (6.5 in.) thick dis-bonded PUR SIPs compared to fully bonded panels with the same thickness. The vertical blue line indicates the serviceability deflection limit of L/180 (13 mm)

Racking Test Results (Dis-bonded tests)

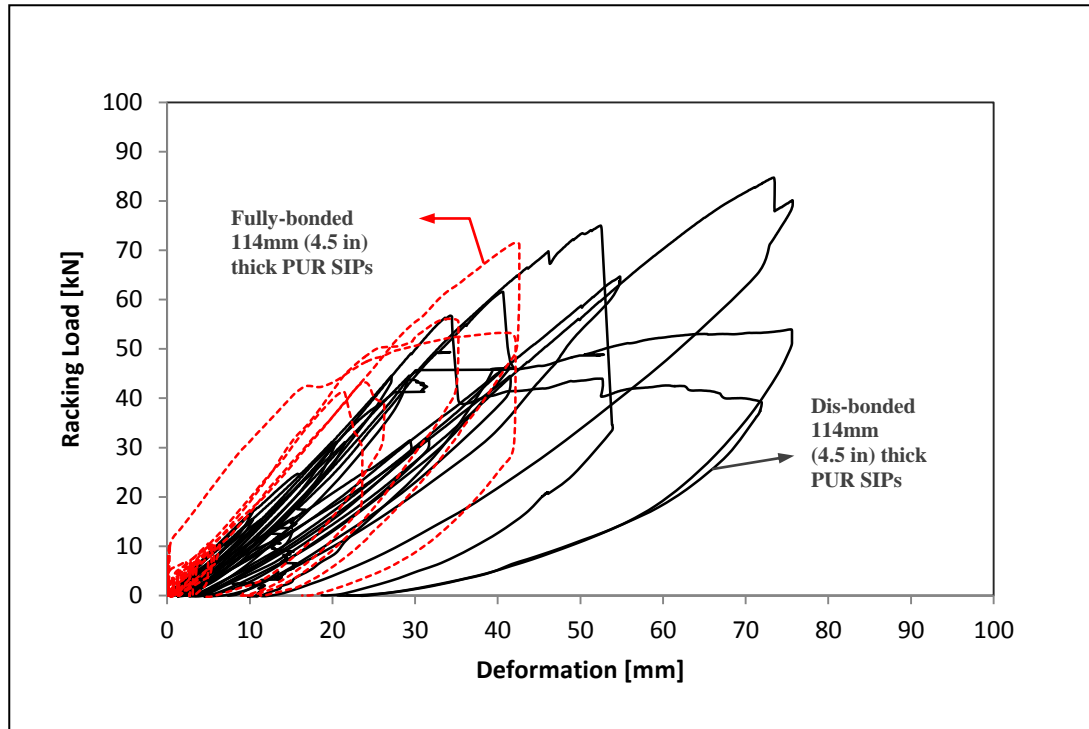


Figure D - 7: Racking load resistance of 114mm (4.5 in.) thick dis-bonded PUR SIPs compared to fully bonded panels with the same thickness

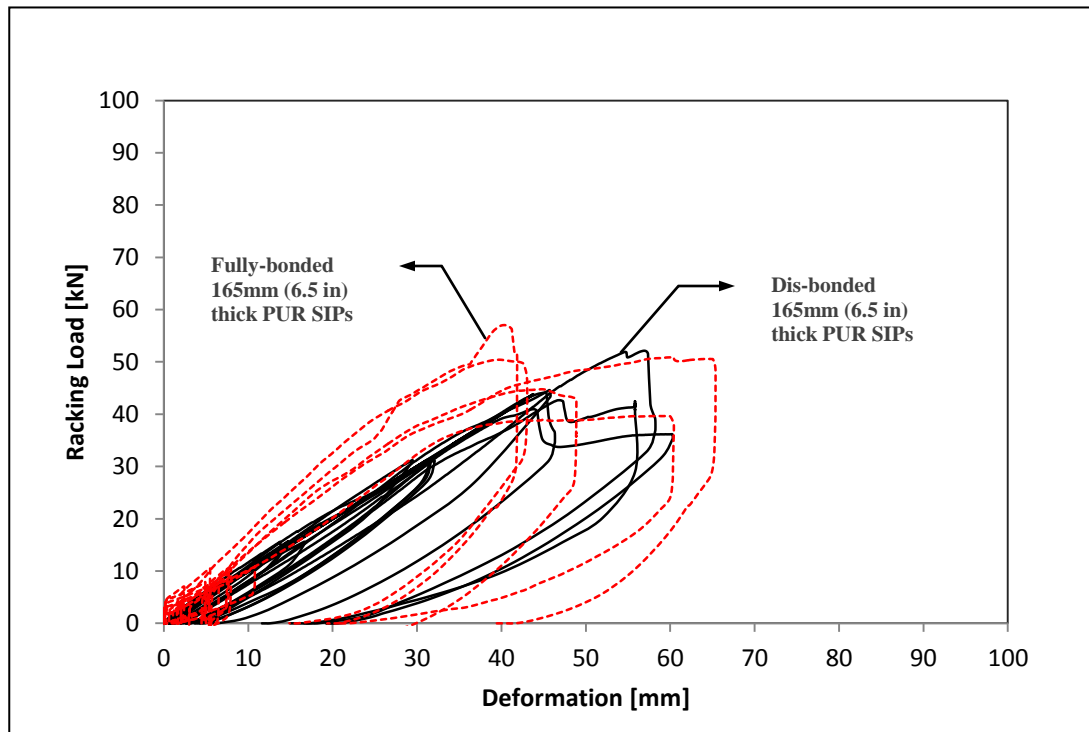


Figure D - 8: Racking load resistance of 165mm (6.5 in.) thick dis-bonded PUR SIPs compared to fully bonded panels with the same thickness

Design Load on a Residential Wall (Location: Winnipeg, Manitoba)

As an example, for a residential house with a width of 10m, flat roof and a non-windswept location and in accordance with NBCC, Appendix C and Part IV (NBCC, 2010):

Panel axial load capacity:

- Average maximum axial load capacity of the dis-bonded 114mm (4.5 in.) thick PUR SIPs from the test results: 58.70 kN
- Width of a panel = 1.22 m
- Linear axial capacity of the panel: $58.70/1.22 = 48.11$ kN/m

Design load:

- Assume Dead Load = 0.5 kPa
- Based on NBCC Snow load, $S = (S_s \cdot C_b \cdot C_s \cdot C_w) + 0.2$

- Where:
 - $S_s = 1.9$ (Winnipeg Snow load)
 - $C_b = 0.8$
 - $C_s = 1.0$
 - $C_w = 1.0$
 - $S_r = 0.2$
- Therefore, Snow load = $(1.9 \times 0.8 \times 1.0 \times 1.0) + 0.2 = 1.72$ kPa
- Factored wall load in this example = $1.5(1.72) + 1.25(0.5) = 3.205$ kPa
- Line-load = $3.205 \times 5.0\text{m} = 16.025$ kN/m

It can be seen that the maximum required design load of 16.025 kN/m is smaller than the average maximum line-load capacity of the dis-bonded 114mm (4.5 in.) thick PUR SIPs of 48.11 kN/m. Therefore, even with 33% partial dis-bond, 114mm (4.5 in.) thick PUR SIPs not only they are capable of handling a regular residential building line-load, but also the failure is anticipated to be non-catastrophic and gradual.

Appendix E: Compression Coupon Test Results

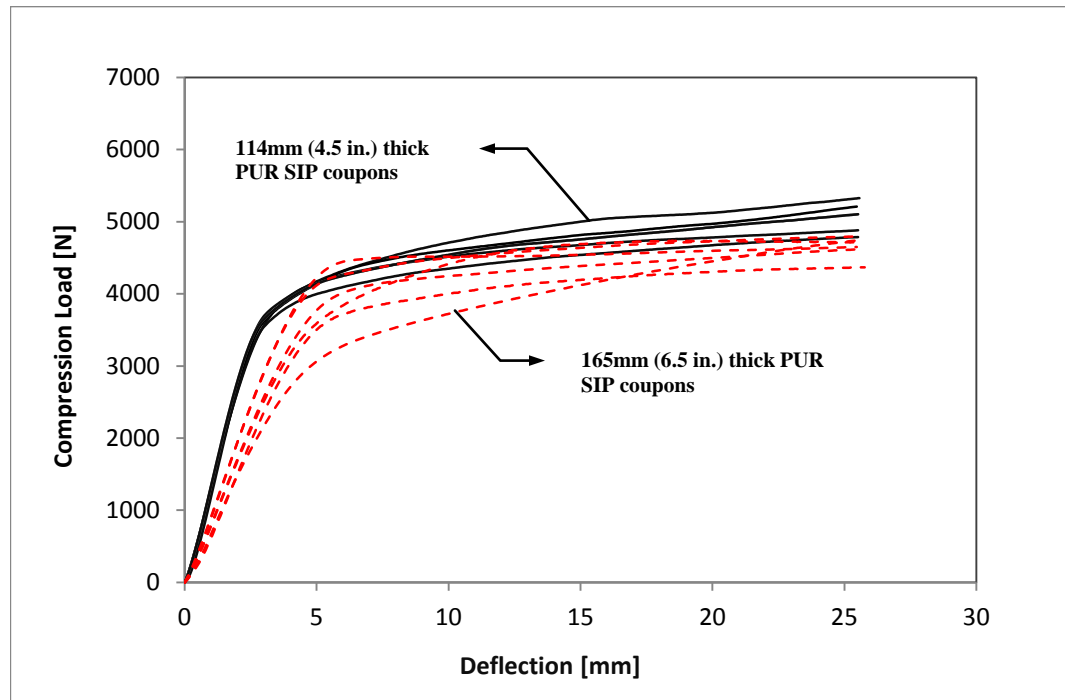


Figure E - 1: All in one compressive tests conducted on 165mm (6.5 in.) and 114mm (4.5 in.) thick PUR SIP coupons with the area of 152 by 152 mm (6 x 6 in.) and 25mm (1 in.) deflection limit

Appendix F: Pull-off Test Results

Table F - 1: Results of all conducted pull-off tests

	Max Load	Delta at Max Load	Tensile (Normal) Stress	Shear Stress	Failure Modes		
60 specimens (New panels)	N	mm	MPa	MPa	Foam	OSB	Bond Interface
PCT 1A	628.35	2.19	0.23	0.21	5	4	1
PCT 1B	550.78	1.96	0.20	0.23	9	1	0
PCT 2A	428.25	2.18	0.15	0.15	9	1	0
PCT 2B	531.93	1.93	0.19	0.19	6	3	1
PCT 3A	647.44	1.76	0.23	0.23	8	2	0
PCT 3B	529.02	2.20	0.19	0.17	8	2	0
Avg.	552.63	2.04	0.20	0.20			
St Dev	78.97	0.18	0.03	0.03	45	13	2
COV	0.14	0.09	0.14	0.17			
60 specimens (Weathered panels)							
WPT 1A	604.68	2.59	0.22	0.21	9	1	0
WPT 1B	564.03	2.21	0.20	0.19	8	1	1
WPT 2A	438.03	1.80	0.16	0.16	8	2	0
WPT 2B	444.99	1.93	0.16	0.16	8	2	0
WPT 3A	523.71	2.21	0.19	0.18	10	0	0
WPT 3B	433.22	2.01	0.16	0.15	5	5	0
Avg.	501.44	2.12	0.18	0.18			
St Dev	73.40	0.28	0.03	0.02	48	11	1
COV	0.15	0.13	0.15	0.13			

Table F - 2: Results of pull-off tests for foam failure only

Specimen	New Panel 1		New Panel 2		New Panel 3		Weathered Panel 1		Weathered Panel 2		Weathered Panel 3	
	A	B	A	B	A	B	A	B	A	B	A	B
Side of the panel												
Average max force of foam-failed plugs only [N]	1070.34	1008.67	643.05	830.94	790.07	759.78	945.94	959.57	462.16	465.85	523.71	459.58
Average Normal Stress [MPa]	0.43	0.41	0.26	0.34	0.32	0.31	0.38	0.39	0.19	0.19	0.21	0.19
Average Normal Stress [MPa]	0.35						0.26					
Total number of plugs	45						48					

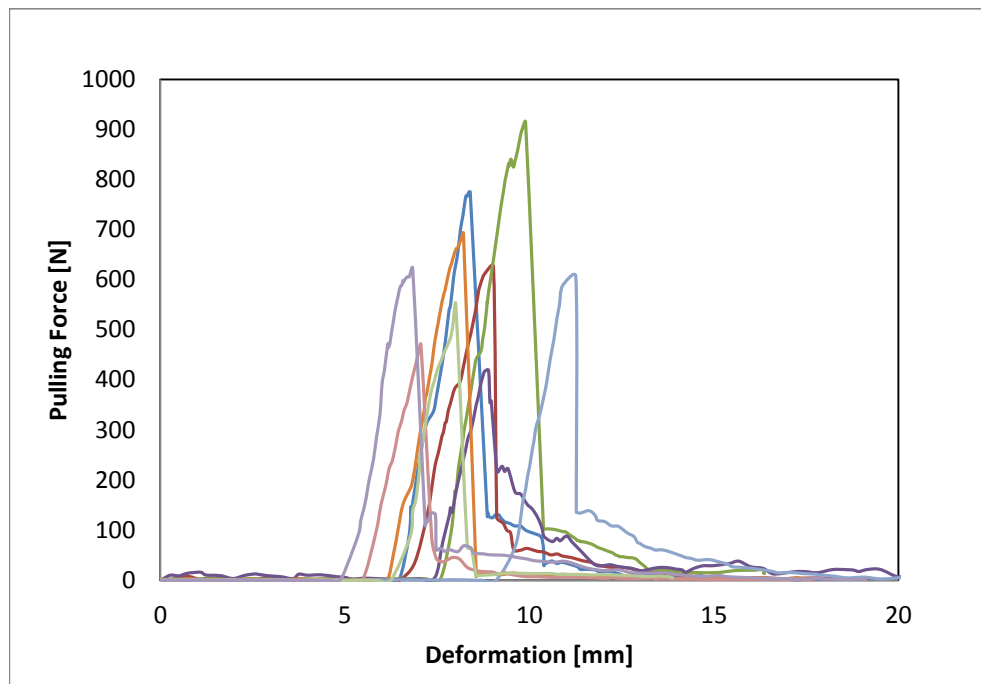


Figure F - 1: Pull-off test results of the New Panel 1 – Samples 1 to 10 Side A of the panel

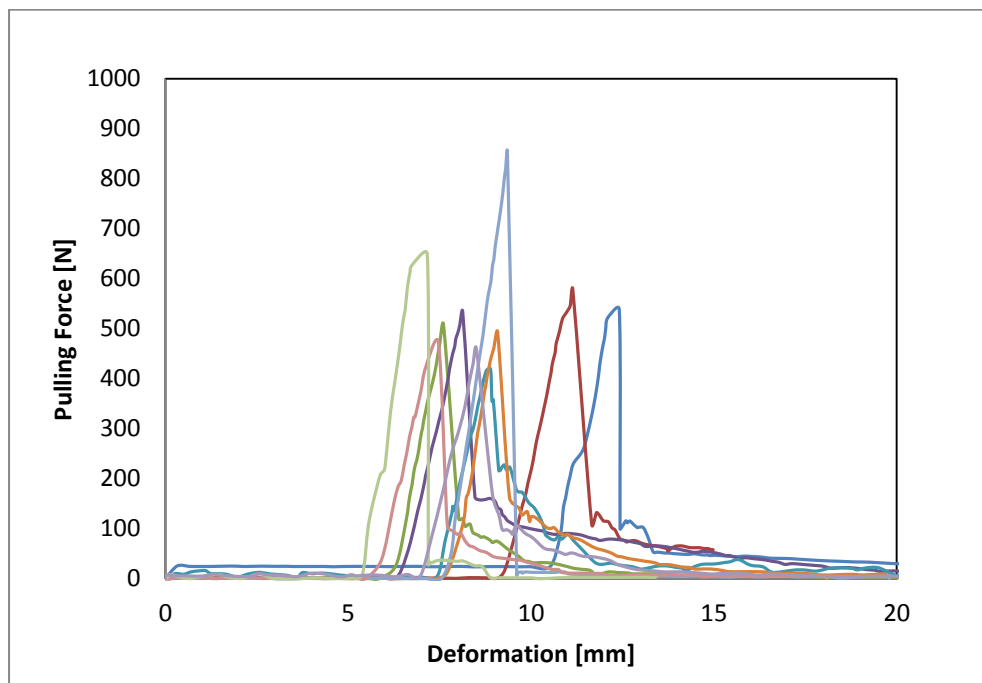


Figure F - 2: Pull-off test results of the New Panel 1 – Samples 1 to 10 Side B of the panel

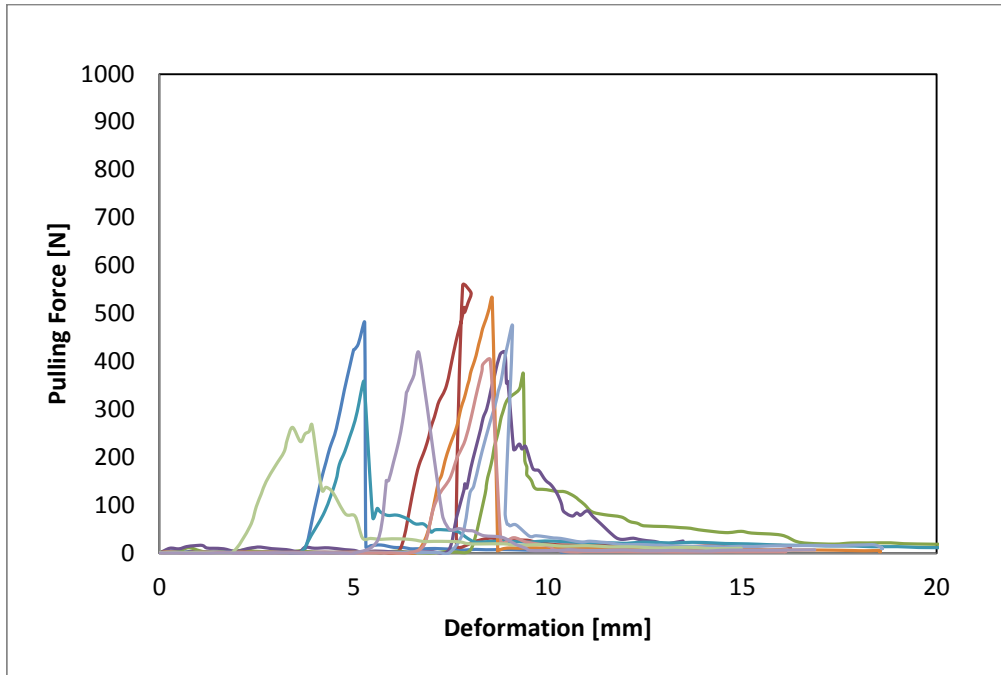


Figure F - 3: Pull-off test results of the New Panel 2 – Samples 1 to 10 Side A of the panel

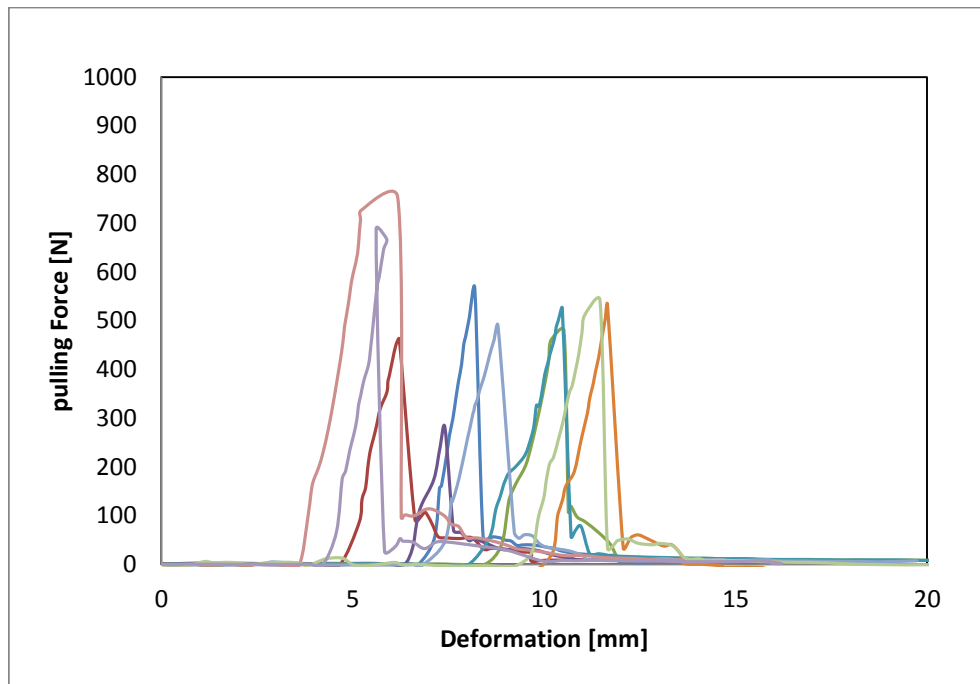


Figure F - 4: Pull-off test results of the New Panel 2 – Samples 1 to 10 Side B of the panel

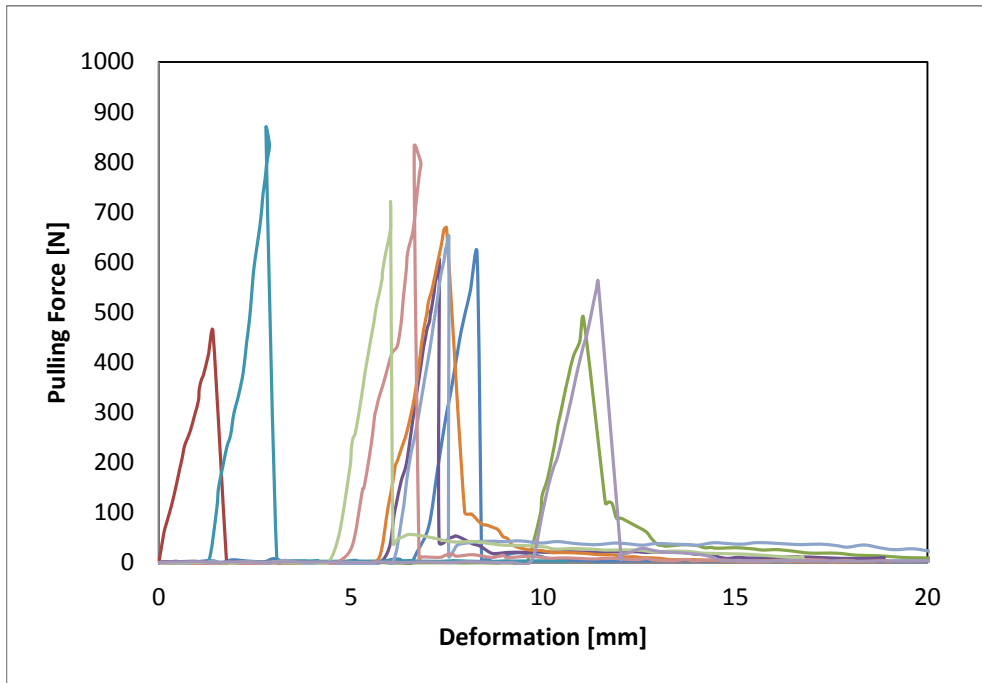


Figure F - 6: Pull-off test results of the New Panel 3 – Samples 1 to 10 Side A of the panel

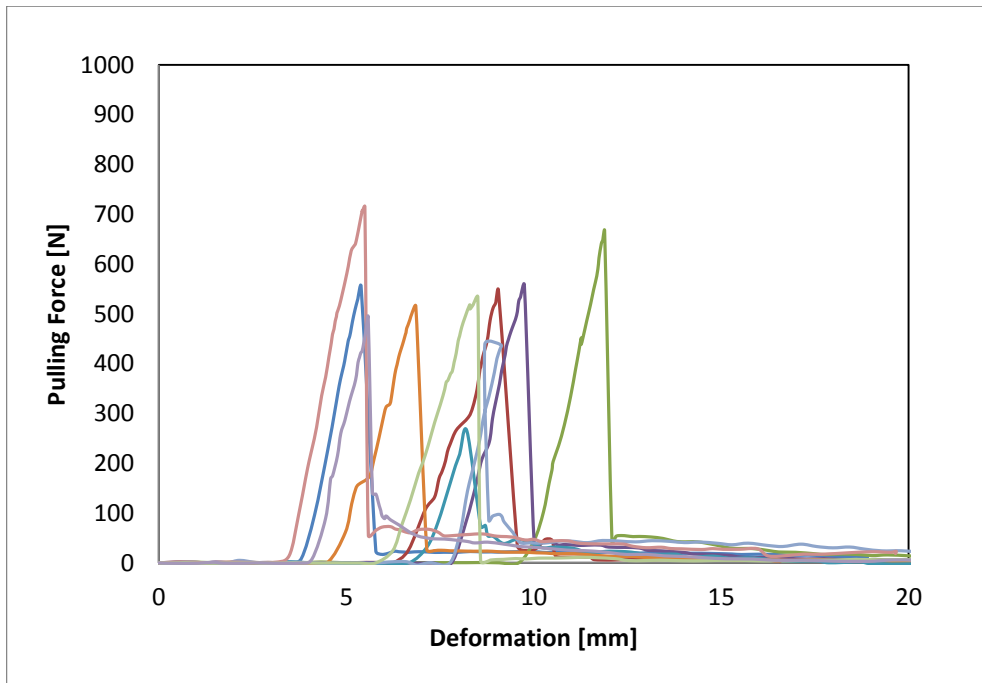


Figure F - 5: Pull-off test results of the New Panel 3 – Samples 1 to 10 Side B of the panel

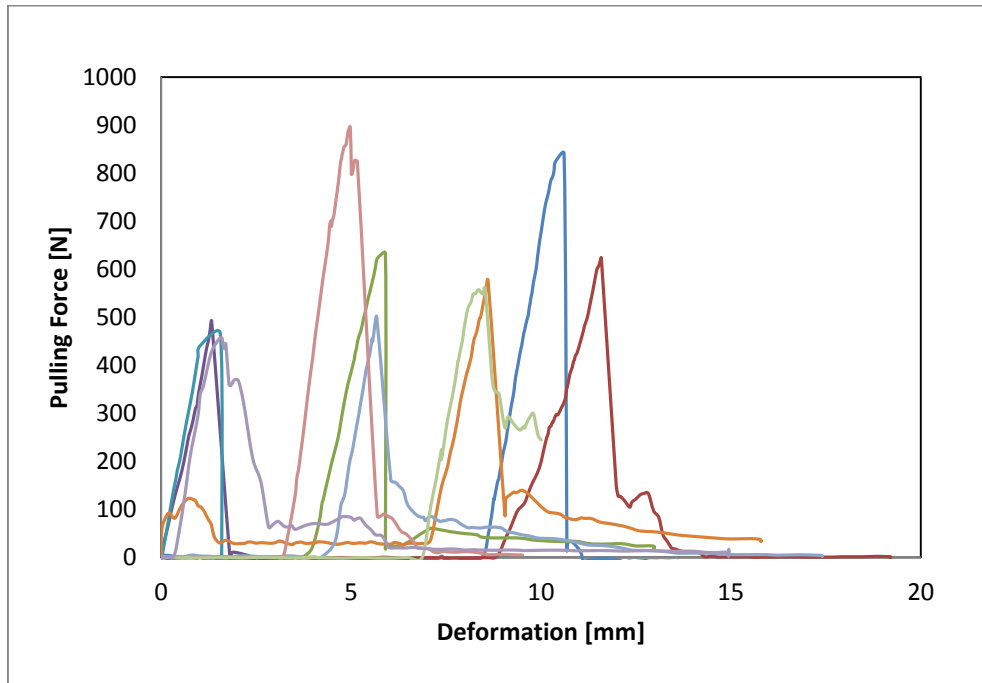


Figure F - 7: Pull-off test results of the Weathered Panel 1 – Samples 1 to 10 Side A of the panel

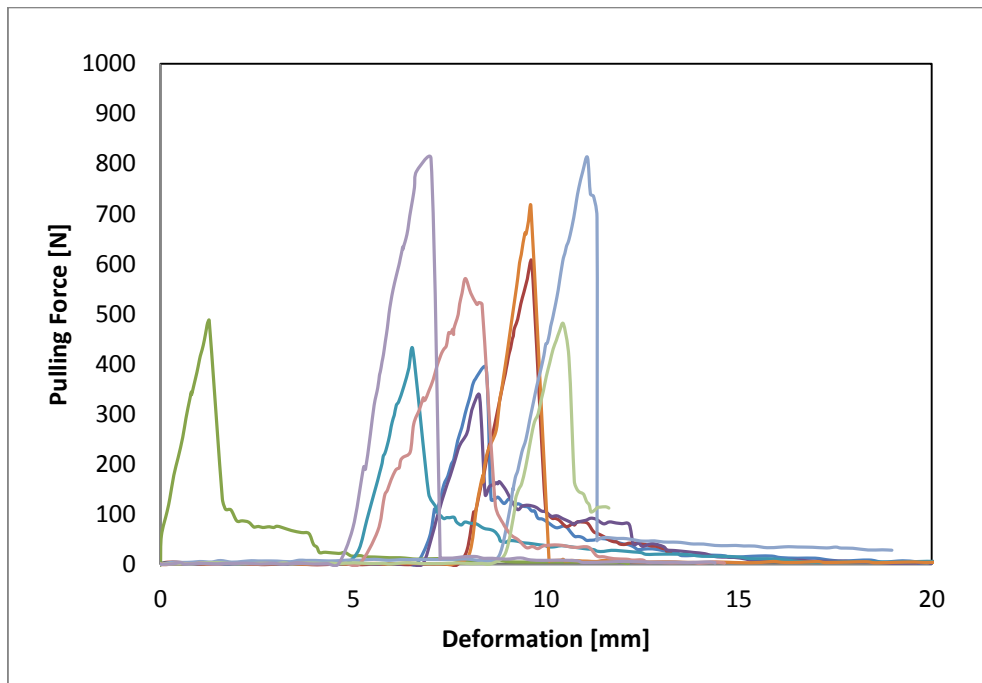


Figure F - 8: Pull-off test results of the Weathered Panel 1 – Samples 1 to 10 Side B of the panel

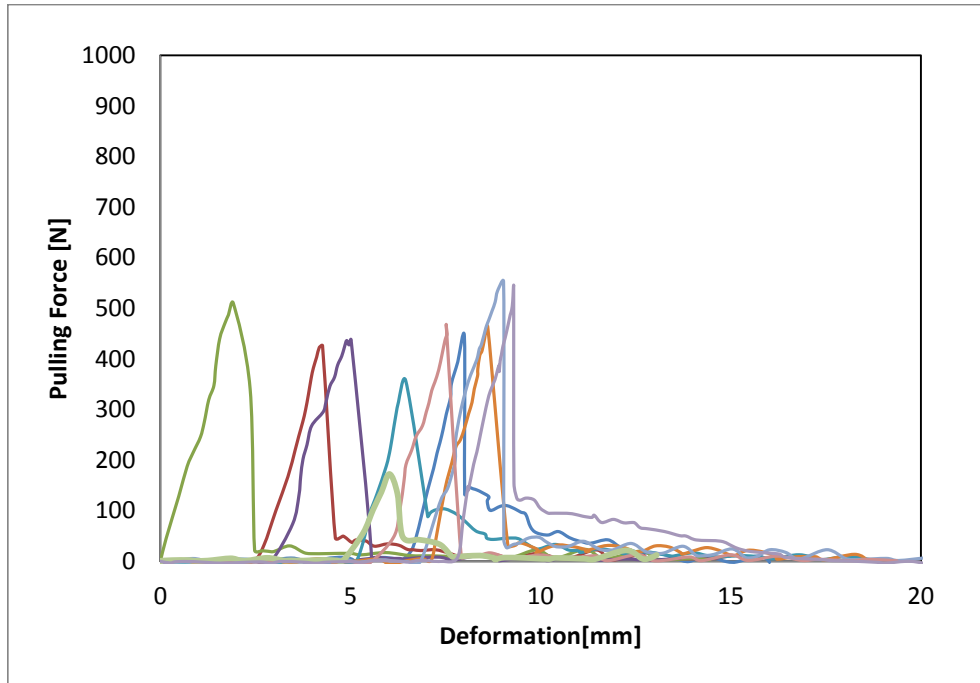


Figure F - 9: Pull-off test results of the Weathered Panel 2 – Samples 1 to 10 Side A of the panel

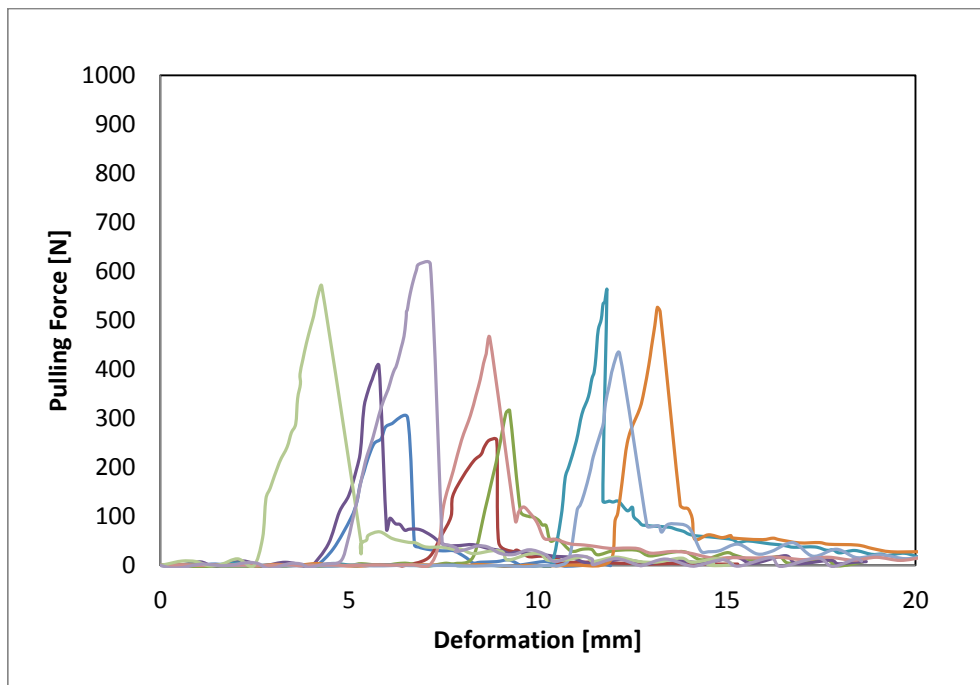


Figure F - 10: Pull-off test results of the Weathered Panel 2 – Samples 1 to 10 Side B of the panel

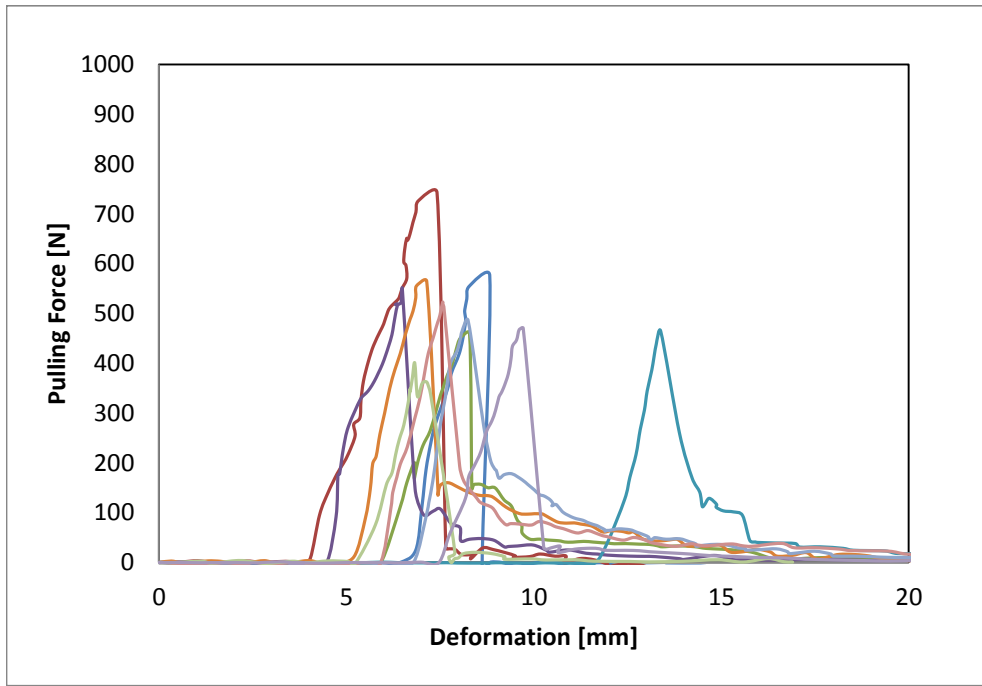


Figure F - 11: Pull-off test results of the Weathered Panel 3 – Samples 1 to 10 Side A of the panel

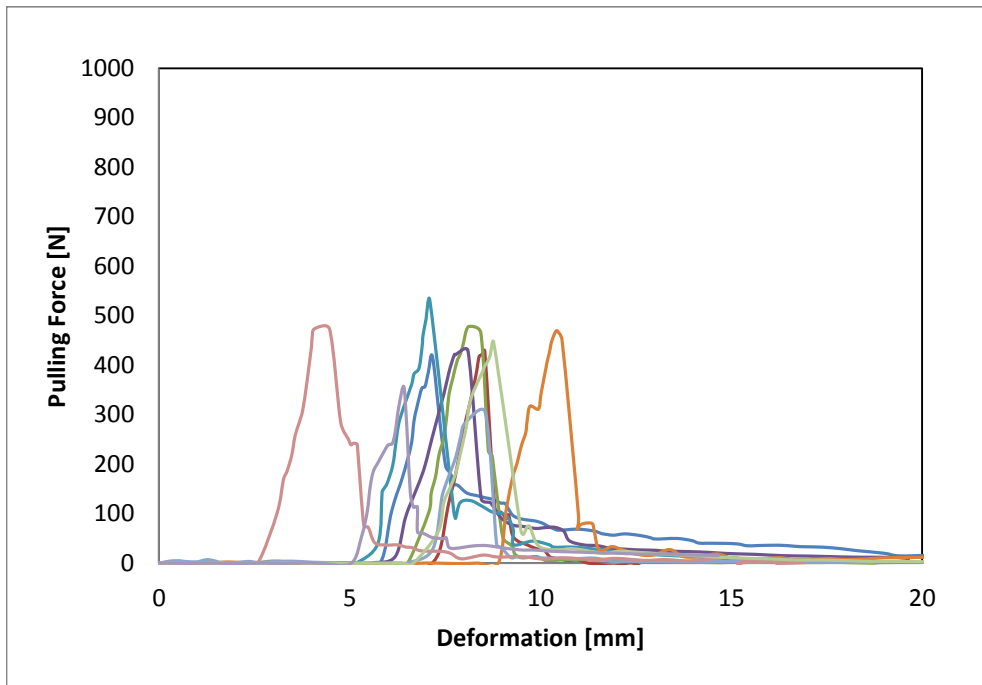


Figure F - 12: Pull-off test results of the Weathered Panel 3 – Samples 1 to 10 Side B of the panel

Appendix G: Modelling Documents

Load vs. Deflection Curves of OSB Specimen Tested for the
Evaluation of the 'E' Values

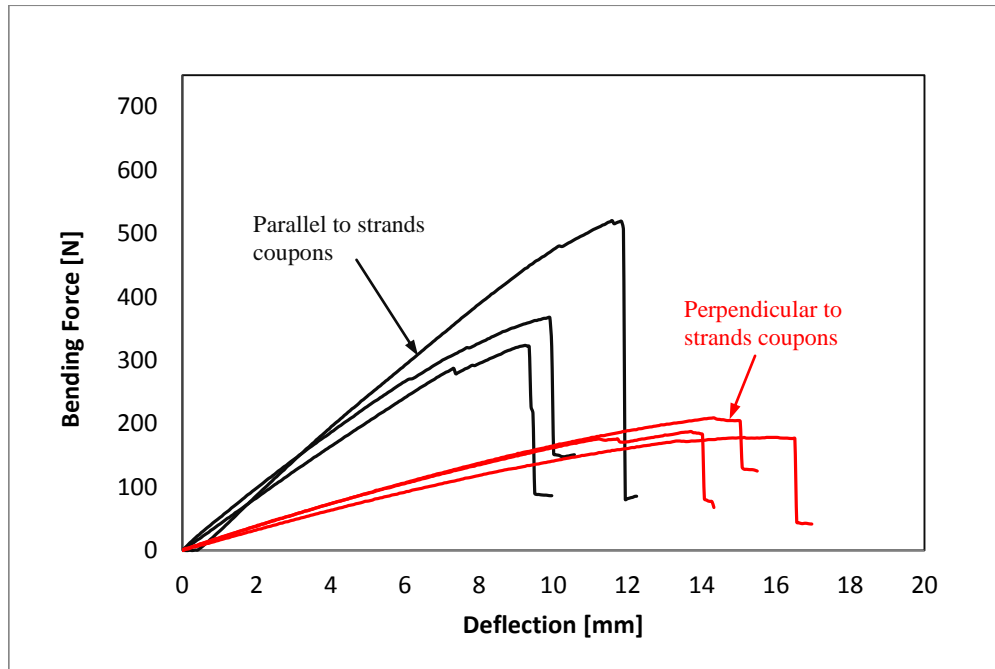


Figure G - 1: Load vs. deflection behaviour of the OSB face-sheet coupons under pure bending test

Axial Load Simulations of Fully-Bonded PUR SIPs (114mm,
4.5 in. thick)

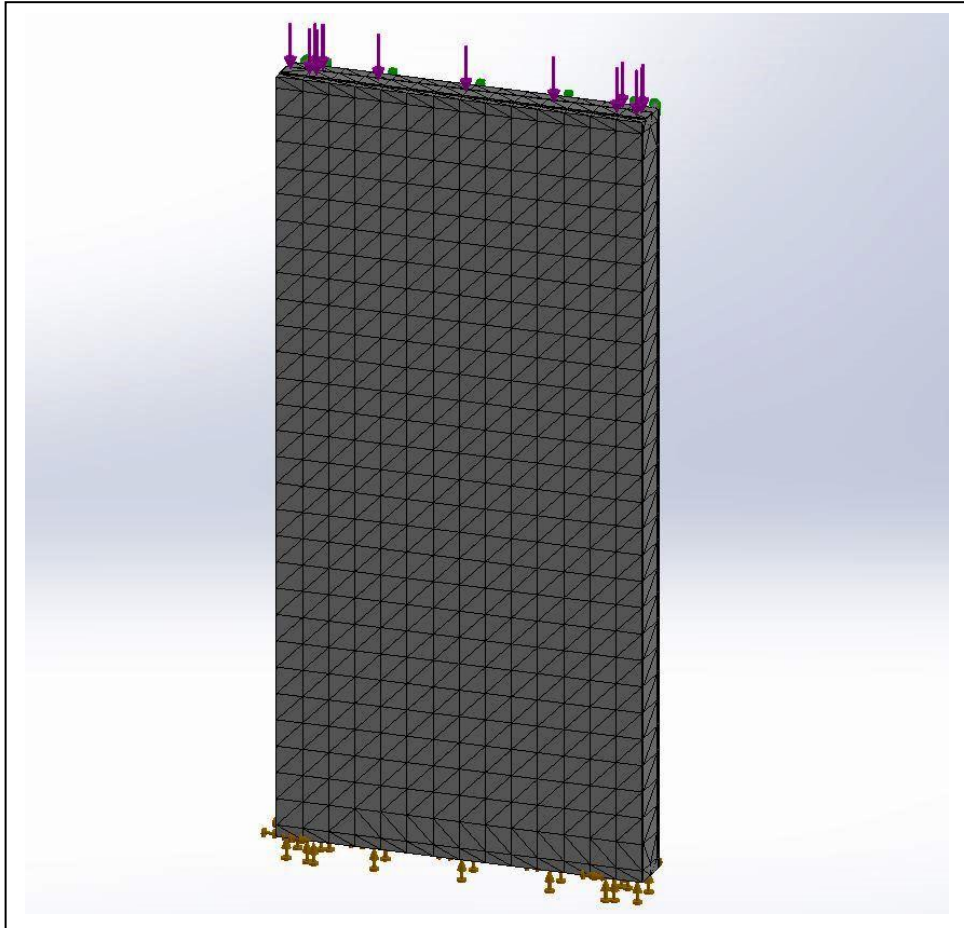


Figure G - 2: Mesh detail of modeled 114mm (4.5 in.) thick fully-bonded PUR SIPs under eccentric axial load (M45A)

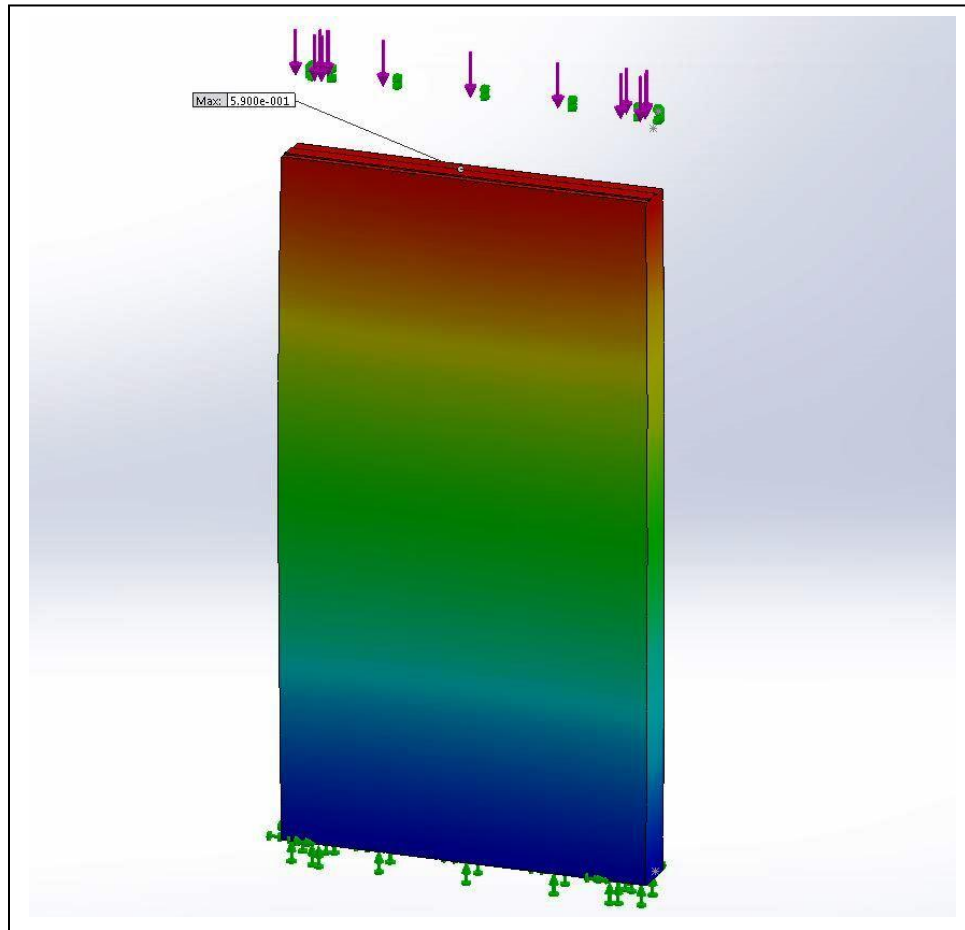


Figure G - 3: Deformation behaviour of modeled 114mm (4.5 in.) thick fully-bonded PUR SIPs under eccentric axial load (M45A) (Red indicates zone of greatest deformation)

Axial Load Simulations of Dis-Bonded PUR SIPs (114mm,
4.5 in. thick)

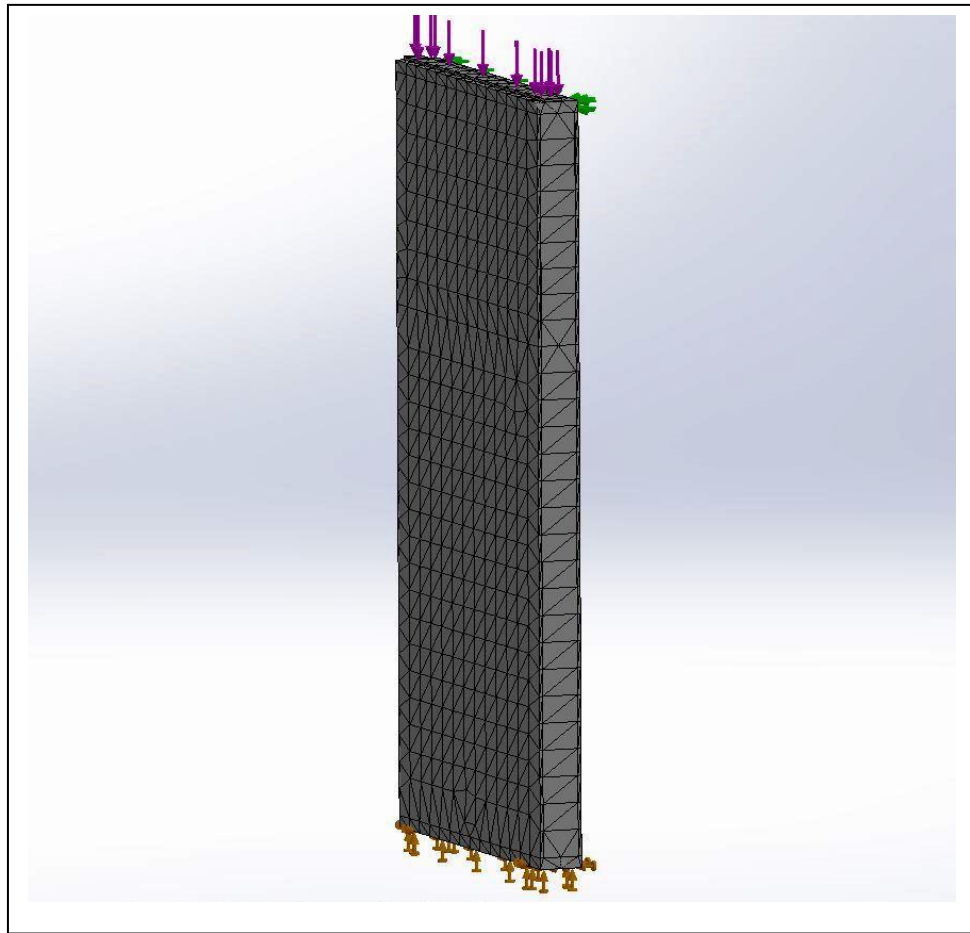


Figure G - 4: Mesh detail of modeled 114mm (4.5 in.) thick partially dis-bonded PUR SIPs under eccentric axial load (MD45A)

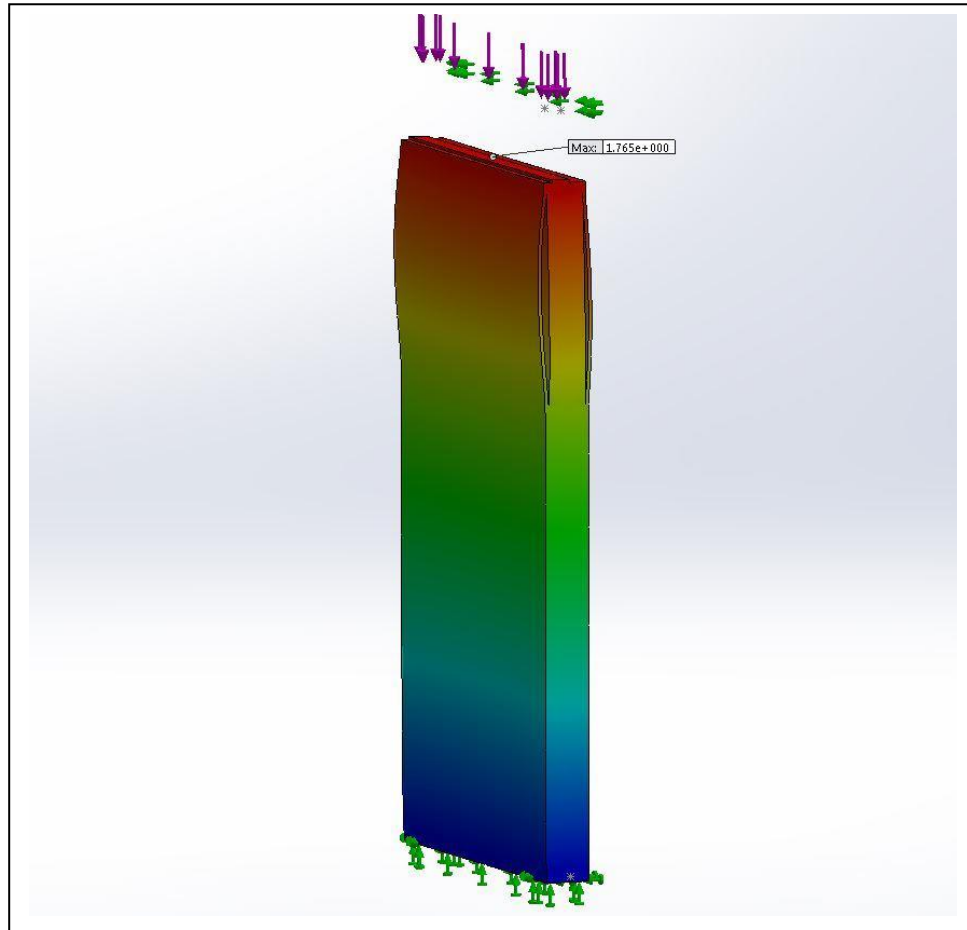


Figure G - 5: Deformation behaviour of modeled 114mm (4.5 in.) thick partially dis-bonded PUR SIPs under eccentric axial load (MD45A) (Red indicates zone of greatest deformation)

Transverse Load Simulations of Fully-Bonded PUR SIPs
(114mm, 4.5 in. thick)

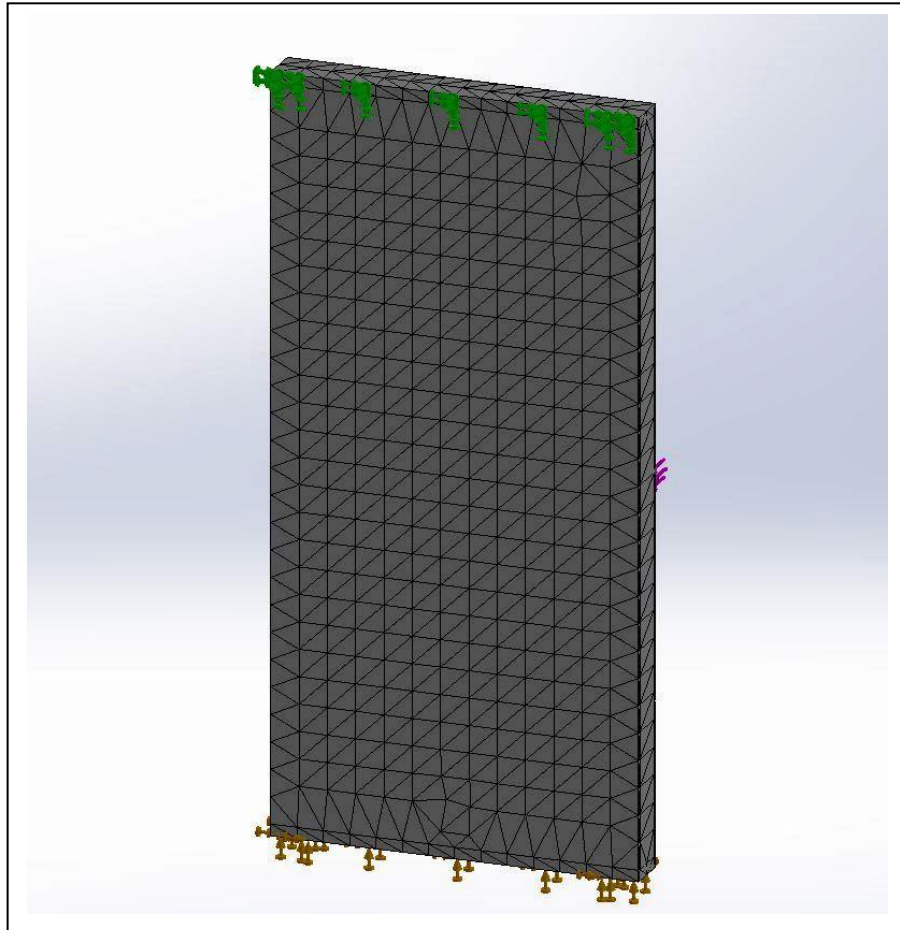


Figure G - 6: Mesh detail of modeled 114mm (4.5 in.) thick fully-bonded PUR SIPs exposed to transverse load (M45T)

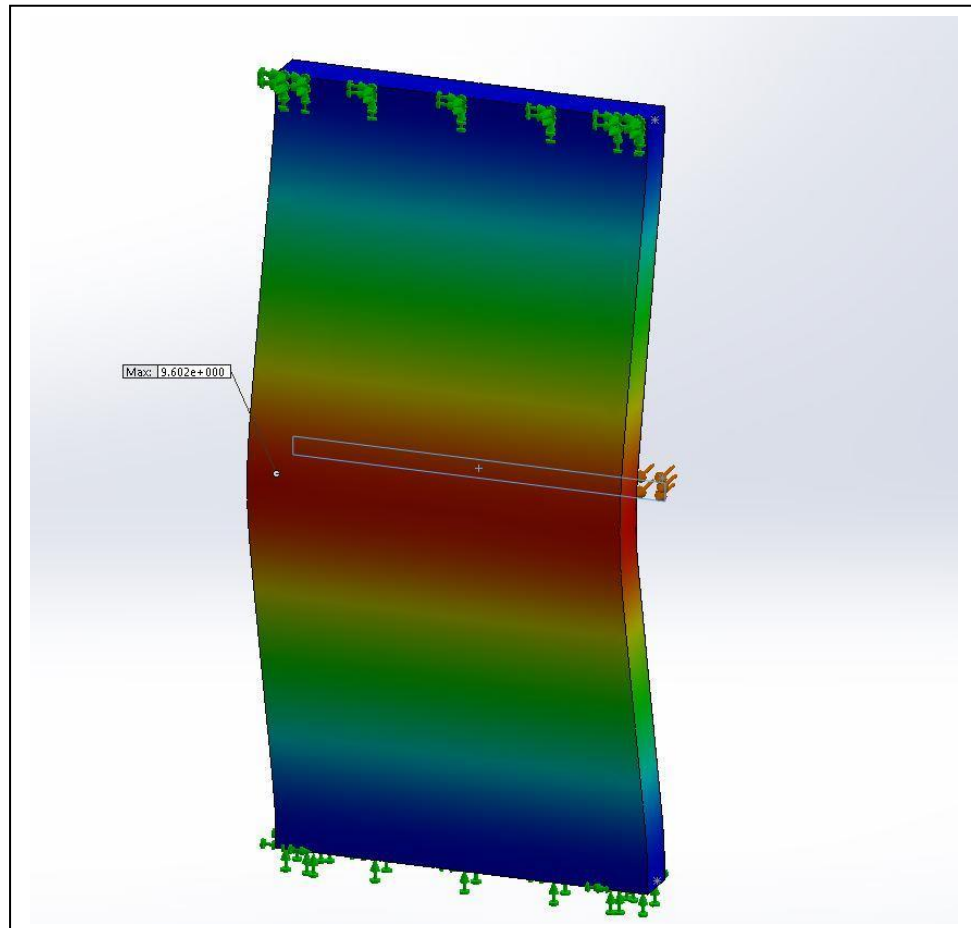


Figure G - 7: Deflection behaviour of modeled 114mm (4.5 in.) thick fully-bonded PUR SIPs exposed to transverse load (M45T) (Red indicates zone of greatest deformation)

Transverse Load Simulations of Dis-Bonded PUR SIPs
(114mm, 4.5 in. thick)

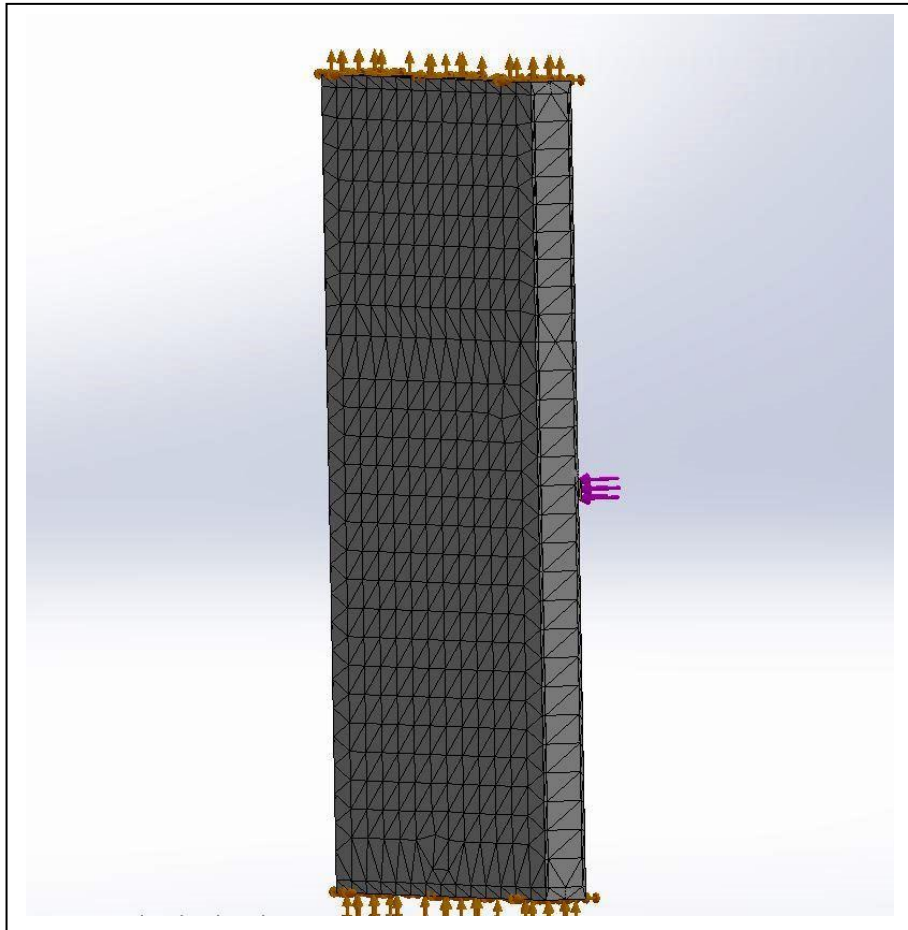


Figure G - 8: Mesh detail of modeled 114mm (4.5 in.) thick partially dis-bonded PUR SIPs exposed to transverse load (MD45T)

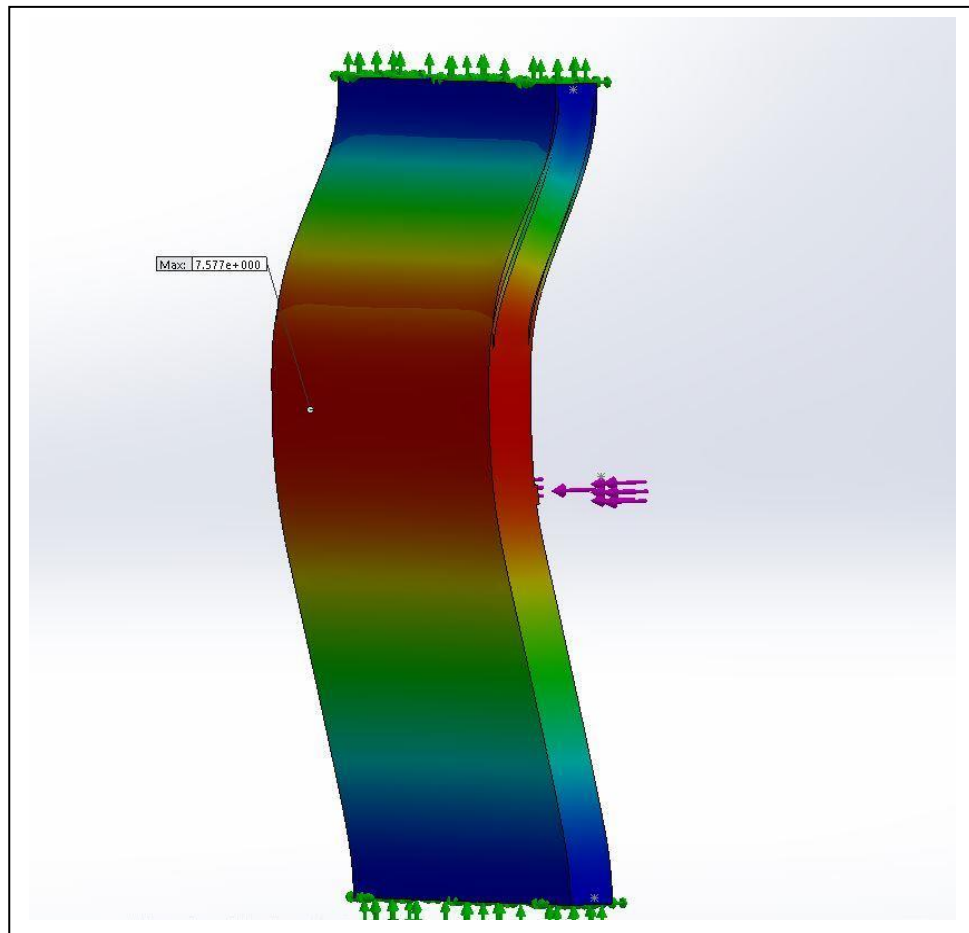


Figure G - 9: Deflection behaviour of modeled 114mm (4.5 in.) thick partially dis-bonded PUR SIPs exposed to transverse load (MD45T) (Red indicates zone of greatest deformation)

Racking Load Simulations of Fully-Bonded PUR SIPs
(114mm, 4.5 in. thick)

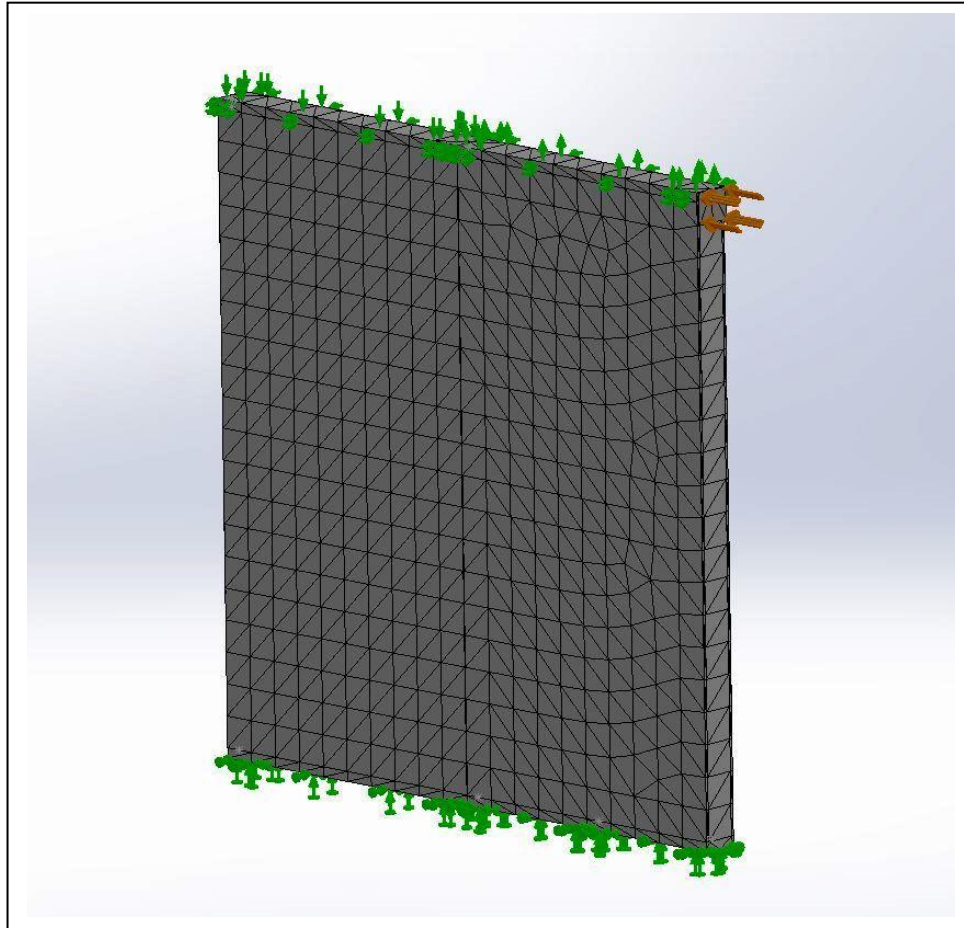


Figure G - 10: Mesh detail of modeled 114mm (4.5 in.) thick fully-bonded PUR SIPs exposed to racking load (M45R)

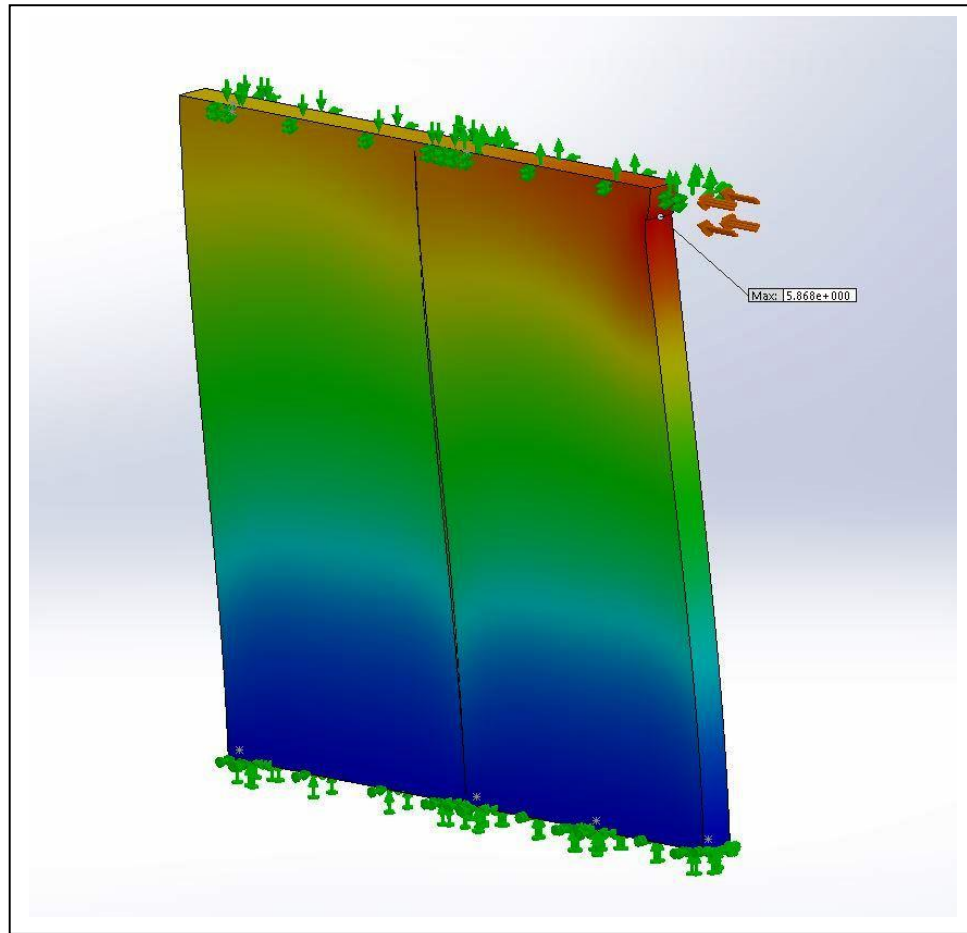


Figure G - 11: Deformation behaviour of modeled 114mm (4.5 in.) thick-fully bonded PUR SIPs exposed to racking load (M45R) (Red indicates zone of greatest deformation)

Racking Load Simulations of Dis-Bonded PUR SIPs
(114mm, 4.5 in. thick)

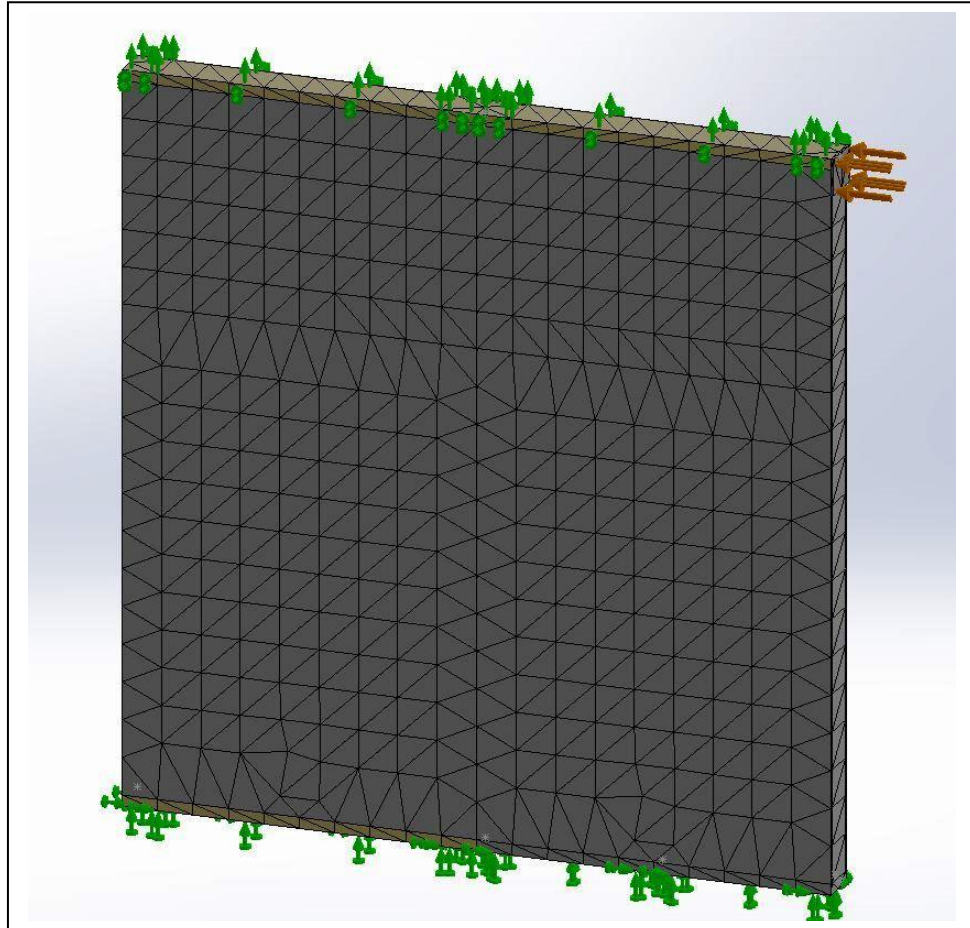


Figure G - 12: Mesh detail of modeled 114mm (4.5 in.) thick partially dis-bonded PUR SIPs exposed to racking load (MD45R)

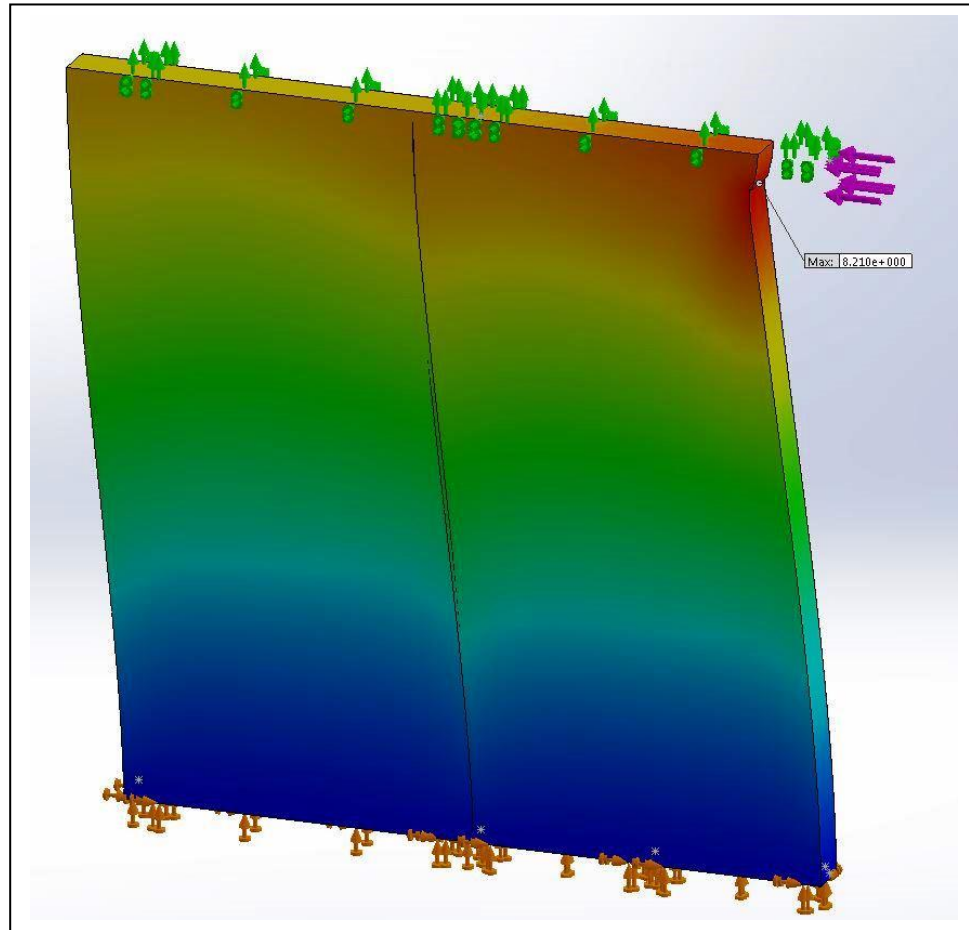


Figure G - 13: Deformation behaviour of modeled 114mm (4.5 in.) thick partially dis-bonded PUR SIPs exposed to racking load (MD45R) (Red indicates zone of greatest deformation)